TESIS DE LA UNIVERSIDAD DE ZARAGOZA

2021

216

Edwin Samir Pinto Maquilón

Thermoeconomic and environmental optimization of polygeneration systems for small-scale residential buildings integrating thermal and electric energy storage, renewable energy and legal restrictions.

Director/es
Serra de Renobales, Luis María

ISSN 2254-7606

Prensas de la Universidad
Universidad Zaragoza

ISSN 2254-7606

Universidad Zaragoza
1542

Tesis Doctoral

THERMOECONOMIC AND ENVIRONMENTAL OPTIMIZATION OF POLYGENERATION SYSTEMS FOR SMALL-SCALE RESIDENTIAL BUILDINGS INTEGRATING THERMAL AND ELECTRIC ENERGY STORAGE, RENEWABLE ENERGY AND LEGAL RESTRICTIONS.

Autor

Edwin Samir Pinto Maquilón

Director/es

Serra de Renobales, Luis María

UNIVERSIDAD DE ZARAGOZA
Escuela de Doctorado

2021

Universidad Zaragoza
1542

Doctoral Thesis

Thermoeconomic and environmental optimization of polygeneration systems for small-scale residential buildings integrating thermal and electric energy storage, renewable energy and legal restrictions

Author

Edwin Samir Pinto Maquilon

Advisor

Prof. Luis María Serra de Renobales

Ph.D. Program in Mechanical Engineering
Universidad de Zaragoza
2021

$\mathcal{A}$ *mi madre que es tan hermosa y la quiero tanto...*♫♫
Dios la tenga en su gloria...
Pa' lante es pa' allá!

$e\pi$

Acknowledgements

Along the revisions of different works, in particular PhD thesis, beyond the technical and scientific aspects, it is a fact that the achievement of a PhD is a merit of the effort and sometimes the sacrifices of a person. However, it is also a fact that to achieve the goal, the PhD student (he/she) has been definitely supported by a group of persons who in different ways helped him/her along the road. My case is not an exception, because I have to acknowledge the support of many important people along my PhD road. First of all, the support of my advisor Luis M. Serra for his enthusiasm and patience but specially for believe in me. Although many people must be acknowledged, I consider that GITSE gathers most of them. In particular, I would like to highlight the unmensurable support of Ana Lázaro and Jose María Marin.

People are the most important; however, the financial aspects also played an important role in my PhD. Therefore, first of all I acknowledge to the mobility program for Latin-Americans offered by Unizar-Santander Universities, since it allowed me to come to Zaragoza for study my PhD. Besides, this work was developed in the frame of the research project ENE2017-87711-R, partially funded by the Spanish Government (Energy Program), the Government of Aragon (Ref: T55-17R), Spain, and the EU Social Fund (FEDER Program 2014-2020 "Building Europe from Aragon") which must be also gratefully acknowledged.

I would like to extend my acknowledge to the Campus Iberus and the EU's Erasmus+ programme for allowing me to carry out my research stay in the LaTep-Université de Pau. Likewise, thanks to Latep group specially to Erwin Franquet for hosting me.

Thanks to Dr. Omar Guerra for his help and advices about optimization issues. I would like to acknowledge his important scientific support along my thesis.

Last but not least, my very special acknowledge is to my wife Maryluz, for showing me her love through her unconditional support in every moment and encouraging me to go ahead.

Agradecimientos

Son muchas las razones que tengo para estar agradecido y muchas personas a quien agradecer, y como es cuestión de sentimientos, la mejor forma de expresarlos es en mi lengua materna. Esta última palabra da pie a la primera persona a agradecer, ayer, hoy y siempre. Y es que... yo quisiera preguntar cual cariño es el más grande del mundo, sin duda nadie se equivocará y sé que todos dirán, que es una bella mujer, una bendición de Dios, es mi mamá$^{\heartsuit\heartsuit\infty}\blacktriangleright$. Ella me enseñó con su ejemplo a no rendirme ante las adversidades, porque pa' lante es pa' allá, pa' atrás ni pa' coger impulso.

A Maryluz$^{\heartsuit\heartsuit}$ mi novia, mi mujer, mi amiga ∞...$\blacktriangleright$ con quien he vivido las experiencias más significativas de mi vida, quien me ha hecho ver el mundo más bonito $\blacktriangleright$. Llegar a este punto es la suma de muchas decisiones, la mayoría entorno a ella, gracias por la travesía y tu apoyo para alcanzar este logro.

GITSE, grupo de ingenieros térmicos soltando exergía, cariño, entusiasmo, alegría, apoyo...en fin, a todos y cada uno, los que están y ya no están, gracias por acompañarme en este camino. Y claro, especialmente a mi equipo de running, Anik* y el entrenador$^{\Phi}$, que indudablemente me impulsaron a seguir adelante en el 2017 y me ayudaron a alcanzar la meta, y aún más, me ayudaron a ver las cosas realmente importantes que van más allá del PhD. A la comandante* por su sonrisa y disposición, un gusto ser su secre. A Luis$^{\natural}$, por continuar conmigo adelante y confiar en mí...por ser humano...mil y mil gracias.

Quiero agradecer también al Dr. Omar Guerra (Optimizerman) por su gran ayuda para abordar la optimización a lo largo de mi tesis y al Dr. Said Pertúz (el genio) por sus brillantes aportes en diferentes aspectos técnico-científicos, pero ante todo gracias a ambos por su colaboración desinteresada siempre que estuvo en sus manos.

Y es que... aquel que nunca ha estado ausente no ha sufrido un guayabo, hay cosas que hasta que no se viven no se saben...$^{\heartsuit}\blacktriangleright$ Así, finalmente, agradezco a familiares y amigos, en especial a mi hermanita Dra. Julieth (Doctora de las que cura) y mi tía Meche (mi segunda madre) por sus oraciones y buenos deseos en todo momento al igual que mi a madrina-suegra, por ser quien es, gracias. Insisto, no hay como agradecer explícitamente a tantas personas que de una u otra forma me han ayudado, pero afortunadamente a cada uno le he agradecido personalmente a lo largo de este camino llamado doctorado.

Merci Beaucoup!

$e\pi$

Abstract

The residential sector, responsible of about 27% of the global energy consumption and 17% of the greenhouse gas emissions, plays a key role in the action to combat climate change. In this sense, polygeneration systems could be considered a suitable alternative to attend the energy demands of residential buildings since they enable an efficient use of natural resources with a low environmental impact. This thesis developed a Mixed Integer Linear Programming (MILP) model to research these kind of systems in a systematic way to integrate renewable energy such as solar and wind energy with thermal and electric energy storage, considering commercial equipment for small-medium scale residential buildings, taking into account both economic and environmental aspects for the optimal design of such systems. The research starts from the suitable way to address the optimization process focused on the selection of the method to select representative days. Through the comparison of different methods, it was demonstrated that its right selection strongly depends on the variability of the time series involved in the analysed system. Besides, a new method was developed in order to improve the results of the optimization process. The developed MILP model was applied to study the feasibility of residential buildings as a microgrid. This innovative approach was found profitable with respect to the current conventional energy systems but it is necessary the application of feed-in tariff schemes or allowing the sale of electricity at reasonable price in order to make them competitive. Further, a thermoeconomic analysis was carried out to evaluate synergies between the components of the energy system. It was shown the importance of considering both thermal and electrical parts in the design of energy systems, highlighting the role of heat pumps and energy storage as key technologies, to achieve more cost-effective and sustainable solutions. Finally, the recent Spanish self-consumption regulations were applied to evaluate its impact on the design of energy systems. Moreover, through the application of multiobjective optimization and the analysis of different trade-off solutions was evaluated if this regulation aligned with European and international goals to combat climate change, and how it could be addressed in order to promote the design of affordable sustainable energy supply systems for the residential buildings. The obtained results suggest to act on the self-consumption regulation in order to achieve more significant reduction of greenhouse gas emissions. Overall, this thesis provided methodologies and useful insights for the design of sustainable energy systems for residential buildings.

Resumen

El sector residencial, responsable del 27% del consumo energético mundial y 17% de emisiones de gases de efecto invernadero aproximadamente, desempeña un papel clave para combatir el cambio climático. Por esto, el uso de sistemas de poligeneración resulta una alternativa apropiada para cubrir las demandas energéticas de los edificios, ya que permiten un uso eficiente de los recursos naturales con un bajo impacto ambiental. En este sentido, esta tesis ha desarrollado un modelo de programación lineal entera mixta (MILP) para investigar estos sistemas de forma sistemática, integrando tecnologías renovables, como la solar y eólica, con almacenamiento de energía térmica y eléctrica, considerando equipos comerciales, teniendo en cuenta aspectos económicos y ambientales en el diseño. La investigación comienza por la forma de abordar el proceso de optimización, partiendo por la elección del método para seleccionar días representativos. Comparando diferentes métodos, se demuestra que su idoneidad depende en gran medida de la variabilidad de las series temporales involucradas en el sistema analizado. Además, se ha desarrollado un nuevo método que mejora los resultados del proceso de optimización. Por otro lado, se ha estudiado la viabilidad del uso de edificios residenciales como microrred. El estudio muestra que resultan rentables con respecto a los sistemas energéticos convencionales actuales, pero es necesario la aplicación de incentivos o permitir la venta de electricidad a un precio razonable para que sean competitivos. Adicionalmente, se han estudiado e identificado sinergias entre los componentes del sistema energético gracias al desarrollo de un modelo termoeconómico, que muestran la importancia de abordar el diseño de los sistemas energéticos considerando conjuntamente tecnologías térmicas y eléctricas, destacando la bomba de calor y los acumuladores de energía como tecnologías claves para lograr soluciones más económicas y sostenibles. Finalmente, se han aplicado las últimas regulaciones españolas de autoconsumo para evaluar su impacto económico y ambiental en el diseño de sistemas energéticos. Además, a través de la aplicación de la optimización multiobjetivo, se analizó si la reciente regulación de autoconsumo se ajusta a las metas europeas e internacionales para combatir el cambio climático. Asimismo, se estudia como podría abordarse la regulación para promover el desarrollo de sistemas energéticos sostenibles para el sector residencial. Los resultados sugieren actuar sobre la regulación de autoconsumo para reducir el impacto ambiental de forma efectiva. En general, esta tesis proporciona metodologías e ideas útiles para el diseño de sistemas energéticos sostenibles capaces de cubrir las demandas de energía de los edificios residenciales.

Contents

Nomenclature

Equipment	
ACH	Absorption chiller
BAT	Batteries
BB	Biomass boiler
CM	Cogeneration module
GB	Gas boiler
GE	Generator
HP	Reversible heat pump
Inv	Inverter
InvC	Inverter charger
Pct	Contracted power from the electric grid
PV	Photovoltaic panels
ST	Solar thermal collectors
TSQ	Thermal energy storage for heating
TSR	Thermal energy storage for cooling
WT	Wind turbine
Energy	
E_d	Electricity demand for appliances
Q_d	Heating demand
R_d	Cooling demand
E_{PV}	Hourly photovoltaic energy production per square meter
E_{ST}	Hourly solar thermal energy production per square meter
E_W	Hourly electrical production of a wind turbine

Ep	Purchased electricity [kWh]
Es	Sold electricity [kWh]
F	Fuel consumption[kWh]
Q	Heat[kWh]
R	Cool[kWh]
E/W	Electricity[kWh]
Decision variables	
Cap	Nominal capacity [*]
Y	Binary variable [0,1]
Economic data	
CIA	Annual investment cost [€/yr]
CRF	Capital recovery Factor
Cu	Component unit cost [€/*]
C_{ope}	Annual operational costs [€/yr]
C_e	Electricity bill cost [€/yr]
C_g	Fuel consumption cost [€/yr]
C_{fix}	Fixed cost bill [€/yr]
C_v	Variable cost of the bill [€/yr]
C_{alq}	Meter equipment rental cost[€/yr]
cp	Purchase electricity/natural gas price [€/kWh]
cs	Electricity sale price [€/kWh]
F_{ind}	Indirect cost factor
F_m	Installation and maintenance cost factor
FNPV	Net Present Value factor
TAC	Total annual cost [€/yr]
Tax_e	Electricity Tax
VAT	Value-added tax
Environmental data	
$CO2_{fix}$	CO_2eq emissions embodied in the components [$kgCO_2eq$/yr]
$CO2_{ope}$	Operational CO_2eq emissions from the fuel combustion and/or from the electric grid [$kgCO_2eq$/yr]
TCE	Total annual CO_2eq emissions [$kgCO_2eq$/yr]
Subscripts	
$_e$	Electricity
$_g$	Conventional or biomass fuel

List of Figures

List of Tables

Chapter 1

Introduction

"Remember, it's a long distance race..."

Nowadays, climate change is a worldwide concern for the humanity. Most of the countries around the world are working to develop energy policies to avoid the depletion of their natural resources as well as to reduce the greenhouse gas emissions, very often expressed in CO_2-equivalent (CO_2eq) emissions. Consequently, renewable energy technologies are a key point in the energy transition in a world that has been driven by fossil fuels for decades, or even centuries.

Polygeneration systems are getting attention since they enable an effective way to achieve a lower consumption of natural resources, a reduction of CO_2 emissions and pollutant emissions as well as economic savings relative to conventional separate production. Likewise, they allow the integration of different technologies with renewable energy, contributing significantly to achieve the worldwide goals concerning energy and environmental policies such as the Paris agreement adopted at the Paris climate conference (COP21) in December 2015, which sets out a global framework to avoid dangerous climate change by limiting global warming to well below 2 °C and pursuing efforts to limit it to 1.5 °C. On the other hand, the residential buildings play an important role in the pathway to combat climate change since they represent about 27% of the world energy consumption. This thesis aims to study methodologies to enable a proper integration of renewable energy technologies for polygeneration systems, a better understanding of these technologies to achieve affordable and sustainable energy solutions for residential buildings and evaluate the impact of the legal restrictions in the pathway to combat the climate change.

1.1 Polygeneration systems in residential buildings

The International Energy Agency (2018) claims that the total building sector consumes nearly 40% of the global final energy consumption in the European Union (EU). Heat demand in the buildings sector accounts for almost 80% of this consumption, mostly in the form of space heating and generally using fossil fuels. Two-thirds of energy consumption in buildings sector is in the residential sector. In turn, in environmental terms, it represents about 30% of direct CO_2 emissions in the European Union (i.e. not including indirect emissions from the use of electricity and district heating). As the buildings sector also accounts for almost 60% of EU electricity consumption, it is also responsible for an important share of indirect CO_2 emissions. In a worldwide perspective, the residential sector represents about 27% of the energy consumption and 17% of the greenhouse gases emissions of the world (Nejat et al., 2015). Thus, the residential buildings are a key component of the energy transition and also play an important role in the policies to mitigate climate change and its impacts. Accordingly, it is one of the objective sectors in the pathway to limit global warming to 1.5 °C according to the last report of the Intergovernmental Panel on Climate Change (IPCC) (Masson-Delmotte et al., 2018).

The design of buildings with low energy consumption has been a matter of research and study during the last two decades (Abel, 1994; Lund et al., 2017). There are approaches oriented to reduce the building's energy demand, through the design of buildings with very low energy requirements (López-Ochoa et al., 2018), but also through the implementation of efficient energy supply systems considering as well the integration of renewable energy technologies (Mancarella, 2014; Pina, 2019).

Recent studies show that the integration of thermal and electrical systems allow to increase the share of renewable energy, and the reduction of CO_2eq emissions (Lund et al., 2017). Hence, the use of polygeneration systems for residential buildings, can be a suitable alternative to reduce economic costs and CO_2eq emissions with respect to the separate production of energy services, thanks to an adequate energy systems integration (Serra et al., 2009). Polygeneration in residential buildings generally refers to the combined production of electricity, heat and cooling (Jana et al., 2017). They consist of different energy technologies, which convert renewable and non-renewable energy resources into the energy services required in the building along the time (Figure 1.1). Internal combustion engines, gas turbines, micro-turbines or fuel cells may act as prime

movers, coupled to an electric generator when required, in which the chemical energy of fossil fuels or biomass is converted into electrical power. The heat released can be used for the production of domestic hot water (DHW) and/or space heating. Further, thanks to the integration of thermally activated technologies such as absorption chillers, cooling production for air conditioning can also be obtained using the available excess of heat produced in periods in which heating space is not required. Mechanical chillers allow also the cooling production thanks to the efficient conversion of electrical energy. In this respect, reversible heat pumps, producing alternatively both, heating or cooling, are also interesting candidate technologies of polygeneration systems in residential buildings that, together with auxiliary boilers, may complement and avoid the oversizing of the prime mover (Rong and Su, 2017). Technologies driven by renewable energies also play a key role in the design of sustainable energy supply systems for residential buildings (Kasaeian et al., 2020; Pinto and Serra, 2018). Renewable energy technologies that can be properly integrated in polygeneration systems for buildings, providing higher flexibility and diversification as well as environmental benefits, can be based on solar energy (e.g. photovoltaic panels, solar thermal collectors, hybrid photovoltaic/thermal), wind energy (e.g. wind turbine generator) or biomass (e.g. biomass boiler), among others. Moreover, they can cover multiple energy demands directly (e.g. electricity from photovoltaic or wind turbines, or heat from solar thermal collectors or biomass boilers) or indirectly by coupling absorption and/or mechanical heat pumps (Pinto et al., 2020; Modi et al., 2017; Ghaem Sigarchian et al., 2018). Nevertheless, non-manageable energy technologies, such as wind or solar energy, are not able of covering alone in a reasonable and competitive way the full demand of energy services of buildings. In this respect the combination of non-manageable renewable energy sources with manageable energy sources (e.g. biomass and/or conventional fossil fuels) and with the integration of energy storage (e.g. electric batteries, thermal energy storage –hot water tanks for heating or chilled water for cooling) allow to reach a significant fraction of renewable energy, to increase the energy security, to reduce the installed capacity of some technologies, to increase the environmental benefits and to reduce the operation costs (Buoro et al., 2014; Pinto et al., 2020).

Consequently, polygeneration systems could be considered as a cutting-edge topic for research aiming to combat the climate change, since it allows the integration of energy-efficient and low-carbon heating and cooling technologies, as well as renewable energy technologies, among others technologies, essential to achieve a sustainable energy future (International Energy Agency, 2017).

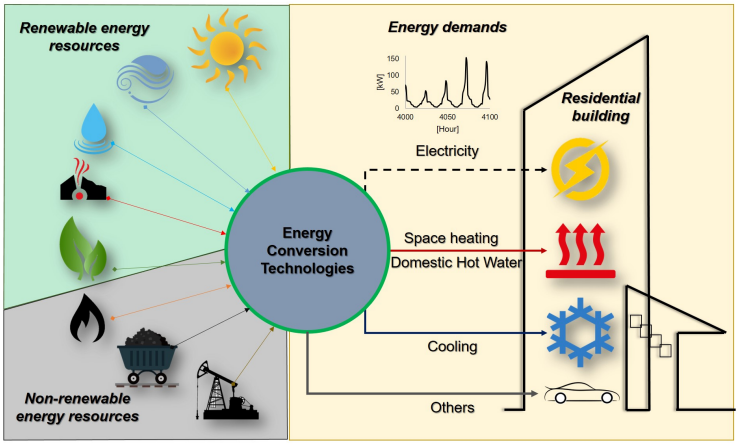

Figure 1.1: Polygeneration system for residential buildings representation.

1.2 Optimization of polygeneration systems

Above mentioned, polygeneration systems could be considered a suitable alternative to reduce both greenhouse emissions and economic costs. However, in order to achieve more efficient and cost effective energy systems effectively, it is necessary to develop better design practices. In this sense, optimization is a remarkable tool in engineering for determining the best, or optimal, value for a decision variable of a system. In energy systems this could be used to minimize the total cost, the fuel consumption and/or the CO_2eq emissions, etc.

Optimization techniques have been widely applied for industrial applications but they have not been so frequently applied for building applications (Ortiga et al., 2007). However, this has changed during the last decades and the use of optimization techniques are also applied for the design of polygeneration systems for residential buildings, becoming one of the most effective approaches for dealing with complex energy systems systematically to obtain the best possible results under certain conditions (Rong and Lahdelma, 2016; Rong and Su, 2017). Nevertheless, the design of polygeneration systems for residential buildings based on optimization techniques could be considered more complex than for industrial applications because usually there are more aspects to be considered, for instance the wide variety of technology options available and great diurnal and annual fluctuations in energy demands and energy prices, among

others (Tapia-Ahumada et al., 2013). Additional factors that increase the complexity include: i) the incorporation of renewable energy sources, such as solar radiation or wind power, which are characterized by intermittent behaviour and non-simultaneity between production and consumption and (ii) the incorporation of energy storage, either electrical and/or thermal, which allow to decouple production from consumption.

Different systematic approaches have been developed for the optimization of energy systems such as heuristic, insight-based, mathematical optimization (Andiappan, 2017). In the case of heuristic approaches, they use rules derived from engineering knowledge and experience and on physical concepts. Since they are often dependent on the experience of the designer, when newly or not established processes are considered, heuristic approaches may not be applicable. In addition, such approach also does not guarantee that the optimal configuration has been revealed (Frangopoulos et al., 2002). Regarding insight-based approaches, they combine principles from thermodynamics and other physical sciences to obtain targets for the optimal system configuration. A prominent example of this approach is the pinch analysis which is used to integrate thermal processes (Kemp, 2007). When insight-based approaches are applied, if the physical target is the optimization objective (e.g. minimization of energy consumption), then these methods provide the solution to the optimization problem. However, if the optimization objective is economic, e.g. minimization of the total cost, then these methods are not very appropriate. Finally, the mathematical optimization approaches considers several possible unit operations and their alternative system configurations, process integration, operating modes and other important matters in a superstructure representation of an energy system (Wakui and Yokoyama, 2014). One of the main advantages of this approach is that it automatically reveals the optimal system configuration (Liu et al., 2011). Consequently, the mathematical optimization approach has been chosen to address the optimization problem herein.

It must be taken into account that, if modelling is inaccurate, simulation and optimization results become unrealistic and useless. Thus, modelling needs to be carefully carried out before optimization is performed (Dincer et al., 2017). Therefore, in this work, an important part lies in the suitable way to model the representative behaviour of the different pieces of equipment of polygeneration systems for residential buildings during the day and along the year, since this fact plays an essential role to achieve good results in the design of such systems (Kotzur et al., 2018).

According to Lozano et al. (2009) and Wakui et al. (2016), two fundamental issues must be addressed in the design of polygeneration systems: the synthesis

of the plant configuration (installed technologies and capacities, etc.) and the operational planning (strategy concerning the operational state of the equipment, energy flow rates, purchase/selling of electricity, etc.). Consequently, herein, the Integrated Design Synthesis Operation Optimization *IDSOO* process is applied to address the design and study of polygeneration systems for residential buildings being one of the most studied and applied in the scientific literature to this end (Rong and Su, 2017). There are different algorithms depending on the mathematical nature and complexity from the relatively straightforward linear programming (LP) to increasingly complex mixed-integer linear programming (MILP), non-linear programming (NLP) and mixed-integer non-linear programming (MINLP) (Andiappan, 2017). For this thesis in particular, MILP is applied to address the optimization of polygeneration systems since the mixed-integer optimization provides a powerful framework for mathematically modelling many optimization problems that involve discrete and continuous variables (Grossmann, 2002).

1.3 Thermal and electric energy integration

Microgrids can be defined as electricity distribution systems containing loads and distributed energy resources (such as distributed generators, storage devices, or controllable loads), that can be operated in a controlled, coordinated way either while connected to the main power network or while islanded according to the Conseil international des grands réseaux électriques *CIGRÉ* (International Council on Large Electric Systems in english) (Oleinikova and Hillberg, 2020). Usually, microgrids are focused on electricity loads; however, this concept has evolved to a wider perspective about the energy integration systems. In this sense, different works about smart energy systems extend their scope to include different energy sectors such as electricity, natural gas, transport, among others in the pathway to achieve 100% renewable energy systems (Lund et al., 2012, 2014; Mathiesen et al., 2015).

Formally, a smart energy system is defined by Lund et al. (2017) as: *an approach in which smart electricity, thermal and gas grids are combined with storage technologies and coordinated to identify synergies between them in order to achieve an optimal solution for each individual sector as well as for the overall energy system.*

In this sense, it is necessary to address the design of energy systems considering technologies which enable the thermal and electrical integration. Thus, technologies such as heat pumps could be considered one of the cornerstone tech-

nologies for the integration of thermal and electrical parts in the pathway to scale up the renewable share in the buildings sector. Further, taking into account the non-manageable nature of the renewable energy technologies, the integration of energy storage helps to overcome this issue. In particular, batteries are considered one of the enabling technologies to increase the share of renewable energy in the new scenario proposed to combat the climate change(IRENA, 2020b). Nevertheless, taking into account the advantages of the electric-thermal synergies, its integration along with thermal energy storage is studied as an interesting alternative to achieve more cost-effective sustainable energy systems (Pinto et al., 2019). The thermal and electric integration in polygeneration systems for residential buildings is an issue hardly studied until now and hence, it is one of the aspects to be addressed in this thesis focused on small size energy systems, below to 500 kW, enabling the study and development of the distributed generation (DG). Concerning the electricity sector, this is because the conventional electricity generation concept has been based on the centralized production driven by fossil fuels, which implies, energy losses about 5% in the transmission lines (above 69 kV) and about 15% in the distribution network (below 69 kV) in the electricity path from the production centres to consumption places. Therefore, bearing in mind to avoid these energy losses, as the environmental considerations became a major concern for humanity and the electrical energy production from renewable sources have been gradually becoming economically feasible, the traditional paradigm of centralised electricity systems is being disrupted by increasing levels of distributed generation (Mehigan et al., 2018). Although this can not be extended to the thermal sector necessarily, all in all, the DG takes advantage of the available energy resources near the consumption places. Besides, the polygeneration system can be connected to the distribution network (grid connected system) or isolated from the grid (standalone), but in all cases provide the energy to attend the user energy demands. Both grid connected and standalone energy systems are studied along the thesis which allows to extend the obtained results to geographic zones where the electric infrastructure is not available, or helping the final users to decide whether or not to be connected to the electric grid.

1.4 Thermoeconomic and environmental analysis

Both economic and environmental aspects are considered herein. Economic aspects encompass operational costs related to the electricity and fuel consumption, and investment costs which include the cost of the equipment, installation and maintenance costs. The sum of both operational and investment costs is the total annual cost of the polygeneration system which is the economic objective function to minimize through the application of the IDSOO process. This allows the evaluation and analysis of energy systems from the economic point of view. On the other hand, environmental aspects are also studied taking into account both the operational CO_2eq emissions and the embodied CO_2eq emissions in the equipment, which are evaluated based on different works about life cycle assessment LCA (International Organization for Standardization, 2006). Besides, multiobjective optimization is carried out in order to obtain different trade-off solutions which can be useful in the decision making process of stakeholders. This also enables to evaluate the feasibility of different technologies from both economic and environmental point of view.

Although the feasibility of the energy systems can be evaluated trough the IDSOO process, a deeper analysis is required in order to know the synergies between technologies and how to address the design of polygeneration systems. This can be carried out through the thermoeconomic analysis.

Concerning thermoeconomics, the first proposal in this field could be attributed to Keenan in 1932, when in a cogeneration plant he apportioned the cost of heat and work taking into account the concepts of irreversibility and thermodynamic efficiency (Second Law), instead of the enthalpy only (First Law) (El-Sayed and Gaggioli, 1989; Valero et al., 2005). However, it was Tribus and Evans (1962) who coined the term "Thermoeconomics" to formulate the interaction between cost and efficiency. Nevertheless, a fruitful research in Thermoeconomics understood as a technique which combines the thermodynamic analysis and the economic optimization of complex energy systems was opened by El-Sayed and Evans (1970) when they applied rigorous calculus methods to the system optimization, incorporating Lagrange multipliers and marginal costs which produced several optimization methods such as Thermoeconomic Functional Analysis (Frangopoulos, 1987), the Engineering Functional Analysis (von Spakovsky and Evans, 1993) or the Intelligent Functional Approach (Frangopoulos, 1991).

Basically, thermoeconomics methods can be divided in two main groups

(Tsatsaronis, 1998): i) Optimization methods that employ marginal costs in order to minimize the cost of a system or a component and ii) cost accounting methods based on average costs.

With respect to cost accounting, it consists of procedures for estimating the total annual cost of production per unit of output for each product from an energy system. The purposes of the cost accounting explicitly are (Lozano and Valero, 1993):

- Determining the actual costs of products.
- Providing a rational basis for pricing products and/or evaluating their profitability.
- Providing means for controlling expenditures.
- Forming a basis for operating decisions and their evaluation.

Although finding the unit costs of the *end* products is important, it is also valuable to trace them through the intermediates in order to make trade-off analyses of the economics of subsystems. Thus, the study of the energy systems based on the internal costs obtained systematically under rational criteria based on the second law of thermodynamics (Lozano and Valero, 1993) enables the comprehension of the interaction of the different components of the energy system. In this sense, thermoeconomic models have been applied to the polygeneration systems, which include thermal and electrical components, in order to stablish synergies between different technologies, specially thermal and electric energy technologies e.g. heat pumps, energy storage, etc. Likewise, interesting and suitable insights can be obtained to address the design of polygeneration systems through the deep understanding of its internal costs.

1.5 Legal framework of polygeneration systems for residential buildings

The challenge for energy policy in this time of energy model transitions is to accelerate and broaden investment in cleaner, smarter and more efficient energy technologies, while ensuring at the same time that all the key elements of energy supply, including electricity networks, remain reliable and robust (International Energy Agency, 2018). In this sense, the energy policies should encourage the deployment of polygeneration systems since they are a suitable

alternative to achieve a lower consumption of natural resources and hence a reduction of CO_2eq emissions (Serra et al., 2009). However, the feasibility of polygeneration systems depends on the applied energy policies and legal framework. Actually, previous studies have demonstrated how some policies could incentive or impede the installation of specific technologies such as cogeneration (Lozano et al., 2010). Sometimes the legal framework of the countries are not well aligned to address the energy transition to a decarbonized and sustainable energy model in accordance with international agreements. For instance, some studies focused on the Spanish regulation considering net metering and net billing have shown how some policies impede the profitability of the photovoltaic technology (Dufo-López and Bernal-Agustín, 2015). Therefore, the study of energy systems taking into account legal restrictions should be carried out in order to verify the real effect of the energy policies in the support and deployment of more efficient and environmental friendly technologies. In turn, the results obtained could help policy makers to take the suitable decisions in favour of the country's energy development.

Herein, the last Spanish self-consumption regulations are evaluated and analysed from the point of view of their promotion of feasible, reliable, efficient and environmental friendly energy systems for residential buildings aligned with European and international objectives on energy and environment.

1.6 Objectives and structure of the thesis

Taking into account the previous introduction, this thesis has five main goals:

I To develop a suitable methodology for the optimization process of polygeneration systems for residential buildings considering the integration of renewable energy and energy storage. In this respect, some methodologies for the selection of representative days for the optimization of polygeneration systems for residential buildings have been studied in order to find an appropriate method to include in the optimization process, avoiding to increase the computational effort, technologies such as wind energy characterized by a stochastic behaviour.

II To study the feasibility of using residential buildings as a microgrids including different energy demands such as electricity, heating, and cooling in a step further to design of polygeneration systems for residential buildings as smart energy systems, in order to promote decentralized energy

generation and renewable energy technologies integration in the residential sector.

III To unveil synergies between different technologies, specially between thermal and electric parts, through the help of thermoeconomic analysis, which allows a deeper understanding of the design of polygeneration systems for residential buildings. Different technologies such as renewable energy technologies, heat pumps, cogeneration and energy storage are thoroughly studied in order to achieve more cost-effective sustainable energy systems.

IV To evaluate the recent Spanish self-consumption regulations from the perspective of their promotion of feasible, reliable, efficient and environmental friendly energy systems for residential buildings with respect to the international energy policies which aim to combat the climate change. This study is focused on the optimization of polygeneration systems for both households (1 dwelling) and residential buildings.

V To develop guidelines for the optimal design of affordable polygeneration systems for small-scale residential buildings oriented to the transition towards decarbonized energy supply systems by the analysis of the multi-objective optimization.

Moreover, the structure of the thesis is presented below:

This first chapter presents the state of the art of the different aspects addressed along the thesis. This includes an overview of the polygeneration systems for residential buildings, the optimization process as a technique to address the design of energy systems, the integration of thermal and electric parts within the energy systems as a cutting edge topic, the thermoeconomic analysis as suitable methodology to study energy systems thoroughly, and the importance of the legal framework to design polygeneration systems for residential buildings aligned to the international agreements to combat the climate change. Besides, the objective and structure of the thesis are defined in this chapter.

The chapter 2 provides the technical, economic and environmental data used for the optimization of polygeneration systems for residential buildings along the thesis. The data encompass the climatic data of Zaragoza and Gran Canaria, which are used to estimate the photovoltaic, solar thermal and wind turbine production, and also the different energy demands namely heating, cooling and electricity for appliances for residential buildings. In addition, this chapter gathers the technical, economic and environmental data of the entire technologies and energy resources considered along the thesis.

The chapter 3 presents a thorough comparison between different methods for the selection of representative days to address the optimization of polygeneration systems such as Averaging, k-Medoids and OPT method. A new method is developed in order to improve some characteristics of the methods studied.

The chapter 4 develops the optimization model which includes both economic and environmental objective functions used along the thesis. The superstructure that considers all candidate technologies is also described in detail.

The chapter 5 proposes the optimization of polygeneration systems for residential buildings as a microgrid. This is carried out in order to research different economic and environmental aspects to be considered in the pathway to evolve from the current conventional energy systems for residential buildings towards microgrid or smart energy systems which enable a higher share of renewable energy technologies.

The chapter 6 develops a thermoeconomic model in order to carry out a comprehensive analysis of the energy system integration. Different technologies are studied in order to find synergies which allow a deeper understanding to address the design of polygeneration systems for residential buildings. In particular, thermal and electrical energy storage are studied to obtain useful insights about these technologies. Besides, the allocation of economic costs in the energy systems is carried out to obtain fair unit cost of the different energy services.

The chapter 7 evaluates the last Spanish self-consumption regulations through the optimization of grid connected polygeneration systems for residential buildings. The RD 900/20015 and RD 244/2019 are compared through the economic optimization of polygenerations systems for residential buildings. In addition, a multiobjective optimization is carried out under the legal restrictions imposed by the RD 244/2019 in order to evaluate affordable sustainable energy supply systems for residential buildings.

Finally, the chapter 8 presents a synthesis of the results obtained, the main contributions and conclusions achieved, followed by the potential future works.

Chapter 2

Data Collection

"Believe and trust!"

In a general view, a polygeneration system for residential buildings converts natural energy resources into appropiate forms of energy to attend the energy demands of the building. The efficiency of these processes depends on the technical, economic and environmental parameters as well as the optimal planning to profit the natural resources at low economic and environmental costs. In this sense, the data collection which include the available energy resources, energy demands, technical equipment data and economic and environmental aspects, among others, plays an important role in the optimal design of the polygeneration systems (Figure 2.1).

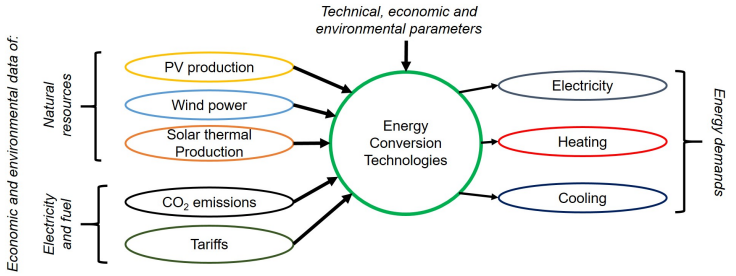

Figure 2.1: Data collection for the optimization of polygeneration systems.

Another important aspect in the design and optimization of polygeneration systems is the considered timeframe, particularly in the case of dynamic systems, in which the representative behaviour of the system should be properly captured. In this respect, the optimization of dynamic energy systems should be carried out in hourly or sub-hourly periods for one or more years (Domínguez-Muñoz et al., 2011). For this work, the timeframe is developed based on hourly periods for one year. In some cases, this is a challenging task, for instance, for the estimation of hourly energy demands, because there are not available hourly data or they are not easy to find; therefore, some approaches must be carried out in order to obtain the hourly energy demands data. On the other hand, in the case of hourly energy resources data, they are available in the climatic databases.

This chapter presents the data that were considered for the optimization of the polygeneration systems for residential buildings studied in this research work. This is addressed in four parts: i) The available natural resources for each considered location (Zaragoza and Gran Canaria); ii) the energy demands for the residential buildings such as electricity, heating and cooling; iii) a comprehensive description of the energy supply technologies for residential buildings including the technical data required for the simulation of their behaviour; and iv) a description of the economic and environmental aspects of the different pieces of equipment and energy resources (fuels and the electric grid).

2.1 Geographic location and climatic data

The natural resources as well as the data from the electric grid and the energy demands depend on the geographic location. Therefore, the first step for the data collection is to define the place of the study. In this work, Zaragoza and Gran Canaria have been chosen as study places, taking into account the differences in natural resources, energy demands and data from the grid that exist between them. This allows to evaluate the design of the polygeneration systems under different conditions and extrapolate the results to other cases.

The energy resources such as solar radiation and wind energy depend on the climatic data. These are required to calculate the energy production of the renewable energy technologies such as solar panels and wind turbines. Besides, the ambient temperature is also required, for instance, to estimate the energy demands of the residential buildings. In this work, the database meteonorm (Meteotest, 2017) has been used to obtain the climatic data for the different locations. The Table 2.1 presents the geographic data of Zaragoza and Gran

Table 2.1: Geographic data of the considered locations.

Parameters	**Zaragoza**	**Gran Canaria**
Latitude	41.7° N	27.9° N
Longitude	1° W	15.4° W
Altitude	249 m	47 m

Canaria.

The climatic data for the design of the polygeneration system herein are:

- Hourly global solar radiation over a tilted surface G_T, at the titled angle β oriented to the south. The tilted angle β is the optimal angle that gives the highest energy output for the whole year, obtained from the photovoltaic geographical information system PVGIS (European Commission JRC, 2019). The Figures 2.2 and 2.3 show the hourly global solar radiation over a tilted surface at $\beta = 36°$ for Zaragoza and for Gran Canaria at $\beta = 26°$ respectively. The solar radiation in Gran Canaria is more stable than in Zaragoza along the year, therefore the annual production of the PV panels and solar thermal collectors is expected to be bigger in Gran canaria than in Zaragoza.

- Hourly ambient temperature T_{amb}: The Figure 2.4 depicts the hourly ambient temperature for Zaragoza and Gran Canaria. Along the year Zaragoza has a higher temperature variation than Gran Canaria. As a result, it would be expected heating and cooling demands in Zaragoza, whereas barely only cooling demand in Gran Canaria.

- Hourly wind speed v_0: The Figures 2.5 and 2.6 show the distribution of the wind speed for Zaragoza and Gran Canaria respectively as a function of their frequencies. The analysis of this kind of distribution is very important to estimate the feasibility of some technologies such as wind turbines. For instance, the cut-in speed to run the wind turbines is about 3.5 m/s and the nominal power usually is reached at 12 m/s. In this sense, a wind turbine in Zaragoza would operate at nominal capacity only about 21% of the year and about 38% of the year would be shutdown, whereas in Gran Canaria about 47% of the year would operate at nominal capacity and about 14% would be shutdown.

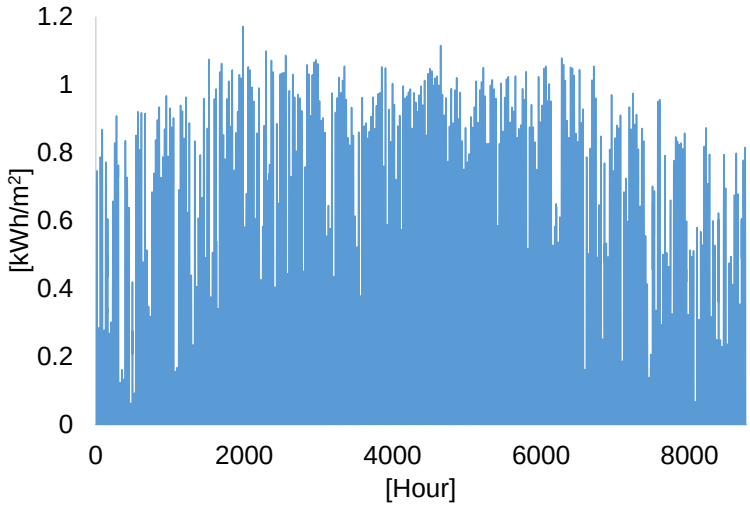

Figure 2.2: Hourly global solar radiation over a tilted surface in Zaragoza (Meteotest, 2017).

2.2 Renewable energy production

Natural resources such as solar radiation or wind energy are considered in this work as an available source of energy for the polygeneration system. The energy production of the different renewable energy technologies considered based on the climatic data of each location must be calculated for the optimization model. Indeed, the actual input data of the optimization model is the energy production of each technology instead of the natural resources.

2.2.1 Photovoltaic production

The hourly electricity production per square meter of the PV panels, $E_{PV}[kW/m^2]$, is calculated as a function of the hourly global solar radiation over a tilted surface $G_T[kW/m^2]$ and the manufacturer data of the PV module (Table 2.2)

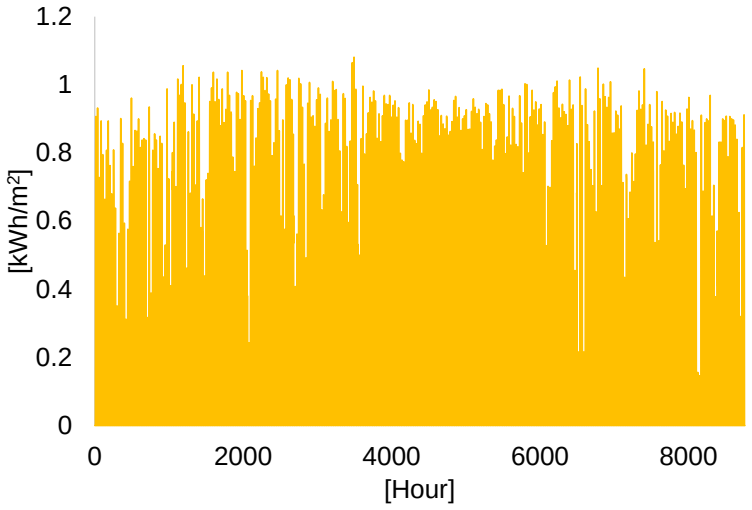

Figure 2.3: Hourly global solar radiation over a tilted surface in Gran Canaria (Meteotest, 2017).

according to the procedures described by Duffie and Beckman (2013). The procedure used to calculate the hourly electricity production per square meter of the PV panels $E_{PV}[kW/m^2]$ (Eq.2.1), take into account the temperature effects over its yield i.e. the energy efficiency of the panel η_{mp} (Eq.2.2) estimating the PV module temperature T_{mod} (Eq.2.3):

$$E_{PV} = \eta_{mp} \cdot G_T \tag{2.1}$$

$$\eta_{mp} = \eta_{mp_{sc}} \cdot \left(1 + \frac{\mu_{V_{oc}}}{V_{mp}} \cdot (T_{mod} - T_{sc})\right) \tag{2.2}$$

$$T_{mod} = T_{amb} + \Delta T_{NOC} \cdot \frac{G_T}{G_{NOC}} \cdot \left(1 - \frac{\eta_{mp}}{0.9}\right) \tag{2.3}$$

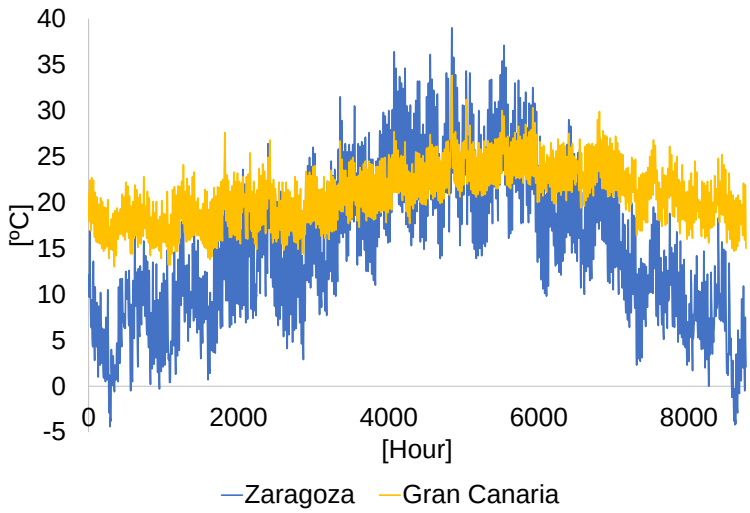

Figure 2.4: Hourly ambient temperature in Zaragoza and Gran Canaria (Meteotest, 2017).

2.2.2 Solar thermal collectors' production

Hourly solar thermal (ST) collectors production per square meter, $E_{ST}[kWt/m^2]$, is calculated based on the solar thermal collector specifications of GK 5000 model (Salvador Escoda S.A, 2017a) presented in the Table 2.3, according to the procedure described by Duffie and Beckman (2013).

Unlike PV production, ST production is not a continuous function proportional to the solar radiation necessarily, but a piecewise function (Eq. 2.4).

$$E_{ST} = max(\eta_o \cdot G_T - a_1 \cdot \Delta T_m - a_2 \cdot \Delta T_m^2, 0) \tag{2.4}$$

In this work, ΔT_m is calculated as the temperature difference between the absorber and the ambient temperature (Salvador Escoda S.A, 2017b). An assumption done for the calculation of E_{ST} is to set the absorber temperature at 60°C. Besides, it is assumed that the E_{ST} production temperature is in between

Table 2.2: PV panel manufacturer data (Atersa, 2017).

Parameter	Value	Description
Model	A-255P	-
Power	255 W	PV nominal capacity
Area	1.63 m^2	PV Surface area
$\eta_{mp_{sc}}$	15.6%	Standard Conditions Maximum power point efficiency
T_{sc}	25 °C	Standard condition temperature
V_{mp}	30.76 V	Maximum power voltage
$\mu_{V_{oc}}$	0.32%/°C	Temperature coefficient of open-circuit voltage
G_{NOC}	0.8 kW/m^2	Irradiation at NOC (Normal Operating Cell Condition)
Δ_{NOC}	27 °C	Temperature difference at NOC

Table 2.3: Technical data for the solar thermal collector (Salvador Escoda S.A, 2017a).

Parameter	Value	Description
Model	GK 5000	-
η_o	80.1%	Optical efficiency
a_1	3.188 $W/(m^2 \cdot K)$	1^{st} order heat loss coefficient
a_2	0.11 $W/(m^2 \cdot K^2)$	2^{nd} order heat loss coefficient

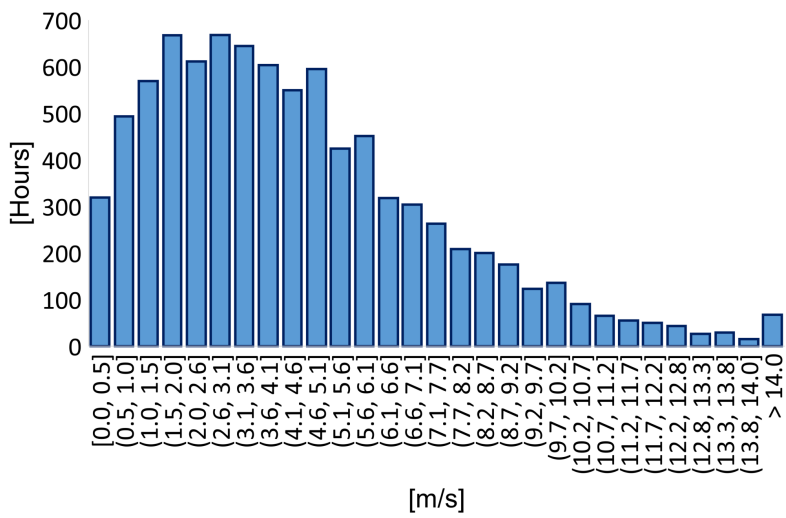

Figure 2.5: Wind speed distribution Zaragoza (Meteotest, 2017).

40-60°C, which is the range temperature of the heating demand.

These assumptions were verified by setting the inlet temperature at 40°C and varying the mass flow between 50-180 l/h. It was checked that for a commercial ST collector area of 5 m^2, outlet temperatures up to 90 °C could be reached under these conditions. This was carried out because the temperature is not considered as a variable in the optimization model, so it has to be guaranteed the suitable operation conditions beforehand.

2.2.3 Wind turbine production

Hourly wind power production, $E_W[kW]$, is calculated as a function of wind speed $v_0[m/s]$ and the production curve of the wind turbine (WT).

A correction air density factor F_ρ is applied to take into account the rate temperature changes with the altitude z. Besides, it is applied the log law to extrapolate the wind speed from a reference height z_a to the hub turbine height

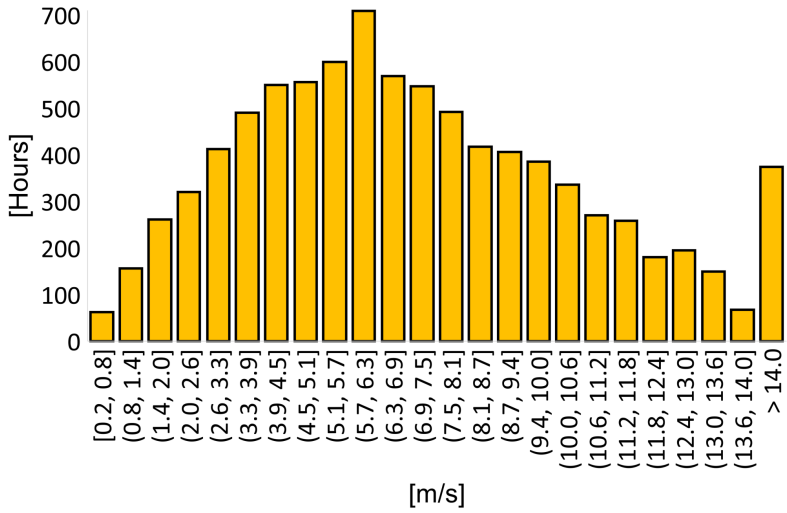

Figure 2.6: Wind speed distribution in Gran Canaria (Meteotest, 2017).

z_t (Manwell et al., 2009). The relations to calculate the wind power production $E_W[kW]$ are described as follows:

$$E_W = f(v_c) \cdot F_\rho \tag{2.5}$$

$$v_c = v_0 \cdot \frac{Ln(z_t/z_0)}{Ln(z_a/z_0)} \tag{2.6}$$

$$F_\rho = \frac{T_0 \cdot (P_0 - 0.011837 \cdot z + 4.7910^{-7} \cdot z^2)}{P_0 \cdot (-B \cdot z + T_0)} \tag{2.7}$$

Where,
v_c: Corrected wind speed m/s.
z_0: Surface roughness length, 0.25 m for a terrain characterized by many trees, hedges, few buildings.
B: Standard temperature gradient 0.0065 K/m.

T_0 and P_0: Temperature and pressure at sea level conditions, 288.15 K and 101.29 kPa respectively.

Wind power production depends on the wind turbine performance, which in turn depends on the capacity scale. In this work, as an approach, it has been used 2 different wind turbines in order to represent 2 different wind turbines groups according to their capacity: residential wind turbines up to 20 kW and commercial wind turbines from 21 kW to 100 kW (Orrell and Poehlman, 2017).

Therefore, wind turbines of 3 kW (Bornay, 2017) of capacity and 30 kW (Aeolos, 2006) of capacity have been chosen to represent the groups of WT used for households and buildings application respectively. The power production curves are depicted in the Figures 2.7a and 2.7b for nominal capacities of 3 and 30 kW respectively.

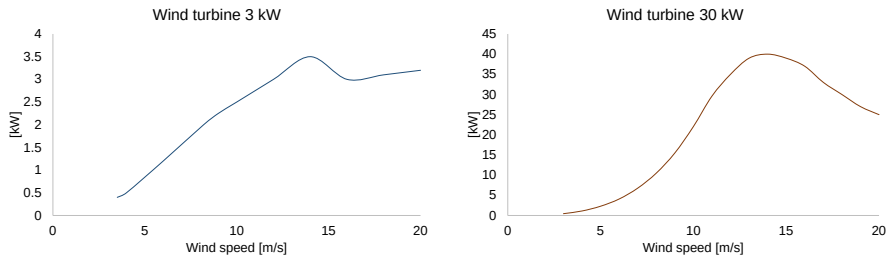

(a) (b)

Figure 2.7: Power production of the reference wind turbines: a) Turbine of 3kW (Adapted from Bornay (2017) ; b) Turbine of 30 kW (Adapted from Aeolos (2006)).

2.3 Energy demands for residential buildings

Polygeneration systems in this work should provide the energy services (electricity, heating and cooling) required by the residential building. Therefore, the estimation of the energy demands for residential buildings plays an important role in the design of the energy systems. These depend on the location, the building envelope and the specific human behaviour, among other factors.

Nevertheless, herein pretends to estimate hourly energy demands for residential buildings in Spain, based on statistical annual data, by applying some hourly profiles and engineering common procedures. Normally, the statistical data are given per square meter or per number of inhabitants in order to be scaled proportional to the residential building size.

2.3.1 Unit Space heating and cooling demands

The procedure to estimate the hourly space heating and cooling demands is in the simplified diagram depicted in the Figure 2.8. This procedure takes the annual energy demands data to be daily distributed by applying the degree days, and finally, the hourly energy demands data are obtained by using an hourly distribution function.

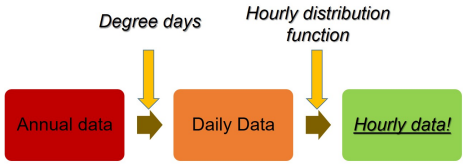

Figure 2.8: Procedure to estimate hourly data of space heating and cooling demands.

In detail, starting from the reference annual unit energy demand (Table 2.4) obtained from the technical report of IDAE (2009), these annual data are daily distributed by applying the *Degree Days method*. This method is more used for the estimation of space heating than for cooling demands, because it does not consider the humidity and solar gains to calculate the refrigeration load (Frederiksen and Werner, 2013); however, according to the work which proposes an enthalpy-based CDD method to take into account both latent and sensible heat, the error between its proposed method and the classical CDD method is only about 2% (Shin and Do, 2016). Taking this into account and despite of eventual solar gains, degree days method has been considered suitable to estimate both space heating and cooling demands.

Heating degree days (HDD) and cooling degree days (CDD) are calculated with base temperatures of T_{bh}=15 °C, for space heating and T_{bc}=21 °C, for cooling. These values were chosen as suitable for Spain according to Valor et al.

Table 2.4: Annual space heating and cooling demands (IDAE, 2009).

Location	**Unit space heating demand** uSH_{ref} $[kWht/m^2yr]$	**Unit cooling demand** uCD_{ref} $[kWht/m^2yr]$
Zaragoza	40.6	11.4
Gran Canaria	3.5	11.1

(2001). Heating and cooling degree days are calculated as the sum of the differences between daily average ambient temperature and the base temperature (ASHRAE, 2009).

$$HDD[^\circ C \cdot day] = \frac{\sum_{t=1}^{24}(T_{bh} - T_{amb}(t))^+}{24} \tag{2.8}$$

$$CDD[^\circ C \cdot day] = \frac{\sum_{t=1}^{24}(T_{amb}(t) - T_{bc})^+}{24} \tag{2.9}$$

The heating and cooling degree days per month, HDD_m and CDD_m respectively, are calculated as:

$$HDD_m = \sum_{d=1}^{d_f} HDD(d) \tag{2.10}$$

$$CDD_m = \sum_{d=1}^{d_f} CDD(d) \tag{2.11}$$

As a simplification, it settles heating and cooling months. This is helpful from the optimization point of view, since the binary variables which determine the operational mode of some components such as heat pumps, can be set beforehand and thus, the computational cost can be reduced. To do this, it is assumed that the operational mode is set for an entire month or group of days; being aware of that daily operational changes are not considered. This is carried out by applying two restrictions: the number of degree days per month must be greater than the number of days of the month d_f and the difference between heating and cooling degree days of the month $_m$ must be above five degree days (Eqs. 2.12 and 2.13).

$$if([HDD_m > d_f] \wedge |HDD_m - CDD_m| > 5) \rightarrow HDD_m; else \rightarrow HDD_m = 0 \quad (2.12)$$

$$if([CDD_m > d_f] \wedge |HDD_m - CDD_m| > 5) \rightarrow CDD_m; else \rightarrow CDD_m = 0 \quad (2.13)$$

The Figure 2.9a shows the heating and cooling degree days per month whereas the Figure 2.9b presents the considered effective heating and cooling months in Zaragoza. On the other hand, the Figure 2.10a shows the heating and cooling degree days per month whereas the Figure 2.10b presents the considered effective heating and cooling months in Gran Canaria. According to the degree days method applied, a residential building in Gran Canaria has only cooling demands, whereas in Zaragoza, residential buildings have both space heating and cooling demands.

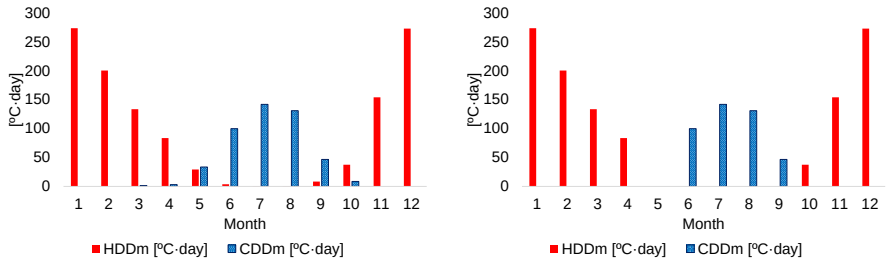

(a) (b)

Figure 2.9: a) Monthly Degree days b) Heating and cooling months in Zaragoza.

Following, the annual degree days for heating (Eq. 2.14) and cooling (Eq. 2.15) are calculated. Based on these, unit space heating $uSH[kWht/m^2]$ (Eq. 2.16) and cooling $uSC[kWht/m^2]$ (Eq. 2.17) demands per day are calculated.

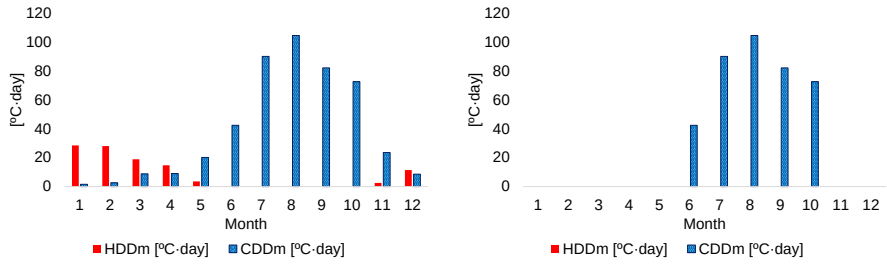

(a) (b)

Figure 2.10: a) Monthly Degree days b) Heating and cooling months in Gran Canaria.

$$HDD_a = \sum_{m=1}^{12} HDD_m \tag{2.14}$$

$$CDD_a = \sum_{m=1}^{12} CDD_m \tag{2.15}$$

$$uSH(d) = uSH_{ref} \cdot \frac{HDD(d)}{HDD_a} \tag{2.16}$$

$$uCD(d) = uCD_{ref} \cdot \frac{CDD(d)}{CDD_a} \tag{2.17}$$

Finally, the hourly unit energy demand for space heating and cooling are obtained by applying an hourly distribution function (Figures 2.11a and 2.11b) to each unit energy demand per day. The hourly distribution function has been calculated taking as a reference the available energy demands data of an urban district of 5000 dwellings located in Zaragoza (Ramos, 2012). According to the source of the data, every day of each month has the same profile. Although the more number of dwellings, the smoother the energy demands profile, this work has been assumed that the profile can be scalable to any residential building size. Another assumption is that these profiles have been applied also for residential buildings located in Gran Canaria, in this case for the cooling demand.

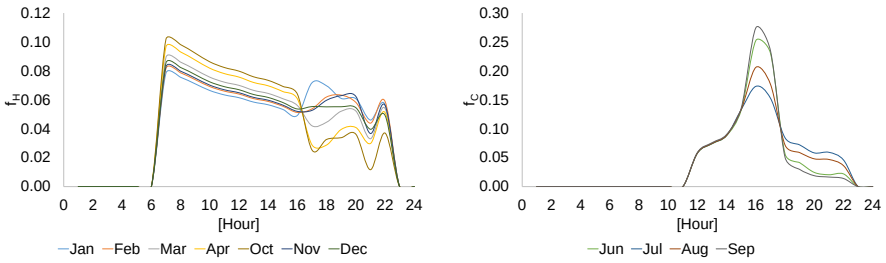

(a) (b)

Figure 2.11: Hourly distribution function for a) space heating b) cooling demand (Ramos, 2012).

Therefore, the unit space heating and cooling demands per hour are calculated as follows:

$$uSH(d,h) = f_H(d,h) \cdot uSH(d) \tag{2.18}$$
$$uCD(d,h) = f_C(d,h) \cdot uCD(d) \tag{2.19}$$

2.3.2 Domestic hot water demand

The estimation of the domestic hot water (DHW) energy $Q_{DHW}[kWht]$ starts from its annual consumption V_{DHW_a} in m^3, which is proportional to the number of inhabitants N_p and the reference consumption per day $V_{DHW_{ref}} = 28\ l/day \cdot person$ (IDAE, 2017). The annual consumption is distributed per month m by applying a distribution factor f_{mv} (Viti, 1996). The monthly energy required to heat up the monthly water volume up to 60°C is calculated considering the water network supply temperature (AENOR, 2005). The monthly energy is divided by the days of the month d_f to obtain the daily DHW energy, and distributed by means of an hourly distribution function f_{DHW} shown in the Figure 2.12 (Ramos, 2012). This procedure assumes that the hourly DHW energy demand is the same for each day of the month.

$$V_{DHW_a} = 365 \cdot N_p \cdot V_{DHW_{ref}} \tag{2.20}$$

$$V_{DHW}(m) = f_{mv} \cdot V_{DHW_a} \tag{2.21}$$

$$Q_{DHW}(m) = 1.161 \cdot V_{DHW}(m) \cdot (60 - T_{red_m}) \tag{2.22}$$

$$Q_{DHW}(d) = \frac{Q_{DHW}(m)}{d_f} \tag{2.23}$$

$$Q_{DHW}(d,h) = f_{DHW}(h) \cdot Q_{DHW}(d) \tag{2.24}$$

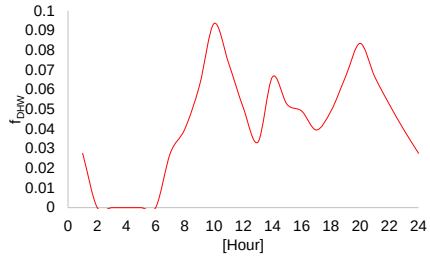

Figure 2.12: Hourly distribution function for DHW (Ramos, 2012).

2.3.3 Unit Electricity demand for appliances

Similar to the DHW energy demand procedure, the estimation of the unit electricity demand for appliances $uEd[kWh/m^2]$, starts from the annual consumption reference $uEd_{ref} = 28.7\ kWh/m^2$ (IDAE, 2011a). This annual consumption is distributed per month by applying a monthly distribution factor f_{me} (Marín Giménez, 2004). In turn, monthly electricity demand is divided by the number of days d_f of each month to obtain the daily electricity demand. Finally, the hourly electricity demand is obtained by applying the hourly distribution factor f_E shown in the Figure 2.13, which in this case, depends on the season (Marín Giménez, 2004).

$$uE_d(m) = f_{me} \cdot uE_{d_{ref}} \tag{2.25}$$

$$uE_d(d) = \frac{uE_d(m)}{d_f} \tag{2.26}$$

$$uE_d(d,h) = f_E(h) \cdot uE_d(d) \tag{2.27}$$

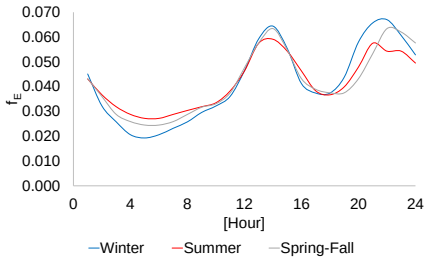

Figure 2.13: Hourly distribution function for electricity demand (Marín Giménez, 2004).

2.3.4 Set of Energy demands for residential buildings

The methodology explained above aims to give the hourly unit function of each energy demand for the residential building. This allows the calculation of the energy demands for the residential building depending on its size. To do this, it has been defined an area of 102.4 m^2 with 3 inhabitants per dwelling (IDAE, 2011d). Therefore, the energy demands are estimated based on the number of dwellings N_{dw} in the residential building to be considered in the study. For this purpose, the total area of the building A_{rb} and the number of inhabitants N_p in the building is calculated as follows:

$$A_{rb} = 102.4 \cdot N_{dw} \tag{2.28}$$

$$N_p = 3 \cdot N_{dw} \tag{2.29}$$

Three energy demands are considered in this work namely, heating Q_d, cooling R_d and electricity for appliances E_d. Heating demand consists of space

heating and domestic hot water DHW (Eq. 2.30), considering a low temperature radiant heating indoor end system, with operation temperatures about of 45 °C, with the possibility to reach temperatures about 60 °C for DHW. In the case of Gran Canaria, heating is equivalent to the DHW demand since there is not space heating demands.

$$Q_d = uSH(d,h) \cdot A_{rb} + Q_{DHW}(d,h) \tag{2.30}$$

$$R_d = uCD(d,h) \cdot A_{rb} \tag{2.31}$$

$$E_d = uE_d(d,h) \cdot A_{rb} \tag{2.32}$$

It is worthy to say that along this work, most of the research consider a residential building made up of 50 dwellings located in Zaragoza. However, there are some cases of study which consider a residential building of 40 dwellings, for instance, the cases of study located in Gran Canaria. Consequently, the Figures 2.14 and 2.15 depicts the different energy demands obtained from the procedure above explained. The Figure 2.14 shows the hourly heating, cooling and electricity demands for a residential building of 50 dwellings in Zaragoza. The peak energy demands for heating is about 274 kWt in December, for cooling is about 293 kWt in July and for electricity is about 30 kWe in different periods along the winter season according to its hourly profile.

The Figure 2.15 shows the hourly heating, cooling and electricity demands for a residential building of 40 dwellings in Gran Canaria. As mentioned before, in this case the heating demand corresponds only to the domestic hot water which peak demand is about 65 kWt in February, the cooling peak demand is about 183 kWt in July and the electricity peak demand is about 24 kWe in different periods along the winter season according to its hourly profile.

2.4 Energy technologies for residential buildings

In this section, a comprehensive revision about the technical, economic and environmental data concerning the equipment used to convert the energy resources to final energy is carried out. Based on the idea of performing preliminary design and/or general analysis of polygeneration systems, a survey about different technologies and branches has been carried out in order to obtain suitable average or representative data. In a general approach, the energy technologies of the equipment can be classified in the prime movers, intermediate energy conversion technologies and energy storage systems. Following this classification, firstly, it

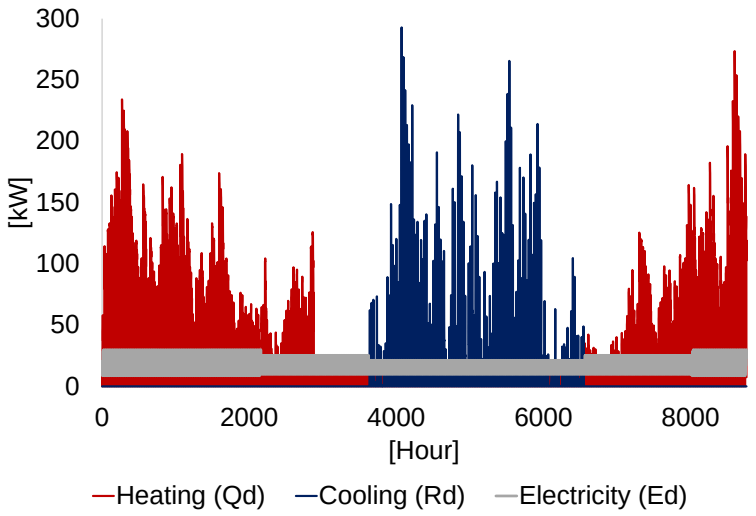

Figure 2.14: Energy demands for a residential building composed of 50 dwellings in Zaragoza.

is presented the technical data of the equipment, except for the renewable energy technologies, which have been explained in the previous section. Secondly, the economic data which encompass acquisition, installation and maintenance costs of the equipment are presented. Finally, the environmental data of the equipment, corresponding to the greenhouse gas emissions, expressed in CO_2-equivalent (CO_2eq) emissions embodied in each component are presented.

2.4.1 Description and technical data

This part defines the main technical data for most of the components of the equipment. A brief description about its function and operation is carried out, followed by the definition of their main technical parameters. The technologies presented herein are the result of a revision of the most suitable technologies utilized in polygeneration systems for residential buildings. The technologies

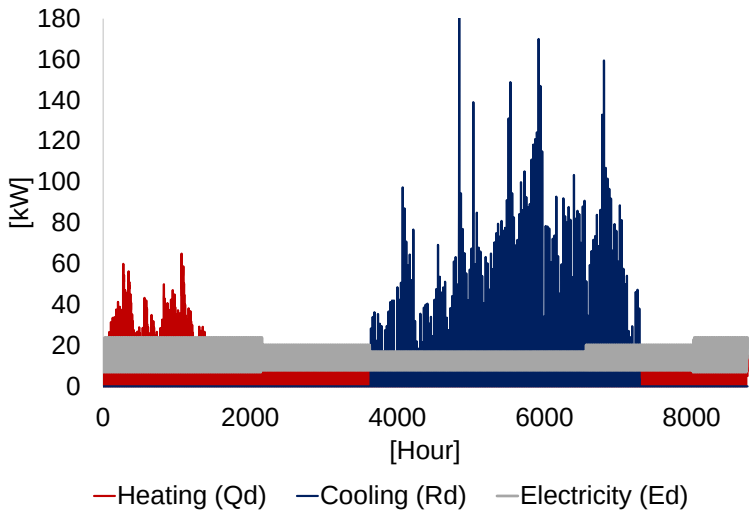

Figure 2.15: Energy demands for a residential building composed of 40 dwellings in Gran Canaria.

have been chosen based on its maturity and availability in the market, taking the most representative data for each technology.

Prime movers

Prime movers transform energy from natural resources into electricity and heat. Taking into account that researching studies aim to energy systems 100% driven by renewable energy (Mathiesen et al., 2015), in this work, renewable energy technologies are considered as feasible prime movers. In this sense, prime movers can be classified in conventional and renewable technologies. Among conventional technologies are the reciprocating internal combustion engines (RICE) and gas boiler (GB). On the other hand, among renewable energy technologies are the PV modules, biomass boilers (BB), wind turbines and ST collectors.

Reciprocating Internal Combustion Engine (RICE): There are several types of prime movers driven by fossil fuels (Al Moussawi et al., 2016, 2017); however, in accordance to the scale of this study (small to medium size residential buildings) and technical data, reciprocating internal combustion engines have been chosen as the most suitable for this study. Some of the advantages of the reciprocating internal combustion engines which make them appropriate for this study are mentioned below (Darrow et al., 2017):

- ✠ High power efficiency with part-load operational flexibility.
- ✠ Fast start-up.
- ✠ Relatively low investment cost.
- ✠ Good load following capability.

The RICE transform chemical energy through the combustion of fossil fuels into mechanical energy. Coupling with an electric generator transforms this mechanical energy into electricity. In the conversion processes, energy is lost as heat (Figure 2.16). When the electricity is the only useful product, the set of engine plus electric generator is called generator (GE). Usually, this is considered as a prime mover in conventional standalone energy systems when unlimited number of hours per year is required (Kaderbhai, 2017)

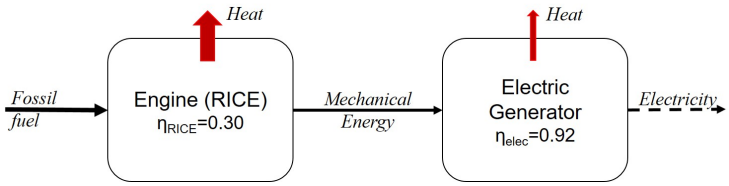

Figure 2.16: Energy conversion system Engine-Electric Generator.

On the other hand, when both heat and electricity are useful products of the set is called cogeneration module (CM). As already explained, cogeneration can be defined as the simultaneous generation in one process of thermal energy and electrical and/or mechanical energy (EU, 2004). Also, it is widely known as combined heat and power CHP (Darrow et al., 2017). Figure 2.17 shows a schematic diagram of the generator and cogeneration module.

Technical parameters such as efficiency and partial load have been considered to define the technical data of RICE for this work. Taking into account average

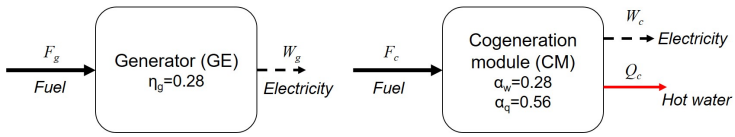

Figure 2.17: Scheme of a generator (Left) and cogeneration module (Right).

Table 2.5: RICE Partial Load operation.

Item	**Load level**	**Operation model (PL)**		
		CM 1	**CM 2**	CM_{set}
1	Maximum load	100%	100%	100%
2	...	100%	75%	88%
3	...	75%	75%	75%
4	...	75%	50%	63%
5	...	50%	50%	50%
6	Minimum Load	50%	0%	25%

values for combined heat and power systems (Darrow et al., 2017), the electric efficiency α_ω for both generator and cogeneration module is considered about 28%, whereas the thermal efficiency for cogeneration module α_q is considered about 56% (Yanmar, 2017). The efficiency can vary as a function of the engine load; nonetheless, it has been considered that it remains constant along its work range, defining a minimum operational partial load (PL). Some CM can modulate up to 50% (CogenGreen, 2014), whereas others can modulate up to 6% with additional electronic devices (Yanmar, 2017). A common practice to maintain constant the efficiency is to install several units which allow to apply load control by shutting down individual engines while keeping the others at nearly-nominal load. Table 2.5 presents an example of a cogeneration modules set modulation. The CM set consists of 2 CMs. Each CM can modulate up to 50%, hence, the CM set can modulate up to 25%. However, taking into account that exist electronic devices which allow to modulate up to about 6%, it could be a suitable approach to consider CM set partial load up 15% for residential buildings applications where up to 2 CMs can be installed. On the other hand, for household applications, PL of about 30% could be considered a good approach.

In terms of minimum capacity, it can be found generators from 1 kWe (Ayerbe, 2018), whereas cogeneration module are available from 5 kWe (Dar-

row et al., 2017). Nonetheless, some CHP technologies have been developed for household applications reaching nominal capacities of about 1 kWe (Honda, 2003; Axiom Energy Group, 2020).

Gas boiler: This component can modulate to produce hot water Q_b at temperature up to about 90 °C as a result of the fossil fuel F_b combustion (Figure 2.18). A constant efficiency η_b of 0.96 is considered in the process (Baxi, 2020).

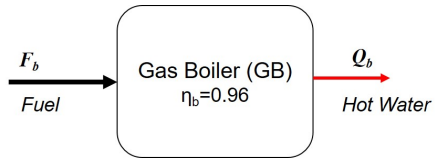

Figure 2.18: Gas boiler scheme.

Biomass boiler: Similar to the gas boiler, hot water Q_{bb} at temperature up to about 90 °C is obtained as a result of the biomass (in this case pellets) F_{bb} combustion (Figure 2.19). A constant efficiency η_b of 0.90 is considered in the process (Baxi, 2020).

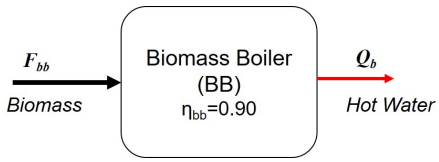

Figure 2.19: Biomass boiler scheme.

Intermediate energy conversion technologies

Intermediate energy conversion technologies convert the energy product provided by prime movers into energy services. Concerning thermal equipment, these can be divided in mechanically and thermally activated technologies. Mechanically activated technologies refers to heat pumps basically. They use electricity to drive the vapour compression technology to provide heat or cooling. On the other hand, thermally activated technologies refers to any technology which use heat as a main source to provide cooling. Mainly, three types of the

thermally activated technologies exist, i.e., absorption chiller, adsorption chiller and desiccant dehumidifier. Nevertheless, only the absorption technologies have been chosen because they are the maturer technology and the most efficient among them (Liu et al., 2014). In some cases, specific intermediate energy conversion technologies are used to adequate the useful energy for subsequent uses. This is the case of the inverter (Inv) or inverter- charger (InvC), which can be seen as auxiliary or complementary components. The first converts the electricity in direct current *dc* to alternating current *ac*, and the second converts the electricity in both directions.

Heat pumps: Heat pumps are vapour compression chiller based on the inverse Rankine cycle driven by electricity. They produce heat or cool driven by electricity (Figure 2.20). A ratio $rcap_{HP}$ between nominal cooling and heating capacities of about 0.9 has been estimated. In conventional applications, when only cool is produced, they are known as mechanical chiller.

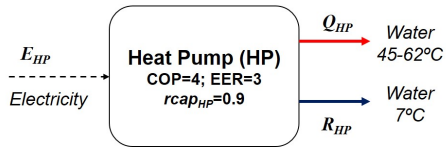

Figure 2.20: Heat pump scheme.

Focused on the development of the high efficiency energy systems, and taking into account the wide commercial availability in terms of size range, water/ground–water technology has been chosen as a reference for this study. Based on different catalogues, both coefficient of performance $COP = 3.0$ for heating production and energy efficiency ratio $EER = 4.0$ for cooling production have been considered constants for this study. The values used herein have been estimated taking into account the manufacturers data and the ambient temperature. The COP is the ratio between heat produced and electricity to produce it, whereas, the second one, EER is the ratio between the cooling produced and the electricity to produce it. The minimum commercial capacity available in the market is about 5 kWt for the residential sector (Daikin, 2019; Enertres, 2017).

Absorption chiller: Among the absorption chiller technologies such as single, double and triple effect technologies, the single-effect absorption chiller tech-

nology has been considered herein because of its maturity and suitability for small scale residential buildings. This component produces chilled water R_{ach} at 7°C driven by hot water Q_{ach} at about 90°C and a small amount of electricity E_{ach}. This last can be negligible in most of the cases (Figure 2.21). According to the technical report of U.S. Department of Energy (2017), the COP is about 0.7 and the minimum commercial capacity is about 17 kWt. In this case, the COP is the ratio between the cooling produced and the heat used to produce it.

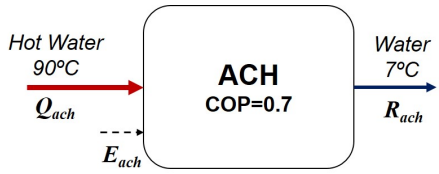

Figure 2.21: Absorption chiller scheme.

Inverter and Inverter-Charger: In the purpose to integrate renewable energy technologies such as PV modules or wind turbine as well as batteries, auxiliary components such as inverters (Inv) and inverter-chargers (Inv-C) must be used. Inverters convert direct current *dc* into alternating current *ac* and Inverter-Chargers can do it in both directions (Figure 2.22). Moreover, they are used to adequate some electrical parameters such as voltage (V) and frequency (Hz) which are required for a suitable performance of the energy system. The capacity of these components is calculated as a function of the power to be managed for them, nonetheless, an oversize factor F_{inv} of about 20% is applied in a conservative way. The efficiency η allows to take into account the energy losses in the conversion process. In this study, the efficiency for the inverter is 0.98 based on the available data of some manufacturers (Fronius, 2016; SMA, 2014), and for the inverter-charger is 0.94 taken the average data of different catalogues (SMA, 2013; Victron, 2017).

The Inverter-charger allows the integration of batteries in the energy systems. Figure 2.23 shows a relation between battery voltage and *ac* power consumption. These relations are used to select a priori the suitable battery voltage to use in the energy system. According to this, for small size systems as household, the battery voltage should be about 24-48 Vdc whereas for medium size systems as residential buildings applications, it should be about 96-192 Vdc

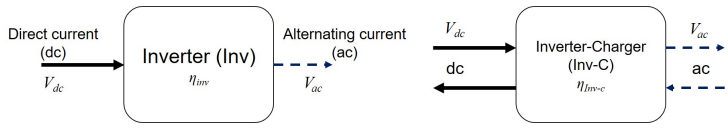

Figure 2.22: Scheme of a) Inverter b)Inverter-charger.

(SMA, 2013).

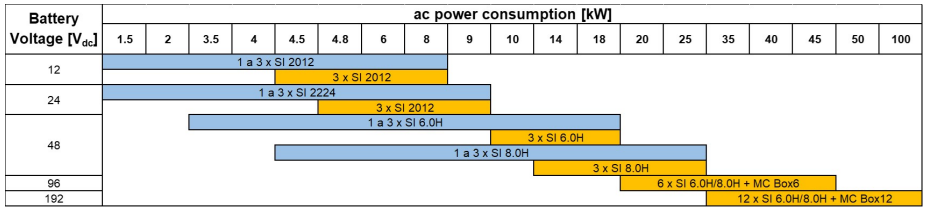

Figure 2.23: Relation between the *dc* battery voltage and *ac* power consumption (Adapted from SMA (2013)).

Energy storage systems (ESS)

Energy storage systems can offer some benefits such as: i) decoupling the energy demand from the energy production, ii) to take advantage of the difference time shift electricity prices in grid connected systems which allow to reduce the operational cost, iii) and to increase the renewable energy consumption since its production can be stored and consumed at other different time when the energy is demanded by the user.

Thermal Energy Storage (TES): In this work, short thermal energy storage are considered as candidate technologies. Stainless steel tanks are used to store thermal energy by using water as a storage medium. Two thermal energy storage are considered, hot water storage tank (TSQ) and cold water storage tank (TSR). In the first case, hot water at about 40-80°C, Q_{in}, can be provided by GB, HP, CM or ST, whereas cold water at about 7°C, R_{in}, can be provided by HP or ACH. There are energy losses per time unit in both tanks due to the heat transfer with the surroundings Q_l and R_l in TSQ and TSR respectively (Figure 2.24).

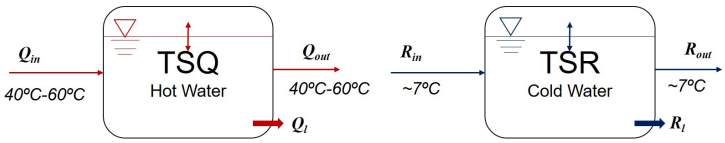

Figure 2.24: Thermal Energy Storage scheme.

A loss thermal factor λ to consider the hourly energy losses is defined in accordance to the expected capacities Cap_{TS}. This is based on the obtained heat transfer results depicted in the Figure 2.25. These results agree with the manufacturer data of Lapesa (2020). Equations 2.33 and 2.34 presents the piecewise functions for the heating and cooling loss thermal factor respectively.

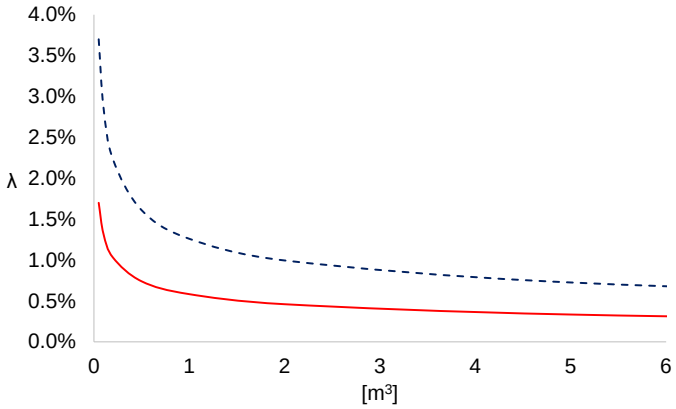

Figure 2.25: Hourly energy loss factor λ for TES . For polyurethane insulation tank with thickness 6 cm. Convection coefficient 10 W/m^2K.

$$\lambda_h = \begin{cases} 2\% & if \quad Cap_{TSQ} \leq 0.3\ m^3 \\ 0.5\% & if \quad 0.3\ m^3 < Cap_{TSQ} \leq 1\ m^3 \\ 0.2\% & if \quad 1\ m^3 < Cap_{TSQ} \end{cases} \tag{2.33}$$

$$\lambda_c = \begin{cases} 3\% & if \quad Cap_{TSR} \leq 0.3\ m^3 \\ 1.5\% & if \quad 0.3\ m^3 < Cap_{TSR} \leq 1\ m^3 \\ 0.5\% & if \quad 1\ m^3 < Cap_{TSR} \end{cases} \tag{2.34}$$

Batteries: Electrical energy storage (Batteries) converts chemical energy into electrical energy by employing chemical reactions (Cho et al., 2015). There are different technologies in development; however, Lead Acid and Lithium-Ion technologies are the most mature and commercially available technologies in the market nowadays, moreover, these are the most suitable technologies bearing in mind the scale of the energy systems of this work (IRENA, 2017).

They charge electricity provided by electric prime movers, Eb_{in}, and discharge electricity Eb_{out}, by means of electrochemical processes. The losses of energy E_l during the charge-discharge process in each time step are calculated through the round trip efficiency η_{rt} (Figure 2.26).

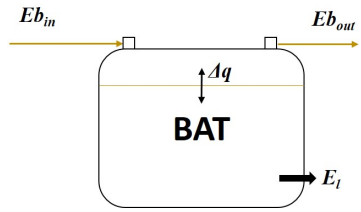

Figure 2.26: Battery scheme.

Different technical parameters must be considered in the optimization model for its proper operation. Maximum deep of discharge DOD is defined for batteries to avoid premature failures. During the batteries lifetime operation, the number of charge-discharge cycles has to be lower than the maximum number of cycles that provoke the failure $N_{c,failure}$, indicated by the manufacturer. This is verified by applying the equivalent full cycle to failure ageing method described by Dufo-López et al. (2014). For both technologies, models of capacity q are applied to calculate their dynamic behaviour in the equipment. Lithium-Ion batteries are modelled according to DiOrio et al. (2015), taking into account both, the maximum charge current $I_{max,c}$ established by manufacturer and the charge ratio α_c in A/Ah given by Homer Energy (2016). On the other hand, Lead-Acid batteries (LA) are modelled by applying the $KiBaM$ model described by Manwell and McGowan (1993), which requires three parameters, calculated

Table 2.6: Technical parameters for Lead Acid and Lithium-Ion batteries (IRENA, 2017). K and c based on lead acid batteries Sunlight (2015).

Technical Parameter	**Lead Acid**	**Lithium-Ion**
Round trip efficiency η_{rt}	82%	95%
Number of cycles failure $N_{c,failure}$	1500 cycles	2000 cycles
Deep of discharge DOD	50%	90%
Self-discharge	0.0104 %/hour	0.0042 %/hour
K	0.11 h^{-1}	-
c	0.53	-

on the basis of manufacturers' data catalogues: K, the rate constant; c, the fraction of the capacity that may hold available charge; and the maximum capacity of the battery q_{max}, as a function of K and c. The capacity models for both technologies are explained in detail in the Appendix A. Table 2.6 presents the technical data used for the both types of batteries.

2.4.2 Economic data

The total investment cost TIC for the project includes equipment investment, installation and maintenance costs, possible repositions, etc. This is divided in annuities CIA, which are calculated by applying the capital recovery factor CRF based on an annual interest rate i along the lifetime of the project n. Mathematically is expressed as:

$$CIA = CRF \cdot TIC \tag{2.35}$$

$$TIC = (1 + F_{ind}) \cdot \sum_{j \in J} Cu_j \cdot Cap_j \cdot (1 + FNPV_j) \cdot (1 + Fm_j) \cdot (1 + VAT) \tag{2.36}$$

$$CRF = \frac{i \cdot (1+i)^n}{(1+i)^n - 1} \tag{2.37}$$

$$FNPV_j = \sum_{r=0}^{n_{repo_j}} \frac{y_{repo}}{(1+i)^{r \cdot n_j}}; y_{repo} = \begin{cases} 0 & if \quad r = 0 \\ 1 & if \quad r > 1 \end{cases} \tag{2.38}$$

$$n_{repo_j} = \begin{cases} 0 & if \quad n = n_j \\ [\frac{n}{n_j}] & if \quad n > n_j \end{cases} \tag{2.39}$$

Where,

F_{ind}: Factor to consider indirect costs of the project (e.g. engineering cost). This value is estimated in 0.2 (Guadalfajara, 2016).
CRF: Capital Recovery Factor, at interest rate $i = 5\%$ and at lifetime project $n = 20$ years. Based on these data $CRF = 0.082\ yr^{-1}$.
Cu: Unit acquisition cost (Unit price) of the component j. example: $Cu_{HP} = 400\ €/kWt$.
Cap: It refers to the capacity of the component, example: A cogeneration module of 10 kWe, so $Cap = 10\ kWe$.
$FNPV$: Net Present Value Factor to consider the possible repositions of the components during the lifetime of the project n. The number of repositions n_{repo} is the integer value of the ratio between the lifetime project n and the estimated lifetime of each component n_j when $n > n_j$.
Fm: Factor to consider installation and maintenance costs.
VAT: Value-added tax. In Spain, this is 0.21 in the peninsula and 0.03 in Gran Canaria.

The values of the Cu and Fm have been collected based on the revision of different catalogues, technical reports and benchmarking. The maintenance costs for most of the equipment such as PV panels, wind turbines, etc, are only about 1% of the total installation cost of the component according to NREL (2016) , therefore, in these cases, the Fm corresponds mainly to the installation costs.

Prime movers

Reciprocating Internal Combustion Engine (RICE): The unit cost of the cogeneration module depends on its capacity. According to the report for the Federal Ministry for Economic Affairs and Energy of Germany (Wünsch et al., 2014), the unit cost can vary from 15000 to 2750 €/kWe, for capacities from 1 to 50 kWe. On the other hand, according to the report for the U.S. Environmental Protection Agency (Darrow et al., 2017), the unit cost for cogeneration modules is in between 1500-2900 US$/kWe for capacities from 5kWe to 10 MWe. These values correspond to the total unit installation costs.
In the case of the generators, the Figure 2.27 presents the unit cost as a function of its nominal capacity for two branches (Ayerbe, 2018). These values do not include installations costs.

Based on the previous reports, the Table 2.7 presents the values taken in this research work for Cu and Fm for the cogeneration module and generator. For both technologies, the lifetime considered is 10 years. This means that one reposition is expected to be carried out during the project lifetime.

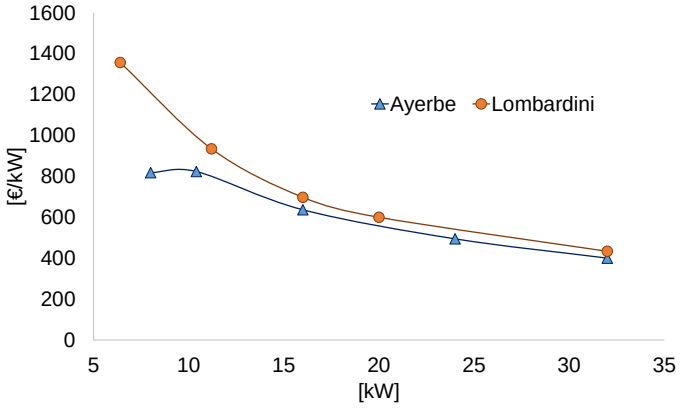

Figure 2.27: Unit price vs Capacity for GE (Adapted from (Ayerbe, 2018)).

Table 2.7: Unit price and installation costs for CM and GE considered in this research work.

Technology	**Cu [€/kWe]**	**Fm [Adim]**
Cogeneration module	1150	0.7
Generator	600	0.2

Boilers: The Figure 2.28 presents the unit cost of the gas boiler(GB) with respect its nominal capacity. The unit cost of this component is about 50-100 €/kWt (Baxi, 2020), therefore a Cu of 80 €/kWt is a suitable approach. Additional components such as expansion tank, heating circuit, among others parts, must be considered in the installation costs. A Fm value of about 0.5 is considered for this component and the lifetime 20 years, so it is not expected any reposition during the project lifetime. For the biomass boiler (BB), the unit cost of this component is about 240 €/kWt (Baxi, 2020) and it is assumed that the installation and maintenance costs as well as the lifetime are the same as the gas boiler.

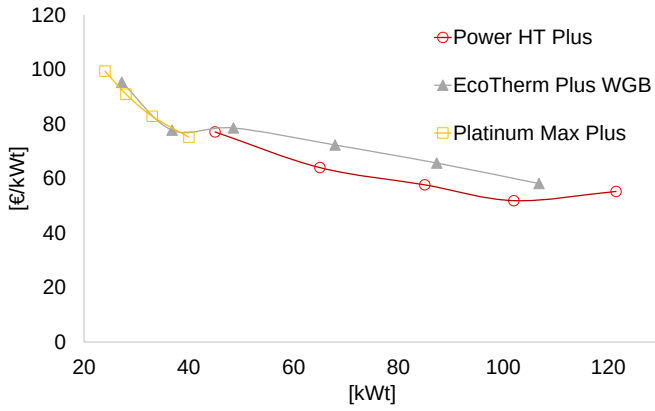

Figure 2.28: Unit price vs Capacity for GB (Baxi, 2020).

Table 2.8: PV Installed unit cost per sector considered in this research work (Fu et al., 2017).

Sector	**Capacity**	$US\$/kW_{dc}$
Residential	3-10 kW	2800
Commercial	10 kW - 1 MW	1850
Utility	$>$ 2 MW	1030

PV panels: Economic data for PV technology are based on the U.S. solar photovoltaic system cost benchmarking (Fu et al., 2017). This report classifies the economic data according to the application sector or capacity. For instance, residential systems have a capacity about 3-10 kW, commercial systems about 10 kW-2 MW and utility scale systems $>$ 2MW. Table 2.8 presents the installed unit cost of this technology according to its installed capacity.

Based on these data and taking into account the price of PV panels (Atersa, 2019), the estimated values for Fm are about 1.8 and 0.9 for residential and commercial systems respectively. Regarding the lifetime of this component, the expected lifetime for the PV system is above 20 years (Fu et al., 2017).

Table 2.9: Wind turbine installed unit cost per sector considered in this research work (Orrell and Poehlman, 2017).

Sector	**Capacity**	$US\$/kW$
Residential	$<$ 21 kW	11953
Commercial	10 kW - 1 MW	7389

Wind Turbines: The economic data for the wind turbine systems were based on the benchmarking report of the Pacific Northwest National Laboratory (Orrell and Poehlman, 2017). Similar to the PV panels, this report classifies the economic data according to the application scale (Table 2.9).

Based on these data and taking into account different branches (Aeolos, 2006; Bornay, 2017; Enair, 2019), the unit cost for wind turbines considered in this work is about 2300 €/kW and the Fm values are 2 and 0.9 for residential and commercial systems. The expected lifetime for the wind turbines is about 20 years.

Solar thermal Collectors: The economic data for the solar thermal collectors were taken from the Plan de energías renovables (IDAE, 2011b) and the report about flat plate solar thermal collectors (Rockenbaugh et al., 2016). Based on those reports and taking into account the price of some collectors (Salvador Escoda S.A, 2017a), the unit cost of solar collectors is about 257 €/m^2 with a Fm of 1.5 which include among others pumping system, regulation system and structure.

Intermediate energy conversion technologies

Heat Pumps: The Figure 2.29 presents the unit cost of different models of heat pumps water-water (Terra) and water-air (EW) as a function of their capacity (Daikin, 2019; Enertres, 2017). Based on these data, the unit cost for capacities above 60 kWt is estimated about 400 €/kWt, and the Fm is estimated in 0.5. The lifetime of the component is 20 years.

Absorption Chiller: Economic data are based on the report of U.S. Department of Energy (2017). According to it, the unit cost for single stage absorption chillers with capacity below 175 kWt is about 485 €/kWt and the Fm value concerning the installation costs is about 1.5.

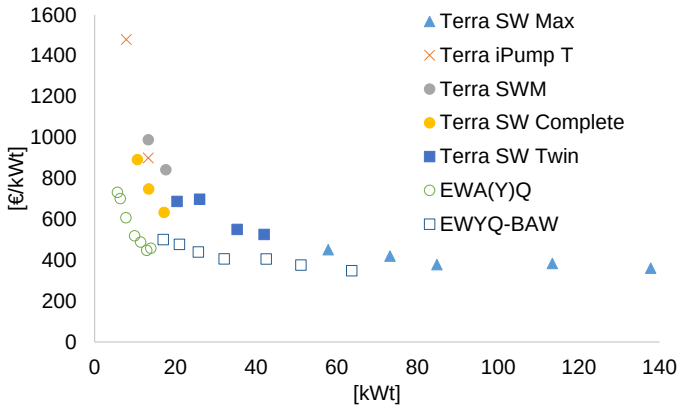

Figure 2.29: Unit price vs Capacity for HP (Daikin, 2019; Enertres, 2017).

Inverter and Inverter-Charger: Economic data for these components are estimated based on commercial catalogues (Rainbow Power Company, 2019; Victron Energy, 2019). Based on these data, the unit cost is estimated in about 400 €/kW for inverters, and 774 €/kW for inverter-chargers. Regarding installation costs, for the inverter, these are included in the PV systems, and for the inverter-chargers Fm is estimated in about 0.25 (Ardani et al., 2016). The lifetime for both inverter and inverter-chargers is 15 years.

Energy Storage Systems (EES)

Thermal Energy Storage: The economic data for the thermal energy storage are estimated based on the manufacturer catalogues (Baxi, 2020; Enertres, 2017). The unit cost for thermal energy storage for heating and cooling is about 212 and 257 €/kWht respectively. The installation cost is estimated in about Fm=0.1, and the lifetime of the tanks is 15 years.

Batteries: The economic data for the Lead Acid and Lithium-Ion batteries were taken from the International Renewable Energy Agency report (IRENA, 2017). According to this, the unit cost for Lead Acid and Lithium-Ion batteries

Table 2.10: Summary of the main economic data for the different technologies for residential buildings applications.

Component	Cu [€/*]	Fm	n_r [Years]	Reference
GE	600 €/kWe	0.7	10	(Ayerbe, 2018)
CM	1150 €/kWe			(Darrow et al., 2017)
PV	113.4 €/m^2	0.9	20	(Fu et al., 2017)
WT	2330 €/kW	0.9	20	(Orrell and Poehlman, 2017)
ST	257 €/m^2	1.5	20	(IDAE, 2011b; Salvador Escoda S.A, 2017a)
BB	240 €/kWt	0.5	20	(Baxi, 2020)
GB	80 €/kWt			
HP	400 €/kWt	0.5	20	(Daikin, 2019; Enertres, 2017)
ACH	485 €/kWt	1.5	20	(U.S. Department of Energy, 2017)
TSQ	212 €/kWht	0.1	15	(Baxi, 2020; Enertres, 2017)
TSR	257 €/kWht			
BAT: Lithium-Ion	370 €/kWh	0.25	12	(IRENA, 2017)
BAT: Lead Acid	129 €/kWh	0.25	7	
Inv	400 €/kW	0	15	(Rainbow Power Company, 2019; Victron Energy, 2019)
InvC	774 €/kW	0.25	15	

is about 129 and 370 €/kWh respectively, and the lifetime is 9 years for Lead Acid batteries and 12 years for Lithium-Ion batteries. Regarding the installation costs Fm, it has been estimated in about 0.25 (Ardani et al., 2016).

The Table 2.10 summarizes the main economic data for the different technologies for residential buildings applications.

2.4.3 Environmental data

The CO_2eq emissions embodied in the equipment are taken into account based on the Life Cycle Assessment (LCA) carried out over each technology, which is a very recognized analysis for reporting potential environmental loads and resources consumed in each step of a product along the life cycle (from the extraction of natural resources to the decommissioning) (Caro, 2019). The literature data about LCA is used to estimate the unit CO_2eq emissions embodied in each component CO_2U. The CO_2eq emissions embodied in the equipment are divided per the number of the project lifetime in order to assess its annual environmental impact. The LCA studies are based on the ISO 14040 methodology (International Organization for Standardization, 2006), which describes the following steps:

1. *Goal and scope definition*: Definition of the research objective; the scope; the system boundaries used for the analysis: "Cradle to grave" (from the extraction of raw materials from the earth to the disposal at the end),

"Cradle to gate" (from the extraction of raw materials from the earth to the factory gate), etc; the functional unit, etc.

2. *Life-cycle inventory (LCI)*: Quantifies the flows of materials, energy and emissions in each stage of the life cycle.

3. *Life-cycle impact assessment (LCIA)*: This step aims to evaluate the environmental impact of the quantities obtained in the LCI analysis. This process associates the inventory data to different categories such as depletion of nonrenewable primary energy resources, global warming, potential toxicity, etc.

4. *Interpretation*: This step is extremely important since different conclusions and recommendations must be obtained as a result of the process LCA for the decision-makers.

For this work, only CO_2eq emissions associated to the global warming impact have been considered. This collection data is only an approach to consider the environmental impact of the components. We have to be aware that the LCA depends strongly on the electricity grid mix technologies in the location considered, and the period in which was carried out the analysis. Therefore, for a specific project, the data must be verified and updated.

PV technology: Different studies have been considered to estimate the CO_2eq emissions embodied in the PV panels (Frischknecht et al., 2015; Fthenakis and Raugei, 2017). Most of them include both PV panels and inverters. Besides, in some cases the CO_2eq emissions are presented as a function of the PV production. Therefore, some approaches have been considered to estimate the CO_2eq emissions embodied for the PV panels per m^2. The average data obtained for the CO_2eq emissions embodied is about 161 $kgCO_2eq/m^2$ for PV panels and 191 $kgCO_2eq/kW$ for the inverters. In the case of inverter-chargers, the same value of the inverters is taken because of their physical similarity.

WT Technology: The CO_2eq emissions embodied in the wind turbine systems have been estimated based on the study of two wind turbines of different capacities, 4.5 MW and 250 W (Tremeac and Meunier, 2009). This study does not consider only the turbine but the tower, foundation and all the components to be taken into account for the wind turbine installation. Similar to PV technology, in some cases the information is given as a function of the WT production. Therefore, some approaches have been carried out to estimate the

CO_2eq emissions embodied per kW of installed capacity. The average data obtained for the wind turbine system is about 720 $kgCO_2eq/kW$. The obtained results have been compared with other studies to check that they are reasonable data (Bonou et al., 2016; Fleck and Huot, 2009).

Thermal energy storage: The CO_2eq emissions per stored energy for the thermal energy storage are calculated as the ratio between the amount of CO_2eq emissions emitted in the stainless steel production process according to (ISSF, 2015; Renzulli et al., 2016), and the energy stored in the tanks. The inlet/outlet temperature difference for the tank for heating is about 10 °C and 5 °C for the tank for cooling and it is assumed a thickness of 5 mm for the tanks. Based on these data, the CO_2eq emissions embodied for heating and cooling energy storage are estimated in about 31 and 62 $kgCO_2eq/kWht$ respectively. These results are in accordance to the data of Beccali et al. (2016).

Batteries: The CO_2eq emissions embodied for the Lithium-Ion batteries have been estimated based on the review about the environmental impact of Li-Ion batteries (Peters et al., 2017). The average data for LFP (Lithium Ion Phosphate) and NMC (Nickel Manganese Cobalt oxide) technologies, which are the most used for stationary application, is about 160 $kgCO_2eq/kWh$. In the case of the lead acid batteries, the CO_2eq emissions have been estimated taking the average data of the studies about the comparative life cycle assessment of battery storage systems for stationary applications (Hiremath et al., 2015) and the environmental consequences of the use of batteries in low carbon systems (McManus, 2012). Based on these studies, the estimated value of CO_2eq emissions embodied for Lead Acid batteries is about 60 $kgCO_2eq/kWh$.

The CO_2U for components such as solar thermal collectors, cogeneration module, gas boiler, heat pumps, and absorption chillers has been taken directly from previous studies. Table 2.11 summarizes the CO_2eq emissions embodied data used in this work for each component.

2.5 Fossil fuels, biomass and electric grid data for residential buildings

In this section, the technical, economic and environmental data about the electric grid and different fuels used in the energy systems are presented.

Table 2.11: Summary of CO_2eq emissions embodied in the equipment.

Component	$CO_2U[kgCO_2eq/*]$	**References**
CM/GE	65 $kgCO_2eq/kWe$	(Carvalho, 2011)
PV	161$kgCO_2eq/m^2$	(Frischknecht et al., 2015; Fthenakis and Raugei, 2017)
WT	720 $kgCO_2eq/kW$	(Bonou et al., 2016; Fleck and Huot, 2009)
ST	95 $kgCO_2eq/m^2$	(Guadalfajara, 2016)
BB/GB	10 $kgCO_2eq/kWt$	(Carvalho, 2011)
HP	160 $kgCO_2eq/kWt$	
ACH	165 $kgCO_2eq/kWt$	
TSQ	31 $kgCO_2eq/kWht$	(ISSF, 2015; Renzulli et al., 2016; Beccali et al., 2016)
TSR	62 $kgCO_2eq/kWht$	
BAT: Lithium-Ion	160 $kgCO_2eq/kWh$	(Peters et al., 2017)
BAT: Lead Acid	60 $kgCO_2eq/kWh$	(Hiremath et al., 2015; McManus, 2012)
Inv	191 $kgCO_2eq/kW$	(Frischknecht et al., 2015; Fthenakis and Raugei, 2017)
InvC		

Table 2.12: Normalized power from the electric grid (Ministerio de Industria turismo y comercio, 2006; Endesa, 2014).

Type of electric system	Tariff	Available normalized power from the electric grid Pct_{nom} [kW]								
Single phase 230 V	2.0	1.15	1.725	2.3	3.45	4.6	5.75	6.9	8.05	9.2
Three phases 3x230/400V	2.1	10.392	13.856	-	-	-	-	-	-	-
	3.0	17.321	20.785	24.249	27.713	31.177	34.641	43.648	55	..

2.5.1 Electricity tariffs

The electric grid is a complex infrastructure which provides electricity to the users. According to the scale and scope of this work, the technical standard for the energy systems is in the low voltage level range 230 V/400 V. Available normalized contracted power Pct can be selected according to the requirements of the polygeneration system (See Table 2.12).

The economic evaluation of the grid connected systems requires the hourly electricity prices from the electric grid. The most common practice is to sign up a contract from the electricity supplier company. Tables 2.13 and 2.14 present the electricity tariffs according to the type of contract and location. The electricity bill is calculated taking into account a fixed term $cPct$ proportional to the contracted power, and the variable term proportional to the hourly electricity consumption and price cp. Besides, electricity tax $Tax_e = 0.0513$ (5.13%) and the electricity meter equipment rental cost C_{alq_e} of 16.32 €/yr (IDAE, 2016) should be considered and the VAT must be applied.

In some cases, there is also the option to purchase and/or sell electricity at

Table 2.13: Electricity tariffs in Spain (Peninsula)(Endesa, 2019, 2018).

Time-of-use tariff	Contracted power [kW]	Time period	Winter (h)	Summer (h)	cPct [€/kW yr]	cp[€/kWh]
Tariff 2.0 DHS	Pct<10	P1	14-23	14-23	47.816	0.173941
		P2	1;8-13;24	1 h;8-13;24		0.099554
		P3	2-7	2-7		0.076838
Tariff 2.1 DHS	10<Pct<15	P1	14-23	14-23	50.187	0.187157
		P2	1;8-13;24	1;8-13;24		0.11527
		P3	2-7	2-7		0.082849
Tariff 3.0 A	15<Pct<30	P1	19-22	12-15	41.951	0.192699
		P2	9-18;23-24	9-11;16-24	25.17	0.172904
		P3	1-8	1-8	16.78	0.129289
	30<Pct<50	P1	19-22	12-15	41.951	0.188567
		P2	9-18;23-24	9-11;16-24	25.17	0.168758
		P3	1-8	1-8	16.78	0.125166
	50<Pct<100	P1	19-22	12-15	41.951	0.185322
		P2	9-18;23-24	9-11;16-24	25.17	0.165525
		P3	1-8	1-8	16.78	0.121922
	100<Pct<250	P1	19-22	12-15	41.951	0.183892
		P2	9-18;23-24	9-11;16-24	25.17	0.164085
		P3	1-8	1-8	16.78	0.120491

Table 2.14: Electricity tariffs in Gran Canaria (Aura Energía, 2019).

Time-of-use tariff	Contracted power [kW]	Time period	Winter (h)	Summer (h)	cPct [€/kW yr]	cp[€/kWh]
Tariff 2.1 DHA	10<Pct<15	P1	12-21	13-22	44.44	0.190047
		P2	1-11;22-24	1-12;23-24		0.109184
Tariff 3.0 DHS	Pct>15	P1	18-21	11-14	40.72889	0.144944
		P2	8-17;22-23	8-10;15-23	24.43748	0.125146
		P3	1-7;24	1-7;24	16.29141	0.092048

spot price. Figure 2.30 shows the hourly electricity prices obtained from the Red Eléctrica de España for the year 2018 (REE, 2019c).

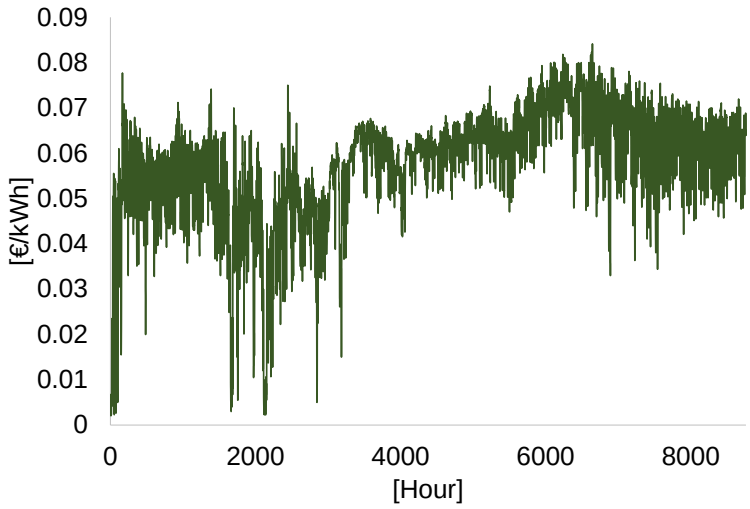

Figure 2.30: Spot electricity prices for Spain 2018 (REE, 2019c).

2.5.2 Natural gas, gasoil and biomass tariffs

For grid connected systems, the components which work due to the fuel combustion usually use natural gas. On the other hand, for standalone systems located in remote areas, the fuel utilized is usually gasoil A for the cogeneration module and generator and gasoil for heating for the gas boiler. However, since there is not natural gas network in Gran Canaria, gasoil instead of natural gas is used in this location for both systems.

The bill cost of the natural gas encompasses a fixed and a variable term. The fixed term depends on the annual gas consumption level C_{fg}. For instance,for a household the expected annual consumption could be below 5000 kWh/yr, therefore the user must pay 61.8 €/yr regardless the consumption, but can not

Table 2.15: Natural gas (Endesa, 2018), gasoil and pellets (IDAE, 2019a) tariffs.

Fuel	Tariff	C_{fg} [€/yr]	cp_g[€/kWh]	Annual consumption limit [kWh/yr]
Natural gas	3.1	61.8	0.063125	≤ 5000
	3.2	112.2	0.05845	5000−50000
	3.3	650.64	0.050523	50000−100000
	3.4	971.64	0.046843	>100000
Gasoil A (IDAE, 2018)	N/A	N/A	0.1174	N/A
Gasoil for heating (IDAE, 2018)			0.0678	
Pellets (IDAE, 2019a)			0.04	

consume more than 5000 kWh/yr of natural gas (See Table 2.15). On the other hand, the variable term is proportional to the amount of gas consumption at retail price cp_g (Endesa, 2018). Besides, the gas meter equipment rental cost C_{alq_g} of 7.2 €/yr (IDAE, 2016) should be considered and the VAT must be applied.

For the biomass boilers, pellets are used as a fuel. The prices for the different fuels have been taken from the Instituto para la Diversificación y ahorro de la Energía (IDAE) and the taxes are included (Table 2.15).

According to the IDAE, the biomass prices have remained stable for the last 3 years (IDAE, 2019a). Therefore, the price of 0.04 €/kWh was considered as a good approach.

2.5.3 CO_2eq emissions

The environmental evaluation of grid connected systems requires to take into account the CO_2eq emissions from the grid. The hourly CO_2eq emissions from the electric grid are available in the Red Electrica Española web (REE, 2019a). The Figure 2.31 depicts the hourly CO_2eq emissions corresponding to the year 2018 from the grid for Zaragoza (Peninsula) and Gran Canaria. There is a remarkable difference between them due to the prime movers used in the utilities of each location. The installed capacity of the renewable energy technology in the Peninsula and Gran Canaria in 2018 was about 48.5% and 19.7% and their shares in the total annual generation was about 40.1% and 10.5% respectively (REE, 2019b). Because of this, CO_2eq emissions values are higher and more stable along the year in Gran Canaria than in Zaragoza.

On the other hand, for the components which work by the fuel combustion, such as combustion engines or gas boilers, both grid connected and standalone systems require the evaluation of the CO_2eq emissions which are proportional to the fuel combustion. The CO_2eq emissions factor for the natural gas is

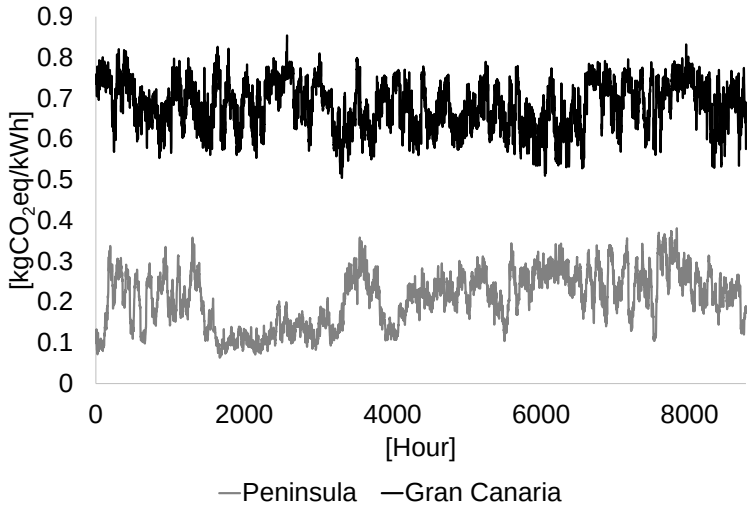

Figure 2.31: CO_2eq emissions of 2018 from the electric grid for Peninsula (Gray) and Gran Canaria (Black) (REE, 2019a).

about 0.203-0.2044 $kgCO_2eq/kWh$ (Miteco, 2020; footprint, 2016) and 0.294 $kgCO_2eq/kWh$ for gasoil (footprint, 2016). In the case of biomass, the CO_2eq emissions factor for the pellets is about 0.063 $kgCO_2eq/kWh$ (Giuntoli et al., 2017).

2.6 Closure

In this chapter have been presented the technical, economical and environmental data required and used for the optimization of the polygeneration systems for small-scale residential buildings studied in this Ph.D Thesis. Specifically, the data that have been collected and/or obtained are: i) climatic data for each considered location; ii) renewable energy resources available in each analysed location; iii) energy demands for the residential buildings (electricity, heating and cooling); iv) technical data based on commercial equipment of the candidate technologies that can supply energy to residential buildings; v) economic and environmental data of the candidate technologies and vi) economic and environmental data of considered fuels and electric grid.

The procedures to calculate both renewable energy production and energy demands for small-medium scale residential buildings located in Zaragoza and Gran Canaria have been presented in this chapter. The renewable energy production was calculated based on available technical data of commercial equipment in the market. The energy demands were calculated based on the *degree days method* taking into account the annual consumption data for residential buildings obtained from the Spanish technical reports. In Zaragoza, the heating demand comprises space heating and domestic hot water demands. There is space heating demand from January to April and from October to December, whereas there is demand of domestic hot water demand all year. Regarding cooling and electricity demands, the former goes from June to September whereas there is electricity demand for appliances and lightning all year. In the case of Gran Canaria, the heating demand corresponds only to the domestic hot water demand along the year. As regards cooling and electricity demands, the former goes from June to October whereas there is electricity demand for appliances and lightning all year.

On the other hand, a comprehensive revision of the updated technical, economic and environmental data of the equipment for the energy supply system for small-medium scale residential buildings was carried out. The data were collected from several catalogues, technical reports and benchmarkings. Likewise, technical, economic and environmental data from the electric grid, natural gas network and different fuels were also collected.

In environmental terms, it is noteworthy the difference between the CO_2eq emissions from the electric grid between Zaragoza and Gran Canaria. In average annual values, the the CO_2eq emissions in Gran Canaria is about three times the CO_2eq emissions in Zaragoza due to the higher share of installed capacity of renewable energy technology in the Peninsula (Zaragoza).

It is worthy to say that renewable energy production, energy demands for residential buildings, and economic and environmental data (CO_2eq emissions) from the electric grid were collected for a year in hourly resolution which enable the data processing, and hence, enhance the results of the optimization of the energy systems for residential buildings.

Chapter 3

Data processing: Methods for the selection of representative days

"Just follow your instincts, even when going against the tide."

The optimal design of polygeneration systems for buildings is a challenging task, due to the wide variety of energy resources, available technologies, and significant diurnal and seasonal fluctuations in energy demands and tariffs (Tapia-Ahumada et al., 2013). The incorporation of renewable energy technologies such as wind turbines, photovoltaic panels, and solar thermal collectors can further increase the complexity of the system design because of their intermittent behaviour due to the non-manageable nature of the availability of the energy resource. Mixed Integer Linear Programming (MILP) is widely utilized for the design of polygeneration systems (Pina et al., 2020; Rong and Su, 2017; Carvalho et al., 2012). Ideally, the optimization of an energy system should consider hourly or sub-hourly periods throughout one or more years. Nonetheless, the solution of MILP problems can easily become intractable as the computational effort increases with the size of the problem, and more specifically with the number of binary variables, which are widely used in synthesis problems and to model the performance of components. The size of the problem is proportional to the number of time series (e.g. number of energy demands or

renewable energy production considered, among others), and consequently the system complexity increases as more time series are included.

A viable approach to reduce the complexity of the optimization problem is to reduce the number of time periods by employing typical or representative days, which enables the reasonable reproduction of the behavior of the system throughout long time periods such as months, or one or several years, reducing the computational effort significantly. There are several methodologies for the selection of representative days, such as graphical methods (Ortiga et al., 2011), statistical methods (Chen, 2013), aggregation methods (Schütz et al., 2018; Kotzur et al., 2018), and the OPT method (Poncelet et al., 2017). Aggregation methods such as the Averaging, k-Means, k-Medoids, and hierarchical clustering, could be considered the most common alternatives for the design of energy systems (Schütz et al., 2018). For instance, an aggregation method has been utilized along with a first-order Markov model, to generate synthetic daily horizontal irradiation to design photovoltaic systems (Muselli et al., 2000, 2001). Within the aggregation methods, k-Medoids is considered as the most reliable (Schütz et al., 2018; Kotzur et al., 2018). However, the variability of the original time series is smoothed when aggregation methods are employed to obtain representative days (Kotzur et al., 2018). Despite not being an exact method, the OPT method has also been applied to select representative days for a system that encompasses time series with high variability such as electricity demand, photovoltaic and wind energy production (Poncelet et al., 2017). Aggregations methods have been previously compared (Schütz et al., 2018; Kotzur et al., 2018), but non-exact methods, such as the OPT, have not been included to date in the comparison of methods for the selection of representative days.

The aim of this chapter is to show the advantages and disadvantages of some methodologies for the selection of representative days and select the most suitable for each optimization problem. Besides, as a result of the analysis of different methods, a new method is proposed which comprises the advantages of the analysed methods. The chapter starts from the description of some methodologies for the selection of representative days such as the Averaging, k-Medoids (Domínguez-Muñoz et al., 2011) and OPT (Poncelet et al., 2017) methods. Then, a new methodology called kM-OPT (Pinto et al., 2020) based on the k-medoids and OPT methods is proposed as an alternative to overcome some of the disadvantages of the before mentioned methodologies. Next, the discussion and analysis of the methods for the selection of representative days explained herein is carried out. Finally, conclusions based on the discussion and analysis are presented as closure. The time series are referred to as attributes herein. Values for each attribute c corresponding to a time period t (1-8760

hours) or a day d (1-365 days) and hour h (1-24 hours) can be represented as $x_(c,t)'$ or $x_(c,d,h)'$.

3.1 Averaging method

This method has been employed previously in several works (Schütz et al., 2018), usually by averaging hourly data for each month. The model can be described as:

$$\bar{x}_{c,m,h} = \frac{\sum_{d=d_0}^{d_f} x'_{c,d,h}}{d_m} \tag{3.1}$$

where:
$\bar{x}_{c,m,h}$: average value of the attribute c for each month m at each hour h.
$x'_{c,d,h}$: value of the element in the time series x' corresponding to the attribute c in day d and hour h for each month m.
d_0: starting day of month m.
d_f: final day of month m.
d_m: number of days in each month m, hence, it is the weight of the respective representative day.

An advantage of this method is that the typical days obtained have a clear order. Nonetheless, the aggregation is based on the original sequence of the days and not on the similarity between days (Kotzur et al., 2018).

3.2 *k*-Medoids method

This method aims to group the days of the year into clusters so that the cluster members are as similar as possible. The cluster is then represented by a single day, which is the medoid in this case. Figure 3.1 shows the graphic representation of this method.

When different attributes with different scales are taken into account, the input time series must be normalized, so it is evaluated on the same scale (Kotzur et al., 2018).

$$x_{c,t} = \frac{x'_{c,t} - min\{x'_c\}}{max\{x'_c\} - min\{x'_c\}} \tag{3.2}$$

The k-Medoids method for the selection of representative days is based on the optimal plant location problem. In the location problem, k plants must be

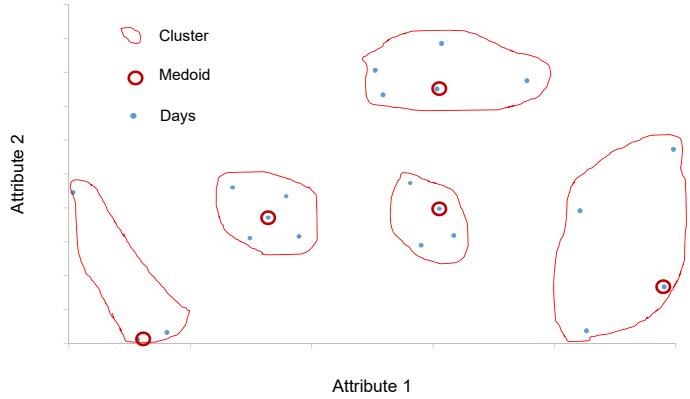

Figure 3.1: Graphic representation of the k-Medoids method.

located in n cities in such a way as to minimize the total distance from the plants to the n cities they supply. In the k-Medoids method, the location of a plant is interpreted as the selection of a medoid, and the distance between each city and the nearest plant is interpreted as the dissimilarity dis between an object and the representative object of the cluster to which it belongs (Domínguez-Muñoz et al., 2011). Therefore, the first step is to define the matrix ψ that contains all the attributes, in which the number of columns is defined by the product of the number of time steps N_h (usually 24 hours for each attribute) and number of attributes N_c, and the number of rows corresponds to the number of periods N_i $i \in I$, where I is the set of periods considered (usually $N_i = 365$ days).

$$\psi = \begin{bmatrix} x_{1,1,1} & \cdots & x_{1,N_h,1} & \cdots & x_{N_c,N_h,1} \\ \vdots & \ddots & \vdots & \ddots & \vdots \\ x_{1,1,N_i} & \cdots & x_{1,N_h,N_i} & \cdots & x_{N_c,N_h,N_i} \end{bmatrix} \tag{3.3}$$

The second step is to define the dissimilarity matrix D, which is composed of the distance (dissimilarity) between two elements p and q of the matrix ψ, and every element is calculated by the Euclidean distance:

$$dis(p,q) = \sqrt{\left(\sum_{h=1}^{N_h} |\psi_{p,h} - \psi_{q,h}|^2\right)} \tag{3.4}$$

$$D = \begin{bmatrix} 0 & dis(1,2) & ... & ..... & dis(1,N_i) \\ dis(2,1) & 0 & & & \vdots \\ \vdots & & \ddots & & \vdots \\ \vdots & & & 0 & \vdots \\ sim & ... & ... & ..... & 0 \end{bmatrix} \tag{3.5}$$

The MILP model for the k-Medoids method is:

$$Minimize \sum_{i=1}^{N_i} \sum_{j=1}^{N_i} dis(i,j) \cdot z_{i,j} \tag{3.6}$$

Subject to:

$$\sum_{i=1}^{N_i} z_{i,j} = 1, \forall j \in 1,2,..,N_i \tag{3.7}$$

$$z_{i,j} \leq u_i, \forall i \in 1,2,..,N_i \tag{3.8}$$

$$\sum_{i=0}^{N_i} u_i = N_k \tag{3.9}$$

$$u_i, z_{i,j} \in \{0,1\} \tag{3.10}$$

$z_{i,j}$ is a binary variable equal to 1 if and only if the object j is assigned to the cluster of which i is the representative object (medoid). The number of clusters N_k is defined by the user. The representative day is selected when $u_i = 1$, and its weight ω_i corresponds to the number of days in each cluster k calculated by:

$$\omega_i = \sum_{j=1}^{N_i} z_{i,j} \tag{3.11}$$

$$\sum_{i=1}^{N_i} \omega_i = N_i \tag{3.12}$$

The reproduction of the series from representative days does not necessarily preserve the original days, and, therefore, a scale factor is calculated a posteriori.

$$\mu_i^c = \frac{\sum_{j=1}^{N_i} \sum_{g=1}^{N_h} x_{j,g}^c}{\omega_i \cdot \sum_{g=1}^{N_h} x_{i,g}^c} \tag{3.13}$$

The scale factor is applied considering that the extreme values of the original time series are not exceeded.

$$x_{scaled,i,g}^c = min[\mu_i^c \cdot x_{i,g}^c, maxX^c], x_{i,g}^c \in X^c \tag{3.14}$$

The aforementioned methods are types of aggregation methods that lead to smooth representative days, which underestimate the variability of the original time series (Kotzur et al., 2018).

3.3 OPT method

This method was proposed by Poncelet et al. (2017) and consists of fitting the data duration curve obtained from representative periods ($DCrep$) to the duration curve of the original time series (DC). The procedure for selecting the representative days is: i) similarly to the k-Medoids method, input time series must be normalized to be evaluated on the same scale; ii) normalized duration curves (NDC) are computed from the normalized time series; iii) normalized duration curves are divided in b bins in the ordinate, in our case a set of 10 bins of length 0.1, each corresponding to an interval s. A parameter Λ that expresses if data from the original time series c in day i belong to a specific interval, is defined, and iv) each interval is approximated by $\aleph$ (Eq. 3.17), where ω_i is the weight of the representative day $i \in I$ (in other words, ω_i is the number of times that the day i must be repeated to approach the original NDC); N_i is 365 in the case of representative days for a year (See Figure 3.2).

The difference between the length L_s and $\aleph$, in each interval s is taken as an error metric ($error_{c,s}$). The optimization model minimizes the sum of the error terms, for all attributes c considered in every interval s, by selecting a single set of representative periods with their corresponding weights ω_i. The MILP model for this method is written as:

$$Minimize \sum_c \sum_s error_{c,s} \tag{3.15}$$

Subject to:

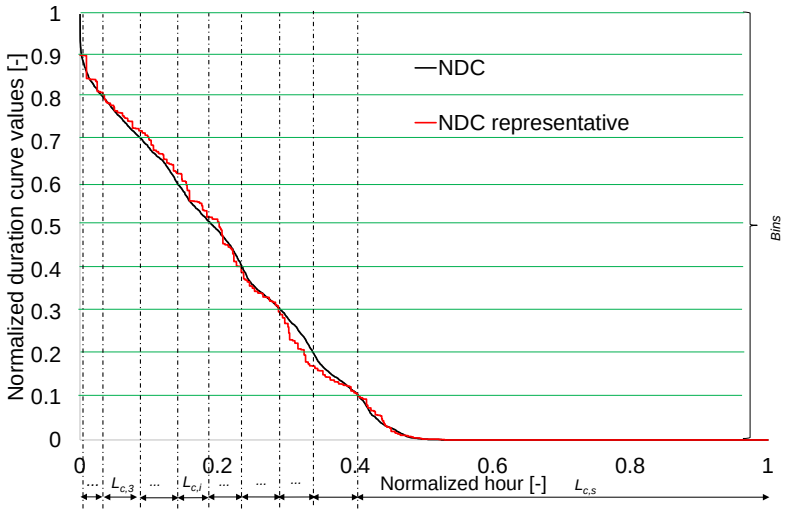

Figure 3.2: Graphical description of OPT method (Adapted from Poncelet et al. (2017)).

$$error_{c,s} = |L_{c,s} - \aleph| \tag{3.16}$$

$$\aleph = \sum_{i=1}^{N_i} \sum_{h=1}^{N_h} \frac{\omega_i}{N_i} \cdot \Lambda_{c,s,i,h} \tag{3.17}$$

$$\sum_{i \in I} u_i = N_k \tag{3.18}$$

$$\omega_i \leq u_i \cdot N_i \tag{3.19}$$

$$\sum_{i \in I} \omega_i = N_i \tag{3.20}$$

$$u_i \in \{0,1\}; \omega_i \in \mathbb{R}_0^+, \ \forall i \ \in \ I \tag{3.21}$$

One of the drawbacks of the OPT method is that the global optimum is challenging to reach. The work of Poncelet et al. (2017) managed three attributes (photovoltaic production, wind production, and electricity load) to select two representative days. The optimization process was stopped after six hours, obtaining good results. However, when dealing with six or more attributes it is more difficult to reach good results in a reasonable time, especially to preserve the area under the curve of each attribute. A scale factor, similar to the procedure described for k–Medoids method, has been applied to address this issue. All runnings that applied the OPT method (results are presented in section 3.5), were stopped after six hours as well.

3.4 Mix *k*M-OPT method

As already explained, aggregation methods lead to smoothed typical periods that underestimate the variability of the original time series (Kotzur et al., 2018), and the OPT method has the disadvantage that the global optimum is difficult to reach. Therefore, a combination of the k-Medoids and OPT methods is proposed to tackle these downsides, reducing the smoothing of typical periods and reaching the global optimum, improving the optimization results of the polygeneration systems. The new procedure is described as follows: the k-Medoids and OPT models are combined in a single model Mix kM-OPT. The function to be minimized in the OPT method is converted into a variable $errorOPT$, defined as:

$$errorOPT = \sum_{c} \sum_{s} error_{c,s} \tag{3.22}$$

The model is optimized as k-Medoid method. This means minimizing the distance of each component of the cluster with respect to the medoid. Simultaneously, $errorOPT$ is calculated, obtaining an $errorkM-OPT$ value, which indicates how close the representative duration curves are to the original curves, by applying the original k-Medoid method. The lower the $errorOPT$ value is, the closer the duration curves from representative days are to the original curves. Therefore, the model can be optimized again, with a new restriction:

$$errorOPT \leq LimOPT \tag{3.23}$$

Where $LimOPT$ is a value defined by the user, lower than $errorkM-OPT$. The lower the $LimOPT$, the global optimum becomes more difficult to reach. A

trade-off value must be found to improve the original models without entailing in excessive computational time. Herein, $LimOPT$ is approximately 90% of $errorOPT$.

3.5 Discussion and analysis of methods

The accuracy of using representative days can be evaluated by defining a metric to estimate how close the set of representative periods are with respect to the reference case, in which hourly (8760 periods) entire year data were considered. In this work, the Root-Mean-Square Error $RMSE$ was selected to evaluate the set of representative days obtained from different methods. $RMSE$ expresses the similarity of the distribution of values and their frequency of occurrence for every representative duration curve with respect to the original ones. The lower the $RMSE$, there is a better fit with the original representative duration curve.

$$RMSE_c = \frac{\sqrt{\frac{1}{8760} \cdot \sum_{h=1}^{8760} (DC_{c,h} - DC_{rep_{c,h}})^2}}{max\{DC_c\} - min\{DC_c\}} \tag{3.24}$$

This section evaluates the suitability of using representative days obtained from different methods to optimize polygeneration systems. Unlike other works, which have studied, among other things, the feasible number of representative days for the optimization of polygeneration systems (Kotzur et al., 2018; Domínguez-Muñoz et al., 2011), herein a fixed number of representative days is considered to compare different methods for the selection of representative days.

Some considerations must be made to guarantee the suitability of the representative days obtained. Averaging method, usually one representative day for each month of the year is considered (Pina et al., 2020). In the case of k-Medoids, eight to 12 representative days are sufficient and have provided good results in previous works (Domínguez-Muñoz et al., 2011; Kotzur et al., 2018). In the case of the OPT method, previous works have selected two representative days and obtained good results (Poncelet et al., 2017), therefore, 12 representative days are considered herein (and sufficient to obtain adequate results as well). For the optimization of the polygeneration systems, two additional days corresponding to peak heating and cooling demands are considered to guarantee that energy demands are always met, with the corresponding impact on the annual investment cost, but not on the annual operational cost.

Table 3.1: Set of representative days i obtained from each method, with respective weights for grid-connected and standalone systems in Zaragoza.

Item	Grid-Connected						Standalone					
	k-Medoids		OPT		Mix kM-OPT		k-Medoids		OPT		Mix kM-OPT	
	i	ω	i	ω	i	ω	i	ω	i	ω	i	ω
1	37	38	1	39	37	36	9	23	1	18.1	21	6
2	62	25	12	4.4	62	27	31	34	19	32.9	37	47
3	112	50	32	35.6	112	44	38	51	25	36.6	116	21
4	116	22	48	29.7	116	24	116	21	58	33.9	136	16
5	175	33	161	19.4	175	37	136	17	123	32.7	147	51
6	208	24	167	56.1	220	22	141	33	166	42.7	158	62
7	221	11	170	2.2	221	14	147	37	182	17.5	166	15
8	241	58	179	11.6	241	50	165	70	186	44.5	175	34
9	287	22	262	32.7	287	25	166	15	231	10.3	240	15
10	291	34	279	67.6	291	37	240	15	290	54.8	300	41
11	339	36	332	54.4	339	35	276	33	310	31.8	339	48
12	352	12	360	12.2	352	14	346	16	362	9.2	352	9

3.5.1 Set of representative days, Metrics and Duration Curves

Tables 3.1 and 3.2 present the set of representative days obtained from each method, along with the respective weights for Zaragoza and Gran Canaria respectively, for both grid connected and standalone energy systems. In the case of grid connected systems, seven attributes have been considered namely the energy demands for 40 dwellings (Q_d, R_d, E_d), renewable energy production (E_{PV}, E_W (30 kW), E_{ST}) and CO_2eq emissions provoked by the electricity from the grid. For standalone systems, the CO_2eq emissions are not required. As aforementioned, one representative day for each month was obtained from the averaging method, and different days were obtained from the other methods, which do not necessarily match each month.

Based on the representative days obtained, the corresponding duration curves for each attribute were built, followed by the calculation of the respective $RMSE$ and $ErrorOPT$ values.

Tables 3.3 and 3.4 present the $RMSE$ values for each attribute and the $ErrorOPT$ values obtained for each method. The $RMSE$ values obtained from the Averaging method are higher than those obtained from other methods. The wind energy production attribute, E_W, presented the highest $RMSE$ value and therefore, the Averaging method presents the weakest approach to the original values. The lowest $RMSE$ values, in general, were obtained from

Table 3.2: Set of representative days i obtained from each method, with respective weights for grid-connected and standalone systems in Gran Canaria.

Item	Grid-Connected						Standalone					
	k-Medoids		OPT		Mix kM-OPT		k-Medoids		OPT		Mix kM-OPT	
	i	ω	i	ω	i	ω	i	ω	i	ω	i	ω
1	40	24	31	28.5	40	24	32	21	1	43.1	32	21
2	52	21	45	63.9	52	21	122	22	65	41.5	122	23
3	58	26	67	0	58	26	124	36	70	0	138	17
4	120	26	89	4.4	120	26	138	17	85	0.2	147	25
5	127	44	121	12.8	127	44	147	25	100	15.7	149	24
6	138	30	122	58.1	138	24	149	23	102	25	176	41
7	186	23	152	35	186	29	176	42	173	48	189	31
8	205	29	219	33.5	226	29	189	31	197	43	190	31
9	264	38	227	53.6	264	38	190	31	229	31	266	30
10	266	29	289	51.1	266	29	266	30	288	24.4	326	34
11	281	28	362	20.6	281	28	351	28	319	56.8	351	29
12	360	47	364	3.6	360	47	359	59	352	36.2	359	59

the OPT method. $ErrorOPT$ represents how close the representative duration curves are to the original ones, and $RMSE$ expresses the similarity between the distribution of values and their frequency of occurrence for every representative duration curve with respect to the original curves. The values obtained from the Mix kM-OPT method are usually intermediate values between those obtained from the k-Medoids and OPT methods. This does not occur necessarily for all attributes, because $ErrorOPT$ is an absolute value that considers all attributes simultaneously (fitting consider the entire set and not individual values).

Figures 3.3 and 3.4 depict some duration curves that aid in the visualization of the accuracy of each method to reproduce the reference DC (original duration curve). In agreement with the values presented in the previous tables, it is observed that E_W and CO_2eq emissions are not well reproduced by the Averaging method because these attributes present the highest variability.

3.5.2 Application of the methods for selecting representative days in the polygeneration systems optimization

The analysis of the duration curves in the previous section gives some clues of the suitability of the different methods. However, the application of these methods in the optimization of polygeneration systems is required in order to achieve better insights for their selection in different applications. To this end,

Table 3.3: *ErrorOPT* values obtained for each method and *RMSE* values for each attribute corresponding to the different methods for grid-connected and standalone systems in Zaragoza.

Grid-Connected								
Method	*RMSE*							*ErrorOPT*
	Q_d	R_d	E_d	E_{PV}	E_W	E_{ST}	CO_2	
Averaging	3.2%	2.3%	0.0%	3.7%	20.6%	7.2%	7.2%	-
k**-Medoids**	2.8%	1.8%	1.0%	1.9%	3.7%	1.6%	4.4%	0.83
OPT	1.6%	1.6%	0.6%	1.5%	1.6%	1.6%	1.6%	0.36
Mix k**M-OPT**	2.7%	1.5%	0.9%	1.6%	3.7%	1.1%	4.2%	0.74
Standalone								
Method	*RMSE*							*ErrorOPT*
	Q_d	R_d	E_d	E_{PV}	E_W	E_{ST}	CO_2	
Averaging	3.2%	2.3%	0.0%	3.7%	20.6%	7.2%	-%	-
k**-Medoids**	1.6%	1.7%	1.2%	2.1%	2.9%	1.7%	-%	0.55
OPT	1.3%	1.5%	1.1%	1.0%	1.7%	1.0%	-%	0.16
Mix k**M-OPT**	2.7%	1.6%	1.1%	2.1%	2.5%	1.6%	-%	0.50

Table 3.4: *ErrorOPT* values obtained for each method and *RMSE* values for each attribute corresponding to the different methods for grid-connected and standalone systems in Gran Canaria.

Grid-Connected								
Method	*RMSE*							*ErrorOPT*
	Q_d	R_d	E_d	E_{PV}	E_W	E_{ST}	CO_2	
Averaging	0.0%	1.6%	0.0%	3.0%	16.0%	8.9%	8.9%	-
k**-Medoids**	0.9%	1.3%	0.5%	1.6%	1.7%	2.0%	2.9%	0.62
OPT	1.3%	2.1%	0.6%	2.0%	2.0%	2.2%	1.3%	0.29
Mix k**M-OPT**	0.8%	1.4%	0.7%	1.6%	1.6%	2.1%	2.7%	0.56
Standalone								
Method	*RMSE*							*ErrorOPT*
	Q_d	R_d	E_d	E_{PV}	E_W	E_{ST}	CO_2	
Averaging	0.0%	1.6%	0.0%	3.0%	16.0%	8.9%	-%	-
k**-Medoids**	1.0%	1.6%	1.2%	2.0%	2.1%	2.1%	-%	0.45
OPT	0.6%	1.4%	0.0%	1.7%	1.3%	2.4%	-%	0.16
Mix k**M-OPT**	1.0%	1.6%	1.2%	1.5%	2.1%	1.6%	-%	0.41

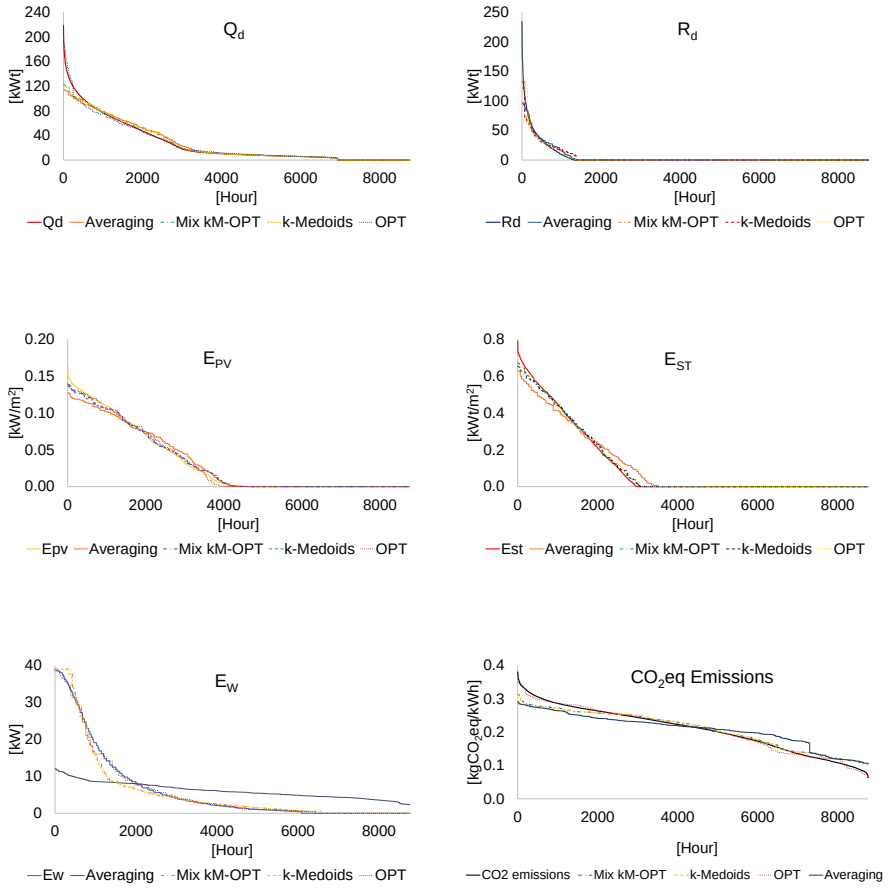

Figure 3.3: Comparison of the original duration curve (Reference) and the duration curves obtained from the analyzed methods for the selection of representative days for Q_d, R_d, E_{PV},E_{ST}, E_W and CO_2eq emissions attributes in Zaragoza.

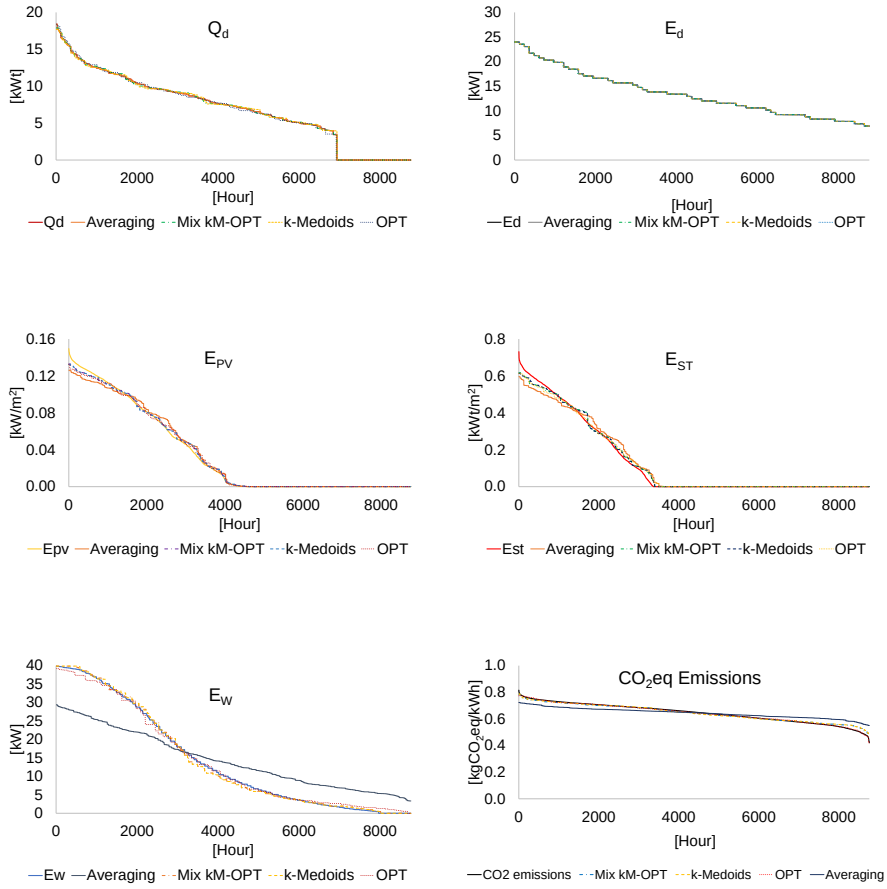

Figure 3.4: Comparison of the original duration curve (Reference) and the duration curves obtained from the analyzed methods for the selection of representative days for Q_d, E_d, E_{PV},E_{ST}, E_W and CO_2eq emissions attributes in Gran Canaria.

the polygeneration systems were optimized minimizing the total annual cost, using different sets of representative days (obtained from different methods). These results were compared to a reference case that considered hourly data throughout the entire year (8760 hours). Optimization was carried out for grid-connected and standalone systems, yielding an optimal configuration along with its optimal operation. A mixed integer linear programming (MILP) model was developed to carry out this study. In the case of the grid-connected systems, the electricity sale to the grid is not allowed. The candidate technologies considered herein are generator (GE), cogeneration module (CM), photovoltaic (PV), solar thermal collectors (ST), wind turbine (WT), heat pump (HP), gas boiler (GB), absorption chiller (ACH), thermal energy storage (TSQ and TSR) and Lithium-Ion batteries (BAT). Regarding storage devices, they are considered as short-term energy storage. As a particular restriction, for the reference case (8760 hours), the stored energy must be the same at the beginning and at the end of the year. On the other hand, in the different cases which use representative days, the stored energy at the beginning and at the end of the representative day must be the same. Concerning to the fuel consumption, in this study there is acces to the natural gas network in Zaragoza for grid connected systems but not for standalone systems, whereas in Gran canaria there is not acces to natural gas neither for grid connected systems nor standalone systems. Therefore, for standalone systems gasoil A is used to drive the generator and cogeneration module, whereas the gas boiler uses gasoil for heating. In this study, biomass technology was not considered as part of the superstructure and technical details such as partial load of equipment were disregarded. The detailed description of the optimization model is presented in the next chapter. The results presented herein were published in the journal Renewable Energy (Pinto et al., 2020).

Table 3.5 shows the optimization results obtained for the grid-connected polygeneration system located in Zaragoza. Regarding the synthesis, the same technologies (PV, CM, HP, TSQ and TSR) are present in the optimal solutions obtained with different sets of representative days. The value of the contracted power from the grid is different when the k-Medoids set of representative days was applied. The OPT set performed better as only the TSR sizing error was higher than 5% (but still lower than 20%). The other sets of representative days presented sizing errors under 20% except for the TSR obtained with the k-Medoids set. Regarding electricity consumption from the grid, error is below 10% except for the k-Medoids set, which was approximately 14%. The error associated with natural gas consumption was under 2% for all sets of representative days. The errors associated with the total annual cost and CO_2eq emissions were below 2% for all sets of representative days.

Table 3.5: Results of the optimization of the grid-connected polygeneration system in Zaragoza, corresponding to the sets of representative days shown in Table 3.1. The reference case considers 365 days (8760 hours).

Technology	**Reference**	**Averaging**	***k*-Medoids**	**OPT**	**Mix *k*M-OPT**
Pct [kW]	$34.6_{1,2,3}$	$34.6_{1,2,3}$	$31.2_{1,2,3}$	$34.6_{1,2,3}$	$34.6_{1,2,3}$
CM $[kWe]$	15.2	14.5	15.7	15.7	15.4
PV $[kW]$	27.4	29.6	30.3	27.6	29.9
WT $[kW]$	0	0	0	0	0
ST$[m^2]$	0	0	0	0	0
HP $[kWt]$	231.3	232.8	224.1	233.7	237.5
GB $[kWt]$	61.4	65.1	69.6	59.2	60.7
ACH $[kWt]$	0	0	0	0	0
TSQ $[kWht]$	2.3	2.3	2.3	2.3	2.3
TSR $[kWht]$	32.7	30	46.4	28.3	21.2
BAT$[kWh]$	0	0	0	0	0
Electricity [kWh]	*36630*	*34028*	*31649*	*34133*	*33076*
Natural gas CM [kWh]	*250287*	*241932*	*248526*	*258462*	*247067*
Natural gas GB [kWh]	*57611*	*60544*	*55213*	*50943*	*56352*
Total Economic cost [€/yr]	**60086**	**59523**	**59599**	**59781**	**59593**
Total CO_2eq emissions $[kgCO_2eq/yr]$	**74969**	**73449**	**73404**	**74973**	**73527**

Table 3.6 shows the results of the standalone polygeneration system located in Zaragoza. In this case, the set of representative days obtained from the Averaging, *k*-Medoids, and OPT methods resulted in the same optimal configuration composed of CM, PV, WT, HP, GB, TSQ, TSR, and Bat. ST and ACH were not included. The utilization of the representative days from the Mix *k*M-OPT method results in the previous configuration but includes ACH (although it could be neglected). Regarding design, PV and WT are not well-sized by using the Averaging set of representative days. The sizing errors obtained for PV and WT are approximately 6% and 33% for the *k*-Medoids set, 11% and 20% for the OPT set, and 6% and 20% for the Mix *k*M-OPT set. HP and GB sizing errors are below 10% for all sets of representative days (for the Mix *k*M-OPT set it was under 5%). Concerning energy storage, TSQ and Bat are barely considered (and therefore could be disconsidered). TSR presented sizing errors below 20% for all sets of representative days. For gasoil consumption, the error was approximately 29% for Averaging, 2% for *k*-Medoids, 5% for OPT and 1% for Mix *k*M-OPT set. In terms of total annual cost, all sets of representative days presented errors of approximately 1% except for the Averaging set, which presented an error of about 4%. For the CO_2eq emissions, the Averaging set presented an error of approximately 27%, *k*-Medoids about 2%, OPT about 4% and Mix *k*M-OPT approximately 0.2%.

Table 3.6: Results of the optimization of the standalone polygeneration system in Zaragoza corresponding to the sets of representative days shown in Table 3.1. The reference case considers 365 days (8760 hours).

Technology	**Reference**	**Averaging**	***k*-Medoids**	**OPT**	**Mix *k*M-OPT**
CM $[kWe]$	23.3	18.9	23	23	23.3
PV $[kW]$	43	25.1	40.3	38.2	45.5
WT $[kW]$	8.6	43.7	5.7	6.9	6.7
ST$[m^2]$	0	0	0	0	0
HP $[kWt]$	167.4	177.4	155.4	153.2	168
GB $[kWt]$	120.8	126.4	122.6	122.4	125.5
ACH $[kWt]$	0	0	0	0	0
TSQ $[kWht]$	2.9	1.8	2.8	1.1	5.8
TSR $[kWht]$	153.2	134.4	175.8	180	170.9
BAT$[kWh]$	1.3	16.5	1.9	2.3	1.5
Gasoil CM[kWh]	*230721*	*91380*	*233120*	*234681*	*227990*
Gasoil GB [kWh]	*139568*	*169887*	*144578*	*154499*	*140700*
Total Economic cost [€/yr]	**81243**	**77743**	**80304**	**81137**	**82157**
Total CO_2eq emissions $[kgCO_2eq/yr]$	**115160**	**84130**	**117031**	**120326**	**114913**

Results of the optimization for Gran Canaria are presented in Tables 3.7 and 3.8 for grid-connected and standalone systems, respectively. For the grid-connected system, all sets of representative days provided the same optimal configuration, composed of PV, WT, HP, GB, and TSR. Unlike the reference system, each set included ST in the optimal configuration. Regarding contracted power, only the OPT set resulted in the same Pct as the reference case. In terms of design, the Averaging set resulted in sizing errors are much higher than 5%, for most technologies, especially for renewable energy based. For the *k*-Medoids, OPT and *k*M-OPT sets, the sizing errors obtained were below or approximately 20% for all technologies. Despite the high sizing errors obtained from Averaging, the total annual cost error was only about 2%. This result confirms that, similarly to Zaragoza, the total annual cost error is not sufficient to evaluate the suitability of a method. For the other analysed sets, the total annual cost error was about 1%. For electricity from the grid, the obtained error was below 5% for all sets of representative days, except for the Averaging set, which presented an error above 20%. The gasoil consumption errors for the Averaging, *k*-Medoids, OPT, and Mix *k*M-OPT sets were approximately 18%, 23%, 7% and 16% respectively. In terms of total CO_2eq emissions errors, for Averaging the error was approximately -21%, for OPT approximately -3% and for *k*-Medoids and *k*M-OPT, about 1%.

For the standalone system in Gran Canaria, the set of representative days obtained from the Averaging, OPT and *k*M-OPT methods result in the same

Table 3.7: Optimization results for grid-connected polygeneration system in Gran Canaria, corresponding to the sets of representative days shown in Table 3.2. The reference case considers 365 days (8760 hours).

Technology	**Reference**	**Averaging**	**k-Medoids**	**OPT**	**Mix kM-OPT**
Pct [kW]	$31.2_{1,2}$-17.3_3	$34.6_{1,2}$-17.3_3	$34.6_{1,2}$-17.3_3	$31.2_{1,2}$-17.3_3	$34.6_{1,2}$-17.3_3
GE [kWe]	0	0	0	0	0
PV [kW]	23	14.7	19.1	24.6	21.8
WT [kW]	8.4	16.2	8.6	7.2	7.8
ST[m^2]	0	7	8	7	6
HP [kWt]	158.5	165.6	165.3	159.8	169.1
GB [kWt]	15.5	13.8	12.8	14.1	12.9
ACH [kWt]	0	0	0	0	0
TSQ [$kWht$]	0	0	0	0	0
TSR [$kWht$]	61.4	48	48.6	59.1	53.4
BAT[kWh]	0	0	0	0	0
Electricity [kWh]	*68361*	*51843*	*71557*	*66270*	*70587*
Gasoil GB [kWh]	*23458*	*19276*	*17950*	*21865*	*19734*
Total Economic cost [€/yr]	**33020**	**32298**	**32835**	**32837**	**33372**
Total CO_2eq emissions [$kgCO_2eq/yr$]	**56030**	**44128**	**56652**	**54412**	**56629**

optimal configuration, which included GE, PV, WT, HP, GB, TSQ and TSR. A similar configuration was obtained by using the k-Medoids set of representative days, but TSQ was not included. Regarding design, the TSQ included was so insignificant it could be disconsidered. When using the Averaging set of representative days, the technology sizing errors were much higher than 5%, especially for WT technology, similar to the result obtained for the grid-connected system. Using the other sets of representative days, sizing errors obtained were below 20% for all technologies, except for the OPT set where the sizing error for WT was about 24%. For gasoil annual consumption, the errors were below 2%, except for the Averaging set, with an error of approximately 49%. In terms of total annual cost, the obtained error was approximately 1% except for the Averaging set, which presented an error of about 15%. In terms of CO_2eq emissions, the errors obtained were approximately 1%, except for the Averaging set, with an error of approximately -45%.

3.5.3 Qualitative evaluation of methods for the selection of representative days

The QFD technique (Kiran, 2017) was applied to evaluate the suitability of each method for the synthesis and design of polygeneration systems, estimating which method is useful for each case. To this end, the criteria shown in Table 3.9 (based on the engineering criteria practice) were applied. A score is applied to the sizing

Table 3.8: Optimization results for the standalone polygeneration system in Gran Canaria, corresponding to the sets of representative days shown in Table 3.2. The reference case considers 365 days (8760 hours).

Technology	**Reference**	**Averaging**	**k-Medoids**	**OPT**	**Mix kM-OPT**
GE $[kWe]$	25.6	25.8	25.5	25.3	25.5
PV $[kW]$	30.5	14.0	26.9	24.4	27.1
WT $[kW]$	18.7	38.2	19.9	23.2	20.0
ST$[m^2]$	0	0	0	0	0
HP $[kWt]$	158.5	163.2	164.5	164.5	165.1
GB $[kWt]$	13.9	12.7	15.4	13.1	14.5
ACH $[kWt]$	0	0	0	0	0
TSQ $[kWht]$	1.6	2.9	0	2.3	0.9
TSR $[kWht]$	61.4	52.7	50.2	50.2	49.1
BAT$[kWh]$	0	0	0	0	0
Gasoil GE[kWh]	*143270*	*54827*	*144171*	*147134*	*144685*
Gasoil GB [kWh]	*45306*	*42070*	*46231*	*44646*	*46037*
Total Economic cost [€/yr]	**48166**	**41086**	**47861**	**48783**	**47985**
Total CO_2eq emissions $[kgCO_2eq/yr]$	**60643**	**33601**	**60954**	**61371**	**61070**

errors E_{sz} of each component. Capacities with a deviation above 20% are not considered acceptable and, therefore they receive a score of 0. A deviation between 5% and 20% is considered reasonably accurate, receiving a score of 1, and a deviation below 5% is considered good accuracy and receives a score of 2. The maximum score that can be reached for each group of technologies is 6 for renewable energy technologies, 8 for electricity/heating/cooling production technologies, and 6 for energy storage technologies.

The QFD results for each system and location are presented in Tables 3.10-3.13. For grid-connected systems, the maximum score was 34, obtained from the OPT method, followed by Mix kM-OPT and k-Medoid methods, and for standalone systems, the maximum score was 26, obtained from Mix kM-OPT method followed by k-Medoids and OPT methods.

3.5.4 Reduction of computational effort by using representative days

The purpose of using representative days instead of entire year data is to reduce the computational time required for the optimization of polygeneration systems. Table 3.14 presents data related to the number of variables, constraints, and elapsed time for the optimization of a grid-connected polygeneration system using entire year data and using representative days. All runs were performed on an Intel Core i5-6200 CPU @ 2.3 GHz, with a memory of 8 GB and 64-bit

Table 3.9: Criteria for the evaluation of methods for the selection of representative days by QFD.

Sizing Error (E_{sz})	**Score**
$E_{sz} > \|20\%\|$	0
$\|5\%\| < E_{sz} \leq \|20\%\|$	1
$E_{sz} \leq \|5\%\|$	2
Group of technologies	**Max Score**
Renewable Energy (RE)	6
Electricity/Heating/Cooling Production Technologies (E/H/C)	8
Energy Storage (ES)	6
Polygeneration system (PS)	***20***

Table 3.10: QFD results for the grid-connected system in Zaragoza.

Method	Renewable Energy				E/H/C Production Technologies					Energy Storage				Polygeneration system
	PV	WT	ST	*Score RE*	CM	HP	GB	ACH	*Score E/H/C*	TSQ	TSR	Bat	*Score ES*	*Score*
Averaging	1	2	2	*5*	2	2	1	2	*7*	2	1	2	*5*	*17*
k-**Medoids**	1	2	2	*5*	2	2	1	2	*7*	2	0	2	*4*	*16*
OPT	2	2	2	*6*	2	2	2	2	*8*	2	1	2	*5*	*19*
*k***M-OPT**	1	2	2	*5*	2	2	2	2	*8*	2	0	2	*4*	*17*

Table 3.11: QFD results for the standalone system in Zaragoza.

Method	Renewable Energy				E/H/C Production Technologies					Energy Storage				Polygeneration system
	PV	WT	ST	*Score RE*	CM	HP	GB	ACH	*Score E/H/C*	TSQ	TSR	Bat	*Score ES*	*Score*
Averaging	0	0	2	*2*	1	1	2	0	*4*	0	1	0	*1*	*7*
k-**Medoids**	1	0	2	*3*	2	1	2	0	*5*	2	1	0	*3*	*11*
OPT	1	1	2	*4*	2	1	2	0	*5*	0	1	0	*1*	*10*
*k***M-OPT**	1	0	2	*3*	2	2	2	0	*6*	0	1	1	*2*	*11*

Table 3.12: QFD results for the grid-connected system in Gran Canaria.

Method	Renewable Energy				E/H/C Production Technologies					Energy Storage				Polygeneration system
	PV	WT	ST	*Score RE*	GE	HP	GB	ACH	*Score E/H/C*	TSQ	TSR	Bat	*Score ES*	*Score*
Averaging	0	0	0	*0*	2	2	1	2	*7*	2	0	2	*4*	*11*
k-**Medoids**	1	2	0	*3*	2	2	1	2	*7*	2	0	2	*4*	*14*
OPT	1	1	0	*2*	2	2	1	2	*7*	2	2	2	*6*	*15*
*k***M-OPT**	2	1	0	*3*	2	1	1	2	*6*	2	1	2	*5*	*14*

Table 3.13: QFD results for the standalone system in Gran Canaria.

Method	Renewable Energy				E/H/C Production Technologies					Energy Storage				Polygeneration system
	PV	WT	ST	*Score RE*	GE	HP	GB	ACH	*Score E/H/C*	TSQ	TSR	Bat	*Score ES*	*Score*
Averaging	0	0	2	*2*	2	2	1	2	*7*	0	1	2	*3*	*12*
k-**Medoids**	1	1	2	*4*	2	2	1	2	*7*	0	1	2	*3*	*14*
OPT	1	0	2	*3*	2	2	1	2	*7*	0	1	2	*3*	*13*
*k***M-OPT**	1	1	2	*4*	2	2	2	2	*8*	0	1	2	*3*	*15*

Table 3.14: Number of variables and runtime for the optimization of polygeneration system using entire year data and sets of representative days.

Number of days	Variables		Constraints	Runtime		
	Integer	Total		Hours	Minutes	Seconds
365	21	928763	1270363	1	27	6
14	21	35824	48888	0	0	8

system. Similar results were also obtained for standalone systems. It must be highlighted that the global optimum using 8760 hours was achieved because the optimization model did not consider many technical details such as partial load of equipment. Otherwise, calculation time could increase up to several days. However, these results demonstrated that there is a remarkable reduction in runtime, of about three orders of magnitude, which is significant when a detailed design is required.

3.6 Closure

The performance of three different methods were compared for the selection of representative days for the optimization of polygeneration systems. Two different systems were considered, standalone and grid-connected located, in two different locations in Spain, Zaragoza and Gran Canaria. The locations presented different climatic conditions, natural resources and energy demands, covering a wide range of possibilities that enable the extension of the results to other case studies. In general terms, the use of representative days in the optimization of polygeneration systems was more accurate for grid connected than standalone systems. The OPT method could be considered the best option for grid-connected systems. In the case of standalone systems, the methods yielded similar results. For instance, in Gran Canaria the Mix kM-OPT method performed best, but in Zaragoza the k-Medoids and Mix kM-OPT methods presented the same score.

The stochastic variability of the attributes has strong influence and must be taken into account when assessing the most suitable method for the selection of representative days. The Averaging method is not adequate to address with attributes with high stochastic variability, such as wind energy; however, it is a good alternative to tackle attributes such as solar energy.

It is important to highlight that the total annual cost is not a determinant factor when evaluating the suitability of a method for the selection of representative days. When the Averaging method was applied to grid-connected systems in Gran Canaria or standalone systems in Zaragoza, the annual cost errors of the optimal systems were below 2% with respect to the corresponding reference cases, but the optimal designs were significantly different than those obtained for the reference systems.

Regarding conventional technologies to produce electricity/heating/cooling, all methods performed well when sizing the components. In the case of energy storage, which are short-term storage , although there is no connection between the selected representative days to model its continuous dynamic behaviour, the sizing errors observed were below 20% in most cases. Herein only thermal energy storage for cooling TSR was feasible in the optimal configurations, and the best results were obtained when applying the OPT method, achieving errors under 5% in Gran Canaria for grid-connected systems. When TSQ and Bat were part of the optimal configuration, sizes were negligible.

From the point of view of operation, the electricity and fuel consumption obtained from the application of k-Medoids, OPT and Mix kM-OPT methods presented good fit with the reference system. The results obtained for stan-

dalone systems were remarkable, with fuel consumption errors below 5%.

In general, based on the obtained results, the OPT method seems to be the best alternative to select representative days. However, computational effort can be very high in the process to obtain the global optimum and, as a consequence, it is advisable to stop the optimization process before the global optimum is reached. It has been demonstrated herein that the k-Medoids method results can be improved by combining the k-Medoids and the OPT methods obtaining a new method called kM-OPT. However, the computational effort and cost of this new method is higher with respect to the former.

The importance of reducing RMSE metric values was highlighted, to improve the results of the optimization of polygeneration systems by using representative days. The lowest RMSE values were obtained with the OPT method, and it was observed that the best results for grid-connected systems were also obtained by applying this method. Nonetheless, when this method is applied, it is more difficult to reach the global optimum, which entails an uncertainty associated with the application of the OPT method. The kM-OPT method allows the achievement of a global optimum, which is an advantage with respect to the OPT method, but does not necessarily mean that results were improved.

As a final global conclusion, the synthesis and optimization of polygeneration systems using appropriate sets of representative days provide a good and reasonable approach and pre-design in terms of configuration, sizing and operation. However, due to the complexity of the problem, an appropriate method for the selection of a set of representative days should be applied, as these highly complex polygeneration systems should meet several energy demands (heating, cooling and electricity in the analyzed cases), using manageable (electricity from the grid, fossil fuels, or biomass) and non-manageable (e.g., solar and wind) energy resources considering several candidate energy conversion technologies (cogeneration, heat pumps, wind turbines, solar PV panels, solar thermal collectors, mechanical and absorption chillers) as well as short-term energy storage.

Chapter 4

Optimization model for polygeneration systems

"What came first, the chicken or the egg?"

Integrated design, synthesis and operation optimization (IDSOO) of polygeneration systems is applied to determine simultaneously the components, capacity of the components and operational strategies of the energy supply system, based on one or more than one criteria over a planning horizon subject to different types of constraints such as technical, economic and legal restrictions. For the design of polygeneration systems for residential buildings, Mixed Integer Linear Programming (MILP) and Mixed Integer Non-Linear Programming (MINLP) techniques are widely used in the literature (Rong and Su, 2017).

Depending on the level of detail required for the analysis of the energy system, different model-based approaches can be carried out to address the IDSOO of polygeneration systems. For instance, the model can explicitly describe the relationship between energy products and components by using input-output matrix (Mancarella, 2009), or it can use thermodynamic models to describe the conversion process of the different energy products along with the coupling of production of different components (Fazlollahi and Maréchal, 2013).

In this work, a MILP model has been developed for the IDSOO of polygeneration systems. The optimization problem can be seen as a three-level decomposition problem (Rong and Su, 2017). One level is the synthesis which consists in the selection of the optimal system configuration based on the cor-

responding superstructure. This can be carried out by using binary variables (0,1). The second level is the design which consists of the sizing of each technology selected. This can be carried out by using continuous variables. The third level consists in the optimization of the operation which means the operating condition of each component based on the load profile. This can be carried out by using binary variables which can represent ON-OFF operation as well as partial load, or, the operation can be continuous with the ability to modulate up to nominal load. Synthesis and design can be carried out simultaneously, therefore the three-levels problem becomes a two-levels problem. In order to obtain the global optimum, the three levels must be solved simultaneously. In computational terms, the bigger the number of binary variables are, the higher computational effort is. Therefore, it is highly recommended to reduce binary variables as much as possible. As mentioned before, synthesis and design can be solved simultaneously, this can be the case when the nominal capacity of the candidate technologies are fixed. However, from other perspective, the capacity of each technology can be considered as a continuous variable, in this case the use of binary variables to select technologies can be avoided and the synthesis and design are solved simultaneously likewise. This methodology makes sense for preliminary designs and general analysis of polygeneration systems, being aware of the fact that there is not selection of a specific equipment but a representative one based on average data. By applying this methodology, a significant reduction in the computational solution time is achieved.

On the other hand, bearing in mind the IDSOO of sustainable polygeneration system for residential buildings, superstructure optimization methodology is one of the most applied approaches for this purpose. This methodology defines the system superstructure which includes all candidate technologies as well as the interactions between them based on feasible processes and integration. Based on this, an optimization model which combines among others, economic, environmental and technical restrictions is developed. Finally, the resulting model is solved by applying standard solvers or developing specific algorithms (Yokoyama et al., 2015; Gong and You, 2015; Rong and Su, 2017), some common standard commercial optimization softwares are LINGO (LINDO Systems Inc, 2013), GAMS (GAMS Development Corporation, 2019) or CPLEX (IBM, 2019), among others (See Figure 4.1).

Taking into account the above mentioned process, this chapter presents a comprehensive description of the system superstructure and the optimization model with the different restrictions used along this research work for the design of sustainable polygeneration systems for residential buildings. The solver LINGO (LINDO Systems Inc, 2013) has been used to develop and solve the

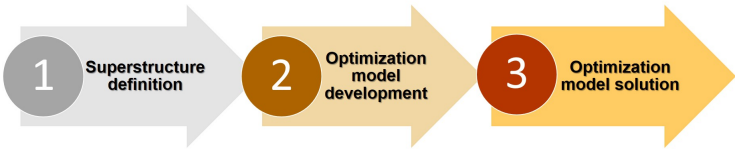

Figure 4.1: Optimization process scheme.

optimization model.

4.1 Superstructure

The superstructure depicted in Figure 4.2 considers the candidate technologies and the feasible connections between them. The system is composed of electrical and thermal parts, as well as components facilitating the integration of both parts. The electrical part consists of the electric grid (only for grid connected systems) from which an specific power can be contracted Pct; photovoltaic modules PV whose power production W_{PV} is proportional to the solar irradiance and modules area A_{PV}; wind turbines WT whose power production W_W is the result of the power production E_W multiplied by the number of turbines N_{WT}; inverter Inv which converts the direct current produced from renewable energy technologies such as PV to alternating current; batteries BAT which can store electrical energy and inverter-charger $InvC$ which converts alternating current to direct current and viceversa. When the excess of electricity produced by PV or WT can not be sold to the electric grid or stored in batteries, it is wasted by a dissipater. The thermal part consists of different components which produce or store thermal energy. Regarding equipment to produce heat, they consist of a conventional boiler GB that consumes fossil fuel F_{GB}, a biomass boiler BB that consumes pellets F_{BB} and a solar thermal collectors ST whose heat production Q_{ST} is proportional to the solar irradiance and the solar collectors area A_{ST}. Concerning the production of cooling, a single-effect absorption chiller ACH

uses heat to produce cooling water R_{ACH}. Also, the thermal energy storage for heating TSQ and cooling TSR, which can charge/discharge thermal energy are considered as candidate technologies. Components such as the cogeneration module CM, converting the energy of fossil fuels F_{CM} into electricity W_C and heat Q_C, and the reversible heat pump HP which converts the electricity E_{HP} into thermal energy either heating Q_{HP} or cooling R_{HP}, allow the integration of electric and thermal parts.

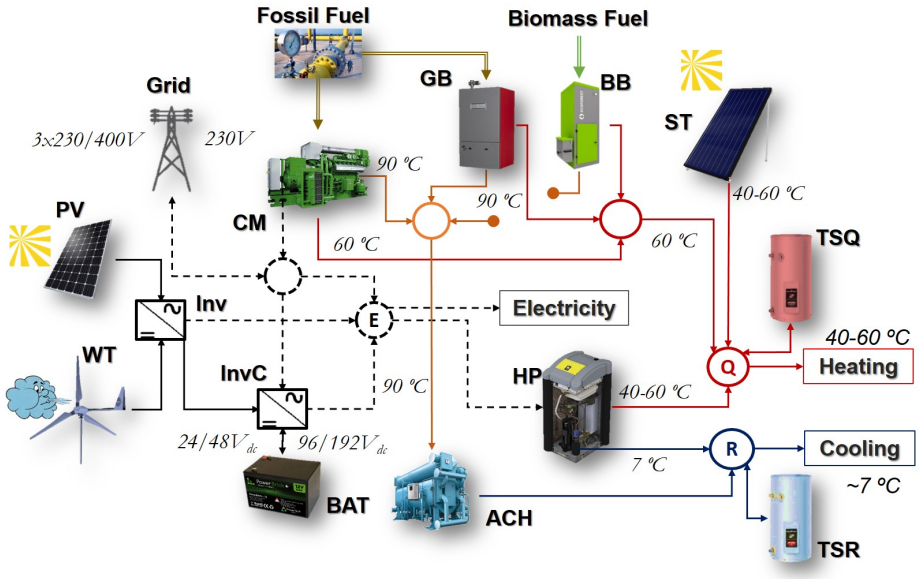

Figure 4.2: Superstructure.

From the point of view of operation, the electrical part considers a three-phase alternating current bus (*ac*-bus) with an operating low voltage (230/400V) and a direct current bus (*dc*-bus) with an operating voltage depending on the *ac* power. For the thermal part, a low temperature radiant heating indoor end system was considered, with operation temperatures about 45 °C, in addition, temperatures about 60 °C are required for DHW. The required thermal energy for space heating and DHW can be provided by the heat pumps, solar thermal collectors, cogeneration module and boilers. In the case of cooling demands,

temperatures of about 7-12 °C are considered, and the required energy can be provided by the reversible heat pumps and the absorption chiller. The activation temperature for the absorption chiller is about 90 °C, and the thermal energy can be produced by the boilers and/or the cogeneration module. Reversible heat pumps can operate in heating or cooling mode, but it is not allowed to operate simultaneously in both modes. The Figure 4.3 depicts a detailed scheme of the superstructure with their feasible connections. Notice that the reversible heat pump HP is represented by two virtual heat pumps HPQ for heating mode and HPR for cooling mode.

4.2 Optimization model

Polygeneration systems allow a suitable energy systems integration to achieve lower consumption of natural resources, reduction of CO_2eq emissions as well as economic savings relative to conventional separate production (Serra et al., 2009). Nonetheless, to achieve it, an optimization process must be carried out to determine the best or optimal values for the decision variables of the energy system, e.g., energy technologies to be installed, operational strategies for each power generation unit, etc. To this end, energy system modelling, simulation, and optimization approaches are used. If modelling is inaccurate, simulation and optimization results become unrealistic and useless. Thus, modelling needs to be carefully carried out before optimization is performed (Dincer et al., 2017). A general mathematical formulation of an optimization problem is described as follows:

$$Min/Max \;\; ObjF = f(X,Y) \tag{4.1}$$

Subject to:

$$H(X,Y) = 0 \tag{4.2}$$

$$G(X,Y) \leq 0 \tag{4.3}$$

$$X \in \mathbb{R}^n \tag{4.4}$$

$$Y \in \{0,1\}^q \tag{4.5}$$

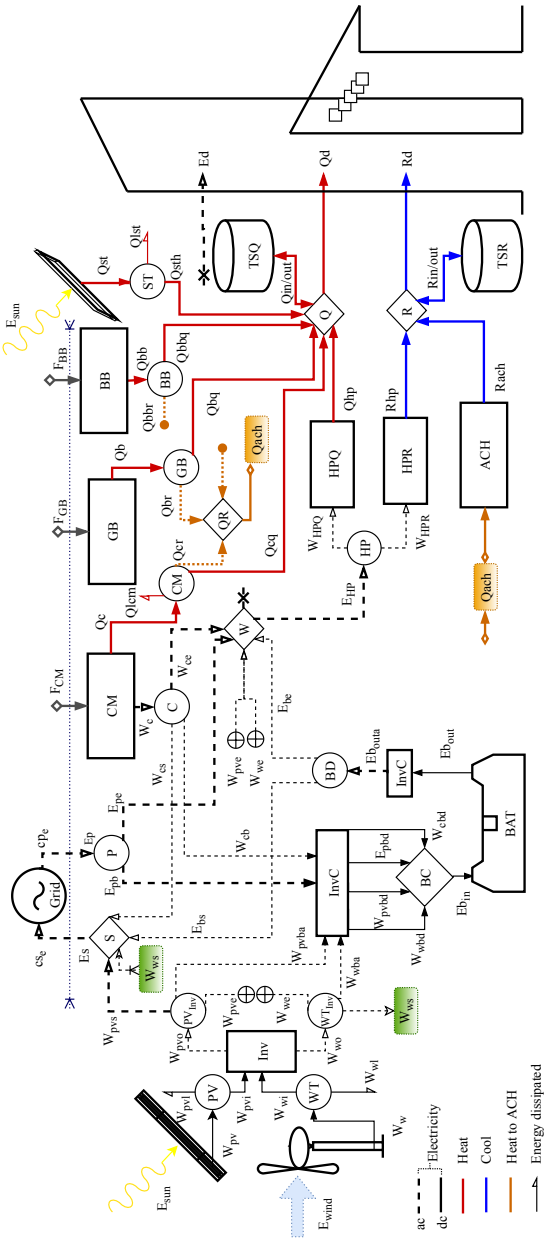

Figure 4.3: Detailed scheme of the considered superstructure with feasible connections.

Where $H(X,Y)$ represents the set of equations, for example, energy balance and $G(X,Y)$ represents the set of inequalities, for example, capacities restrictions. Both of them are the constraints of the optimization model. The optimization problem consists of finding the decision variables values which satisfy the set of equations and inequalities in order to optimize [$Minimize(Min)$ or $Maximize(Max)$] the objective function $ObjF$.

The timeframe for the optimization of the polygeneration systems in this study is one year or 365 days with hourly resolution. However, depending on the complexity of the model (as explained in the previous chapter), typical or representative days can be used to reduce the computational complexity. N_{rep} represents the number of representative days considered for the energy system optimization and ω the weight of each day. For instance, when the entire 365 days are considered, $N_{rep} = 365$ and $\omega = 1$ (See chapter 3). In this sense, it is defined a set of representative days D_{rep} with N_{rep} elements. Each representative day consists of a set H of 24 time periods of 1 hour. However, since the electric tariffs depend on the time of use, three different time periods are also defined along the day namely $P1, P2, P3$ in order to calculate the electric bill cost (See Table 2.13).

The optimization model is adjusted depending on the type of study. In general terms, the type of study carried out along this work can be divided in grid connected and standalone energy systems. The main difference between them is the absence of the electric grid in the standalone systems. To do this, a parameter Υ_{gc} is used to select the case of study. The $\Upsilon_{gc} = 1$ when the energy system considers electric grid, on the other hand, when $\Upsilon_{gc} = 0$, there is not option to interact with the electric grid. Besides, the energy system can or can not have access to the natural gas network. This depends on the location of the residential building and/or the type of study carried out. Therefore, along the study, the access option to the electric grid and natural gas network is defined beforehand in accordance to the type of study.

In this study, two objective function have been considered for the optimization of polygeneration systems:

- ♦ Minimize the total annual cost TAC (Economic optimization):

$$Min\ TAC \tag{4.6}$$

- ♣ Minimize the total annual CO_2eq emissions TCE (Environmental optimization):

$$Min\ TEC \tag{4.7}$$

4.2.1 Economic optimization

The total annual cost TAC is composed for the investment annual cost CIA and the operational cost C_{ope}.

The economic objective function is:

$$Min\ TAC = Min(CIA + C_{ope}) \tag{4.8}$$

The annual investment cost CIA is the annuity to reimburse the loan of the total investment cost (See section 2.4.2).

The operational annual cost C_{ope} is the sum of the annual electricity bill cost C_e (for grid connected systems) and the annual fuel consumption cost C_g.

$$C_{ope} = C_e + C_g \tag{4.9}$$

Subscript $_e$ indicates electricity and subscript $_g$ indicates conventional and/or biomass fuels.

The electricity bill C_e is composed of a fixed part C_{fix_e}, and the variable cost C_{v_e} (Eq. 4.10). The C_{fix_e} is proportional to the contracted power Pct at $cPct$ price in €/kWe (Eq. 4.11). C_{v_e} (Eq. 4.15) is calculated based on the electricity consumption Ep at cp_e price and the sale electricity Es at cs_e price. Values of cp_e and cs_e in €/kWh depend on the time-of-use electricity tariff. Besides, tax Tax_e and the equipment rental cost C_{alq_e} of the electricity are considered. The contracted power Pct is selected by applying the dot product between the vector of normalized power from the electric grid $Pct_{nom} \in \mathbb{R}^m$ (Table 2.12) and the binary variable vector Y_{Pct} in accordance to the time-of-use period (Eq. 4.12), taking into account that neither the purchased electricity nor the sale electricity can exceed the contracted power (Eq. 4.14). For contracted power below to 15 kW, only one normalized power is selected, on the other hand, above 15 kW (low voltage) up to three different normalized powers can be selected. In this sense, a set of time-of-use electricity tariff I with up to three elements is defined.

$$C_e = ((C_{fix_e} + C_{v_e}) \cdot (1 + Tax_e) + C_{alq_e}) \cdot (1 + VAT) \cdot \Upsilon_{gc} \tag{4.10}$$

$$C_{fix_e} = \sum_{i=1}^{3} cPct(i) \cdot Pct(i) \tag{4.11}$$

For each electric tariff period i:

$$Pct(i) = \sum_{k=1}^{m} Pct_{nom}(k) \cdot Y_{Pct}(i,k) \tag{4.12}$$

$$\sum_{k=1}^{m} Y_{Pct}(i,k) \leq 1; \;\; Y_{Pct}(i) \in [0,1]^m \tag{4.13}$$

$$Pct(i) \geq Ep(i,d,h) + Es(i,d,h) \; \forall \; i \in I, \; d \in D_{rep} \; \wedge \; h \in H \tag{4.14}$$

$$C_{v_e} = \sum_{d=1}^{N_{rep}} \omega(d) \cdot \left(\sum_{h=1}^{24} (cp_e(i,d,h) \cdot Ep(i,d,h) - cs_e(i,d,h) \cdot Es(i,d,h)) \right)$$
$$\forall \; i \in I, \; d \in D_{rep} \; \wedge \; h \in H \tag{4.15}$$

C_g is the cost of the conventional fuel cost (Eq. 4.16). When there is access to the natural gas network, it represents the natural gas bill cost which is composed of a fixed part related to the annual natural gas consumption C_{fix_g}, and a variable part proportional to the fuel consumption C_{v_g} .Additionally, the equipment rental cost C_{alq_g} was also considered. When there is no access to the natural gas network, there are not fixed costs, hence the fuel cost is proportional only to the gasoil and/or biomass consumption.

$$C_g = ((C_{fix_g} + C_{alq_g}) + C_{v_g}) \tag{4.16}$$

$$C_{v_g} = \sum_{d=1}^{N_{rep}} \omega(d) \cdot \left(\sum_{h=1}^{24} cp_g \cdot F_g(d,h) \right) \tag{4.17}$$

4.2.2 Environmental optimization

The total annual CO_2eq emissions TCE is composed of a fixed part $CO2_{fix}$ corresponding to the annual CO_2eq emissions embodied in the components and the variable part $CO2_{ope}$ corresponding to the annual CO_2eq emissions due to the fossil fuels and pellets combustion, and/or electricity consumption from the grid during the operation system.

The environmental objective function is:

$$Min \; TCE = Min(CO2_{fix} + CO2_{ope}) \tag{4.18}$$

The annual CO_2eq emissions embodied in each component is the product of the unit CO_2eq emissions CO_2U by its capacity, divided by the lifetime project n. The repositions carried out during the lifetime of the installation n_{repo} are also considered in the fixed part $CO2_{fix}$ (Eq. 4.19). The operational CO_2eq emissions (Eq. 4.20) encompass the annual CO_2eq emissions associated to the combustion of each fuel $CO2_g$ (Eq. 4.21), and the CO_2eq emissions associated to the electricity from the grid $CO2_{gc}$ (Eq. 4.22).

$$CO2_{fix} = \sum_{j \in J} CO_2U(j) \cdot Cap(j) \cdot \frac{(1 + n_{repo})}{n} \tag{4.19}$$

$$CO2_{ope} = \sum_{d=1}^{N_{rep}} \omega(d) \left(\sum_{h=1}^{24} (CO2_g(d,h) + CO2_{gc}(d,h)) \right) \tag{4.20}$$

$$CO2_g(d,h) = \sum_{j \in J} (CO2(j) \cdot F(j,d,h)) \; \forall \; d \in D_{rep} \; \wedge \; h \in H \tag{4.21}$$

$$CO2_{gc}(d,h) = CO2_{grid}(d,h) \cdot (Ep(d,h) - Es(d,h)) \cdot \Upsilon_{gc} \; \forall \; d \in D_{rep} \; \wedge \; h \in H \tag{4.22}$$

4.2.3 Technical and physical restrictions

Installation of technologies: The Installation of the components is determined by the binary variable Y_{ins} taking into account the maximum capacity of each component $max\ Cap$. Then, the technology can or can not be installed according to the expression:

$$Cap(j) \leq Y_{ins}(j) \cdot max\ Cap(j) \; \forall j \in J \tag{4.23}$$

Energy balance: Energy balance is carried out in each node of the superstructure for every day d and hour h. The variable u represents the in/out energy (electricity E/W, heating Q or cooling R) value in each time step.

$$\sum u^{in}(\Gamma,d,h) - \sum u^{out}(\Gamma,d,h) = 0 \;\; \forall \, \Gamma \in \{W/E, Q, R\}, \; d \in D_{rep}, \; h \in H \tag{4.24}$$

Equipment efficiency: Efficiency of every component of the superstructure has been considered. F represents the fuel consumption of the component.

$$BB : \eta_{BB} \cdot F_{BB} - Q_{BB} = 0 \tag{4.25}$$
$$GB : \eta_{GB} \cdot F_{GB} - Q_{GB} = 0 \tag{4.26}$$
$$HPQ : Q_{HP} - W_{HPQ} \cdot COP = 0 \tag{4.27}$$
$$HPR : R_{HP} - W_{HPR} \cdot EER = 0 \tag{4.28}$$
$$CM : \alpha_w \cdot F_{CM} - W_C = 0 \tag{4.29}$$
$$CM : \alpha_q \cdot F_{CM} - Q_C = 0 \tag{4.30}$$
$$ACH : R_{ACH} - COP_{ACH} \cdot Q_{ACH} = 0 \tag{4.31}$$

Energy storage: In the case of energy storage, the stored energy at the beginning of the day ($h = 1$) must be equal at the end of the day ($h = 24$) (Eq. 4.32), due to the use of representative days. On the other hand, when the entire days of the year is considered (8760 hours), the stored energy at the beginning of the year must be equal at the end of the year (Eq. 4.33).

$$S(d, 1) = S(d, 24) \tag{4.32}$$
$$S(1, 1) = S(365, 24) \tag{4.33}$$

The energy stored S is evaluated in each time step taking into account their energy loss factor λ to consider the hourly energy losses. In the case of batteries, λ corresponds to the self-discharge value. For each energy storage technology j:

$$S(j, d, h) = S(j, d, h-1) \cdot \lambda + u^{in}(j, d, h) - u^{out}(j, d, h) \; \forall \; d \in D_{rep} \; \wedge \; h \in H \tag{4.34}$$

For batteries, besides the hourly energy losses, the round trip efficiency η_{rt} is also considered and modelled by applying a charge efficiency η_{ch}, and discharge efficiency η_{dis} to the charge I_{ch} and discharge I_{dis} currents, and the charge Eb_{in} and discharge Eb_{out} energies respectively. In addition, the number of cycles N_c must be lower or equal to the cycle life of the battery $N_{c,failure}$. The number of cycles N_c is the ratio between the total amount of energy discharged by the battery along its lifetime and its nominal capacity. The stored energy of each technology depends on the dynamic behaviour (See in Appendix A a detailed description of the battery model).

$$\eta_{rt} = \eta_{ch} \cdot \eta_{dis} \tag{4.35}$$
$$Eb_{in}(d,h) \cdot \eta_{ch} - I_{ch}(d,h) \cdot V_{dc} = 0 \; \forall \; d \in D_{rep} \; \wedge \; h \in H \tag{4.36}$$
$$Eb_{out}(d,h) - \eta_{dis} \cdot I_{dis}(d,h) \cdot V_{dc} = 0 \; \forall \; d \in D_{rep} \; \wedge \; h \in H \tag{4.37}$$
$$N_c \leq N_{c,failure} \tag{4.38}$$

Renewable energy technologies: For renewable energy production technology, the aim is to find the surface areas of the PV modules A_{PV} and solar thermal collectors A_{ST}, and the number of wind turbines N_{WT}.

$$PV : W_{PV} = E_{PV} \cdot A_{PV} \tag{4.39}$$
$$ST : Q_{ST} = E_{ST} \cdot A_{ST} \tag{4.40}$$
$$WT : W_W = E_W \cdot N_{WT} \tag{4.41}$$

Installed capacity: For each component, the energy production is equal or lower than its nominal capacity. In the case of energy storage, its stored energy must be equal or lower to their nominal capacity

$$u(\Gamma, d, h) \leq Cap(j) \; \forall \; \Gamma \in \{W/E, Q, R\}, j \in J, \; d \in D_{rep}, \; h \in H \tag{4.42}$$
$$S(j, d, h) \leq Cap(j) \forall \; j \in J, \; d \in D_{rep}, \; h \in H \tag{4.43}$$

Operational restrictions: Partial load PL of the engine in the case of the generator or the cogeneration module is considered by applying a binary variable Y_{ON} along with the $BigM$ number. In this way, the engine can modulate according to the expression:

$$W_{CM/GE} - PL \cdot Cap_{CM/GE} \geq - BigM \cdot (1 - Y_{ON}) \tag{4.44}$$
$$W_{CM/GE} \leq BigM \cdot Y_{ON} \tag{4.45}$$

4.3 Multiobjective optimization

Depending on the study, two different objective functions could be considered for the optimization of polygeneration systems: minimization of economic and/or

environmental costs. Nevertheless, the minimization of the economic costs is often opposite to the minimization of the environmental impact. Therefore, when both of them are going to be optimized, multi-objective optimization must be carried out, since it allows the optimization of contradictory criteria simultaneously. Thus, the aim is no longer seek to determine an optimal solution, but to find a set of compromise solutions instead (Yalaoui et al., 2013).

In order to carry out a multi-objective optimization, herein, a Pareto solution's set are found by means the ε-constraint method (Haimes et al., 1971). This means that different solutions can be obtained by optimizing one of the objective functions f_1 whereas the value of the other objective function f_2 is fixed in different selected sequential values. This procedure can be carried out as many times as required modifying the value of the objective function f_2 to create the Pareto front as it is shown in the Figure 4.4. The optimal solutions in between the single-objective optimization solutions ($Opt f_1$ and $Opt f_2$) are known as trade-off solutions or non-dominated solutions. These solutions define the Pareto front and the solutions above this curve are the dominated solutions.

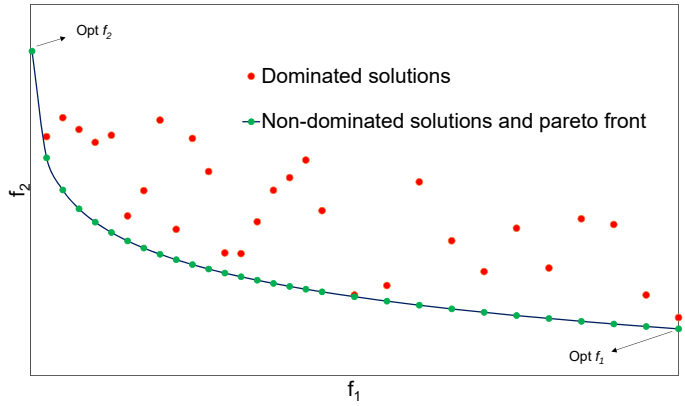

Figure 4.4: Pareto front.

4.4 Closure

This chapter starts from the explanation of the integrated design, synthesis and operation optimization (IDSOO) of polygeneration systems focused on the Mixed Integer Linear Programming (MILP) approach. As part of the *IDSOO* procedure, the superstructure which comprises the candidate technologies and the feasible connections between them is described in detail.Then, a Mixed Integer Linear Programming (MILP) model has been developed to carry out the optimization of the synthesis and operation of the energy systems for residential buildings simultaneously. The structure of the MILP model allows to address the optimization of polygeneration system for residential buildings for both grid connected and standalone energy systems. Besides, depending on the type of study, the model can be applied for both single or multiobjective optimization.

A comprehensive description of the MILP model is carried out starting from both objective functions considered herein namely the total annual cost and the total annual CO_2eq emissions. The objective functions are subject to different technical and physical restrictions such as the energy balance carried out in each node of the superstructure, the equipment efficiency considering the yield of each component, and operational restrictions such as the partial load of the engine, among others.

The MILP model could be considered the cornerstone of this work since all the studies carried out are based on the described model.

Chapter 5

Residential buildings as a microgrid

"Suddenly, you see the light."

According to the U.S Department of Energy, microgrid can be defined as "a group of interconnected loads and distributed energy resources within clearly defined electrical boundaries that acts as a single controllable entity with respect to the grid. A microgrid can connect and disconnect from the grid to enable it to operate in both grid-connected or island-mode" (Ton and Smith, 2012). Microgrids have been identified as a key component for improving power reliability and quality, besides they offer a viable solution for integrating Distributed Energy Resources (DERs), including in particular variable and unpredictable renewable energy sources, low-voltage and medium-voltage into distribution networks (Chauhan et al., 2020). However, this definition could be considered limited in the new worldwide perspective taking into account the recent works about smart energy systems which show the advantages of integrate different energy services beyond the electricity (Lund et al., 2017).

In the mainframe of microgrids, energy communities is a new arisen concept, which typically refers to the cooperation among the consumers (or prosumers), in order to accomplish the satisfaction of their communities (e.g. neighbourhood) energy needs using solely local production sources (Oleinikova and Hillberg, 2020). In this sense, residential buildings could be considered an energy community, and hence a microgrid.

Unlike previous works about microgrids and standalone energy systems, which only focus on the electricity load (Cagnano et al., 2020; Al-falahi et al., 2017), the design of energy systems for residential buildings usually takes into account several energy demands such as electricity, heating and cooling.

As a result, this chapter proposes the optimization of polygeneration systems for residential buildings, taking the residential building as an energy community or microgrid, considering different energy demands, i.e. electricity, heating and cooling. Thus, it is expected to find synergies between the electrical and thermal part in order to demonstrate the importance of having a wider perspective which include the entire energy demands in the design of energy systems for microgrids aiming to achieve more cost-effective alternatives.

However, for the sake of the clarity, this work focuses only on the design of energy systems. Electric and control operational issues with the grid are out of the scope of this work.

In order to research economic and environmental aspects to be considered in the pathway to evolve from the current energy systems for residential buildings towards energy communities or microgrids, the optimization of the polygeneration system for a residential building located in Zaragoza made up of 50 dwellings is addressed considering three cases:

1. **Conventional energy system as a reference case:** This case considers as conventional, a grid connected energy system made up of a gas boiler and a mechanical chiller to attend the heating and cooling demands of the residential building respectively. The electricity and cooling demands of the residential building fully depend on the electric grid. This means that, in case of any outage, the electricity and cooling demands cannot be attended. This is not a microgrid but it is considered a good reference system to compare the advantages of the subsequent energy systems.

2. **Grid connected polygeneration system:** In this case, the energy demands of the residential building could be attended by a polygeneration system connected to the grid. In this way, some electricity could be purchased from the grid when there is not enough production in the polygeneration system but the electricity sale to the grid is not allowed. As a result, the energy demands of the residential building depends also on the electric grid. However, in case of any outage, depending on the period of time, the polygeneration system could be or not enough to cover the energy demands. Therefore, the residential building is not considered a microgrid since can operate barely in island mode.

3. **Grid connected self-sufficient polygeneration system:** In this case the energy demands can be attended by the electric grid; nonetheless, in case of any outage, the residential building has a self-sufficient polygeneration system to cover all the energy demands. As a result, the residential building can be considered as a microgrid. The design of the polygeneration system is carried out not allowing the purchase of electricity from the grid in the peak days for summer ($d = 6$) and winter ($d = 14$). In this way, it is guaranteed the self-sufficiency of the polygeneration system for the residential building. The optimization is subject to:

$$E_p(6, h) = 0 \; \forall \; d \in D_{rep} \; \wedge \; h \in H \; peak \; day \; in \; summer \tag{5.1}$$

$$E_p(14, h) = 0 \; \forall \; d \in D_{rep} \; \wedge \; h \in H \; peak \; day \; in \; winter \tag{5.2}$$

Besides, the energy system must be connected to the grid in order to work as a microgrid. This means that the system must contract a power Pct from the grid. Therefore, the optimization must be also subject to:

$$Pct(d, h) > 0 \; \forall \; d \in D_{rep} \; \wedge \; h \in H \tag{5.3}$$

The above mentioned cases are studied under the assumption of the availability to access to the natural gas network.

Next, the $IDSOO$ process, explained in the previous chapter, is applied to the three above mentioned cases to obtain the optimal energy system to attend the energy demands of a residential building composed of 50 dwellings located in Zaragoza (Figure 2.14). The technical data for the equipment are presented in the chapter 2, the economic and environmental data for the equipment are presented in the Tables 2.10 and 2.11 respectively. Regarding the electric and fuel tariffs, they are presented in the Tables 2.13 and 2.15 respectively. Except for the conventional energy system, the superstructure depicted in the Figure 4.2 is optimized minimizing the total annual cost considering specific restrictions in accordance to the case of study.

5.1 Conventional energy system as a reference case

The Figure 5.1 shows the reference system configuration made up of the electric grid, a mechanical chiller and the gas boiler. From the operational point of view, the Figure 5.2 depicts the representative dynamical behaviour of the

conventional system in summer and winter days. In a summer day, the electricity demand E_d is covered only by the electric grid E_{pe} (Figure 5.2a) and the cooling demand R_d is covered by a mechanical chiller R_{mch} (Figure 5.2b) which in turn is driven by the electricity supplied by the grid E_{mch}. There is not space heating demand but domestic hot water demand, which is covered by the gas boiler. On the other hand, in a winter day, there are only electricity demand, which is covered by the electric grid (Figure 5.2c) and heating demand Q_d, which is covered by the gas boiler Q_{bq} (Figure 5.2d).

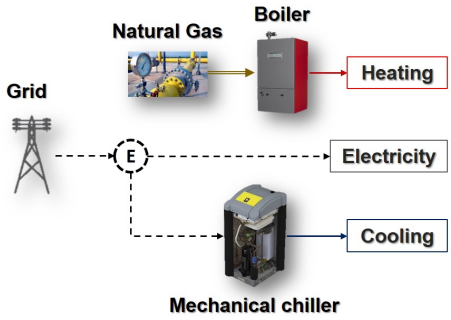

Figure 5.1: Conventional grid connected energy system configuration.

The Table 5.1 presents the results of the economic optimization of the conventional energy system. These results are used as a reference to evaluate the following cases.

5.2 Grid connected polygeneration system

The Figure 5.3 shows the optimal configuration of a grid connected polygeneration system. In this case, the electricity sale to the grid is not allowed and the electricity demand can be attended by the grid, the cogeneration module and/or the PV panels. The heating demand can be covered by the gas boiler, the heat pump (heating mode) and/or the cogeneration module. The cooling demand can be attended by the heat pump (cooling mode) and by the thermal energy storage for cooling.

The Table 5.2 presents the results of the economic optimization of the grid connected polygeneration system. In comparison with the conventional system, both the contracted power and the electricity consumption from the grid de-

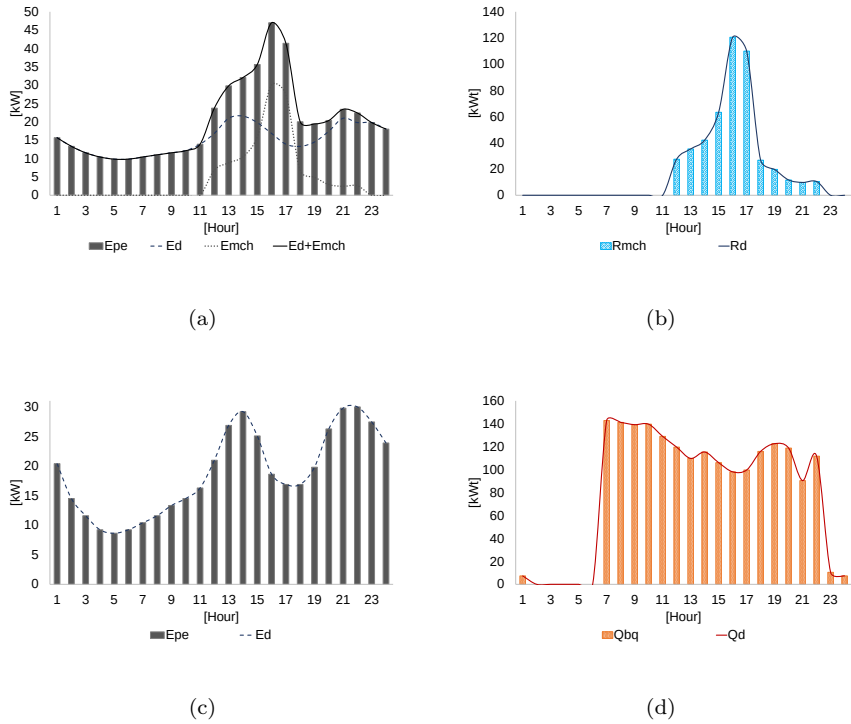

Figure 5.2: Optimal operation of a conventional energy system: a) Electricity operation in a summer day b) Cooling operation in a summer day c) Electricity operation in a winter day d) Heating operation in a winter day.

crease about 72%, whereas the natural gas consumption increases about 18%. In general terms, the total annual cost and the CO_2eq emissions are reduced about 16% and 10% respectively.

The Figures 5.6 and 5.5 show the operation of the grid connected polygeneration system in a summer and winter day respectively. In summer, the polygeneration system made up of the cogeneration module W_{ce}, PV panels W_{pve} and the electric grid E_{pe}, covers the electricity demand E_d but also run the heat pump in cooling mode E_{hp} (Figure 5.4a). In the morning, from 1 to 7 hours the electricity comes mainly from the grid E_{pe} due to the low elec-

Table 5.1: Results of the conventional energy system.

Technology	**Grid connected**		
	Install Cap	**CIA[€/yr]**	CO_2**fix [kg**CO_2eq**/yr]**
$Pct_{1,2,3}$ [kW]	$110.9_{1,2}$-20.8_3	-	-
Mch	362 kWt	22747	2603
GB	274 kWt	3824	137
	CIA / $CO2_{fix}$	*26571*	*2740*
	Annual operational costs		
Fuel	**Consumption [kWh/yr]**	**Energy cost [€/yr]**	CO_2**ope [kg**CO_2eq**/yr]**
Electricity	161495	42673	33341
Natural Gas	303757	18401	61663
	C_{ope}/ $CO2_{ope}$	*61074*	*95004*
	TAC/ TCE	**87645**	**97744**

Table 5.2: Results of the grid connected polygeneration system without electricity sale.

Technology	**Grid connected polygeneration system**		
	Install Cap	**CIA[€/yr]**	CO_2**fix [kg**CO_2eq**/yr]**
$Pct_{1,2,3}$ [kW]	$31.2_{1,2,3}$	-	-
CM	17 kWe	6254	111
PV	40 kW/255 m^2	6404	2053
Inv	48 kW	3296	912
HP	238 kWt	16654	1906
GB	126 kWt	1762	63
TSR	132 kWht	6445	819
	CIA / $CO2_{fix}$	*40814*	*5864*
	Annual operational costs		
Fuel	**Consumption [kWh/yr]**	**Energy cost [€/yr]**	CO_2**ope [kg**CO_2eq**/yr]**
Electricity	43087	10935	9184
Natural Gas	359592	21566	72997
	C_{ope}/ $CO2_{ope}$	*32501*	*82181*
	TAC/ TCE	**73315**	**88046**

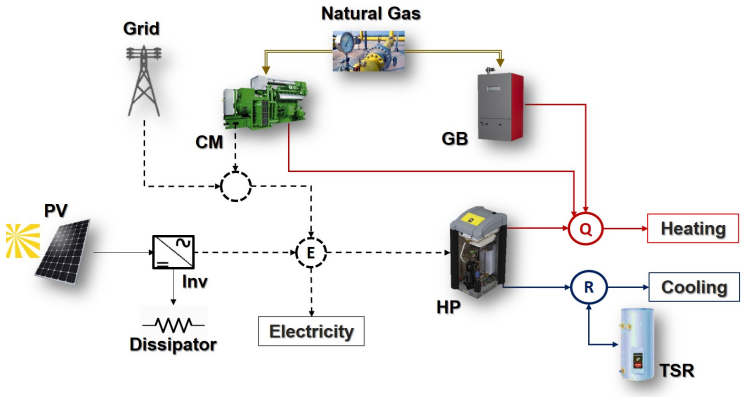

Figure 5.3: Optimal configuration of a grid connected polygeneration system without electricity sale.

tricity tariff. From 8 to 18 hours, the electricity comes mainly from the PV panels W_{pve}. Finally, from 19 to 24 hours, the electricity comes mainly from the cogeneration module W_{ce}. On the other hand, the Figure 5.4b depicts the operation of the polygeneration system to cover the cooling demand R_d. This is attended by the heat pump R_{hp}; however, the thermal energy storage TSR helps to cover the cooling demand in the hours 16, 17 and 20-22 R_{out}, taking advantage the energy stored R_{in} from the PV panels.

In winter, the Figure 5.5a depicts the electricity operation of the polygeneration system. From 1 to 8 hours the electricity comes mainly from the grid E_{pe} due to the low electricity tariff. From 9 to 18 hours the electricity comes from both the cogeneration module W_{ce} and the PV panels W_{pve}. Finally, from 19 to 24 the electricity comes from both the cogeneration module W_{ce} and the electric grid E_{pe}. The Figure 5.5b depicts the operation of the polygeneration system to cover the heating demand Q_d. This is attended by the heat pump Q_{hp}, the cogeneration module Q_{cq} and the gas boiler Q_{bq}. Note that the heat pump is driven mainly by the electric grid in the hours 7 and 8, and by the PV panels from 9 to 18 hours to take advantage the low electricity price.

It is worthy to say that the polygeneration system is not self-sufficient because it is not able to cover the peak demands without the electric grid support. In the summer peak day, the electricity peak is about 70 kWe (Figure 5.6a) and the total electricity capacity of the polygeneration system is about 57 kWe.

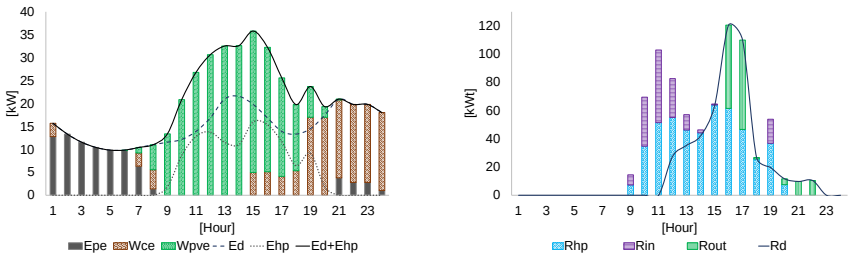

(a) (b)

Figure 5.4: Optimal operation of a grid connected polygeneration system: a) Electricity operation in a summer day b) Cooling operation in a summer day.

5.3 Grid connected self-sufficient polygeneration system

In this case the polygeneration system is connected to the grid but it is sized to be able of covering all energy demands of the building without support of the electric grid, i.e. it must be self-sufficient in island mode. Therefore, in this case it works as a microgrid. To do this, the superstructure (Figure 4.2) is optimized minimizing the total annual cost subject to the Eqs. 5.1, 5.2 and 5.3. The Table 5.3 presents the results of the optimal configuration of the grid connected self-sufficient polygeneration system without sale of electricity (Figure 5.7).

The total annual cost obtained increases about 5% with respect to the previous case, and the CO_2eq emissions decrease about 1.2%. Even so, this case is interesting since both the total annual cost and CO_2eq emissions of this alternative remains lower than the conventional system in about 12%. In terms of design and configuration, with respect to the previous case, the cogeneration module and PV capacities increase about 73% and 12% respectively. The heat pump capacity decreases about 28% whereas the gas boiler capacity increases about 24%. The batteries are selected but its capacity is negligible. Regarding the contracted power, it was reduced about 44% with respect to the previous case. In fact, it was selected the minimum available contracted power from the grid due to the restriction of being connected to the electric grid Eq. 5.3.

The Figure 5.8 allows the visualization of the operational behaviour of a

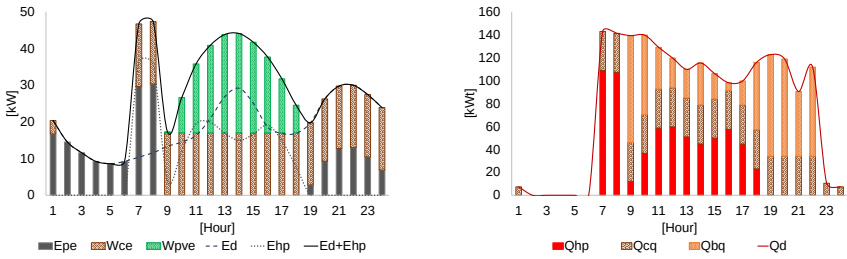

(a) (b)

Figure 5.5: Optimal operation of a grid connected polygeneration system: a) Electricity operation in a winter day b) Heating operation in a winter day.

residential building as a microgrid when the electricity sale to the grid is not allowed. The Figure 5.8a depicts the operation of the electricity demand in a winter day (no peak). Electricity from the grid E_{pe} covers most of the electricity demand E_d from 1 to 8 hours since is the lowest price of the electric tariff (See Table 2.13). The rest of day the cogeneration module W_{ce} covers most of the electricity demand E_d and run the heat pump E_{hp}, supported by the PV panels W_{pve} from 9 to 18 hours. On the other hand, the Figure 5.8b depicts the operation of the electricity demand in the peak day of winter. In this case, the electricity demand E_d and the electricity to run the heat pump E_{hp} is covered only by the cogeneration module W_{ce} along the day supported by the PV panels W_{pve} from 10 to17 hours. Thus, it is demonstrated that the polygeneration system is able to cover all the energy demands of the building in island mode in any time, thereby the building can be considered a microgrid.

As a result, the first conclusion of this analysis is that *under the current economic conditions, for a residential building located in Zaragoza is profitable to work as a microgrid with respect to the conventional system, but in comparison with the unrestricted grid connected polygeneration system (previous case), it is not enough profitable to work as a microgrid if it is not allowed to sell electricity.* On the other hand, based on the obtained results, an standalone system could be an interesting alternative since, apparently, the optimization of the studied energy system without the restriction Eq. 5.3 could lead "to leave the grid".

Consequently, the next questions arise:

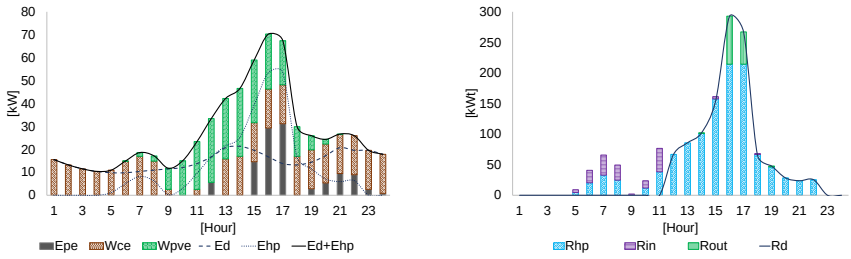

(a) (b)

Figure 5.6: Optimal operation of a grid connected polygeneration system in a peak summer day: a) Electricity operation- b) Cooling operation.

¿Which would be the sale electricity price to make the residential building profitable enough to work as a microgrid?.

¿How much is the cost to disconnect from the electric grid?

Grid connected self-sufficient polygeneration system allowing the sale of electricity

The former of the previous questions is answered in this subsection. Thus, the sale electricity price is evaluated from 0 up to a point when the grid connected self-sufficient polygeneration system is more profitable than the polygeneration system for a residential building not self-sufficient in which electricity sale is not allowed (section 5.2). This is achieved when the sale electricity price is about 75% of the purchase electricity price. The obtained optimal configuration is depicted in the Figure 5.9. Note that batteries are no selected at all.

The Table 5.4 presents the results of the optimal configuration of a grid connected self-sufficient polygeneration system when it is allowed the sale of electricity at 75% of the purchase price. Concerning the optimal configuration, the only difference with respect to the previous case (Grid connected self-sufficient polygeneration system without sale electricity option) is that the batteries have not been selected. However, the capacity of the different components change considerably. In this case, there is a remarkable increase in the PV capacity,

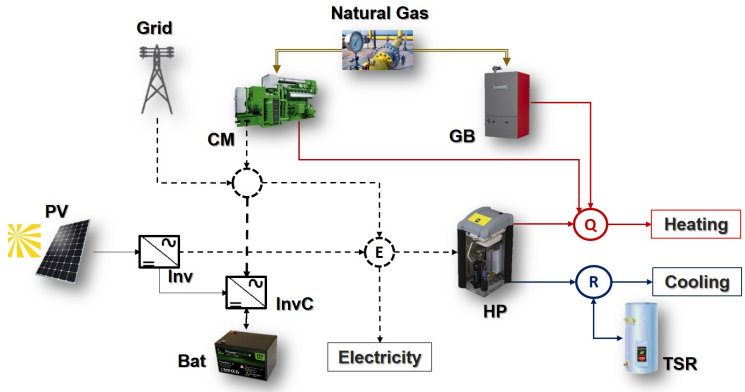

Figure 5.7: Optimal configuration of the grid connected self-sufficient polygeneration system without sale of electricity.

above 100%, since the electricity sale is allowed. For the same reason, the contracted power increases as well. The heat pump capacity increases about 63%, the thermal energy storage capacity for cooling decreases significantly, about 78%, whereas the gas boiler capacity remains approximately constant. Note that the net cost of the electricity bill is negative which is not allowed under the current Spanish self-consumption regulation. In this case we are not considering legal restrictions (they will be analysed in the chapter 7), but it is shown that they play an important role in both the design of polygeneration systems and the evaluation of the profitability of a microgrid. In environmental terms there is a CO_2eq emissions reduction of about 20% with respect to the reference conventional energy system, and about 10% with respect to the previous case of grid connected polygeneration system.

The Figure 5.10 allows the visualization of the operational behaviour of a residential building as a microgrid when the electricity is sold at 75% of the purchase electricity price. In both summer and winter days, most of the PV production is sold to the electric grid. As mentioned before, the contracted power increases in order to allow the sale of the PV production.

Table 5.3: Results of the Grid connected self-sufficient polygeneration system without electricity sale.

Technology	**Grid connected self-sufficient polygeneration system - Not sale**		
	Install Cap	**CIA[€/yr]**	CO_2**fix [kg**CO_2eq**/yr]**
$Pct_{1,2,3}$ [kW]	$17.3_{1,2,3}$	-	-
CM	29 kWe	10805	191
PV	45 kW/288 m^2	7294	2339
Inv	54 kW	3718	1029
HP	172 kWt	12045	1378
GB	156 kWt	2180	78
TSR	255 kWht	12454	1583
Bat LA	1 kWh	55	13
InvC	1 kW	128	15
	CIA / $CO2_{fix}$	*48609*	*6603*
Annual operational costs			
Fuel	**Consumption [kWh/yr]**	**Energy cost [€/yr]**	CO_2**ope [kg**CO_2eq**/yr]**
Electricity (Purchased)	26738	6273	**5799**
Electricity (Sold)	0	0	
Natural Gas	367326	22004	74567
	C_{ope}/ $CO2_{ope}$	*28277*	*80366*
	TAC/ TCE	**76886**	**86969**

Table 5.4: Results of the Grid connected self-sufficient polygeneration system selling electricity.

Technology	**Grid connected self-sufficient polygeneration system- Sale allowed**		
	Install Cap	**CIA[€/yr]**	CO_2**fix [kg**CO_2eq**/yr]**
$Pct_{1,2,3}$ [kW]	$43.6_{1,2}$ 17.3_3	-	-
CM	30 kWe	11021	195
PV	97 kW/622 m^2	15614	5007
Inv	116 kW	8036	2224
HP	280 kWt	19594	2242
GB	155 kWt	2164	77
TSR	55 kWht	2661	338
	CIA / $CO2_{fix}$	*59180*	*10089*
Annual operational costs			
Fuel	**Consumption [kWh/yr]**	**Energy cost [€/yr]**	CO_2**ope [kg**CO_2eq**/yr]**
Electricity (Purchased)	26026	8259	**-18368**
Electricity (Sold)	122704	20403	
Natural Gas	427423	25411	86767
	C_{ope}/ $CO2_{ope}$	*13267*	*68399*
	TAC/ TCE	**72447**	**78488**

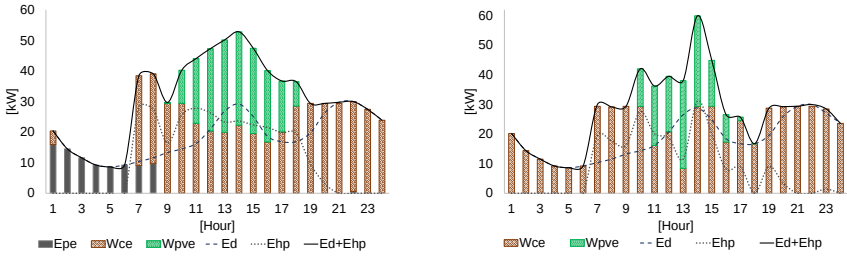

(a) (b)

Figure 5.8: Optimal operation of a residential building as a microgrid when electricity sale is not allowed: a) Electricity operation in a winter day (no peak) b) Electricity operation in the peak day of winter.

5.4 Standalone polygeneration system

The answer to the question *¿How much is the cost to disconnect from the electric grid?* is answered in this section. Based on the results obtained in the previous section, in this case the superstructure is optimized to obtain an energy system self-sufficient (Eqs. 5.1 and 5.2) but in this case it is not restricted to be connected to the electric grid, this means that:

$$Pct(d,h) \geq 0 \; \forall \; d \in D_{rep} \; \wedge \; h \in H \tag{5.4}$$

The Table 5.5 presents the results of the optimization considering the new contracted power constraint (Eq. 5.4). As expected, if the electricity sale is not allowed, it is not profitable for a self-sufficient energy system to be connected to the electric grid because of the fixed costs associated to the electric grid connection. However, it could be interesting to evaluate the profitability of the standalone energy systems taking into account that there is an interest in part of the society for "leaving the grid" (Khalilpour and Vassallo, 2015).

The total annual cost is about 13% lower than the conventional system; however, the CO_2eq emissions increase about 4%. This result shows the benefits of the electric grid in Spain (peninsula) in the aim to diminish the greenhouse gases emissions. However, it also turns out attractive leaving the grid, taking into account the volatility of the electricity prices and the resilience of the renewable

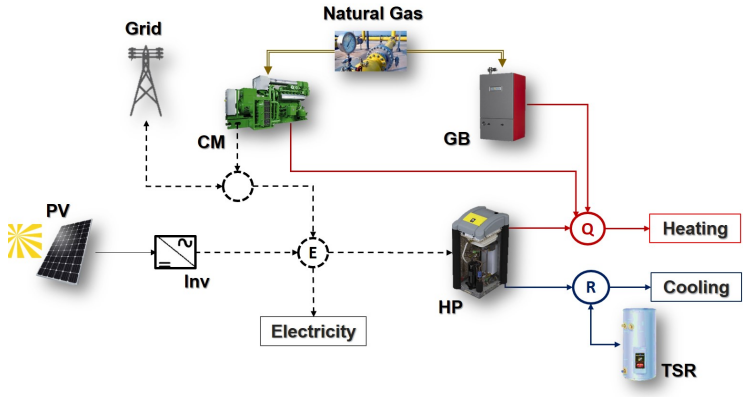

Figure 5.9: Grid connected self-sufficient polygeneration system allowing the sale of electricity.

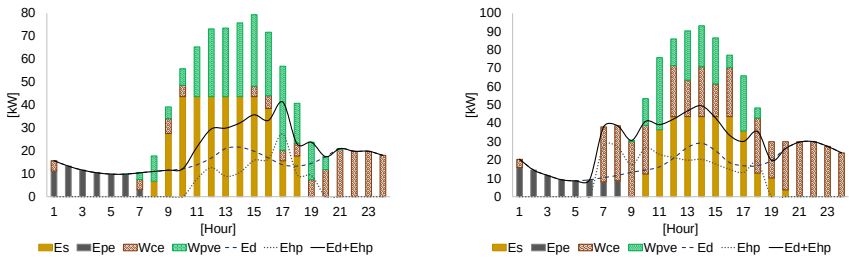

(a) (b)

Figure 5.10: Optimal operation of a residential building as a microgrid when the electricity is sold at 75% of the purchase electricity price: a) Electricity operation in a summer day b) Electricity operation in a winter day.

energy technologies. In fact, the Covid-19 crisis has shown the renewable energy technologies as the most resilient to the lockdown measures (IEA, 2020). Thus, in a near future, standalone polygeneration systems could be and interesting alternative from both economic and environmental point of view.

Table 5.5: Results of the standalone polygeneration system for a residential building.

Technology	**Standalone polygeneration system**		
	Install Cap	**CIA[€/yr]**	CO_2**fix [kg**CO_2eq**/yr]**
CM	30 kWe	10918	193
PV	41 kW/262 m^2	10918	2107
Inv	49 kW	3383	1565
HP	161 kWt	11236	1286
GB	155 kWt	2168	78
ACH	10 kWt	1470	86
TSR	252 kWht	12313	1565
Bat LA	1 kWh	34	8
InvC	0.5 kW	79	9
	CIA / $CO2_{fix}$	*48172*	*6268*
	Annual operational costs		
Fuel	**Consumption [kWh/yr]**	**Energy cost [€/yr]**	CO_2**ope [kg**CO_2eq**/yr]**
Natural Gas	469560	27799	95321
	C_{ope}/ $CO2_{ope}$	*27799*	*95321*
	TAC/ TCE	**75971**	**101588**

The Figure 5.11 depicts the optimal configuration of a standalone polygeneration system for a residential building. In this case the absorption chiller and the battery are selected in the optimal configuration. In terms of equipment capacity, the cogeneration module capacity up to 30 kWe along with the PV capacity of about 40 kW allow the polygeneration system to operate in island mode.

Concerning the energy storage, note that although the battery was selected in the optimal configuration, it could be disregarded as its capacity is only about 1 kWh. This is a very interesting result, since a battery bank is widely used in standalone energy systems because of its reliability and flexibility (Chauhan and Saini, 2014), but also it is one of the components to be reduced because of its high cost (Tawfik et al., 2018). The obtained results show the advantage of the thermal energy storage, in this case for cooling, in order to reduce (or avoid) the battery bank. Taking into account that electric and control operational issues are not considered in this study, it is not appropriate to talk about the total replacement of batteries in a standalone energy system; however, it claims the importance of considering thermal energy storage as a complement to achieve more cost-effective energy systems.

Consequently, the next chapter addresses the optimization of standalone

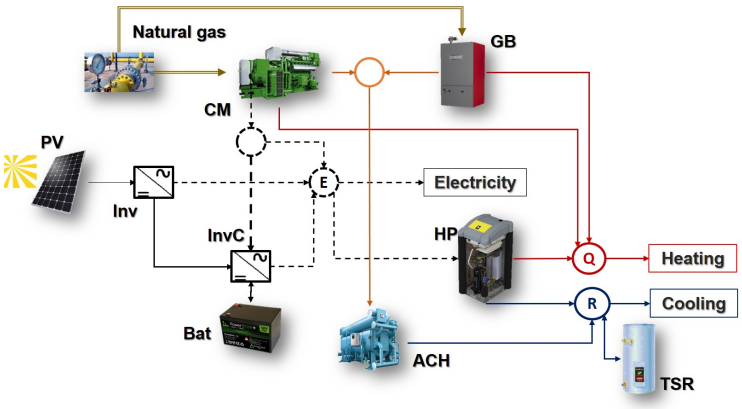

Figure 5.11: Standalone polygeneration system configuration.

polygeneration systems thoroughly in a systematic way in order to identify the synergies in the integration of electrical and thermal components for the design of polygeneration systems for residential buildings.

5.5 Closure

It was studied the feasibility of using residential buildings as a microgrid from the economic point of view. To this end, it was carried the optimization of energy systems for different cases from the conventional energy systems for residential buildings up to energy communities or microgrid. In general, the results have shown the profitability of polygeneration systems, highlighting the feasibility of the PV panels, the heat pump and thermal energy storage for cooling.

The deployment of energy buildings as microgrid is feasible from the economic point of view with respect to the current conventional energy systems but not in comparison with a grid connected polygeneration system not self-sufficient. In fact, the results could encourage to leave the electric grid, depending only in the natural gas network and renewable technologies. According to the results of the analysed case, only when the sale of electricity is allowed at about 75% of the purchased price, the polygeneration for a residential building as a microgrid starts to be profitable with respect to the unrestricted grid connected polygeneration system. However, for more accurate analyses, the evaluation could consider feed-in tariff schemes and/or legal restrictions.

Although a battery bank is widely used in standalone systems and microgrids, the results show that the integration of the thermal and electric parts allows to reduce the battery bank capacity. Since electrical and control issues were not considered in the optimization model, it is not appropriate to say that batteries can be avoided (although it was the obtained result), but it was demonstrated that they can be reduced when thermal energy storage, in this case for cooling, is considered. So, in general terms, the design of energy systems for residential buildings as a microgrid should be carried out taking into account not only electrical load, but all energy demands, i.e. electricity, heating and cooling in order to achieve more cost-effective alternatives.

According to the obtained results, technologies such as PV panels, reversible heat pumps and the thermal energy storage could be considered as interesting alternatives to reduce both the economic costs and CO_2eq emissions. Regarding PV panels, restrictions of space have not been considered in order to estimate the potential of this technology. However, this aspect should be considered when a particular project must be evaluated.

Chapter 6

Integration of thermal and electrical energy storage, and renewable energy resources in the design of the polygeneration systems

"A friendly hand...thanks Cabezudo."

The previous chapter studied the feasibility of using residential buildings as a microgrid from the economic point of view. Along the study, it was found, among other results, that a self-sufficient energy system could be an appealing alternative even off-grid, i.e. as a standalone energy supply system. Further, it was found an interesting result about the electrical and thermal energy storage. To be specific, the results showed that batteries were barely required in the optimal configuration of the polygeneration system and they were displaced/substituted by the cooling thermal energy storage. This is a very interesting result, since a battery bank is widely used in standalone energy systems because of its reliability and flexibility (Chauhan and Saini, 2014), but also it is one of the components aiming to be reduced owing to its high cost

(Tawfik et al., 2018). As shown in the previous chapter, in a polygeneration system there is a connection among thermal and electrical plant components, therefore this chapter aims to identify synergies between both parts in order to achieve a deeper understanding of the different technologies involved in a polygeneration system and their relations to achieve more cost-effective energy systems for residential buildings. This is addressed through the help of the thermoeconomic analysis, because it enables unveil the different internal costs within the energy system as well as the aspects that generate them. In this way, it is possible to better understand the relationship among the different plant components and evaluate their relations.

The chapter starts with a brief description of thermoeconomic analysis of energy systems. Different concepts such as productive structure and the definition of fuel and product in the system are highlighted. Then, different optimal configurations are obtained from the optimization of different superstructures which are becoming progressively more complex along the integration process of different candidate technologies. Finally, a sensitivity analysis of the natural gas price is carried out in order to evaluate different technologies that could be disregarded owing to its current high cost.

6.1 Thermoeconomic analysis of energy systems

Thermoeconomics is a technique which combines the thermodynamic analysis and economics with the purpose of revealing opportunities of energy and cost savings in the analysis, diagnosis, and optimization of energy conversion systems unveiling the internal costs of the system (Lozano and Valero, 1993; Serra, 1994; Bejan et al., 1996; El-Sayed, 2003). Although the first work about thermoeconomics is attributed to Keenan (1932), the works developed by Gaggioli (1961) and Tribus and Evans (1962) could be considered as the starting point of the real development of thermoeconomics (Valero et al., 2005). The main applications of the thermoeconomic analysis developed right now can be divided in: i) cost accounting, which calculates average costs and helps to provide rational cost assessment to the final products of energy systems (Lozano and Valero, 1993); ii) diagnosis of plants operation, which general objective is the detection of inefficiencies and calculation of their economic effects in operating plants (Lazzaretto et al., 2006); iii) the design and optimization of energy systems, which implies the selection of the design parameters of the system that minimize/maximize a specific objective function subject to different restrictions such as technical, economic, environmental, etc. (Lozano et al., 1996); iv) evaluation

of different design alternatives encompassing the selection of the plant structure (Guelpa and Verda, 2020). Thus, the thermoeconomic analysis is applied herein to calculate the costs of the internal mass and energy flows and final products, identifying the contribution of investment and operational costs in optimized standalone energy supply systems. The internal costs analysis unveils the resources consumed for each component and hence, enable the identification of possible synergies between components.

In the thermoeconomic analysis, a productive structure depicts a graphical representation of the resources distribution throughout the energy system. This is made up of productive units, which represent the energy transformation carried out in physical components (Figure 6.1), and junctions and branchings (Figure 6.2), which represent the possible structural interactions between mass and energy streams that are a consequence of the productive plant components interactions.

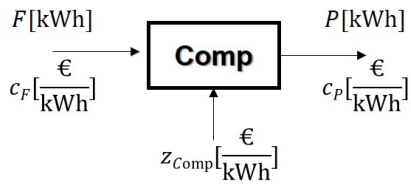

Figure 6.1: Scheme of a generic subsystem indicating fuel, product, unit thermoeconomic cost of fuel and product, and investment cost per kWh of product.

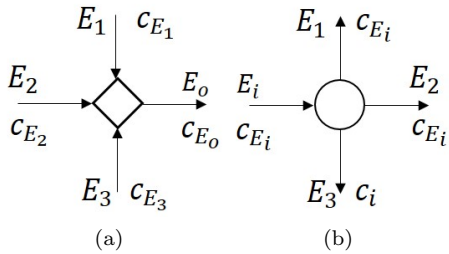

Figure 6.2: Structural interactions between energy streams: a) Junction; b) Branching.

The Figure 6.1 depicts the scheme of a generic subsystem or component ($Comp$) indicating fuel, product and investment cost per kWh. The production costs, which is a cost balance applied to the subsystem, can be expressed as:

$$c_P \cdot P = c_F \cdot F + z_{comp} \cdot P \tag{6.1}$$

$$z_{comp} = \frac{Investment\ cost}{\sum_{h=1}^{8760} P(h)} \tag{6.2}$$

Where in this chapter,
c_P is the unit cost of the product in €/kWh.
c_F is the unit cost of the fuel in €/kWh.
F is the annual fuel consumption in kWh.
P is the annual product in kWh.
z_{comp} corresponds to the annual investment cost of the component per unit of product obtained in €/kWh. In this work, the investment cost consists of the purchase costs of the component plus installation and maintenance costs.

This equation can be also read as:
$Product\ cost(€) = Operational\ costs(€) + Investment\ cost(€)$.
Therefore, the unit product cost is composed of both operational and investment unit costs.

This equation can also be written as:

$$c_P = c_F \cdot \frac{F}{P} + z_{comp} \tag{6.3}$$

$$c_P = c_F \cdot k_F + z_{comp} \tag{6.4}$$

Where, k_F is the unit energy consumption, which is the inverse of its efficiency.

In the case of junctions and branchings, as they are virtual components, one of their characteristics is that they do not have irreversibility. Thus, when a single stream is obtained by several streams (Junction), Figure 6.2a, the unit cost of the output stream can be calculated as:

$$c_{E_o} = \frac{\sum_i c_{E_i} \cdot E_i}{E_o} \tag{6.5}$$

Table 6.1: Annual energy demands for a residential building of 50 dwellings.

Energy service	Annual energy demand [kWh/yr]	% Energy service
Electricity E_d	146950	29.6%
Heating Q_d	291607	58.7%
Cooling R_d	58368	11.7%

On the other hand, when several streams are obtained from a single stream (Branching), Figure 6.2b, the unit cost of the output streams is the same as the inlet stream:

$$c_{E_i} = c_{E_1} = c_{E_2} = c_{E_3} = c_{E_n} \tag{6.6}$$

6.2 Energy systems integration in standalone energy supply systems for residential buildings

The aim of the energy supply system is to cover the energy demands of the residential building. The Table 6.1 presents de total energy demands with their respective weights with respect to the total energy demands of a residential building of 50 dwellings in Zaragoza. According to this, the heating demand doubles the electricity demand and triples the cooling demand approximately. In this sense, *the variation of the unit cost of each service will have an effect in the total cost proportional to the weight of each demand.*

The total annual cost TAC of the energy supply system consists of the operational cost due to the annual natural gas billing cost C_g and the investment annual cost CIA. The users must pay for them through the annual billings of the supplied energy services namely, electricity E_d, heating Q_d, and cooling R_d, at unit cost c_E, c_Q and c_R respectively.

$$TAC = C_g + CIA \tag{6.7}$$

$$TAC = \sum_{h=1}^{8760} [c_E(h) \cdot E_d(h) + c_Q(h) \cdot Q_d(h) + c_R(h) \cdot R_d(h)] \tag{6.8}$$

$$TAC = 146950 \cdot c_E + 291607 \cdot c_Q + 58368 \cdot c_R \tag{6.9}$$

Therefore, the effect of each energy service on the TAC can be calculated as:

$$\frac{\partial TAC}{\partial c_E} = 146950\ €/yr \tag{6.10}$$

$$\frac{\partial TAC}{\partial c_Q} = 291607\ €/yr \tag{6.11}$$

$$\frac{\partial TAC}{\partial c_R} = 58368\ €/yr \tag{6.12}$$

This means that a variation (+/-) in 0.01 €/kWh of the unit cost of the electricity, heating or cooling, leads to increase or decrease the TAC about 1470 €/yr, 2916 €/yr or 584 €/yr respectively.

The optimization of the energy supply systems for residential buildings starts from the superstructure definition described in the chapter 4. As mentioned before, a productive structure must be defined in order to carry out the thermoeconomic analysis. However, the productive structure does not match the physical structure of the energy system necessarily, as this depends on the level of aggregation or disaggregation required for the analysis. In this case, for instance, the Figure 4.2 represents the physical superstructure, whereas the Figure 6.3 depicts the productive superstructure.

Based on the energy demands of the residential building, the productive superstructure can be divided in three parts (Figure 6.3). The Electricity part (grey) is made up of the cogeneration module, photovoltaic panels, wind turbines and batteries. The heating part (red) is made up of heat pump, cogeneration module, gas boiler, biomass boiler, solar thermal collectors and thermal energy storage for heating. And the cooling part (blue) is made up of heat pump, absorption chiller and thermal energy storage for cooling.

The cogeneration module produces electricity W_c to attend the electricity demand or drive the heat pump and produces heat Q_c to drive the absorption chiller or to attend the heating demands. The heat pump is divided in two virtual components: HPQ produces heat Q_{HP} driven by the electricity W_{HPQ} and HPR produces cooling R_{HP} driven by the electricity W_{HPR}. Both electricity flows W_{HPQ} and W_{HPR} come from any component of the electricity part E_{HP}. The absorption chiller can be driven by the cogeneration module Q_{cr}, the gas boiler Q_{br} and/or the biomass boiler Q_{bbr} to produce cooling R_{ACH} to attend the cooling demand.

Given the superstructure depicted in the Figure 4.2, the objective is to identify and study the possible synergies between different components of the su-

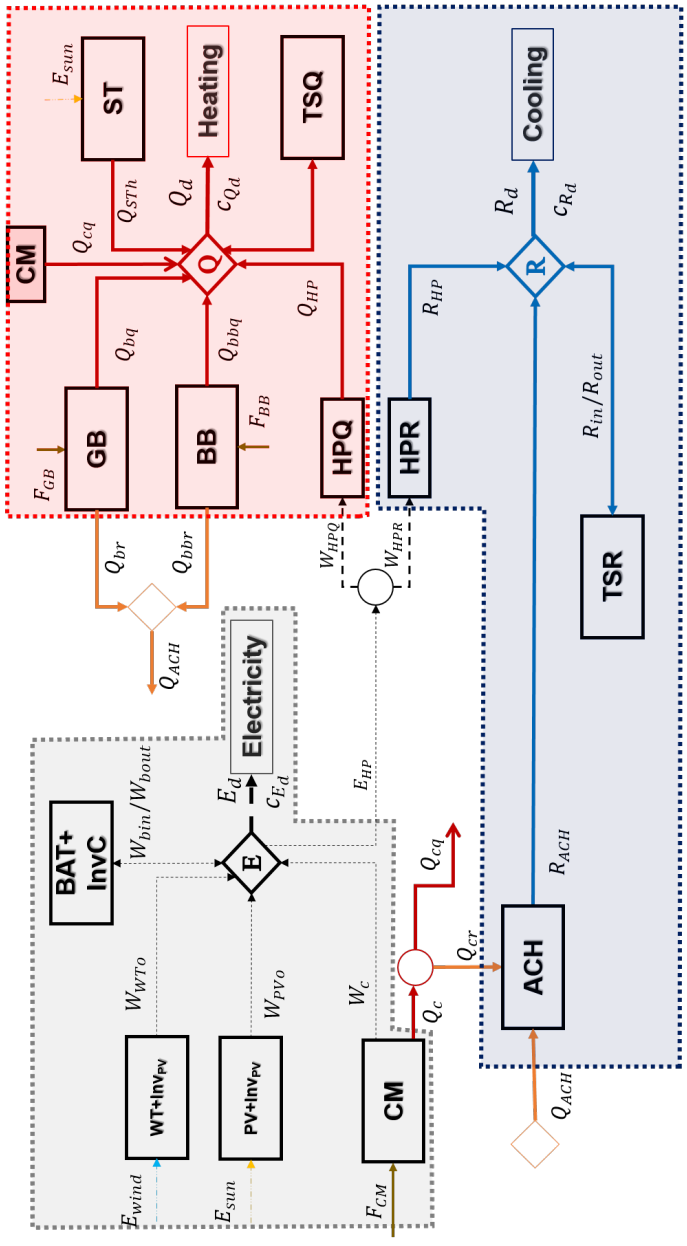

Figure 6.3: Superstructure parts.

perstructure, specially between the thermal and electrical parts. To this end, it is proposed to carry out a progressive integration of the different components, starting from a standalone conventional structure up to reach the complex physical superstructure corresponding to the Figure 4.2 without the electric grid (Chapter 4). In this case, the standalone conventional structure consists of a gas boiler to attend the heating demand, a mechanical chiller to attend the cooling demand and an electric generator to attend the electricity demand and drive the mechanical chiller. Besides, it comprises also batteries to guarantee the continuous energy supply to attend the energy demands.

The superstructure to be optimized is modified progressively from a conventional energy system up to include the entire candidate technologies. Firstly, a conventional standalone energy system is defined as a reference case (Standalone Reference system). As mentioned above, this is made up of an electric generator GE, a mechanical chiller Mch, a gas boiler GB and a battery bank BAT with its respective inverter charger, hereinafter called battery system. Then, the mechanical chiller is replaced by a reversible heat pump HP, this is the first energy system to be studied (Superstructure 1). From this point, different technologies are included progressively increasing the complexity of the superstructure. Thus, the aim is to explain why the optimal configuration changes from one to another along the progressive integration process based on the obtained results from the thermoeconomic analysis. Following, the sub-superstructures studied are defined (See Figure 6.4):

- ♦ Standalone Reference system: GE,Mch, GB and BAT.
- ♦ Superstructure 1: GE, HP, GB, BAT.
- ♦ Superstructure 2: GE, HP, GB, BAT, CM, ACH. The combination of CM and ACH is so-called $CCHP$ (Combined Cooling, Heat and Power).
- ♦ Superstructure 3: GE, $CCHP$, HP, GB, BAT and TES.
- ♣ Superstructure 4: $CCHP$, HP, GB, BAT, TES, BB and ST.
- ♣ Superstructure 5: $CCHP$, HP, GB, BAT, TES, BB, ST and WT.
- ★ Superstructure 6: $CCHP$, HP, GB, BAT, TES, BB, ST and WT and PV.

Along the study, the different configurations are optimized from the economic point of view and the analysis is carried out in annual basis. This means that

Superstructure Complexity		Candidate Technologies											
		Conventional System					CCHP		Thermal Energy Storage	Renewable Energy Technologies			
		GE	BAT	GB	Heat Pump								
					Cooling	Heating	CM	ACH	TS	Biomass	ST	WT	PV
	Reference System	✓	✓	✓	✓	-	-	-	-	-	-	-	-
	Superstructure 1	✓	✓	✓	✓	✓	-	-	-	-	-	-	-
	Superstructure 2	✓	✓	✓	✓	✓	✓	✓	-	-	-	-	-
	Superstructure 3	✓	✓	✓	✓	✓	✓	✓	✓	-	-	-	-
	Superstructure 4	×	✓	✓	✓	✓	✓	✓	✓	✓	✓	-	-
	Superstructure 5	×	✓	✓	✓	✓	✓	✓	✓	✓	✓	✓	-
	Superstructure 6	×	✓	✓	✓	✓	✓	✓	✓	✓	✓	✓	✓

Figure 6.4: Systematic integration of candidate technologies in the energy system.

the relation €/kWh in each energy flow $_y$ is based on the annual cost and the annual energy balance. The total unit cost c_y (Eq. 6.13) is presented separately, operational cF_y (Eq. 6.14) and investment z_y (Eq. 6.15) unit costs. In this way, it is easier to track the impact of each component in the total unit cost.

$$c_y = cF_y + z_y \tag{6.13}$$

$$cF_y = \frac{Annual\ Operational\ Costs\ [€]}{Annual\ Energy\ [kWh]} \tag{6.14}$$

$$z_y = \frac{Annual\ Investment\ Costs\ [€]}{Annual\ Energy\ [kWh]} \tag{6.15}$$

For the sake of clarity, as the entire thermoeconomic analysis is carried out in annual basis, the annual energy of a fuel $\sum_{h=1}^{8760} F(h)$ and the annual energy of a product $\sum_{h=1}^{8760} P(h)$, are expressed hereinafter simply by their corresponding variables F and P.

6.2.1 Standalone reference energy system

The energy supply system of the residential building must cover the electricity, heating and cooling demands. To do this, the standalone conventional system is made up of an electric generator GE to attend the electricity demand, gas boiler GB to attend the heating demand, and a mechanical chiller Mch to attend the cooling demand. The unit investment cost of the mechanical chiller is assumed to be the same that one of the heat pump. A battery bank is also required to guarantee the energy supply to the residential building. This is because the ratio between the maximum and minimum load is above the minimum partial

load of the engine. The Figure 6.5 shows the power required for electricity and cooling demands in the reference energy system for a summer day. Taking into account that the mechanical chiller is driven only by the generator, the cooling demand can be transformed directly in electricity demand. Since the electric generator is not allowed to run below 15% of its nominal capacity, a back-up system such as batteries is required in the time period from 2 to 9 hours. For the reference system, lead acid batteries are selected because they are the most mature and conventional technology in the market (Parra et al., 2017).

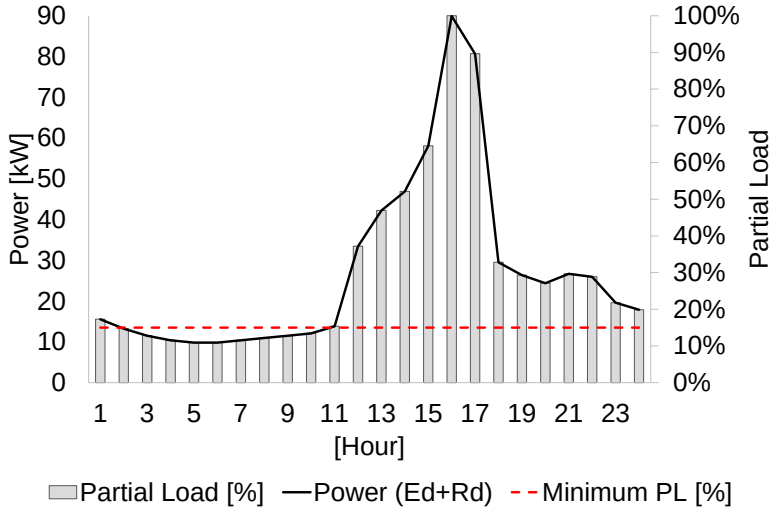

Figure 6.5: Power for electricity and cooling demands vs Partial load in the reference energy system for a summer day.

Economic optimization of the reference system: Table 6.2 presents the installed capacity, investment cost and fuel consumption of the optimal reference energy system. The total annual cost is distributed in 56% and 44% for operational and investment costs respectively (Figure 6.6a). Within the operational cost, 66% is to drive the GE and 34% to drive the GB (Figure 6.6c). Among

the investment costs, the mechanical chiller has the highest share with a 57%, followed by the GE with a 27%, GB 9% and the battery system 7% (Figure 6.6b). Concerning CO_2eq emissions, these are mainly due to the natural gas consumption since the embodied CO_2eq emissions are negligible (Figure 6.6d). Although the use of batteries is mainly due to technical reasons, the batteries also allow the reduction of the GE capacity from 90 kWe to 81 kWe, which is another advantage of the storage systems, they allow the reduction of the equipment capacity production. In this respect, it could be interesting to analyse the capacity factor (CF) of the equipment. First of all, the capacity factor can be defined as a measure of a power plant's actual generation compared to the maximum amount it could generate in a given period of time without any interruption (Morales Pedraza, 2019):

$$CF = \frac{Energy\ production\ [kWh]}{Time\ [h] \cdot Cap\ [kW]} \tag{6.16}$$

For a given energy production, the higher the equipment capacity, the lower the CF is, which means a lower profit of the equipment. Therefore, the use of energy storage systems could be an interesting alternative for both to reduce the equipment capacity and increase its profit. Based on the Eq. 6.16 the capacity factor of the different components of the standalone conventional energy system are calculated. Thus, the electric generator works the whole year producing 162700 kWh/yr with a CF about 0.23, the gas boiler works also the whole year producing 291607 kWht/yr with a CF about 0.12 and the mechanical chiller works four months of the year producing 58368 kWht/yr with a CF about 0.06. The obtained results allow a better approach to evaluate the potential use of other technologies.

In the Table 6.2 and hereafter, the total cost of the natural gas consumption includes the fixed cost whereas the cost of the natural gas consumption of the components, in this case the generator GE and gas boiler GB, corresponds only to the operational costs.

Internal unit costs of the reference system: The Figure 6.7 depicts the optimal configuration of the reference system with their respective annual unit costs. In the electricity part, the use of batteries increases in about 7% the unit cost of the produced electricity, which affect directly the unit cost of the electricity and cooling services. Note that the unit cost of the electricity produced by the electric generator depends highly on its energy efficiency since it consists of about 75% of operational costs and about 25% of investment costs.

Table 6.2: Results of the optimization of the reference system.

Technology	**Install Cap**	**CIA[€/yr]**	CO_2**fix** [kgCO_2eq/yr]
GE	81 kWe	11006	528
Mch	362 kWt	22747	2603
GB	274 kWt	3824	137
BAT LA	20 kWh	787	183
InvC	11 kW	1841	211
Investment annual cost / Embodied CO_2eq ***emissions***		*40204*	*3662*
Annual operational costs			
Fuel	**Consumption [kWh/yr]**	**Energy cost [€/yr]**	CO_2**fix** [kgCO_2eq/yr]
Natural Gas (NG)	884827	51336	179620
NG for GE	581070	32935	117957
NG for GB	303757	17217	61663
Operational Economic cost/ Operational CO_2eq emissions		*51336*	*179620*
Total Economic cost/ Total CO_2eq emissions		**91541**	**183282**

Table 6.3: Unit cost of each energy service for the optimal reference energy system.

Energy service	cF_y**[€/kWh]**	z_y **[€/kWh]**	c_y **[€/kWh]**
c_E	0.2088	0.0844	***0.2932***
c_Q	0.0604	0.0131	***0.0735***
c_R	0.0522	0.4108	***0.4630***

This is the unit cost of electricity stored by the battery W_{bin}, however these ratios change significantly in the unit cost of the electricity discharged by the battery system W_{bout} which consists of about 22% of operational costs and 78% of investment cost, which demonstrated the high impact of the investment cost of the battery system on the unit cost of the electricity. For the heating part is clear the effect of the efficiency of the GB in the unit cost of the heating service since operational unit cost is about 82% of the total unit cost. In contrast, the unit cost of the cooling service depends strongly on the investment cost, because this is about 89% of the total unit cost; nonetheless it should be highlighted the effect of the EER in the operational cost, reducing about 75% the operational unit cost when the electricity is converted into cooling.

The Table 6.3 summarizes the unit costs of each energy service for the reference energy system. These values are taken as a reference to compare the different configurations, and also are used as reference values for the allocation cost in the $CCHP$ module.

The economic and environmental data of the reference system are used to

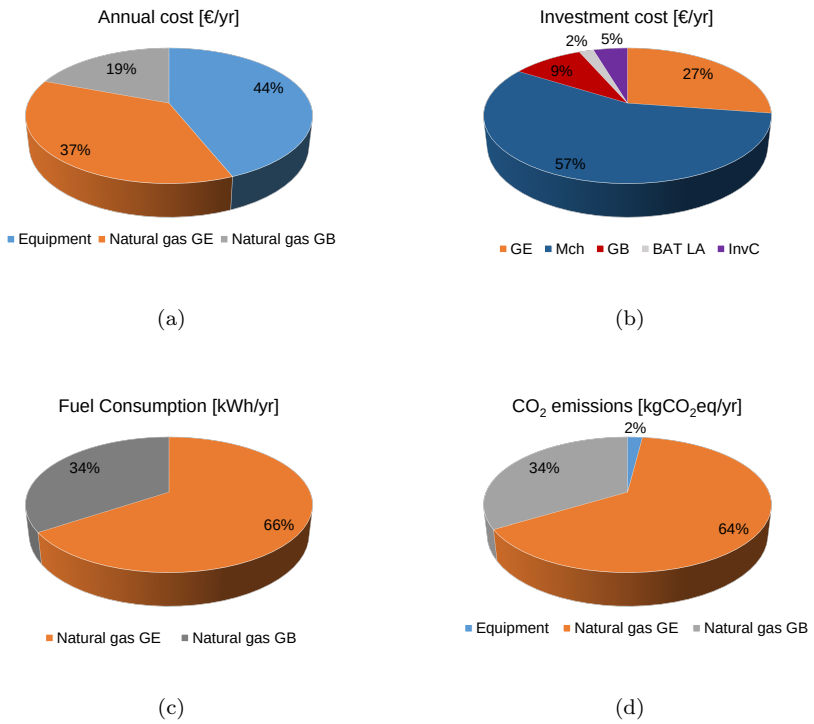

Figure 6.6: Standalone reference system. Breakdown of: a) Total annual cost, b) Investment cost, c) Fuel consumption, d) CO_2eq emissions.

evaluate the different configurations obtained through the systematic analysis.

6.2.2 Superstructure 1: GE, HP, GB, BAT.

In this case, the mechanical chiller Mch is replaced by a reversible heat pump HP and both lead acid (LA) and lithium-Ion (Li-Ion) batteries are considered as candidate technologies in the superstructure. Thus, the HP enables a stronger connection of the electrical and thermal part. In turn, the HP is divided in two virtual components: HPQ to produce heating in winter and HPR to produce cooling in summer (Pina, 2019). Therefore, the resources consumed by the HP

Figure 6.7: Optimal configuration of the standalone reference energy system.

must be distributed in its virtual components (Figure 6.8).

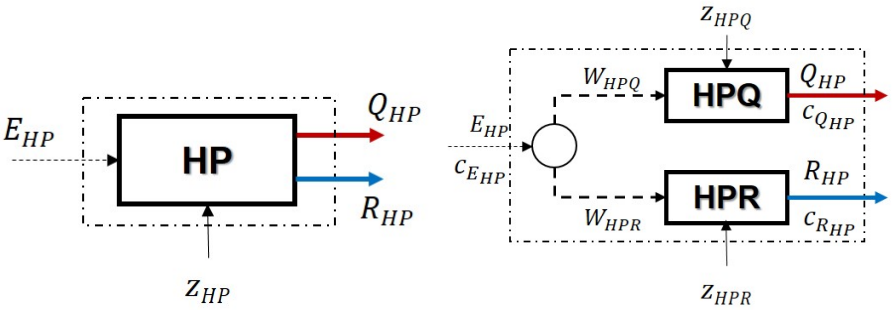

Figure 6.8: Scheme of the heat pump indicating fuel, product and investment costs per kWh: a) Physical structure; b) Productive structure.

The distribution of the costs is carried out based on the Eq. 6.4, as follows:

$$c_{Q_{HP}} = \frac{c_{E_{HP}}}{COP} + z_{HPQ} \tag{6.17}$$

$$c_{R_{HP}} = \frac{c_{E_{HP}}}{EER} + z_{HPR} \tag{6.18}$$

In turn, the distribution of the investment cost of the heat pump $Invest_{HP}$ is distributed in the virtual heat pumps HPQ and HPR proportionally to their annual productions, as follows:

$$Invest_{HP} = z_{HPQ} \cdot Q_{HP} + z_{HPR} \cdot R_{HP} \tag{6.19}$$

$$\frac{z_{HPQ}}{z_{HPR}} = \frac{Q_{HP}}{R_{HP}} \tag{6.20}$$

The unit cost of the products of the virtual heat pumps are obtained by solving the equations 6.17-6.20

Economic optimization of the superstructure 1: Table 6.4 presents the installed capacity, investment cost and fuel consumption of the optimal energy

Table 6.4: Results of the optimization of the superstructure 1.

Technology	**Install Cap**	**CIA[€/yr]**	CO_2**fix [kg**CO_2eq**/yr]**
GE	82 kWe	11091	532
HP	325 kWt	22747	2603
GB	73 kWt	1022	37
BAT LA	19 kWh	729	170
InvC	10 kW	1707	195
Investment annual cost / Embodied CO_2eq ***emissions***		*37296*	*3537*
	Annual operational costs		
Fuel	**Consumption [kWh/yr]**	**Energy cost [€/yr]**	CO_2**fix [kg**CO_2eq**/yr]**
Natural Gas (NG)	892302	51760	181137
NG for GE	642551	36420	130438
NG for GB	249751	14156	50700
Operational Economic cost/ Operational CO_2eq emissions		*51760*	*181137*
Total Economic cost/ Total CO_2eq emissions		**89056**	**184674**

system when the reversible HP, producing heating in winter and cooling in summer, is considered. In general terms, the total annual cost TAC is reduced only about 2.7% and the CO_2eq emissions increase about 0.8 % with respect to the reference system. The TAC is distributed in 58% for operational costs and 42% for investment costs (Figure 6.9a). Concerning the operational costs or fuel consumption, the total natural gas consumption increases with respect to the reference system, because the increase of the fuel by the GE is higher than the fuel reduction by the GB. Within the operational costs, the natural gas is distributed in 72% for the GE and 28% for the GB (Figure 6.9c). Regarding the design, the capacity of the GB decreases about 70% which is reflected in the investment cost breakdown. The share of the GB in the investment cost decreases about 6% with respect to the reference system, whereas the share of the HP investment cost increases about 4% with respect to the mechanical chiller in the reference system (Figure 6.9b). The CO_2eq emissions in this case are distributed in 71% due to the fuel combustion in the GE, 27% due to the fuel combustion in the GB, and 2% due to the embodied CO_2eq emissions in the equipment (Figure 6.9d).

Internal unit costs of the standalone energy system 1: The Figure 6.10 depicts the optimal configuration of the reference system with their respective annual unit costs. Unlike the reference system, the unit cost of the heating service depends on both GB and HPQ. In general terms, the unit cost of the electricity and cooling services decrease about 3% and 38% respectively, whereas the unit cost of the heating service increases about 42% with respect to

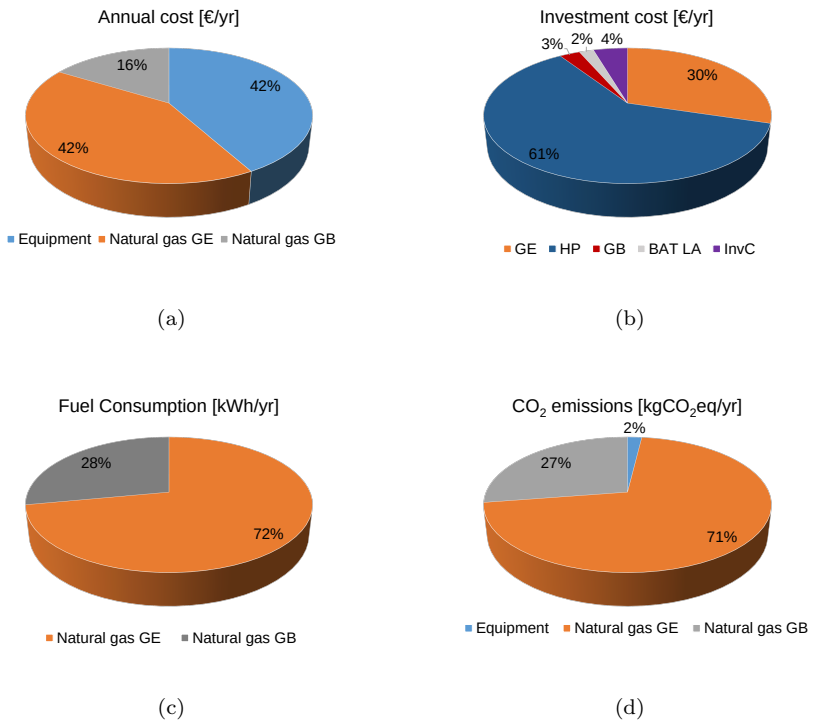

Figure 6.9: Standalone energy system 1. Breakdown of: a) Total annual cost, b) Investment cost, c) Fuel consumption, d) CO_2eq emissions.

the reference system. Even so, the reduction of the total annual cost in absolute terms is about 2000 €. This is due to the relative weight of each energy service in the total annual cost (Eq. 6.9). Note that the reduction of the unit cost of electricity is because the energy stored and delivered by the batteries is reduced with respect to the reference scenario and the unit cost of the battery system is also reduced. As a result, the ratio W_{bout}/W_{ce} decreases, and hence the unit cost of the battery system has a lower impact on the electricity unit cost.

Table 6.5 presents the unit cost of each energy service for the optimal standalone energy system 1. The main difference with respect to the reference scenario is in the heating service unit cost which increases about 42% due to

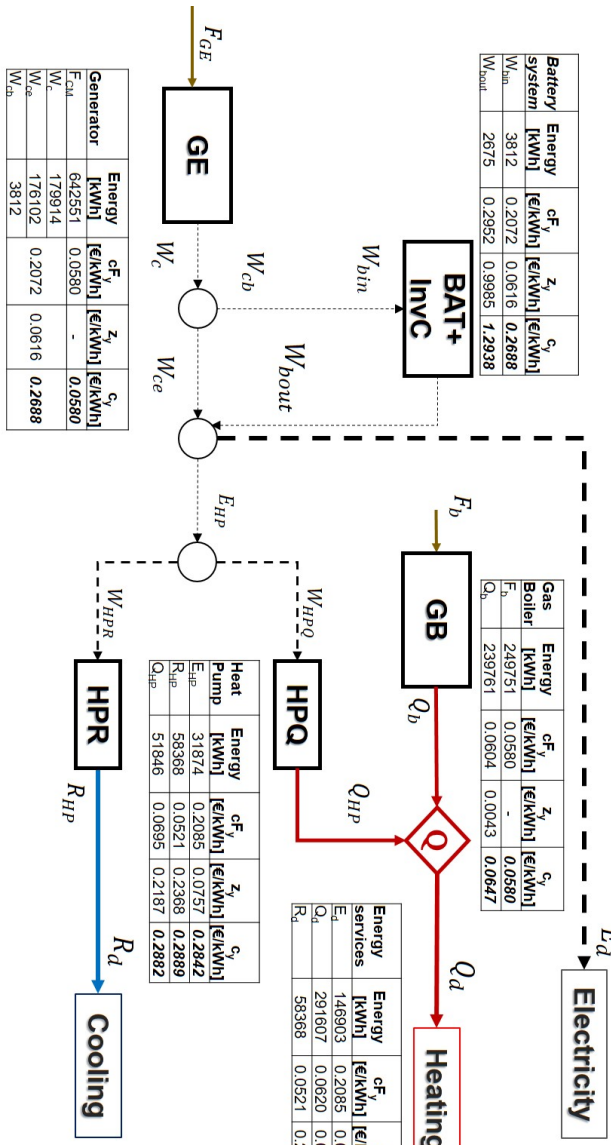

Figure 6.10: Optimal configuration of the standalone energy system 1.

Table 6.5: Unit cost of each energy service for the optimal standalone energy system 1.

Energy service	cF_y[€/kWh]	z_y [€/kWh]	c_y [€/kWh]
c_E	0.2085	0.0757	***0.2842***
c_Q	0.0620	0.0424	***0.1044***
c_R	0.0521	0.2368	***0.2889***

the contribution of the reversible heat pump in the investment cost. Note that the unit investment cost of the heating service is about three times the value of the reference system. On the other hand, the unit cost of the cooling service decreases significantly with respect to the reference system because the investment cost of the heat pump is distributed in both heating and cooling production.

Although the unit cost of the heating service increases, it must be highlighted the advantage of using a reversible heat pump in an energy system for residential building. It allows a better use of investment cost, since the same component produces both heating (in winter) and cooling (in summer). In addition, it enables the reduction of the gas boiler capacity, and hence the reduction of the total investment cost.

6.2.3 Superstructure 2: GE, $CCHP$, HP, GB, BAT.

In this case, the Combined Cooling Heating and Power $CCHP$ made up of the cogeneration module CM and the absorption chiller ACH is included in the superstructure. However, the results of the optimization deliver the same configuration, design and operation than the one of the previous energy system obtained when optimizing the superstructure 1.

6.2.4 Superstructure 3: GE, $CCHP$, HP, GB, BAT and TES.

Now, besides the $CCHP$, the thermal energy storage for heating and cooling are also included as candidate technologies in the superstructure.

Economic optimization of the superstructure 3: The Table 6.6 presents the installed capacity, fuel consumption and operational and investment costs of the optimal energy system. Concerning the optimal configuration, in this case the CM is profitable as a prime mover and a battery system is not required.

Table 6.6: Results of the optimization of the superstructure 3.

Technology	**Install Cap**	**CIA[€/yr]**	CO_2**fix [kg**CO_2eq**/yr]**
CM	36 kWe	13077	231
HP	84 kWt	5859	670
GB	127 kWt	1773	63
ACH	91 kWt	12865	751
TSR	229 kWht	11154	1418
Investment annual cost / Embodied CO_2eq ***emissions***	*44728*	*3134*	
Annual operational costs			
Fuel	**Consumption [kWh/yr]**	**Energy cost [€/yr]**	CO_2**fix [kg**CO_2eq**/yr]**
Natural Gas (NG)	626668	36704	127214
NG for CM	622051	35258	126276
NG for GB	4617	262	937
Operational Economic cost/ Operational CO_2eq emissions	*36704*	*127214*	
Total Economic cost/ Total CO_2eq emissions	**81432**	**130348**	

The selection of the $CCHP$ along with the thermal energy storage for cooling increases the use of the engine and overcome the technical issues regarding the partial load, explained before in the reference system. Thus, a battery bank is not required in this case.

In general terms, there is a remarkable reduction in both total annual cost and CO_2eq emissions of about 11% and 29% with respect to the reference system.

The total annual cost is distributed in 45% and 55% for operational and investment costs respectively (Figure 6.11a).Within the operational costs, most of them are due to the natural gas consumption to drive the cogeneration module. It could be said that the fuel consumption of the gas boiler is marginal (Figure 6.11c). It must be highlighted that this configuration is much more efficient since it allows a remarkable reduction of the natural gas consumption of about 30% with respect to the reference system. *This is one of the advantage of the polygeneration systems, in this case, represented by the* $CCHP$ *system.* Among the investment costs, the cogeneration module and the absorption chiller ($CCHP$) have the highest share with about 58%, followed by the TSR 25%, HP 13% and the GB 4% (Figure 6.11b). Concerning CO_2eq emissions these are mainly on account of the natural gas consumption of the cogeneration module since the CO_2eq emissions due to the natural gas for the gas boiler and the embodied CO_2eq emissions are negligible (Figure 6.11d).

Internal unit costs of the standalone energy system 3: The issue of cost allocation emerges when there is a system producing different products. This is important since the manner in which cost allocation is made will not only affect

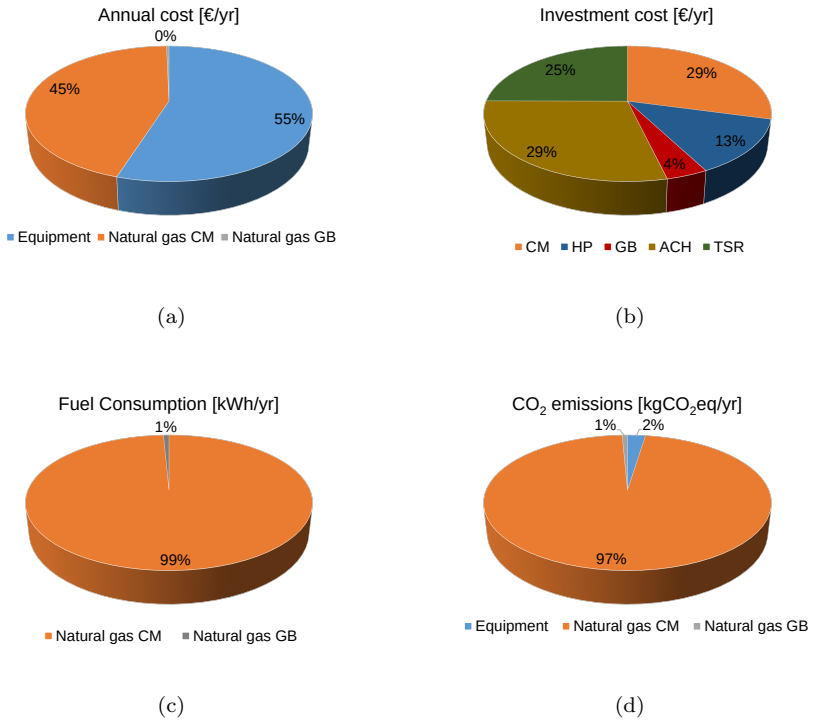

Figure 6.11: Standalone energy system 3. Breakdown of: a) Total annual cost, b) Investment cost, c) Fuel consumption, d) CO_2eq emissions.

the cost of the products but also the information provided to the consumers, which can affect their behaviour (Carvalho, 2011). In this case, the cost allocation process is more complicated with respect to the previous scenarios. This is because the CM produces both electricity and heat, which in turn can drive the absorption chiller and the heat pump. Therefore, the unit cost of the energy services depend strongly on the criteria used to allocate the costs. Taking into account this statement, two different productive structures have been defined in order to visualize the advantage and disadvantage of each one. The productive structure 3-A which considers the $CCHP$ as a subsystem and the productive structure 3-B which defines a subsystem made up of the $CCHP$, the heat pump

and the thermal energy storage for cooling. Both subsystems could be considered as trigeneration systems since they produce electricity, heating and cooling from an unique fuel.

Productive structure 3-A: The Figure 6.12 shows the productive structure of the optimal configuration considering the $CCHP$ as a subsytem enclosed in the control volume $CV-A$. To do this, two virtual absorption chillers $ACH1$ and $ACH2$ are defined. The $ACH1$ is part of the $CCHP$ subsystem driven by the cogeneration module. Thus, the expression to calculate the production costs can be expressed as:

$$\begin{aligned} &c_{W_c} \cdot W_c + c_{Q_{cq}} \cdot Q_{cq} + c_{R_{ACH1}} \cdot R_{ACH1} = \\ &c_{F_{CM}} \cdot F_{CM} + z_{CM} \cdot W_c + z_{ACH1} \cdot R_{ACH1} \end{aligned} \tag{6.21}$$

In order to determine the unit cost of the products, it is proposed to apply the same discount ϱ to all cogenerated products which cross the control volume $CV-A$, in this case W_c, Q_{cq} and R_{ACH1} with respect to their corresponding reference costs obtained in the reference system:

$$\varrho = 1 - \frac{c_{W_c}}{c_{W_{ref}}} = 1 - \frac{c_{Q_{cq}}}{c_{Q_{ref}}} = 1 - \frac{c_{R_{ACH1}}}{c_{R_{ref}}} \tag{6.22}$$

On the other hand, the $ACH2$ is driven by the gas boiler. The cooling produced by both virtual absorption chillers can attend directly the cooling demand R_{ACH_r} or can be stored R_{ACH_TSR}. However, according to the optimal operation of the system throughout the year, the absorption chiller is driven only by the cogeneration module since $Q_{br} = 0$.

The internal costs are presented in the Figure 6.12. The investment cost of the CM is about 19% higher than the GE in the reference system, with the advantage of producing both electricity and heat. Further, the heat produced can be used to attend the heating demands and/or drive the absorption chiller ACH. Therefore, in this case, the operational and investment costs of the CM and ACH are distributed among the electricity, heating and cooling services crossing the border of CV-A. In effect, the unit cost of the electricity, heating and cooling energy flows from the control volume are lower than those obtained in the reference system; even so the unit cost of the heating and cooling services are higher than those obtained in the reference system. Therefore, a new level of aggregation could be applied in order to obtain a fairer unit cost of the

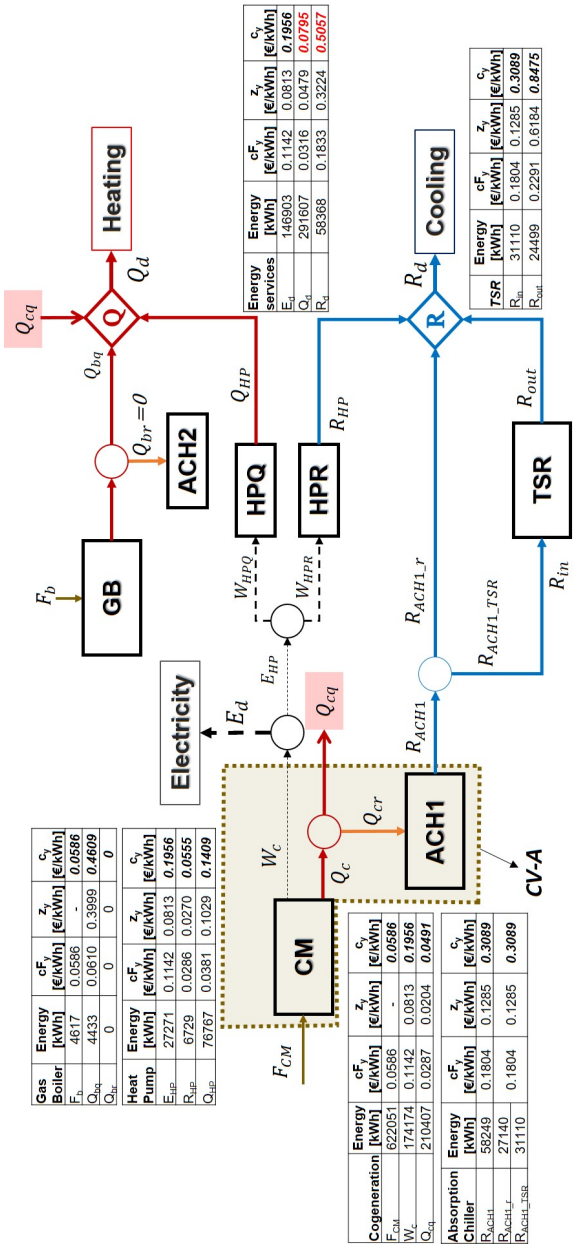

Gas Boiler	Energy [kWh]	cF_y [€/kWh]	z_y [€/kWh]	c_y [€/kWh]
F_b	4617	0.0586	-	*0.0586*
Q_{bq}	4433	0.0610	0.3999	*0.4609*
Q_{br}	0	0	0	*0*

Heat Pump	Energy [kWh]	cF_y [€/kWh]	z_y [€/kWh]	c_y [€/kWh]
E_{HP}	27271	0.1142	0.0813	*0.1956*
R_{HP}	6729	0.0286	0.0270	*0.0555*
Q_{HP}	76767	0.0381	0.1029	*0.1409*

Energy services	Energy [kWh]	cF_y [€/kWh]	z_y [€/kWh]	c_y [€/kWh]
E_d	146903	0.1142	0.0813	*0.1956*
Q_d	291607	0.0316	0.0479	*0.0795*
R_d	58368	0.1833	0.3224	*0.5057*

TSR	Energy [kWh]	cF_y [€/kWh]	z_y [€/kWh]	c_y [€/kWh]
R_{in}	31110	0.1804	0.1285	*0.3089*
R_{out}	24499	0.2291	0.6184	*0.8475*

Cogeneration	Energy [kWh]	cF_y [€/kWh]	z_y [€/kWh]	c_y [€/kWh]
F_{CM}	622051	0.0586	-	*0.0586*
W_c	174174	0.1142	0.0813	*0.1956*
Q_{cq}	210407	0.0287	0.0204	*0.0491*

Absorption Chiller	Energy [kWh]	cF_y [€/kWh]	z_y [€/kWh]	c_y [€/kWh]
R_{ACH1}	58249	0.1804	0.1285	*0.3089*
R_{ACH1_r}	27140	0.1804	0.1285	*0.3089*
R_{ACH1_TSR}	31110			

Figure 6.12: Productive structure 3-A.

energy services. However, it can be observed that useful information related to the energy system integration is unveiled with this productive structure 3-A. For instance, the thermal energy storage for cooling TSR displaces the use of batteries to overcome technical issues as the unit cost of the energy delivered by the thermal energy storage for cooling is about 34% lower than the electricity discharged by the battery system in the previous energy supply system (from the superstructure 1). Note that, even so, the unit cost of the cooling service increases about 75% especially due to thermal energy storage for cooling. Nonetheless, as the relative weight of the cooling service is much lower than the electricity service in the total annual cost (Eq. 6.9), it remains profitable the use of the thermal energy storage for cooling instead of the battery system. As a result, from the thermoeconomic analysis is also demonstrated the advantages of the integration of the thermal and electrical parts to achieve more cost-effective energy supply systems.

On the other hand, although the unit cost of the cooling production of the heat pump decreases substantially, the unit cost of the heating production remains higher than the reference system. Thereby, as mentioned before, aiming to obtain a fairer unit cost of the energy services (lower than the reference system), a new level of aggregation will be applied.

Productive structure 3-B: The unit cost of the energy services should be lower than the unit costs of the reference energy system in order to contribute to the acceptance of the more complex but more efficient energy systems by users which is essential for the success of such systems (Carvalho, 2011). Bearing in mind this statement and based on the results obtained from the productive structure 3-A, the Figure 6.13 shows the productive structure 3-B which defines a subsystem made up of the $CCHP$, the heat pump and the thermal energy storage for cooling enclosed in the control volume $CV - B$. In addition to the virtual absorption chillers mentioned in the previous productive structure, two virtual thermal energy storage for cooling $TSR1$ and $TSR2$ are defined. The $TSR1$ stores the energy flow R_{ACH1_TSR1} which comes from the cogeneration module through the absorption chiller $ACH1$. On the other hand, the $TSR2$ would store the energy flows R_{ACH2_TSR2} and R_{HP_TSR2} coming from the absorption chiller $ACH2$ and the heat pump respectively. However, the optimal operation of the system along the year has shown that both $ACH2$ and $TSR2$ are not required in this case. Thus, in this case the expression to calculate the production costs can be expressed as:

Table 6.7: Unit cost of each energy service for the Productive structure 3-B.

Energy service	cF_y[**€/kWh**]	z_y [**€/kWh**]	c_y [**€/kWh**]
c_E	0.1171	0.1381	***0.2552***
c_Q	0.0299	0.0402	***0.0700***
c_R	0.1849	0.2180	0.4030

$$\begin{aligned} & c_{W_{c-E_d}} \cdot W_{c-E_d} + c_{Q_{cq}} \cdot Q_{cq} + c_{R_{ACH1\_r}} \cdot R_{ACH1\_r} + \\ & + c_{Q_{HP}} \cdot Q_{HP} + c_{R_{HP}} \cdot R_{HP} + c_{R_{out1}} \cdot R_{out1} = \\ & c_{F_{CM}} \cdot F_{CM} + z_{CM} \cdot W_c + z_{ACH1} \cdot R_{ACH1} + z_{HPQ} \cdot Q_{HP} + \\ & + z_{HPR} \cdot R_{HP} + z_{TSR1} \cdot R_{out1} \end{aligned} \tag{6.23}$$

In order to determine the unit cost of the products, it is proposed to apply the same discount ϱ to all cogenerated products crossing the border of the control volume $CV - B$, in this case W_c, Q_{cq}, Q_{HP}, R_{HP}, R_{ACH1_r} and R_{out1} with respect to their corresponding reference costs obtained in the reference system:

$$\begin{aligned} \varrho =& 1 - \frac{c_{W_{c-E_d}}}{c_{W_{ref}}} = 1 - \frac{c_{Q_{cq}}}{c_{Q_{ref}}} = 1 - \frac{c_{Q_{HP}}}{c_{Q_{ref}}} \\ & = 1 - \frac{c_{R_{HP}}}{c_{R_{ref}}} = 1 - \frac{c_{R_{ACH1\_r}}}{c_{R_{ref}}} = 1 - \frac{c_{R_{out1}}}{c_{R_{ref}}} \end{aligned} \tag{6.24}$$

The internal costs of the productive structure 3-B are presented in the Figure 6.13. As expected, the unit costs of the energy services remain lower than the reference values thanks to the re-distribution of the costs in the subsystem enclosed in the control volume $CV - B$.

Table 6.7 summarizes the unit cost of each energy service for the productive structure 3-B. As mentioned before, all unit costs of the energy services remains lower than the reference values. The unit cost of the electricity decreases about 13%, the unit cost of the heating services decreases about 5% and the unit cost of the cooling service decreases about 13% with respect to the reference scenario.

The productive structure 3-A allowed to identify with more detail the formation cost for the different energy services. It was identified the thermal energy storage for cooling as the component which increases the unit cost of the cooling service, but also that helps to avoid the use of the batteries. Since the electricity part has a high weight in the total annual cost, *the use of TSR instead of*

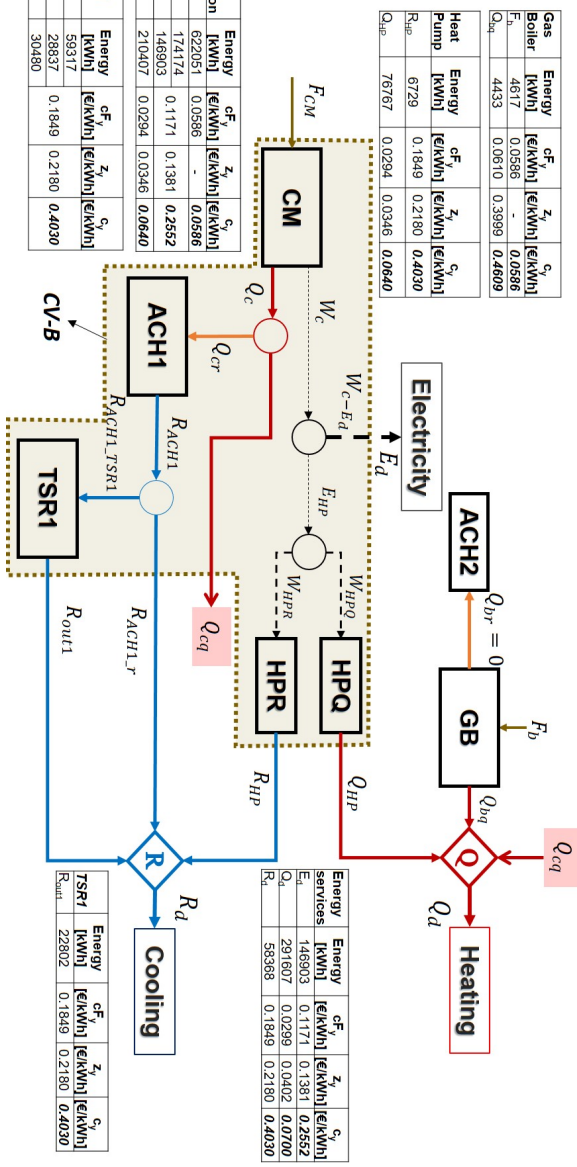

Figure 6.13: Productive structure 3-B.

(or along with) the batteries is an interesting alternative in the integration of the energy system in order to reduce the economic costs and increase the flexibility and reliability of the energy system. On the other hand, the productive structure 3-B leads to achieve a better apportionment of the unit cost of the energy services which is important for the deployment of the polygeneration systems. Therefore, hereinafter the productive structure 3-B is chosen for the next analyses.

6.2.5 Superstructure integrating renewable energy technologies

In this part, renewable energy technologies are included in the superstructure as candidate technologies in order to study their economic feasibility in the integration of the standalone energy systems. The inclusion of the different renewable energy technologies is carried out in a systematic way in order to observe the impact of the different renewable energy technologies in the energy system. Firstly, biomass boiler and solar thermal collectors, next, wind turbines are considered and finally the *PV* technology. However, it has been found that currently only the PV panels are feasible from the economic point of view. This can be explained through the levelized cost of energy *LCOE* of the different technologies, a measure widely used to compare alternative sources of energy. The *LCOE* of each technology can be calculated as the total costs of the technology over an annual period and divided by the energy generated in the same period (Aldersey-Williams and Rubert, 2019):

$$LCOE_{technology} = \frac{Total\ annual\ cost\ of\ technology}{Annual\ energy\ produced\ by\ technology} \tag{6.25}$$

The total annual cost of each technology includes the costs associated to the investment, maintenance, installation, possible repositions, indirect costs, taxes and fuel. For the case of the biomass boiler, it was assumed a capacity factor of 0.12 to estimate the energy generated in a year, based on the capacity factor of the gas boiler for the standalone reference energy system. Thus, by applying the Eq. 6.25, the *LCOE* for each technology is estimated as:

$LCOE_{ST} \approx 0.0752$ €/kWht

$LCOE_{BB} \approx 0.0876$ €/kWht

$LCOE_{WT+Inv} \approx 0.3433$ €/kWh

The unit cost of heating and electricity services of the reference systems are $c_{E_{d_{ref}}} = 0.2932$ €$/kWh$ and $c_{Q_{d_{ref}}} = 0.0735$ €$/kWht$ respectively. Consequently, based on the $LCOE$ presented above, the use of solar thermal collectors, biomass boiler and wind turbines are not profitable under the current conditions. It is worthy to say that the $LCOE$ gives only an idea of the profitability of each technology herein; however, it is not advisable to extrapolate this information to predict the optimal configuration of an standalone energy system since there are some assumptions considered in this measure that can bias the information. For instance, the $LCOE$ for solar thermal collectors and wind turbines is calculated assuming that all the energy produced is consumed. But this is not the case necessarily.

As a result, it is presented the optimal configuration which includes the PV panels. In this case, it is considered a reasonable available surface area of 300 m^2 for urban areas. The optimization model includes the surface area restriction taking into account the minimum distance between panels considering the shading effects. Details about the procedure are explained in the appendix D. Nevertheless, some simulations have been carried out without surface area restriction, finding that the installed surface area reaches a value of about 650 m^2 with a similar optimal configuration.

The Table 6.8 presents the installed capacity, and the operational and investment costs of the optimal configuration of the superstructure 6. As mentioned before, PV panels are selected in the optimal configuration with a surface area of 121 m^2 corresponding to 19 kWe. The surface area of the PV panels covers the entire available surface area (300 m^2), so it is expected that the bigger the available surface area, the more installed capacity of PV panels (as observed in the standalone system studied in the previous chapter). In general terms, remarkable reductions in the total annual cost about 16% and the CO_2eq emissions about 37% are achieved with respect to the reference scenario. A high share of renewable energy resources consumption, in this case PV technology, leads to these reductions. The total annual cost is distributed in 41% for operational costs and 59% for the investment costs (Figure 6.14a). The operational costs correspond to the natural gas consumption to drive the cogeneration module. Similar to the energy system 3, the fuel consumption of the gas boiler is marginal (Figure 6.14c). Concerning the investment costs breakdown, about 26% corresponds to the CM, 26% to the TSR, 19% to the HP, 15% to the ACH, 10% to the PV system (PV panels and Inverter) and 4% to the GB (Figure 6.14b). In environmental terms, the share of the CO_2eq emissions corresponds to the CM 95% and GB 1%. The rest corresponds to the CO_2eq emissions embodied

Table 6.8: Results of the optimization of the superstructure 6.

Technology	**Install Cap**	**CIA[€/yr]**	CO_2**fix [kg**CO_2eq**/yr]**
CM	33 kWe	12096	214
PV	19 kWe/121 m^2	3028	971
Inv	23 kW	1558	431
HP	122 kWt	8551	979
GB	140 kWt	1959	70
ACH	50 kWt	7073	413
TSR	241 kWht	11778	1497
Investment annual cost / Embodied CO_2eq ***emissions***		*46073*	*4575*
	Annual operational costs		
Fuel	**Consumption [kWh/yr]**	**Energy cost [€/yr]**	CO_2**fix [kg**CO_2eq**/yr]**
Natural Gas (NG)	543044	31964	110238
NG for CM	536261	30395	108861
NG for GB	6783	384	1377
Operational Economic cost/ Operational CO_2eq emissions		*31964*	*110238*
Total Economic cost/ Total CO_2eq emissions		**78007**	**114812**

in the equipment (Figure 6.14d).

The only difference between this case and the standalone system studied in the previous chapter is the restriction area. In that case, thanks to the high capacity of the PV panels, twice the capacity obtained here, the battery system began to be profitable since they allowed the system to take advantage the surplus energy from the PV panels which otherwise should be curtailed. Although this is not the only aspect to be considered to evaluate the profitability of the batteries, it is one of the reason to invest in them nowadays. In fact, several island and off-grid communities have invested in large-scale battery storage to balance the grid and store excess renewable energy (IRENA, 2020a). Consequently, this work does not pretend to show the thermal energy storage as solution to replace the batteries in energy systems for residential buildings, but it claims the use of both technologies to achieve more cost-effective and sustainable solutions.

Internal unit costs of the standalone energy system with PV panels: The Figure 6.15 depicts the productive structure of the polygeneration system and the Table 6.9 presents the annual unit costs of the different energy flows. Unlike the standalone energy system 3, in this case four virtual heat pumps are considered. The new ones, $HPQ2$ and $HPR2$, are driven only by the PV panels. In turn, the energy produced by the $HPR2$ can be stored R_{HP2_TSR2} in the $TSR2$ or used directly to attend the cooling demand R_{HP2_r}.

The unit cost of the energy services reduces with respect to the reference

Table 6.9: Unit costs of the productive structure of the standalone energy system with PV panels.

Energy services	**Energy [kWh]**	cF_y **[€/kWh]**	z_y **[€/kWh]**	c_y ***[€/kWh]***
E_d	146903	0.0966	0.1402	***0.2368***
Q_d	291607	0.0279	0.0440	***0.0719***
R_d	58368	0.1649	0.2162	***0.3811***
Renewable Energy	**Energy [kWh]**	cF_y **[€/kWh]**	z_y **[€/kWh]**	c_y ***[€/kWh]***
W_{PVe}	33702	0	0.1361	***0.1361***
Cogeneration	**Energy [kWh]**	cF_y **[€/kWh]**	z_y **[€/kWh]**	c_y ***[€/kWh]***
F_{CM}	536261	0.0589	-	***0.0589***
W_c	150153	0.1167	0.1411	***0.2578***
W_{c_Ed}	121599			
Q_{cq}	190511	0.0293	0.0354	***0.0647***
Heat Pump	**Energy [kWh]**	cF_y **[€/kWh]**	z_y **[€/kWh]**	c_y ***[€/kWh]***
R_{HP1}	15412			
R_{HP1_r}	12257	0.1843	0.2228	***0.4071***
R_{HP1_TSR2}	3155			
Q_{HP1}	74102	0.0293	0.0354	***0.0647***
R_{HP2}	6284			
R_{HP2_r}	3614	0	0.0437	***0.0437***
R_{HP2_TSR2}	2670			
Q_{HP2}	20482	0	0.0735	***0.0735***
Absorption Chiller	**Energy [kWh]**	cF_y **[€/kWh]**	z_y **[€/kWh]**	c_y ***[€/kWh]***
R_{ACH1}	44248			
R_{ACH1_r}	14361	0.1843	0.2228	***0.4071***
R_{ACH1_TSR1}	29887			
Gas boiler	**Energy [kWh]**	cF_y **[€/kWh]**	z_y **[€/kWh]**	c_y ***[€/kWh]***
F_b	6783	0.0589	-	***0.0589***
Q_{bq}	6511	0.0613	0.3009	0.3622
TSR1	**Energy [kWh]**	cF_y **[€/kWh]**	z_y **[€/kWh]**	c_y ***[€/kWh]***
R_{out1}	22423	0.1843	0.2228	***0.4071***
TSR2	**Energy [kWh]**	cF_y **[€/kWh]**	z_y **[€/kWh]**	c_y ***[€/kWh]***
R_{in2}	5825	0.0999	0.1407	***0.2406***
R_{out2}	5713	0.1018	0.2691	***0.3709***

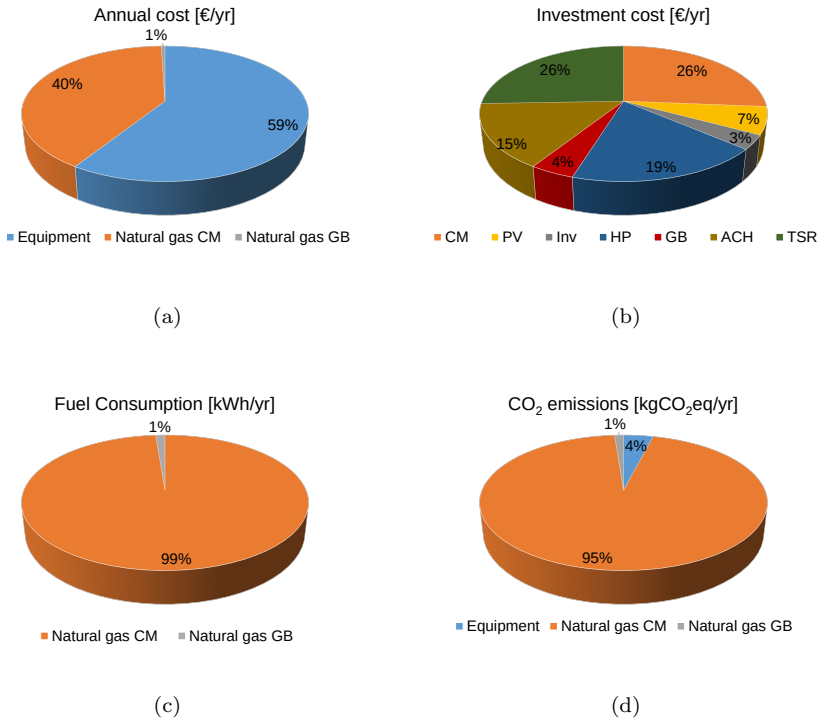

Figure 6.14: Standalone energy system with PV panels. Breakdown of: a) Total annual cost, b) Investment cost, c) Fuel consumption, d) CO_2eq emissions.

system, 19% for electricity, 2% for heating and 18% for cooling. In addition to the advantages of the energy system 3, these reductions are due to the "free" PV energy contribution, since its total unit cost depends only on the PV investment cost.

The unit cost of the different energy services produced from the PV panels are lower or equal to the unit cost of the reference system. The unit cost of the electricity from the solar energy W_{PVe} about 50% and the unit cost of the cooling produced from the solar energy R_{HP2} about 90%. In the case of the unit cost of the heating produced from the solar energy Q_{HP2} is equal to the reference value. Note that in this case, the virtual thermal energy storage

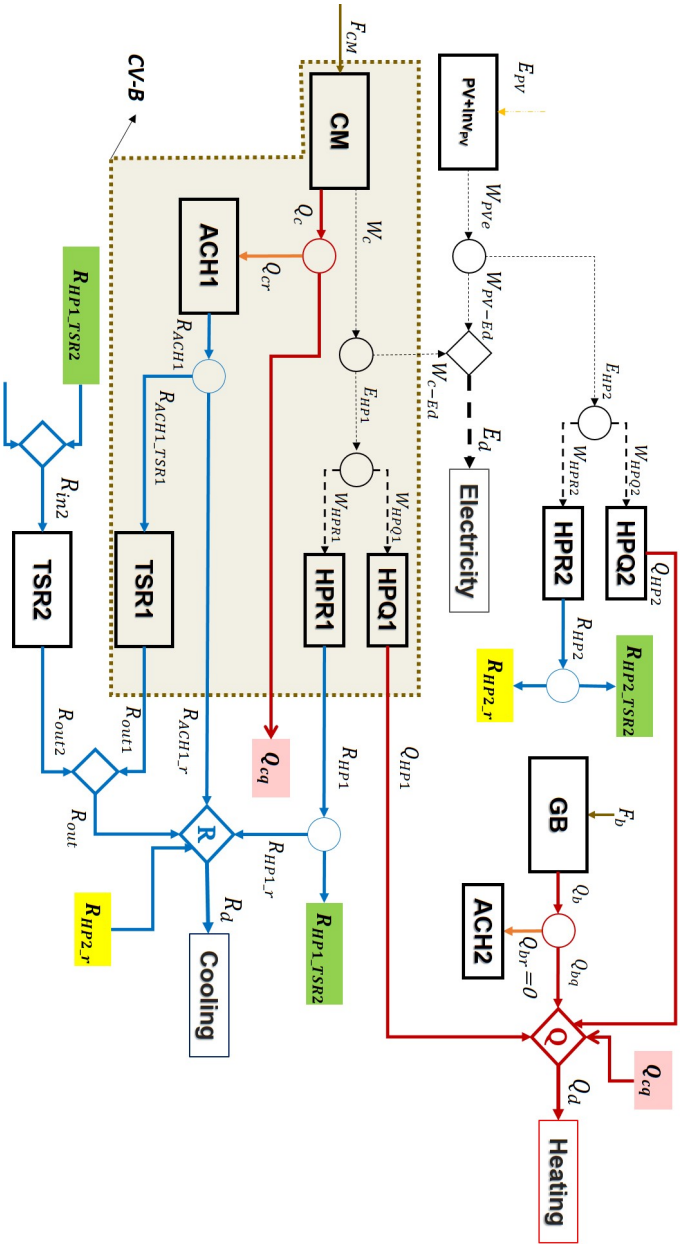

Figure 6.15: Productive structure of the standalone energy system with PV panels.

for cooling $TSR2$ exists to store the energy produced by both virtual heat pumps R_{HP1_TSR2} and R_{HP2_TSR2}. The unit cost of the energy delivered by the thermal energy storage for cooling R_{out2} remains about 20% lower than unit cost of the cooling service of the reference system. These facts remark even more the profitability of the PV panels for the energy systems for residential buildings.

The thorough description of the thermoeconomic model of the optimal standalone energy system with PV panels is presented in the appendix C.

Sensitivity analysis of the natural gas price

Above mentioned, renewable technologies such as biomass boiler, solar thermal collectors and wind turbines are not profitable under the current conditions. However, taking into account the natural gas price uncertainty, and the interest of the standalone energy systems for residential buildings, a sensitivity analysis is carried out in order to evaluate the feasibility of these technologies in other conditions. The available space for collectors restriction remains in this study and it is assumed that there is not restriction to install wind turbines. The Figure 6.16 depicts the investment cost per technology and the CO_2eq emissions for the obtained optimal configurations as a function of the natural gas price.

The current natural gas price is about 0.0468 €/kWh without taxes. According to the graphic, the biomass boiler begins to be profitable when the natural gas price is 1.5 times the current price. As the natural gas price increases, the biomass boiler capacity increases and the gas boiler capacity decreases. On the other hand, the wind turbine technology is profitable when the natural gas price is 2.5 times the current natural gas price. This value coincides with the price of the gasoil A which can be used in remote areas where the natural gas network is not available. The profitability of the wind turbine is also because the PV capacity is restricted to the available space area. Regarding the solar thermal collectors, they are not profitable in any studied case. This fact reasserts that the $LCOE$ is not enough to predict the optimal configuration of standalone energy systems. Concerning the environmental impact, as the natural gas price increases, the CO_2eq emissions decreases because the renewable energy increases. This result also shows the resilience of the renewable energy technologies, especially the PV panels and wind turbine (IEA, 2020). With respect to the batteries, note that they appear in the optimal configuration along with the wind turbine in order to manage the electricity from the non-manageable technologies. The lead acid batteries were the technology selected in the optimal configuration. However, this is a mature technology which is

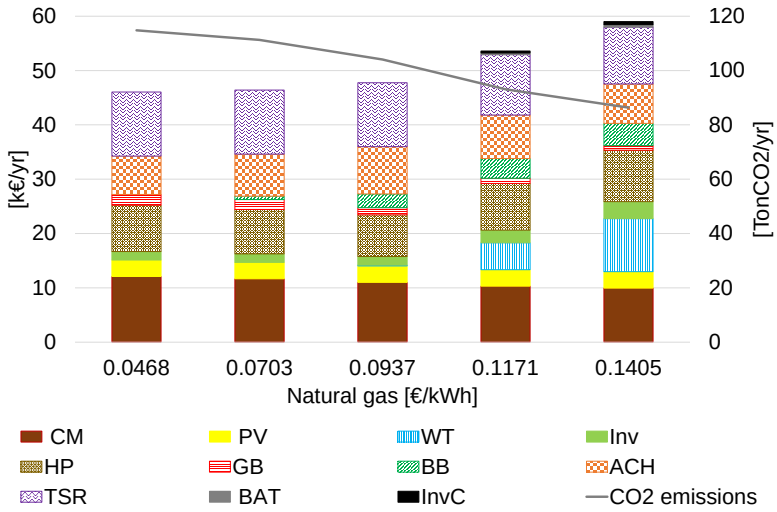

Figure 6.16: Sensitivity analysis of the natural gas price.

hardly to improve its performance or reduce its cost. On the contrary, lithium-Ion technology has a high potential of performance improvement and reduction cost. In fact, the performance and unit cost used in this work were based only on the NMC (Nickel Manganese Cobalt) technology; however, there is a wide range of lithium-Ion technologies which improve its performance IRENA (2017). Consequently, the Table 6.10 presents the results of the optimal configuration of the polygeneration system when the natural gas price is 2.5 times the current natural gas price considering two scenarios: i) Lead acid battery, ii) Lithium-Ion battery under current conditions (See appendix A).

Note that almost the same results are obtained with both battery technologies; nevertheless, the lithium-ion battery requires about the half of the lead acid battery capacity. Thus, the lithium-ion batteries could be considered a competitive technology currently. As mentioned before, this configuration could be an interesting alternative for residential buildings or energy communities located in remote areas nowadays. Renewable energy technologies increase their share

Table 6.10: Results of the optimal configuration of the polygeneration system when the natural gas price is 2.5 times the current natural gas price.

Technology	**Lead Acid Battery**			**Lithium-Ion Battery**		
	Install Cap	**CIA[€/yr]**	CO_2**fix** [**kg**CO_2eq/**yr**]	**Install Cap**	**CIA[€/yr]**	CO_2**fix** [**kg**CO_2eq/**yr**]
CM	28 kWe	10321	182	28 kWe	10321	182
PV	19 kWe/121 m^2	3028	971	19 kWe/121 m^2	3028	971
WT	9 kW	4943	341	9 kW	4943	341
Inv	34 kW	2342	648	34 kW	2342	648
HP	123 kWt	8576	981	123 kWt	8576	981
GB	68 kWt	957	34	69 kWt	963	34
BB	87 kWt	3647	43	87 kWt	3648	43
ACH	57 kWt	7991	467	57 kWt	7991	467
TSR	228 kWht	11107	1412	228 kWht	11107	1412
BAT Li-Ion	-	-	-	4 kWh	363	69
BAT LA	8 kWh	318	74	-	-	-
InvC	2 kW	371	42	2 kW	371	42
	CIA / $CO2_{fix}$	*53602*	*5196*	***CIA*** / $CO2_{fix}$	*53653*	*5191*
	Annual operational costs					
Fuel	**Consumption** [**kWh/yr**]	**Energy cost** [**€/yr**]	CO_2**ope** [**kg**CO_2eq/**yr**]	**Consumption** [**kWh/yr**]	**Energy cost** [**€/yr**]	CO_2**ope** [**kg**CO_2eq/**yr**]
Natural Gas (NG)	360955	52328	73274	361116	52351	73307
NG for CM	360955	51144	73274	361116	51167	73307
NG for GB	0	0	0	0	0	0
Biomass (Pellets)	232427	11249	14643	231913	11225	14610
	C_{ope}/ $CO2_{ope}$	*63578*	*87917*	C_{ope}/ $CO2_{ope}$	*63576*	*87917*
	TAC/ TCE	**117180**	**93113**	**TAC/ TCE**	**117229**	**93108**

in the polygeneration system. On the other hand, technologies such as the gas boiler are used only as backup. The reversible heat pump claims as a key component in the energy system integration and the thermal energy storage for cooling allows the capacity reduction of both the heat pump and the battery system, which lead to reduce the investment cost.

6.3 Closure

A comprehensive thermoeconomic analysis was carried in annual basis on the standalone energy supply system for a residential building composed of 50 dwellings. Different optimal configurations were obtained from the optimization of the different superstructures which were changing progressively along the integration process of different candidate technologies. Results highlight the advantages of the thermoeconomic analysis to study synergies between components based on the formation of costs.

Among the synergies found between the different components, it should be highlighted the relation between the reversible heat pump HP and gas boiler GB as the former leads to reduce the GB capacity and hence the total investment cost. Besides, the HP enables the installation of renewable energy technology such as PV panels. Another remarkable synergy found along the study is between the batteries and thermal energy storage. The thermoeconomic analysis unveiled the impact of the batteries on the total annual cost. Likewise, it was found the thermal energy storage for cooling as a cost-effective alternative to displace the batteries. The point is not to show that one technology displaces another, but the synergy between them to achieve better solutions.

It was studied the importance of the level of aggregation in the thermoeconomic analysis. A lower level of aggregation gives more details of the contribution of each component to the costs formation, however, depending on the type of analysis, a higher level of aggregation could be interesting. Thus, in the analysis of the standalone energy system 3, the high unit cost of the thermal energy storage for cooling and its effect in the final unit cost of the energy services was detected because only the cogeneration module and the absorption chiller were taken as a control volume (a lower level of aggregation). This gave rise to include more technologies in the trigeneration system control volume (a higher level of aggregation) in order to achieve a fairer allocation cost of the different final energy services.

Among the renewable energy technologies, only PV panels are feasible from the economic point of view under the current conditions. It is remarkable the economic and environmental benefits obtained through its integration in the energy system.

A sensitivity analysis of the natural gas showed the potential profitability of the renewable energy technologies in specific conditions. At a natural gas price of about 2.5 times the current prices, most of the renewable energy technologies (except solar thermal collectors) and batteries turn out profitable. This configuration is proposed as an interesting alternative for remote areas. Regarding

battery technologies, it was demonstrated that although the lead acid batteries were selected in the optimal configuration, the lithium-ion batteries is currently a competitive technology.

Chapter 7

Legal restrictions impact on the polygeneration systems design

"Better as a team!"

Several targets and policies have been proposed by the governments around the world in order to encourage a deployment of energy efficient and low carbon grid connected distributed generation. In particular, regulatory and pricing policies such as feed-in tariffs (FiT), net metering or net billing have been applied to support distributed generation DG (International Energy Agency, 2018). A brief description of those pricing policies schemes are presented in the following paragraphs.

Feed-in Tariff (FiT): In this scheme, electricity consumption and generation must be separated and accounted differently. While electricity from the grid is purchased at retail price, the electricity injected to the grid is compensated at a predetermined tariff notified by the regulator which can be higher than retail electricity price (International Renewable Energy Agency, 2019). When the compensation tariff is indeed higher than the retail electricity price, this scheme can be called Buy all, Sell All arrangement (Zinaman et al., 2017).

Net metering or Net energy metering: Under this mechanism, the electricity bill for the net electricity consumption from the grid is accounted after netting

off the electricity injected by the owner into the grid. This requires bidirectional meters, or net meters, which keep account of the net flow of electricity. In this case, the owner receives a credit in kilowatt-hours and typically is compensated for the injected electricity at the retail electricity tariff (International Renewable Energy Agency, 2019).

Net billing: In this scheme, the compensation is monetary. The owner can consume electricity generated by renewable energy installation in real-time and export any surplus generation to the utility grid. All net electricity exports are metered and credited at a predetermined sell rate in the moment they are injected into the grid. The sell rate is lower to the retail rate of electricity (Zinaman et al., 2017).

Several countries, such as Germany or Canada, have applied FiT mechanisms to encourage the renewable technology investment as Buy All, Sell All arrangement. However, this mechanism has evolved to net billing arrangements as self-consumption (offering lower rates for exported energy) (Zinaman et al., 2017; Masson et al., 2016).

In the case of Spain, although different approaches of net metering and net billing have been studied since 2011 (Dufo-López and Bernal-Agustín, 2015), the recent regulations implemented have been focused on the self-consumption. Thus, taking into account the importance of the legal framework to foster low carbon technologies in the pathway to reduce the greenhouse emissions, this chapter aims to study the effect of the Spanish regulations on the design of polygeneration systems for residential buildings and their impact in the policy to combat the climate change. The chapter is divided in two parts: the first one is the design of polygeneration systems for households and residential buildings considering the latest self-consumption regulations, followed by a thoroughly analysis comparing those regulations. The second part aims to stablish some guidelines for the design of affordable sustainable energy supply systems for residential buildings through a multiobjective optimization.

7.1 Comparison of the recent self-consumption regulation in Spain

In the case of Spain, in particular, in the last four years, the Spanish government has implemented two different royal decrees to regulate the self-consumption. The first of them is the Royal Decree RD 900/2015 (Boletin Oficial del Estado, 2015) which was appropriated in 2015 and defined two types of self-consumption

systems: i) Self-consumption type 1: For systems with installed polygeneration system capacity below 100 kW in which energy sale is not allowed and ii) Self-consumption type 2: there was no limit for installed polygeneration system capacity (either lower or upper limit) and energy sale was allowed. The self-consumption type 2 can be considered as a net billing arrangement. In both types, the installed polygeneration system capacity must be lower than or equal to the contracted capacity from the grid. A relevant aspect of this regulation is that it must be applied two types of self-consumption taxes: i) a fix tax proportional to the difference between the charges application power and the contracted power from the grid, in this work this fix tax is applied to the installed polygeneration system capacity; and ii) a variable tax corresponding to the self-consumed energy, depending on time-of-use tariffs. However, for self-consumption type 1 when contracted power from the grid is lower or equal to 10 kW, self-consumption taxes were not applied.

Recently, the Spanish government has released the Royal Decree RD 244/2019 (Boletin Oficial del Estado, 2019) which establishes the administrative, technical and economic conditions for self-consumption. This decree derogates the previous one, RD 900/2015, and settles down two categories of self-consumption: i) self-consumption without surplus electricity production, in which electricity injection to the grid is not allowed, and ii) self-consumption with surplus, in which electricity injection to the grid is allowed. Both self-consumption categories can be applied for individual or collective installations. The self-consumption with surplus type is divided in two types: a) Surplus subject to compensation: In this case, the primary energy must be renewable and the installed polygeneration system capacity must be equal or lower than 100 kW, and b) Surplus no subject to compensation: Self-consumption systems that do not accomplish the requirements to be subjected to compensation or that voluntarily decide do not receive any economic compensation. This could happen, because when a client wants to sell electricity to the grid, some additional administrative and technical requirements should be fulfilled, which also could require to pay additional fees. Then, if the surplus of electricity is a small amount, it could be more interesting to avoid these technical and administrative issues. Besides, in this way, the client can deliver surplus electricity to the grid, with more flexibility of operation and avoiding the additional investment in any dissipater or battery required to manage the excess of electricity produced.

A relevant difference between both regulations is that in the Royal Decree 244/2019 there is neither application of any tax related to self-consumption nor any restriction on the installed self-consumption system capacity with respect to the contracted power from the electric grid. However, in the case of surplus

Table 7.1: Legal restrictions considered for the design of polygeneration systems.

Feature	Based on RD 900/2015		Based on RD 244/2019	
	Individual	Collective	Individual	Collective
Polygeneration system size with respect to the contracted power from the electric grid	Below or equal to contracted grid power		Unlimited	
Mechanism of compensation	Net billing (optional)		Net billing (optional)	
Sale electricity	Surplus electricity (optional)		Surplus electricity only from renewable resources (Optional)	
Charges over self-consumption	When contracted power is above 10 kW or sale electricity is applied	Yes	No	

subject to compensation, i.e. produced with renewable energy, the installed capacity must be equal or lower than 100 kW.

This section aims to compare both regulations by evaluating their impacts on the design of polygeneration systems for the residential sector from the economic and environmental points of view. Although collective installations are not mentioned in the RD 900/2015, in this work both individual and collective installations are studied for both regulations, by considering households as a reference for individual installations, and residential buildings as a reference for collective installations. Three scenarios based on the above-mentioned regulations are considered: i) Scenario 1 in which electricity sale is not allowed; ii) Scenario 2 in which electricity sale is allowed at spot price; and iii) Scenario 3 in which Electricity sale is allowed at 80% purchase price. In addition, Spanish regulation RD 244/2019 establishes that the surplus electricity cannot be greater than the consumed electricity from the grid in economic terms for the billing time, which cannot exceed 1 month; however, in this case due to the procedure applied to select representative days in the optimization model, the considered billing time is one year. This approach is less restrictive and provides higher flexibility to self-consumption arrangements. Scenarios 2 and 3 are proposed as particular examples of the type 2 self-consumption in both regulations (Boletin Oficial del Estado, 2015, 2019), and they are, in fact, net billing arrangements under legal restrictions based on the regulations. Table 7.1 summarizes the legal restrictions considered for the design of polygeneration systems in this work which are mainly based on the aforementioned royal decrees.

The analysis was carried out minimizing the total annual cost whereas the CO_2eq emissions were calculated simultaneously. In this way, the greenhouse gas emissions reduction can be verified, which is one of the aims of the new self-consumption policy (IDAE, 2019b). For both regulations, the legal restrictions in the optimization model to consider the net billing and the maximum self-consumption capacity are expressed as:

$$\sum_{d=1}^{N_{rep}} \omega_d \left(\sum_{h=1}^{24} (cp_e(d,h) \cdot Ep(d,h) - cs_e(d,h) \cdot Es(d,h)) \right) \geq 0 \tag{7.1}$$

$$Cap_{PV} + Cap_{WT} + Cap_{CM} \leq 100[kW] \tag{7.2}$$

For the RD 900/2015, the installed capacity of the polygeneation system must be lower than the contracted power:

$$Cap_{PV} + Cap_{WT} + Cap_{CM} \leq Pct \tag{7.3}$$

The location of this study was carried out for Zaragoza considering individual installations for households and collective installations for residential buildings:

- ☐ Household (Hh): A single dwelling, in which the expected contracted power is below 10 kW; therefore, the electric tariff 2.0 DHS (See Table 2.13) is applied. The available surface area for photovoltaic panels or solar thermal collectors is 100 m^2.
- ⊞ Residential building (RB): It consists of a multifamily residential building composed of 50 dwellings (households). The community can sign-up a collective self-consumption contract for all services. The expected electricity contracted power is above 15 kW; therefore, the electric tariff 3.0A (See Table 2.13) is applied in this case. The available area for photovoltaic panels or solar thermal collectors is 2000 m^2.

A conventional energy system consisting of a gas boiler to attend heating demands, a mechanical chiller driven by electricity from the grid to attend only cooling demands, and electricity also purchased from the grid to cover the electrical demand of appliances is considered as a reference scenario for both cases. The rest of scenarios consider reversible heat pump.

7.1.1 Individual installations-Households

Optimization of the polygeneration system for a household based on RD 900/2015

The optimization of the total annual cost of the superstructure for a household was carried out under the legal restrictions based on the RD 900/2015. The Table 7.2 shows the obtained results for the optimal design of a polygeneration system for a household and the Figure 7.1 shows the optimal configuration.

Table 7.2: Results of the optimization of the polygeneration system for a household based on RD 900/2015.

Technology	**Reference scenario**			**Scenario 1**			**Scenario 2-3**		
	Install Cap	**CIA[€/yr]**	**CO_2fix [kgCO_2eq/yr]**	**Install Cap**	**CIA[€/yr]**	**CO_2fix [kgCO_2eq/yr]**	**Install Cap**	**CIA[€/yr]**	**CO_2fix [kgCO_2eq/yr]**
Pct [kW]	2.3	-	-	1.15	-	-	1.725	-	-
PV	-	-	-	4.9 m^2	181	39	-	-	-
Inv	-	-	-	1 kW	63	17	-	-	-
Mch	6.5 kWt	569	52	-	-	-	-	-	-
HP	-	-	-	5.5 kWt	482	44	5.7 kWt	497	47
GB	20 kWt	414	20	20 kWt	414	20	20 kWt	414	20
TSR	-	-	-	1.3 kWht	81	8	1 kWht	62	3
	CIA / $CO2_{fix}$	*983*	*72*	***CIA*** / $CO2_{fix}$	*1221*	*129*	***CIA*** / $CO2_{fix}$	*973*	*71*
Annual operational costs									
Fuel	**Consumption [kWh/yr]**	**Energy cost [€/yr]**	**CO_2ope [kgCO_2eq/yr]**	**Consumption [kWh/yr]**	**Energy cost [€/yr]**	**CO_2ope [kgCO_2eq/yr]**	**Consumption [kWh/yr]**	**Energy cost [€/yr]**	**CO_2ope [kgCO_2eq/yr]**
Electricity	3230	712	668	3653	704	757	5010	979	1022
Natural Gas	6075	542	1242	550	94	112	524	92	107
	C_{ope}/ $CO2_{ope}$	*1254*	*1910*	C_{ope}/ $CO2_{ope}$	*798*	*869*	C_{ope}/ $CO2_{ope}$	*1071*	*1129*
	TAC/ TCE	**2236**	**1982**	**TAC/ TCE**	**2019**	**998**	**TAC/ TCE**	**2043**	**1200**

The scenario 1 (Figure 7.1a) includes PV, HP, GB and TSR whereas scenarios 2 and 3 (Figure 7.1b) only HP, GB and TSR were included. The results of scenarios 2 and 3 mean that for a household user, it is not profitable at all to sell electricity (type 2 self-consumption), because in those conditions, the potential electricity bill savings and revenues from electricity sale (from the PV panels) do not compensate the self-consumption taxes to pay. By comparing the reference scenario with scenario 1, a significant reduction of about 36% in economic operational costs was achieved, but in terms of total annual cost reduction of a 10% was achieved. The installation of PV panels and TSR enable the contracted power to be reduced up to 50% with respect to the reference scenario. In terms of environmental impact, the total CO_2eq emissions were reduced about 50%. In this scenario, the produced PV electricity that is not self-consumed is dissipated at zero cost.

Optimization of the polygeneration system for a household based on RD 244/2019

The optimization of the total annual cost of the superstructure for a household is carried out by applying RD 244/2019. The optimal configuration is shown in the figure 7.2. This is the same for the three different considered scenarios which includes PV, HP, GB and TSR, the only difference is that an electricity dissipater is not required when sale of electricity is allowed.

The results of scenario 1 based on RD 900/2015 and RD244/2019 are the same (Table 7.2), since there is no application of self-consumption taxes in both

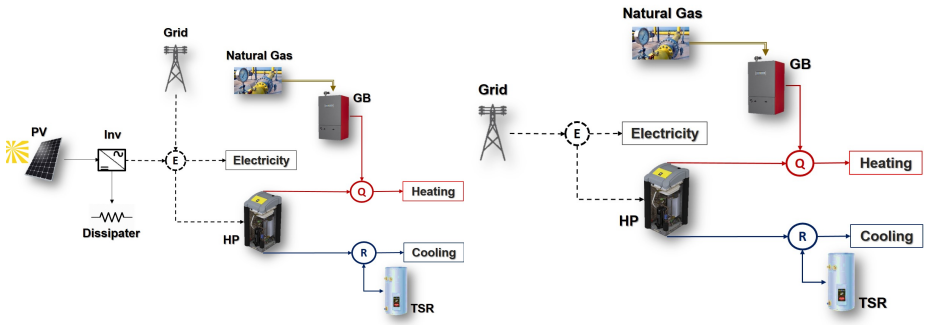

(a) (b)

Figure 7.1: Optimal configuration of a polygeneration system based on RD 900/2015 for a household. a) Scenario 1 and b) Scenarios 2 and 3.

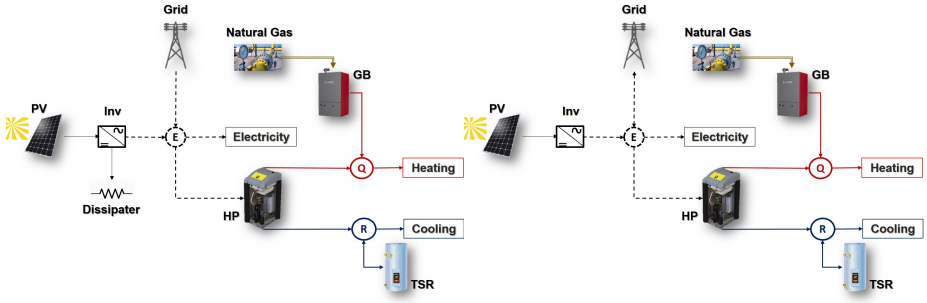

(a) (b)

Figure 7.2: Optimal configuration of a polygeneration system based on RD 244/2019 for a household. a) Scenario 1 and b) Scenarios 2 and 3.

cases. On the other hand, unlike scenarios 2 and 3 based on RD 900/2015, in this case the installation of a polygeneration system based on PV and HP is profitable (Table 7.3). Both scenarios 2 and 3 present the same configuration. The achievements in total economic and environmental costs are quite similar to scenario 1. By comparing scenario 1 with scenarios 2 and 3, the fact of selling electricity increased the PV and HP capacity about 10% and 4% respectively,

Table 7.3: Results of the optimization of the polygeneration system for a household based on RD 244/2019. Scenarios 2 and 3.

Technology	**Scenario 2-3**		
	Install Cap	**CIA[€/yr]**	CO_2**fix [kg**CO_2eq**/yr]**
Pct [kW]	1.15	-	-
PV	5.4 m^2	199	43
Inv	1 kW	70	19
HP	5.7 kWt	497	47
GB	20 kWt	414	20
TSR	1 kWht	62	6
	CIA / $CO2_{fix}$	*1242*	*134*
Annual operational costs			
Fuel	**Consumption [kWh/yr]**	**Energy cost [€/yr]**	CO_2**ope [kg**CO_2eq**/yr]**
Electricity (Purchased)	3550	686	726
Electricity (Sold)	52	-5	
Natural Gas	550	94	112
	C_{ope}/ $CO2_{ope}$	*776*	*839*
	TAC/ TCE	**2017**	**973**

and decreased the TSR capacity about 23%. However, in absolute terms, these variations were not significant in this size scale. Regarding the installation of PV panels, these covered only about 15% of the total available horizontal surface. The obtained results show that for 1 household the possibility of selling electricity to the grid does not provide a significant economic benefit but operational flexibility without dissipating electrical energy.

7.1.2 Collective installations-Residential buildings

By applying the legal restrictions based on the aforementioned regulations, the optimization of the polygeneration systems for residential buildings leads to the optimal configuration shown in the Figure 7.3, which included CM, PV, HP, GB and TSR, and in some scenarios, TSQ as well. An electricity dissipater was required in scenario 1 when there was a surplus of produced PV electricity that was not self-consumed and in scenario 3 by applying RD 244/2019, due to the technical restriction which does not allow to sell electricity above the contracted power (Figure 7.3a). Note that only electricity which come from renewable energy can be sold, therefore, the electricity produced by CM is only for self-consumption. In all cases, primary energy savings PES were positive. See the appendix B for a detailed explanation about PES calculation.

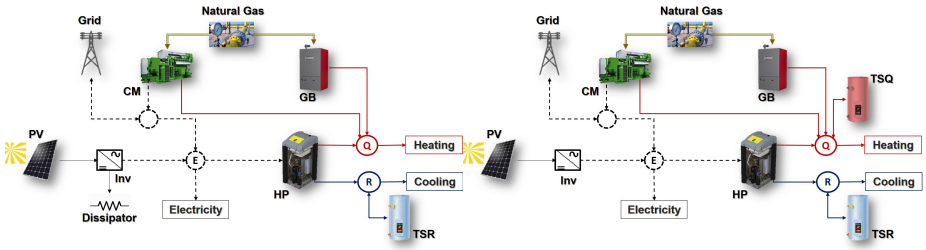

(a) (b)

Figure 7.3: Optimal configuration of a polygeneration system for a residential building based on RD 900/2015 and RD 244/2019. a) Scenarios 1 and 2 (RD 900/2015) and scenario 1 and 3 (RD 244/2019). b) Scenario 3 (RD 900/2015) and scenario 2 (RD 244/2019).

Optimization of the polygeneration system for a residential building based on RD 900/2015

Tables 7.4 and 7.5 show the optimal design of a polygeneration system for a residential building composed of 50 dwellings, by applying legal restrictions based on RD 900/2015. The contracted power for the collective installation was the same for scenarios 1, 2 and 3, with a significant reduction of about 50% with respect to the reference scenario. This is mainly due to the installation of the CM and PV panels. Regarding equipment capacity, the installation of reversible HP instead of a mechanical chiller enables the reduction of the GB capacity. Likewise, the installation of TSR enables the HP capacity reduction. In economic terms, from the reference scenario to scenario 1 there was a reduction of about 27% and 10% in the operational and total annual costs, respectively. From scenario 2 to scenario 3 there was a reduction of about 10% and 1% in the operational and total annual costs, respectively. On the other hand, from the environmental point of view, from reference scenario to scenario 1 there was a reduction of about 16% and 14% in the operational and total CO_2eq emissions respectively. From scenario 1 to 2 there was a reduction below 1% in both operational and total CO_2eq emissions. From scenario 2 to 3 there was a reduction of about 4% and 2% in the operational and total CO_2eq emissions, respectively.Under this regulation there is an important limitation to reach significant economic and environmental savings due to the self-consumption taxes

Table 7.4: Results of the optimization of the polygeneration system by applying the RD 900/2015 for a residential building. Reference scenario and scenario 1.

Technology	**Reference Scenario**			**Scenario 1**		
	Install Cap	**CIA[€/yr]**	CO_2**fix** [**kg**CO_2eq/**yr**]	**Install Cap**	**CIA[€/yr]**	CO_2**fix** [**kg**CO_2eq/**yr**]
$Pct_{1,2,3}$ [kW]	$110.6_{1,2}$-20.9_3	-	-	$55.4_{1,2,3}$	-	-
CM	-	-	-	8 kWe	2941	52
PV	-	-	-	199 m^2	5006	1605
Inv	-	-	-	37 kW	2576	713
Mch	325 kWt	22747	2603	-	-	-
HP	-	-	-	287 kWt	20083	2298
GB	274 kWt	3824	137	98 kWt	1375	49
TSR	-	-	-	44 kWht	2170	276
	CIA / $CO2_{fix}$	*26571*	*2740*	***CIA*** / $CO2_{fix}$	*34152*	*4993*
	Annual operational costs					
Fuel	**Consumption** [**kWh/yr**]	**Energy cost** [**€/yr**]	CO_2**ope** [**kg**CO_2eq/**yr**]	**Consumption** [**kWh/yr**]	**Energy cost** [**€/yr**]	CO_2**ope** [**kg**CO_2eq/**yr**]
Electricity	161495	42681	33341	84905	26275	17972
Natural Gas	303757	18189	62088	302829	18136	61898
	C_{ope}/ $CO2_{ope}$	*60869*	*95429*	C_{ope}/ $CO2_{ope}$	*44411*	*79870*
	TAC/ TCE	**87440**	**98169**	**TAC/ TCE**	**78563**	**84863**

to pay and to the fact that the installed capacity of the renewable energy and cogeneration technologies cannot exceed the contracted power from the grid (Eq. 7.3).

Optimization of the polygeneration system for a residential building based on RD 244/2019

Tables 7.6 and 7.7 show the optimal design of a polygeneration system for a residential building based on the RD 244/2019. The contracted power for the collective installation varies for each scenario, achieving reductions of up to about 69% in scenarios 1 and 2, and up to about 58% in scenario 3 with respect to the reference scenario. The reduction in contracted power is mainly due to the installation of CM and PV panels. Regarding equipment capacity, TSQ capacity is negligible taking into account the size scale. The replacement of the mechanical chiller for a reversible HP enables the GB capacity to be reduced, and the installation of TSR enables the reversible HP capacity to be reduced. In economic terms, from reference scenario to scenario 1 there was a reduction of about 46% and 16% in the operational and total annual costs, respectively. From scenario 1 to scenario 2 there was a reduction of about 8% in the operational cost but it was negligible in the total annual cost. From scenario 2 to scenario 3 there was a reduction of about 37% and 7% in the operational and total annual costs, respectively. From the environmental point of view, from reference scenario to scenario 1 there was a reduction of about 13% and 10% in the operational and

Table 7.5: Results of the optimization of the polygeneration system by applying the RD 900/2015 for a residential building. Scenarios 2 and 3.

Technology	**Scenario 2**			**Scenario 3**		
	Install Cap	**CIA[€/yr]**	CO_2**fix** [kgCO_2eq/**yr**]	**Install Cap**	**CIA[€/yr]**	CO_2**fix** [kgCO_2eq/**yr**]
$Pct_{1,2,3}$ [kW]	$55.4_{1,2,3}$	-	-	$55.4_{1,2,3}$	-	-
CM	8 kWe	2941	52	6 kWe	2206	39
PV	202 m^2	5060	1623	317 m^2	7954	2551
Inv	38 kW	2604	721	58 kW	4094	1133
HP	288 kWt	20134	2304	297 kWt	20751	2375
GB	98 kWt	1375	49	106 kWt	1488	53
TSR	43 kWht	2103	267	27 kWht	1292	164
	CIA / $CO2_{fix}$	*34218*	*5016*	***CIA*** / $CO2_{fix}$	*37865*	*6321*
	Annual operational costs					
Fuel	**Consumption** [**kWh/yr**]	**Energy cost** [**€/yr**]	CO_2**ope** [kgCO_2eq/**yr**]	**Consumption** [**kWh/yr**]	**Energy cost** [**€/yr**]	CO_2**ope** [kgCO_2eq/**yr**]
Electricity (Purchased)	84687	26260	17654	82873	26699	11173
Electricity (Sold)	1046	-92		33994	-6008	
Natural Gas	303441	18171	62023	319647	19089	65336
	C_{ope}/ $CO2_{ope}$	*44339*	*79678*	C_{ope}/ $CO2_{ope}$	*39780*	*76509*
	TAC/ TCE	**78557**	**84694**	**TAC/ TCE**	**77645**	**82830**

total CO_2eq emissions respectively. From scenario 1 to 2 there was a reduction about 10% and 8% in operational and total CO_2eq emissions respectively. From scenario 2 to 3 there was a significant reduction of about 35% and 28% in the operational and total CO_2eq emissions respectively. This is mainly because in scenarios 1 and 2 the exploited area for PV panels is about 32% and 41% respectively, whereas in scenario 3 is about 74%. The available area for installing PV panels is a key factor for the reduction of CO_2eq emissions. The limit value of 2000 m^2 for the available area is an assumption only to evaluate how much PV panels could be installed in the different scenarios.

7.1.3 Individual and Collective installations comparison

The total annual cost and CO_2eq emissions per dwelling were calculated for the case of the residential building consisting of 50 dwellings. These results were compared with individual installations in order to evaluate the advantages and disadvantages of both types of installations from the economic and environmental point of view. It is noteworthy in reference scenario (see Tables 7.8 and 7.9) that in collective installations the cost per dwelling is lower than in individual installations. The reason is the reduction of natural gas cost when its consumption is increased, which is a common feature in most of countries (Eurostat, 2020). Table 7.8 presents the total annual cost and CO_2 emission

Table 7.6: Results of the optimization of the polygeneration system for a residential building by applying RD 244/2019. Reference scenario and scenario 1.

Technology	**Reference Scenario**			**Scenario 1**		
	Install Cap	**CIA[€/yr]**	CO_2**fix** [**kg**CO_2eq/**yr**]	**Install Cap**	**CIA[€/yr]**	CO_2**fix** [**kg**CO_2eq/**yr**]
$Pct_{1,2,3}$ [kW]	$110.6_{1,2}$-20.9_3	-	-	$34.6_{1,2,3}$	-	-
CM	-	-	-	17 kWe	6250	111
PV	-	-	-	256 m^2	5416	2057
Inv	-	-	-	48 kW	3302	914
Mch	325 kWt	22747	2603	-	-	-
HP	-	-	-	254 kWt	17738	2030
GB	274 kWt	3824	137	116 kWt	1618	58
TSR	-	-	-	118 kWht	5254	668
	CIA / $CO2_{fix}$	*26571*	*2740*	***CIA*** / $CO2_{fix}$	*40578*	*5837*
Annual operational costs						
Fuel	**Consumption** [**kWh/yr**]	**Energy cost** [**€/yr**]	CO_2**ope** [**kg**CO_2eq/**yr**]	**Consumption** [**kWh/yr**]	**Energy cost** [**€/yr**]	CO_2**ope** [**kg**CO_2eq/**yr**]
Electricity	161495	42681	33341	44151	11523	9427
Natural Gas	303757	18189	62088	358411	21286	73259
	C_{ope}/ $CO2_{ope}$	*60869*	*95429*	C_{ope}/ $CO2_{ope}$	*32809*	*82686*
	TAC/ TCE	**87440**	**98169**	**TAC/ TCE**	**73387**	**88524**

Table 7.7: Results of the optimization of the polygeneration system for a residential building by applying RD 244/2019. Scenarios 2 and 3.

Technology	**Scenario 2**			**Scenario 3**		
	Install Cap	**CIA[€/yr]**	CO_2**fix** [**kg**CO_2eq/**yr**]	**Install Cap**	**CIA[€/yr]**	CO_2**fix** [**kg**CO_2eq/**yr**]
$Pct_{1,2,3}$ [kW]	$34.6_{1,2,3}$	-	-	$43.5_{1,2,3}$	-	-
CM	17 kWe	6349	112	7 kWe	2411	43
PV	327 m^2	8210	2633	599 m^2	15037	4822
Inv	61 kW	4225	1169	112 kW	7740	2142
HP	279 kWt	19497	2231	297 kWt	20751	2375
GB	112 kWt	1560	56	141 kWt	1970	70
TSQ	3 kWht	115	9	-	-	-
TSR	60 kWht	2942	374	27 kWht	1292	164
	CIA / $CO2_{fix}$	*42897*	*6584*	***CIA*** / $CO2_{fix}$	*49201*	*9616*
Annual operational costs						
Fuel	**Consumption** [**kWh/yr**]	**Energy cost** [**€/yr**]	CO_2**ope** [**kg**CO_2eq/**yr**]	**Consumption** [**kWh/yr**]	**Energy cost** [**€/yr**]	CO_2**ope** [**kg**CO_2eq/**yr**]
Electricity (Purchased)	42888	11276	6815	73650	18635	517
Electricity (Sold)	10463	-878		77127	-13957	
Natural Gas	333248	19860	68116	237516	14434	48548
	C_{ope}/ $CO2_{ope}$	*30258*	*74931*	C_{ope}/ $CO2_{ope}$	*19112*	*49065*
	TAC/ TCE	**73155**	**81515**	**TAC/ TCE**	**68312**	**58681**

Table 7.8: Total annual cost and CO_2eq emissions per dwelling based on RD 900/2015.

Scenarios	**Individual Installation**		**Collective installation**	
	Total Annual cost [€/yr]	**Total CO_2eq emissions [$kgCO_2eq$/yr]**	**Total Annual cost [€/yr]**	**Total CO_2eq emissions [$kgCO_2eq$/yr]**
Reference scenario	2236	1982	1749	1963
Scenario 1	2019	998	1571	1697
Scenario 2	2043	1200	1571	1694
Scenario 3			1553	1657

Table 7.9: Total annual cost and CO_2eq emissions per dwelling based on RD 244/2019.

Scenarios	**Individual Installation**		**Collective installation**	
	Total Annual cost [€/yr]	**Total CO_2eq emissions [$kgCO_2eq$/yr]**	**Total Annual cost [€/yr]**	**Total CO_2eq emissions [$kgCO_2eq$/yr]**
Reference scenario	2236	1982	1749	1963
Scenario 1	2019	998	1468	1770
Scenario 2	2017	973	1463	1630
Scenario 3	2015	973	1366	1174

of the optimal design of a polygeneration system for a residential building by applying legal restrictions based on the RD 900/2015. According to these results, the use of collective installations enables the reduction of the total annual cost per dwelling about 22% with respect to individual installations. However, apart from reference scenario, CO_2eq emissions per dwelling increase by using collective installations in every scenario, about 70% in scenario 1, and about 40% in scenarios 2 and 3, with respect to the emissions corresponding to the individual installations.

Table 7.9 presents the total annual cost and CO_2eq emissions of the optimal design of a polygeneration system for a residential building by applying legal restrictions based on the RD 244/2019. The use of collective installations enables the reduction of the total annual cost per dwelling about 27% in scenarios 1 and 2 and about 32% in scenario 3. In contrast, CO_2eq emissions per dwelling were increased by using collective installations about 77%, 68% and 21% in scenarios 1, 2 and 3 respectively.

The obtained results are remarkable taking into account that the CO_2eq emissions reduction is a very important factor to be considered in the energy

policy. Encouraging the collective installations should lead to decrease both the total annual cost and the CO_2eq emissions per dwelling, but it does not. In the three scenarios, the CO_2eq emissions per dwelling in residential buildings are higher than the obtained from individual installations.

This increase of CO_2eq emissions per dwelling is partly due to the natural gas consumption of the cogeneration module. In order to evaluate the impact of the cogeneration in the CO_2eq emissions, the energy system is optimized not allowing the installation of this technology. Figures 7.4a and 7.4b present the obtained results for a household (Hh), residential building per dwelling considering cogeneration (RB-CM), and residential building per dwelling without cogeneration (RB-Not CM) for both regulations. The economic and environmental impact of the optimization of polygeneration system per dwelling based on the RD 900/2015 is shown in the Figure 7.4a. There is a CO_2eq emissions reduction of about 7-9% when CM technology is not part of the optimal configuration with respect to RB-CM. However, the CO_2eq emissions results in residential building per dwelling remain higher than household results in every scenario.

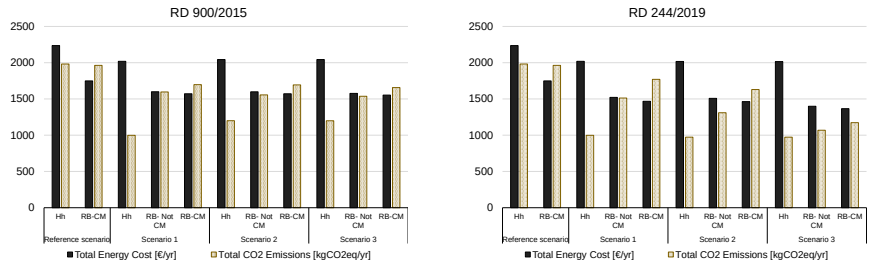

(a) (b)

Figure 7.4: Economic and environmental impact of the optimization of polygeneration system per dwelling: a) RD900/2015; b) RD244/2019.

The economic and environmental impact of the optimization of polygeneration system per dwelling based on the RD 244/2019 is shown in the figure 7.4b. There is a CO_2eq emissions reduction of about 15-20% when CM technology is not part of the optimal configuration with respect to RB-CM. However, the CO_2eq emissions results in residential building per dwelling remain higher

than household results. Unlike RD 900/2015, the RD 244/2019 does not have restrictions on installed self-consumption system capacity, which allows the installation of as much PV panels as possible in scenario 3, leading to reduce the CO_2eq emissions significantly.

The fact that the CO_2eq emissions per dwelling in residential buildings remain higher than household is because the natural gas consumption increases significantly whereas purchased electricity decreases in the residential building per dwelling as depicted in the figure 7.5. This is because under the current natural gas prices structure, the higher the natural gas consumption, the lower the natural gas price. Based on the obtained results, this prices structure should change in order to do not favour a larger consumption of fossil fuels (natural gas), at least for the residential sector (residential buildings-collective installations). In this way, more environmental-friendly technologies based on renewable energies that could be competitive and profitable would not be penalised and higher reductions of CO_2eq emissions would be achieved.

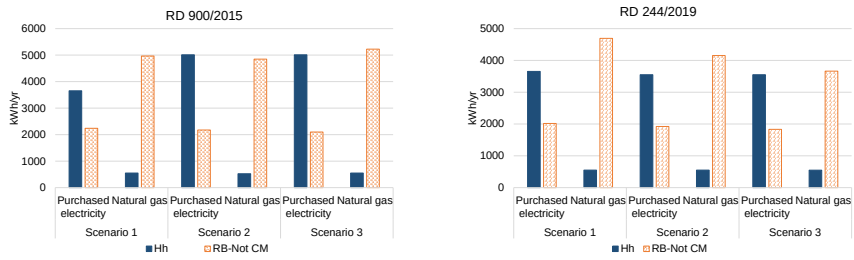

(a) (b)

Figure 7.5: Natural gas consumption Vs purchased electricity per dwelling: a) RD900/2015; b) RD244/2019.

7.1.4 Results comparison of the optimization of polygeneration systems under RD 900/2015 and RD 244/2019

The use of polygeneration systems with respect to conventional systems (reference scenario) provides economic and environmental benefits in all analysed cases. In individual installations (households), economic benefits were about

10%, whereas CO_2eq emissions reductions were about 50%, when PV technology was selected, for both regulations. In collective installations (residential buildings), the economic benefits were about 10% and 20% based on the application of RD 900/2015 and RD 244/2019 respectively. On the other hand, the CO_2eq emissions reduction was only about 14% for both regulations with respect to the reference system, except for the scenario 3 based on RD 244/2019, which enables CO_2eq emissions reduction about 40%, thanks to the installation of a significant capacity of PV, which is profitable due to the economic revenues obtained with self-produced electricity sale at 80% of the retail price. When comparing collective versus individual installations, it was observed that both regulations enable economic benefits of about 25% when using collective installations. However, promoting collective installations could lead to an increase of the CO_2eq emissions up to about 77% with respect individual installations in some scenarios. Therefore, promoting collective installations does not necessarily lead to accomplish the targets of CO_2eq emissions reduction, on the contrary, it could lead to increase the environmental impact under the current conditions.

7.2 Towards the design of affordable sustainable energy supply systems for buildings

Energy consumption in the residential sector plays an important role to mitigate climate change. Polygeneration systems are a suitable alternative enabling efficient use of natural resources with low environmental impact. However, their deployment depends, among other factors, on the economic cost and the legal restrictions. This section analyses the potential reduction of greenhouse gases emissions, expressed in CO_2-equivalent emissions (CO_2eq), in residential buildings installing polygeneration systems and considering the current Spanish self-consumption regulation RD244/2019. Taking as starting point this regulation, it is evaluated, through a multiobjective optimization considering both economic and environmental aspects, the potential CO_2eq emissions reduction of buildings' energy supply systems. In addition, guidelines for the affordable energy supply systems design, as close as possible to zero CO_2eq emissions for small-medium scale residential building, considering the current legal restrictions are proposed.

The multiobjective optimization of the polygeneration system was carried out for 12, 24 and 50 dwellings for three scenarios: scenario 1 in which elec-

Table 7.10: Results of the optimization of the reference systems for 12 and 24 dwellings.

Technology	**12 dwellings**			**24 dwellings**		
	Install Cap	**CIA[€/yr]**	CO_2**fix** [**kg**CO_2eq/**yr**]	**Install Cap**	**CIA[€/yr]**	CO_2**fix** [**kg**CO_2eq/**yr**]
$Pct_{1,2,3}$ [kW]	$24.2_{1,2}$-17.3_3	-	-	$43.5_{1,2}$-17.3_3	-	-
HP	70 kWt	5528	562	141kWt	11055	1125
GB	66 kWt	918	33	131 kWt	1836	66
	CIA / $CO2_{fix}$	*6445*	*595*	***CIA*** / $CO2_{fix}$	*12891*	*1190*
	Annual operational costs					
Fuel	**Consumption [kWh/yr]**	**Energy cost [€/yr]**	CO_2**ope** [**kg**CO_2eq/**yr**]	**Consumption [kWh/yr]**	**Energy cost [€/yr]**	CO_2**ope** [**kg**CO_2eq/**yr**]
Electricity	38759	10755	8002	77518	20298	16004
Natural Gas	72901	5253	14901	145813	9449	29804
	C_{ope}/ $CO2_{ope}$	*16008*	*22903*	C_{ope}/ $CO2_{ope}$	*29748*	*45808*
	TAC/ TCE	**22453**	**23498**	**TAC/ TCE**	**42638**	**46998**

tricity sale is not allowed, corresponding to the case of self-consumption type 1; scenario 2 in which electricity sale is allowed at spot price; and scenario 3 in which electricity sale is allowed at 80% purchase price. Scenarios 2 and 3 are proposed as particular examples of the self-consumption type 2. For comparison, a conventional energy system in which electricity is purchased from the electrical grid, a gas boiler (GB) attends heating demands and a mechanical chiller (MCh) covers only cooling demands, was considered as a reference scenario (Tables 7.10 and 7.11). Note that the 3 cases of study (12, 24 and 50 dwellings) are a scaling from the unit consumption, this allows to have an idea of the potential of the current self-consumption regulation to reduce CO_2eq emissions at affordable cost in different scales taking into account the limit of the installed capacity of 100 kW. In this way, the investors could evaluate the scale of the project to be both profitable and sustainable, being aware of the legal restrictions.

The results of the reference scenarios have been taken into account to calculate the potential reduction in terms of economic cost and CO_2eq emissions as well as the payback for different optimal configurations along the trade-off solutions of the Pareto curve. The payback is calculated as:

$$Payback[yr] = \frac{CI_{trade-off} - CI_{Reference}}{C_{ope_{Reference}} - C_{ope_{trade-off}}} \tag{7.4}$$

Where, CI is the total investment cost of the equipment in €, and C_{op} is the annual operational cost in €/yr.

Table 7.11: Results of the optimization of the reference systems for 50 dwellings.

Technology	**50 dwellings**		
	Install Cap	**CIA[€/yr]**	CO_2**fix [kg**CO_2eq**/yr]**
$Pct_{1,2,3}$ [kW]	$110.9_{1,2}$-17.3_3	-	-
HP	325 kWt	23031	2343
GB	274 kWt	3824	137
	CIA / $CO2_{fix}$	*26855*	*2480*
Annual operational costs			
Fuel	**Consumption [kWh/yr]**	**Energy cost [€/yr]**	CO_2**ope [kg**CO_2eq**/yr]**
Electricity	161495	42681	33341
Natural Gas	303757	18401	62088
	C_{ope}/ $CO2_{ope}$	*61082*	*95429*
	TAC/ TCE	**87938**	**97909**

Multiobjective optimization of the polygeneration systems for residential buildings under legal restrictions

Figures 7.6-7.8 show the Pareto curves for the cases of 12, 24 and 50 dwellings and the Table 7.12 presents the different configurations corresponding to the trade-off solutions along the Pareto curves. All of them are connected to the grid.

The highest reduction in CO_2eq emissions was obtained in scenarios where selling electricity was allowed. The more electricity produced with renewable energy was sold, the higher was the reduction of CO_2eq emissions. Note that in all the analysed cases, when it was not allowed the electricity sale, i.e. scenario 1, it was not possible to reach zero CO_2eq emissions. Therefore, in a horizon oriented to achieve zero greenhouse gases emissions (or lower values), selling electricity produced from renewable energy sources should be allowed. It is noteworthy to remark the Pareto curves shown in figure 7.8 for the case of 50 dwellings, in which the maximum reduction of CO_2eq emissions is the same for scenarios 2 and 3, because under the current self-consumption regulation (Boletin Oficial del Estado, 2019) the installed capacity of renewable energy technology is limited up to 100 kW. Therefore, the current self-consumption regulation, oriented to foster the implementation of decentralized energy supply systems based on renewable energy in buildings, which is also oriented to reach zero CO_2eq emissions, is targeted to small or medium size residential buildings with less than 24 dwellings (based on the considered energy demands). It is difficult and even not possible when increasing the size of the building to obtain zero CO_2eq emissions for residential buildings with more than 24 dwellings

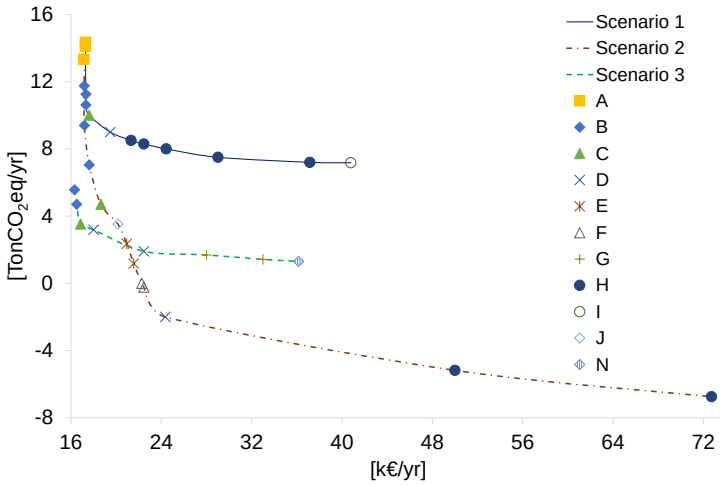

Figure 7.6: Pareto curves of the different scenarios for 12 dwellings case.

(based on the considered energy demands) by applying this regulation (Figure 7.8). If the regulation would allow higher power capacities, the potential of more significant reduction of CO_2eq emissions in big residential buildings would be higher. Therefore, the current self-consumption regulation is not enough to reach long term EU environmental targets on climate neutral by 2050 (European Commission, 2018). Nevertheless, note that as shown in the figures 7.6-7.8 in the three scenarios of the three analysed cases there is a sharp reduction of CO_2eq emissions with a relative small increase of economic cost, showing the feasibility of reducing very significantly in an affordable way the greenhouse gas emissions in residential buildings, as it is analysed in more detail in the next subsection. Consequently, the current Spanish self-consumption regulation (Boletin Oficial del Estado, 2019) is nowadays aligned with EU 2030 climate and energy framework targets (European Commission, 2018), but from the results obtained in this study the current regulation is not appropriate for reaching long term objective of carbon neutral energy supply systems. Therefore, in the mid-term it would be necessary to modify this regulation when more ambitious

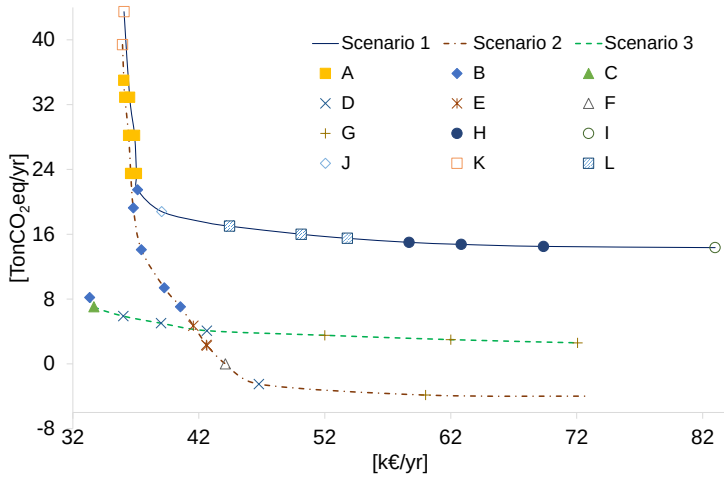

Figure 7.7: Pareto curves of the different scenarios for 24 dwellings case.

objectives on greenhouse gas emissions reduction would be established.

The higher electricity prices encourage electricity sale from renewable energy, which means reducing CO_2eq emissions. However, in the frame of the current regulation (Boletin Oficial del Estado, 2019), there is a point from which the achieved reduction of CO_2eq emissions in scenario 2 are higher than those obtained through scenario 3 (Figures 7.6-7.7). This is due to the billing time restriction, which establishes that the economic value of surplus electricity cannot be greater than the economic value of consumed electricity from the grid in a billing time, which has been considered a year in this study. Therefore, when net billing restriction is applied, the lower the electricity sale price, the higher the potential amount of electricity produced with renewable energy that could be sold to the grid and the higher the potential of reducing CO_2eq emissions. Obviously, the decentralized electricity produced with renewable energy will be sold to the grid when profitable. From the results shown in figures 7.6-7.7, it can be concluded that electricity sold at spot price could be a reasonable and feasible approach. Based on these results, it can be considered that nowadays

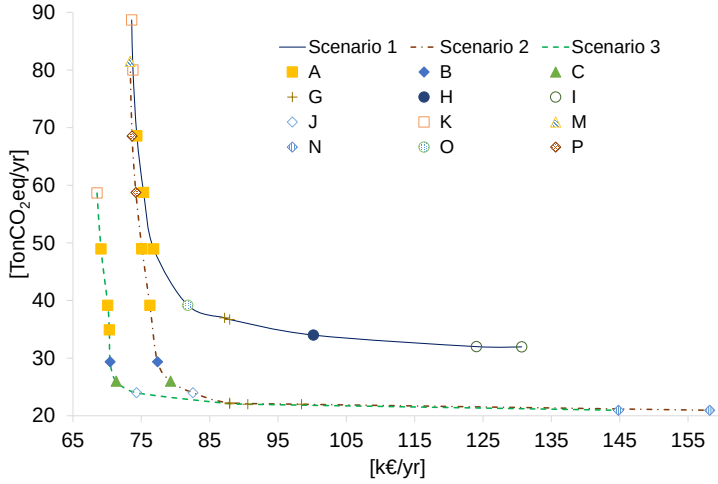

Figure 7.8: Pareto curves of the different scenarios for 50 dwellings case.

the scenario 2, providing interesting economic savings with respect to the reference scenario and with the highest potential of CO_2eq emissions reduction, among the considered scenarios, is an adequate approach combining economic profitability and a good alignment with current EU environmental and energy targets (European Commission, 2018).

The installed capacity of all technologies for the different trade-off solutions are presented below. Among the renewable energy technologies, ST and WT are the less competitive and therefore, they appear in a limited number of trade-off configurations (Table 7.12), when approaching the environmental optimum and significant reduction of CO_2eq emissions must be achieved (Figures 7.9b-7.9c, 7.10b-7.10c,7.11b-7.11c). Although available space is an important restriction to be considered in the design of energy systems for buildings, in this study, this restriction was removed in order to evaluate the technical, environmental and economic feasibility of PV ans ST technologies, as long as the legal restrictions allow to install them. However, note that these technologies compete for the available area. Thus, according to the results, in all cases PV technology prevails

Table 7.12: Different configurations of the trade-off solutions obtained along the Pareto curves.

Configuration	CM	PV	WT	ST	HP	GB	BB	ACH	TSQ	TSR	BAT
A	x	x			x	x	x			x	
B		x			x	x	x			x	
C		x		x	x	x	x			x	
D		x		x	x		x		x	x	
E		x			x		x			x	
F		x		x	x		x			x	
G		x	x	x	x		x		x	x	
H		x	x	x	x		x		x	x	x
I		x	x	x	x		x	x	x	x	x
J		x		x	x	x	x		x	x	
K	x	x			x	x				x	
L		x	x	x	x	x	x		x	x	x
M	x	x			x	x			x	x	
N		x	x	x	x		x	x	x	x	
O		x	x	x	x	x	x		x	x	
P	x	x			x	x	x		x	x	

over the ST technology (Figures 7.9a-7.9b, 7.10a-7.10b,7.11a-7.11b).

BB represents a very interesting alternative to GB and it is selected in most of the configurations (Table 7.12). GB technology is the main boiler in the economic optimum. Nonetheless, BB becomes the main boiler whereas GB tends to disappear in the pathway to reach the environmental optimum (Figure 7.9d-7.11d, 7.12b-7.14b).

CM is not very appropriate in residential buildings for the analysed cases when high CO_2eq emissions reduction must be achieved (Table 7.12). It appears in configurations close to the economic optimum and its feasibility is higher in bigger collective installations (Figure 7.13c,7.14c). In fact, in the case of 12 dwellings, the capacity of the installed CM is very small (1 kW), and although there are commercial CM with such a low capacity (Honda, 2003; Axiom Energy Group, 2020), its feasibility for few dwellings is questionable (Figure 7.12c).

HP appears in all trade-off solutions (Table 7.12) with a very significant capacity in the three considered scenarios (Figures 7.12a, 7.13a, 7.14a). It plays a very interesting role in the production of cooling and heating, as well as in the reduction of greenhouse gas emissions because its installation allows the reduction of capacity of GB and CM. In contrast, the interest of ACH is very limited compared to HP since it is barely selected, and when it does, it is negligible in most of the solutions. ACH presents a high investment cost and

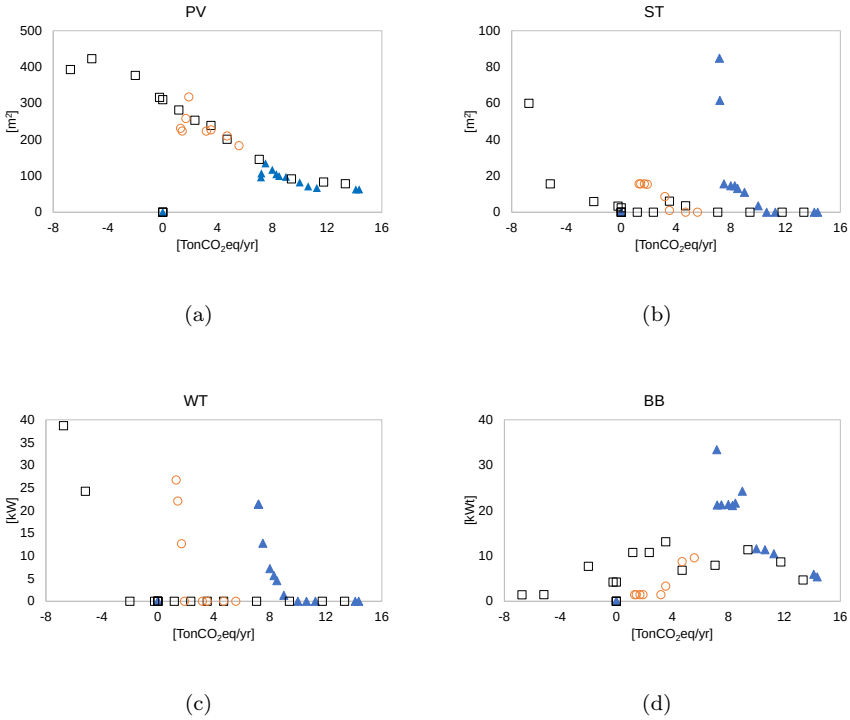

Figure 7.9: Sizing of the renewable energy technologies in the trade-off solutions for 12 dwellings case: scenario 1 (triangle), scenario 2 (square), scenario 3 (circle).

only produces one energy service, cooling (Figures 7.12d, 7.13d, 7.14d).

The installation of energy storage allows i) the match among energy production and energy consumption when energy resources are not manageable, as it is the case of solar (PV and/or ST) and wind energy (WT), and ii) the reduction of the installed capacity of some energy production pieces of equipment, such as HP or CM that thanks to the availability of storing energy they can operate at a high load with lower installed capacity during a longer time period, even when there is not energy consumption, storing the energy produced in order to consume it in the moment where there is a high or peak demand. In this

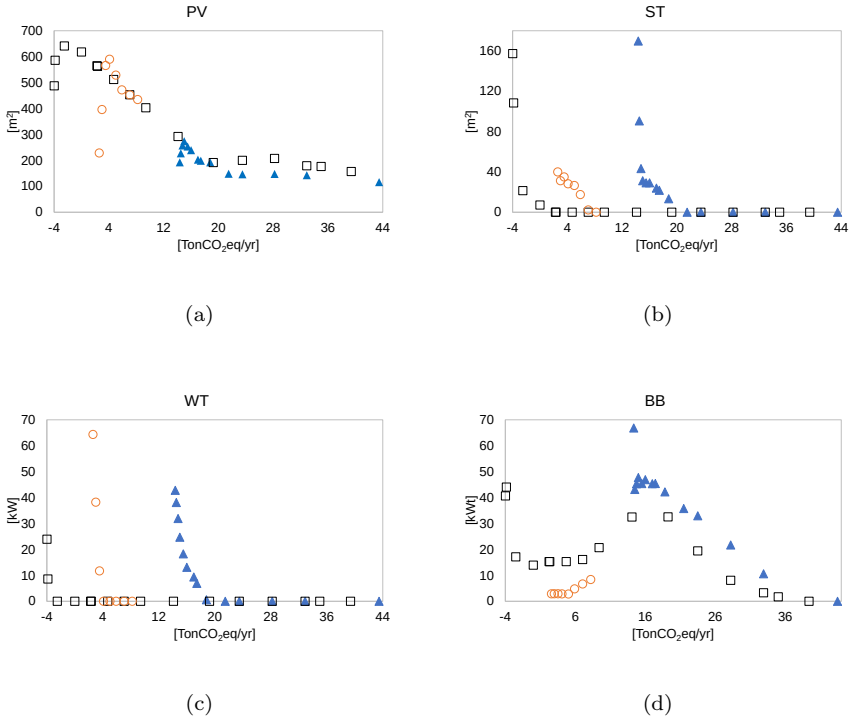

Figure 7.10: Sizing of the renewable energy technologies in the trade-off solutions for 24 dwellings case: scenario 1 (triangle), scenario 2 (square), scenario 3 (circle).

respect BAT appears in a few configurations, due to its high investment cost, when approaching the environmental optimum with a significant production of electricity from non-manageable renewable resources (WT and PV) and there is not the possibility of selling it to the grid, as it is the case of scenario 1. In the case of 12 dwellings BAT are also installed close to the environmental optimum of scenario 2 when there is also installed a significant capacity of PV and WT, and the electricity is sold at spot price, which is a relatively low price. When the electricity price is higher than the spot price (scenario 3), it is more profitable to sell electricity than to store it in the electric batteries (Figure 7.15c, 7.16c,

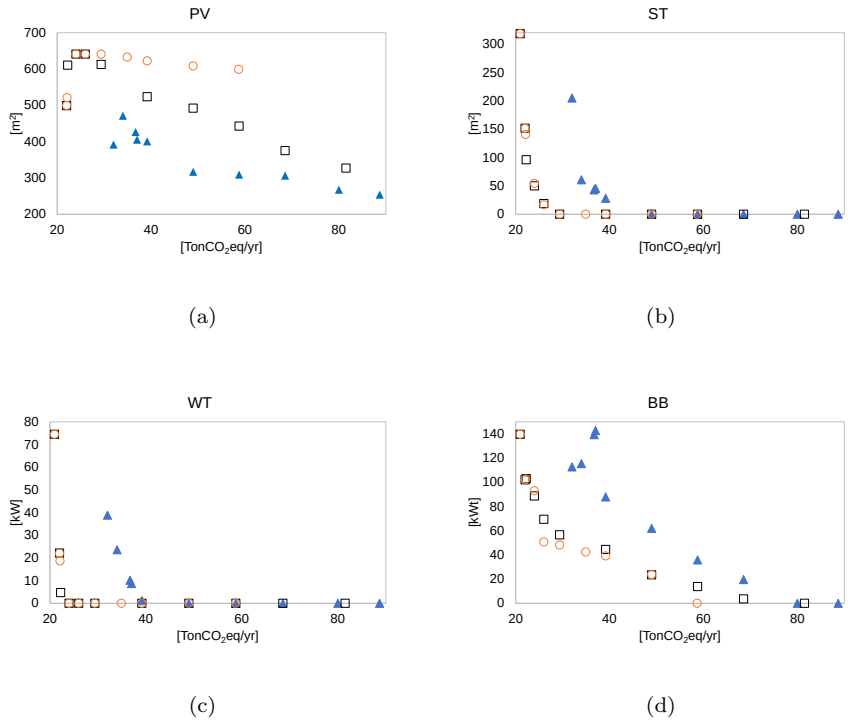

Figure 7.11: Sizing of the renewable energy technologies in the trade-off solutions for 50 dwellings case: scenario 1 (triangle), scenario 2 (square), scenario 3 (circle).

7.17c). TSQ, which is a quite common technology with a lower investment cost than TSR appears in less configurations than the latter (Table 7.12), due to the various different available technological options for the heat production. Furthermore, TSQ is selected in the trade-off solutions close to the environmental optimum (Figures 7.15a, 7.16a, 7.17a). TSR appears in all configurations (Table 7.12) because its operation is closely coupled with HP, allowing the reduction of the installed capacity, with the corresponding reduction of its investment cost (Figures 7.15b, 7.16b, 7.17b).

Selling to the grid electricity produced with renewable energy technologies

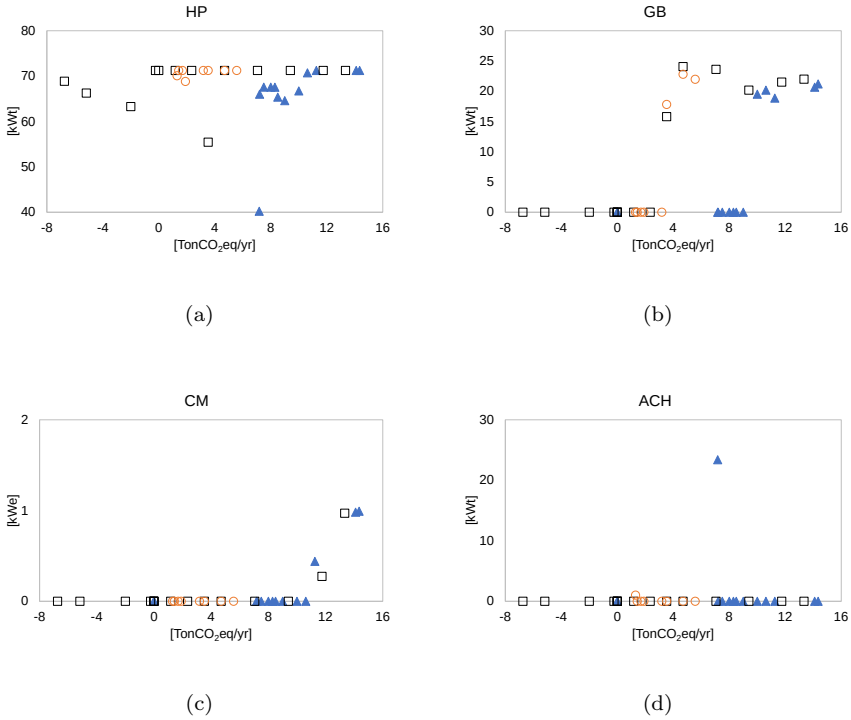

Figure 7.12: Sizing of the electricity/heating/cooling production technologies in the trade-off solutions for 12 dwellings case: scenario 1 (triangle), scenario 2 (square), scenario 3 (circle).

offsets greenhouse gas emissions allowing additional CO_2eq emissions reductions. Therefore, contracted power tends to increase in the pathway towards the environmental optimum in order to enable higher injection of renewable energy to the grid in scenarios 2 and 3 (Figures 7.15d, 7.16d, 7.17d).

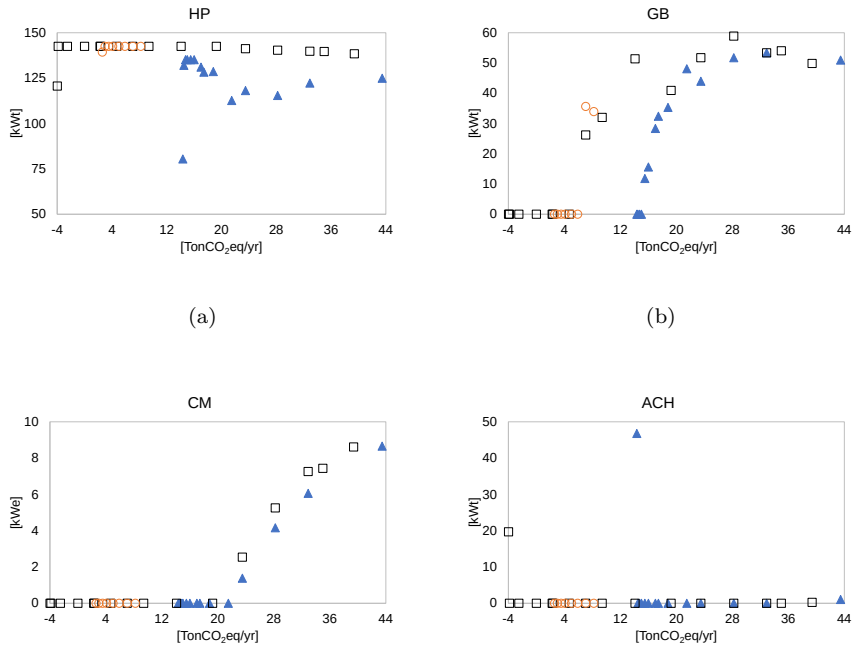

Figure 7.13: Sizing of the electricity/heating/cooling production technologies in the trade-off solutions for 24 dwellings case: scenario 1 (triangle), scenario 2 (square), scenario 3 (circle).

7.2.1 Evaluation of cost and CO_2eq emissions reduction for different trade-off solutions

Different trade-off solutions were obtained along the Pareto curves. Tables 7.13-7.15 present, for the different trade-off solutions, the configuration (CFG), payback (PB), cost reduction (CR) and CO_2eq emissions reduction (CO2R) with respect to the reference scenario. Among the trade-off solutions, those at an annual cost equal to the reference scenario are highlighted. In the scenario 1, CO_2eq emissions reductions up to about 65% were achieved, whereas in scenar-

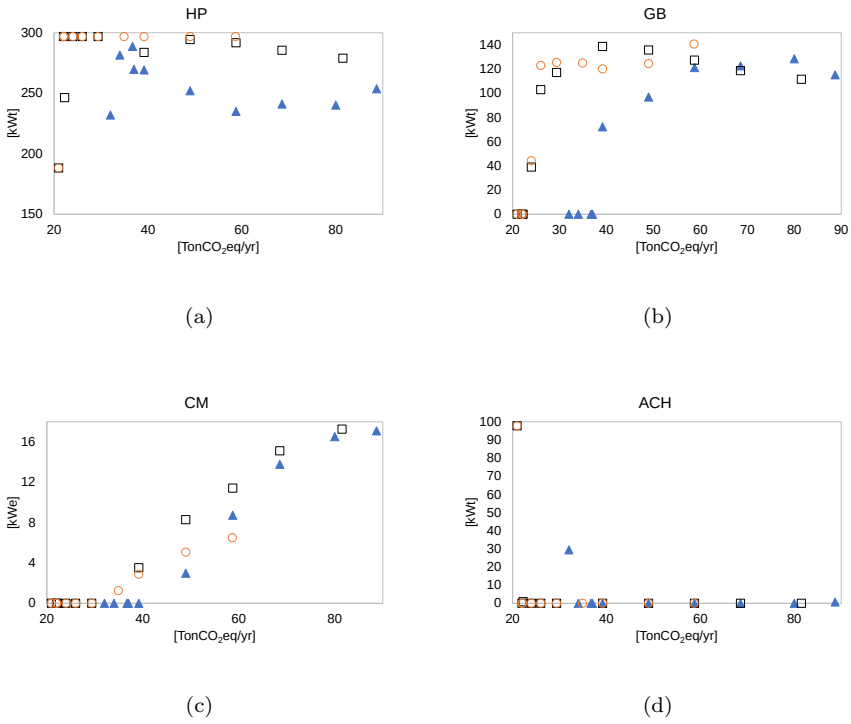

Figure 7.14: Sizing of the electricity/heating/cooling production technologies in the trade-off solutions for 50 dwellings case: scenario 1 (triangle), scenario 2 (square), scenario 3 (circle).

ios 2 and 3, were about 75% - 100%. These results show that nowadays, with the available technology and the current Spanish self-consumption regulation (Boletin Oficial del Estado, 2019), it is possible to achieve remarkable CO_2eq emissions reduction with respect to the conventional systems at an affordable cost. The payback of the aforementioned trade-off solutions is around 10 - 12 years, which could be a reasonable time to recover the investment, taking into account the benefits in the operational costs and environmental aspects. High shares of renewable energy can be considered as an advantage, since the uncertainty on the energy system investment is reduced, due to the lower consump-

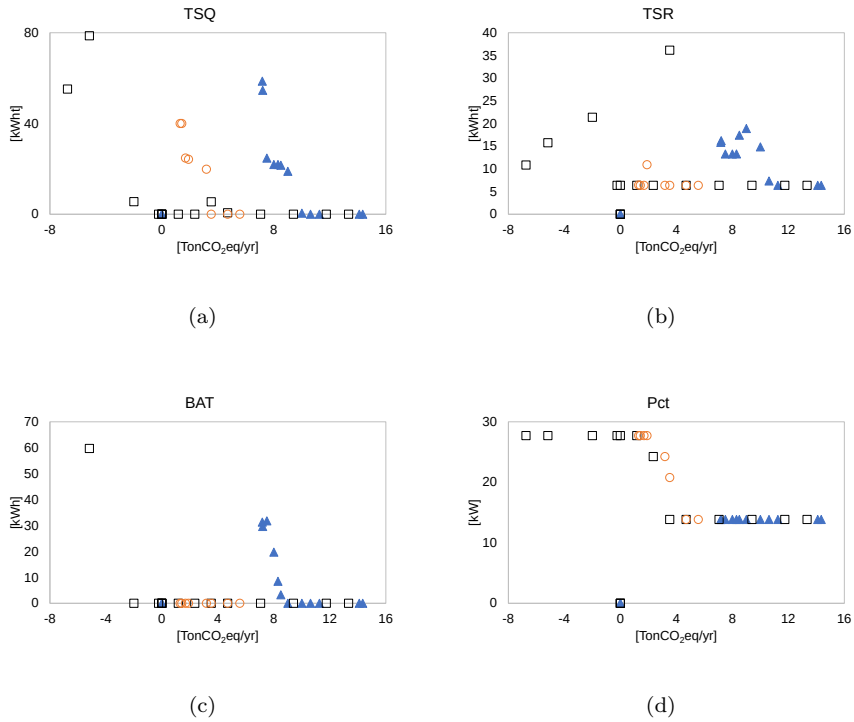

Figure 7.15: Sizing of the energy storage technologies and Pct in the trade-off solutions for 12 dwellings case: scenario 1 (triangle), scenario 2 (square), scenario 3 (circle).

tion of fossil fuels, which experience a high variability of their market prices. On the other hand, in the three analysed cases, the payback period corresponding to 50% CO_2eq emissions reduction is significantly lower thanks to the cost reduction with respect to the reference scenario, reinforcing the economic and environmental interest of such systems for the energy supply of buildings.

Table 7.13: Configuration, payback, total annual cost and CO_2eq emissions reductions for trade-off solutions with respect to the reference scenario in the 12 dwellings case.

Scenario 1				Scenario 2				Scenario 3			
CFG	**PB [yr]**	**CR**	**CO2R**	**CFG**	**PB [yr]**	**CR**	**CO2R**	**CFG**	**PB [yr]**	**CR**	**CO2R**
A	3.3	-23%	-39%	A	3.9	-24%	-43%	B	5.8	-27%	-76%
A	3.3	-23%	-40%	B	3.8	-23%	-50%	B	6.4	-26%	-80%
B	3.3	-23%	-52%	B	4.0	-23%	-60%	C	7.1	-25%	-85%
B	3.3	-23%	-55%	B	5.8	-22%	-70%	D	8.2	-20%	-86%
C	4.1	-22%	-57%	C	7.6	-17%	-80%	***D***	***12.5***	***0%***	***-92%***
D	7.1	-13%	-62%	J	9.2	-10%	-85%	G	17.8	25%	-93%
H	9.5	-5%	-64%	E	9.4	-7%	-90%	G	22.5	47%	-94%
H	***10.8***	***0%***	***-65%***	E	10.2	-4%	-95%	N	25.6	61%	-94%
H	12.9	9%	-66%	F	11.6	-1%	-100%	-	-	-	-
H	17.4	29%	-68%	***F***	***11.8***	***0%***	***-101%***	-	-	-	-
H	24.9	65%	-69%	D	13.6	8%	-109%	-	-	-	-
I	28.2	82%	-69%	H	38.8	123%	-122%	-	-	-	-
-	-	-	-	H	60.5	224%	-129%	-	-	-	-

Table 7.14: Configuration, payback, total annual cost and CO_2eq emissions reductions for trade-off solutions with respect to the reference scenario in the 24 dwellings case.

Scenario 1				Scenario 2				Scenario 3			
CFG	**PB [yr]**	**CR**	**CO2R**	**CFG**	**PB [yr]**	**CR**	**CO2R**	**CFG**	**PB [yr]**	**CR**	**CO2R**
K	6.2	-15%	-8%	K	6.7	-16%	-16%	B	7.2	-22%	-83%
A	5.9	-14%	-30%	A	6.7	-15%	-26%	C	7.8	-21%	-85%
A	5.7	-13%	-40%	A	6.7	-15%	-30%	D	9.1	-16%	-87%
A	4.8	-13%	-50%	A	6.7	-15%	-40%	D	10.6	-9%	-89%
B	4.4	-13%	-54%	A	5.8	-14%	-50%	***D***	***12.4***	***0%***	***-91%***
J	7.1	-8%	-60%	B	4.9	-14%	-59%	G	17.5	22%	-92%
Q	***10.1***	***0%***	***-63%***	B	6.7	-12%	-70%	G	23.1	45%	-94%
L	11.4	4%	-64%	B	8.7	-8%	-80%	G	28.9	69%	-94%
L	15.0	18%	-66%	B	9.7	-5%	-85%	-	-	-	-
L	17.0	26%	-67%	E	10.5	-3%	-90%	-	-	-	-
H	19.5	38%	-68%	E	11.2	0%	-95%	-	-	-	-
H	21.6	47%	-69%	***E***	***11.2***	***0%***	***-95%***	-	-	-	-
H	24.9	63%	-69%	F	12.3	3%	-100%	-	-	-	-
-	-	-	-	D	13.7	10%	-105%	-	-	-	-
-	-	-	-	G	21.2	41%	-108%	-	-	-	-
-	-	-	-	N	28.9	71%	-108%	-	-	-	-

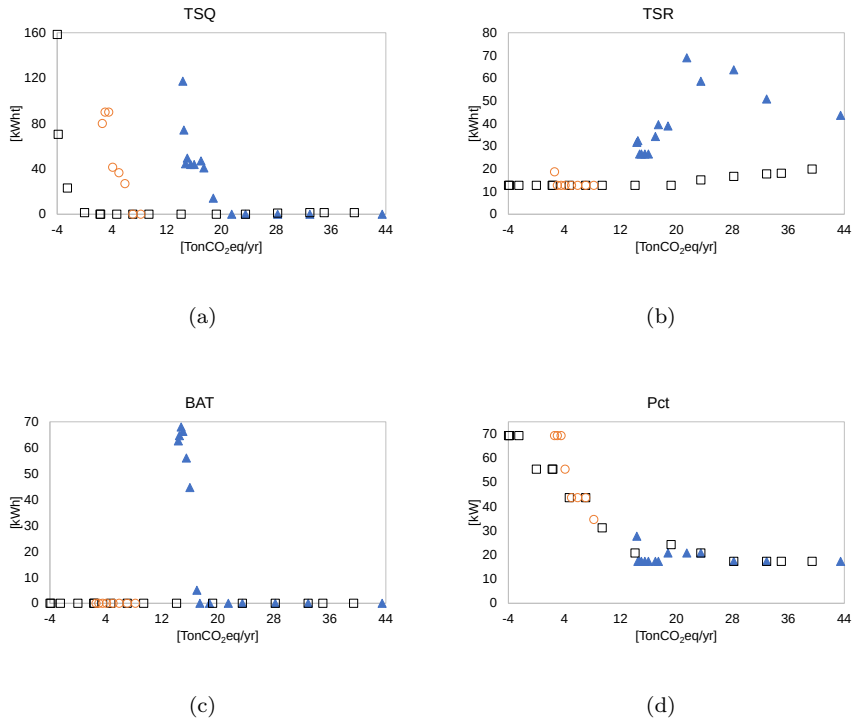

(a) (b)

(c) (d)

Figure 7.16: Sizing of the energy storage technologies and Pct in the trade-off solutions for 24 dwellings case: scenario 1 (triangle), scenario 2 (square), scenario 3 (circle).

7.2.2 Feasible configurations to achieve remarkable reduction of CO_2eq emissions at affordable cost

The simplicity of the configuration is an advantage to be considered as investment criteria. In this sense, among the different trade-off solutions, configuration B (Figure 7.18) has been chosen for its simplicity and convenience in the transition to achieve sustainable energy systems, since allows the gradual replacement of the conventional fuels (natural gas, electricity from the grid) by renewable energy sources. Besides, this configuration was one of the optimal

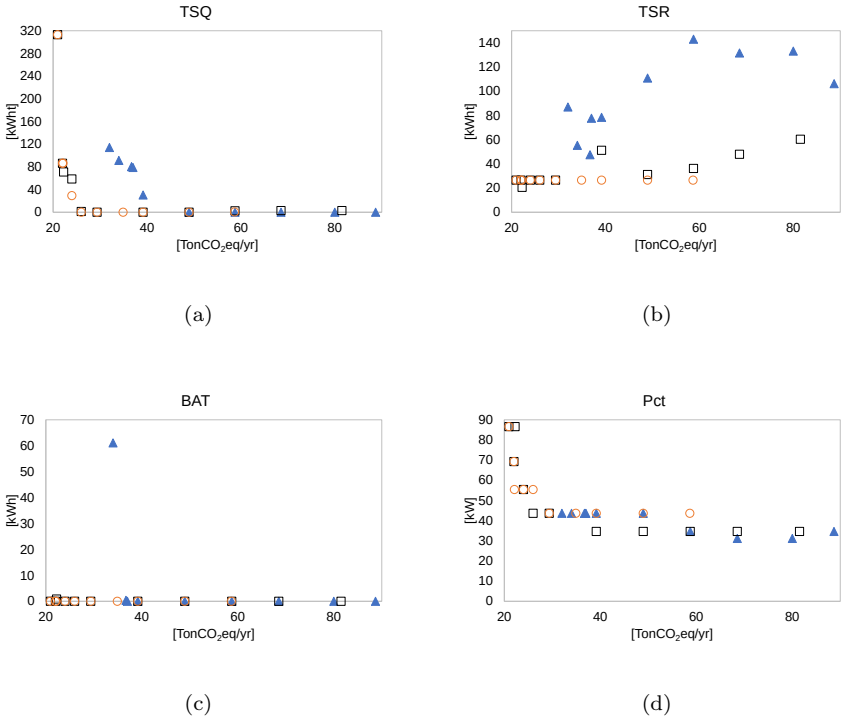

Figure 7.17: Sizing of the energy storage technologies and Pct in the trade-off solutions for 50 dwellings case: scenario 1 (triangle), scenario 2 (square), scenario 3 (circle).

configurations selected in almost all Pareto curves (the only exception is the scenario 1 for 50 dwellings as shown in Table 7.15) and it allows, in some cases, very significant CO_2eq emissions reductions up to 82%, with a little increase of cost, about 13%, with respect to the economic optimum (see figures 7.6-7.8). For the scenario 3, in the case of 24 dwellings, the economic optimum corresponds to the configuration B.

Tables 7.16-7.21 present the results of the design of the configuration B for the different number of dwellings and scenarios, corresponding to the lowest CO_2eq emission values of configuration B depicted in the Pareto curves (Fig-

Table 7.15: Configuration, payback, total annual cost and CO_2eq emissions reductions for trade-off solutions with respect to the reference scenario in the 50 dwellings case.

Scenario 1				Scenario 2				Scenario 3			
CFG	**PB [yr]**	**CR**	**CO2R**	**CFG**	**PB [yr]**	**CR**	**CO2R**	**CFG**	**PB [yr]**	**CR**	**CO2R**
K	6.1	-16%	-9%	M	6.5	-17%	-17%	K	6.7	-22%	-40%
K	6.3	-16%	-18%	P	6.7	-16%	-30%	A	6.2	-21%	-50%
A	6.1	-15%	-30%	P	6.7	-16%	-40%	A	6.1	-20%	-60%
A	5.7	-14%	-40%	A	6.9	-15%	-50%	A	6.0	-20%	-64%
A	5.1	-13%	-50%	A	6.7	-13%	-60%	B	5.8	-20%	-70%
O	7.4	-7%	-60%	B	6.9	-12%	-70%	C	6.4	-19%	-73%
G	9.7	-1%	-62%	C	7.8	-10%	-73%	J	7.1	-15%	-75%
G	***10.0***	***0%***	***-63%***	J	8.9	-6%	-75%	***G***	***10.6***	***0%***	***-77%***
H	14.0	14%	-65%	***G***	***10.0***	***0%***	***-77%***	G	11.3	3%	-78%
I	20.5	41%	-67%	G	13.3	12%	-78%	N	26.6	65%	-79%
I	22.5	49%	-67%	N	37.9	80%	-79%	-	-	-	-

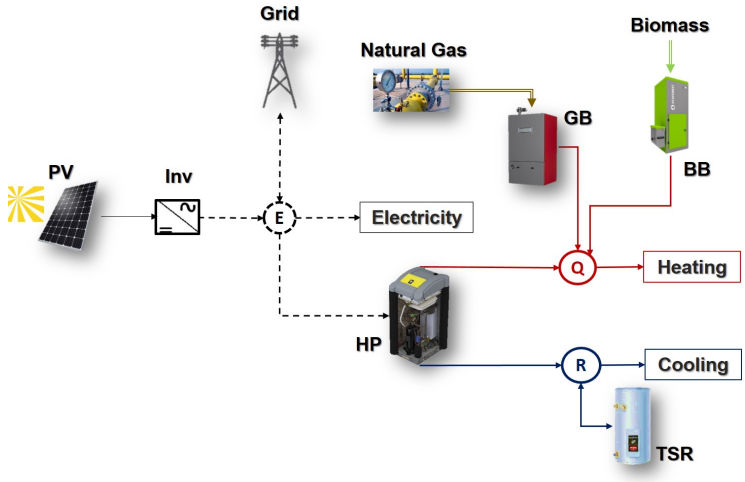

Figure 7.18: Energy system technologies corresponding to the configuration B.

ures 7.6-7.8). In the particular case of the 50 dwellings for the scenario 1, the economic optimum of configuration B, which is very close to the Pareto curve, is presented. In all the selected designs of configuration B shown in the Tables 7.13-7.15, the additional investment in the polygeneration system (with respect to the reference scenario) is compensated with a remarkable reduction in the op-

Table 7.16: Results of the design of the configuration B for a residential building corresponding to the 12 dwellings case.

Technology	**Scenario 1**			**Scenario 2**		
	Install Cap	**CIA[€/yr]**	CO_2**fix** [**kg**CO_2eq/**yr**]	**Install Cap**	**CIA[€/yr]**	CO_2**fix** [**kg**CO_2eq/**yr**]
Pct	13.9 kW	-	-	13.9 kW	-	-
PV	71 m^2	1789	574	146 m^2	3654	1172
Inv	13 kW	921	255	27 kW	1881	520
HP	71 kWt	4944	566	71 kWt	4980	570
GB	20 kWt	282	10	24 kWt	330	12
BB	11 kWt	477	6	8 kWt	333	4
TSR	7 kWht	358	45	6 kWht	310	39
	CIA / $CO2_{fix}$	*8770*	*1456*	***CIA*** / $CO2_{fix}$	*11488*	*2317*
	Annual operational costs					
Fuel	**Consumption** [**kWh/yr**]	**Energy cost** [**€/yr**]	CO_2**ope** [**kg**CO_2eq/**yr**]	**Consumption** [**kWh/yr**]	**Energy cost** [**€/yr**]	CO_2**ope** [**kg**CO_2eq/**yr**]
Electricity (Purchased)	35236	7131	7399	30044	6201	3436
Electricity (Sold)	-	-	-	14784	-1131	
Natural Gas	0	71	0	0	71	0
Biomass	27939	1352	1760	20547	994	1294
	C_{ope}/ $CO2_{ope}$	*8554*	*9159*	C_{ope}/ $CO2_{ope}$	*6137*	*4731*
	TAC/ TCE	**17324**	**10615**	**TAC/ TCE**	**17625**	**7048**

erational cost which leads to a total annual cost reduction. The operational cost reduction is proportional to the reduction of electricity consumption from the grid and the fossil fuel consumption. Hence, a remarkable reduction of CO_2eq emissions is also achieved. In the case of 12 dwellings, the GB technology was selected only to cover heating peak demands, i.e. it was selected as an auxiliary boiler. In these cases, the natural gas cost corresponds to the fixed cost of the natural gas contract, so this is the cost for the availability of this service. In the case of 24 dwellings, the natural gas consumption by the GB technology is always lower than the biomass consumption, therefore, GB technology works as an auxiliary boiler as well. A similar situation occurs in the case of 50 dwellings for scenarios 2 and 3; however, in scenario 1 does not. For this scenario, as aforementioned, the economic optimum of the configuration B is presented, which is close to the economic point of this pareto curve. In this particular case, GB technology is the main boiler, since the natural gas consumption is higher than the biomass consumption. This is due to the natural gas tariff is lower than the biomass price. Note that the natural gas tariff depends on the natural gas consumption and its cost is lower when the gas consumption increases.

Based on the obtained results, when comparing the case of 12 dwellings for the scenario 1 with respect to the reference system, it is observed that an additional investment cost of 36% leads to reduce the total annual cost in about 23% and total CO_2eq emissions in about 55%. For the scenario 2, an additional

Table 7.17: Results of the design of the configuration B for a residential building corresponding to the 12 dwellings case-Scenario 3.

Technology	**Scenario 3**		
	Install Cap	**CIA[€/yr]**	CO_2**fix** [**kg**CO_2eq**/yr**]
Pct	13.9 kW	-	-
PV	210 m^2	5272	1691
Inv	39 kW	2713	751
HP	71 kWt	4980	570
GB	23 kWt	319	11
BB	9 kWt	367	4
TSR	6 kWht	310	39
	CIA / $CO2_{fix}$	*13961*	*3067*
Annual operational costs			
Fuel	**Consumption [kWh/yr]**	**Energy cost [€/yr]**	CO_2**ope** [**kg**CO_2eq**/yr**]
Electricity (Purchased)	2760	5609	4
Electricity (Sold)	28537	-4387	
Natural Gas	0	71	0
Biomass	25847	1251	1628
	C_{ope}/ $CO2_{ope}$	*2543*	*1632*
	TAC/ TCE	**16504**	**4699**

Table 7.18: Results of the design of the configuration B for a residential building corresponding to the 24 dwellings case.

Technology	**Scenario 1**			**Scenario 2**		
	Install Cap	**CIA[€/yr]**	CO_2**fix** [**kg**CO_2eq**/yr**]	**Install Cap**	**CIA[€/yr]**	CO_2**fix** [**kg**CO_2eq**/yr**]
$Pct_{1,2,3}$ [kW]	$20.8_{1,2,3}$	-	-	43.6_1-$34.6_{2,3}$	-	-
PV	148 m^2	3727	1195	453 m^2	11369	3646
Inv	28 kW	1918	531	85 kW	5852	1619
HP	113 kWt	7875	901	142 kWt	9961	1140
GB	48 kWt	672	24	26 kWt	366	13
BB	36 kWt	1501	18	16 kWt	676	8
TSR	69 kWht	3363	427	13 kWht	620	79
	CIA / $CO2_{fix}$	*19056*	*3096*	***CIA*** / $CO2_{fix}$	*28843*	*6505*
Annual operational costs						
Fuel	**Consumption [kWh/yr]**	**Energy cost [€/yr]**	CO_2**ope** [**kg**CO_2eq**/yr**]	**Consumption [kWh/yr]**	**Energy cost [€/yr]**	CO_2**ope** [**kg**CO_2eq**/yr**]
Electricity (Purchased)	48536	12122	10331	51304	14375	-2594
Electricity (Sold)	-	-	-	68461	-5158	
Natural Gas	3752	358	767	0	71	0
Biomass	115754	5603	7293	49812	2411	3138
	C_{ope}/ $CO2_{ope}$	*18082*	*18390*	C_{ope}/ $CO2_{ope}$	*11700*	*544*
	TAC/ TCE	**37138**	**21486**	**TAC/ TCE**	**40543**	**7049**

Table 7.19: Results of the design of the configuration B for a residential building corresponding to the 24 dwellings case-Scenario 3.

Technology	**Scenario 3**		
	Install Cap	**CIA[€/yr]**	CO_2**fix [kg**CO_2eq**/yr]**
$Pct_{1,2,3}$ [kW]	$34.6_{1,2,3}$	-	-
PV	435 m^2	10909	3498
Inv	81 kW	5615	1554
HP	142 kWt	9961	1140
GB	34 kWt	474	17
BB	8 kWt	352	4
TSR	13 kWht	620	79
	CIA / $CO2_{fix}$	*27931*	*6292*
Annual operational costs			
Fuel	**Consumption [kWh/yr]**	**Energy cost [€/yr]**	CO_2**ope [kg**CO_2eq**/yr]**
Electricity (Purchased)	56972	15070	-196
Electricity (Sold)	62795	-11354	
Natural Gas	83	77	17
Biomass	33188	1606	2091
	C_{ope}/ $CO2_{ope}$	*5400*	*1912*
	TAC/ TCE	**33331**	**8204**

Table 7.20: Results of the design of the configuration B for a residential building corresponding to the 50 dwellings case.

Technology	**Scenario 1**			**Scenario 2**		
	Install Cap	**CIA[€/yr]**	CO_2**fix [kg**CO_2eq**/yr]**	**Install Cap**	**CIA[€/yr]**	CO_2**fix [kg**CO_2eq**/yr]**
$Pct_{1,2,3}$ [kW]	$43.6_{1,2,3}$	-	-	$43.6_{1,2,3}$	-	-
PV	309 m^2	7764	2490	613 m^2	15377	4931
Inv	58 kW	3996	1106	115 kW	7914	2190
HP	236 kWt	16513	1890	297 kWt	20751	2375
GB	167 kWt	2331	83	117 kWt	1638	59
BB	7 kWt	292	3	57 kWt	2373	28
TSR	141 kWht	6865	873	27 kWht	1292	164
	CIA / $CO2_{fix}$	*37761*	*6444*	***CIA*** / $CO2_{fix}$	*49345*	*9747*
Annual operational costs						
Fuel	**Consumption [kWh/yr]**	**Energy cost [€/yr]**	CO_2**ope [kg**CO_2eq**/yr]**	**Consumption [kWh/yr]**	**Energy cost [€/yr]**	CO_2**ope [kg**CO_2eq**/yr]**
Electricity (Purchased)	100897	24229	21242	103127	25041	9530
Electricity (Sold)	-	-	-	62260	-4756	
Natural Gas	189521	11926	38738	1012	149	207
Biomass	48184	2332	3036	156804	7589	9879
	C_{ope}/ $CO2_{ope}$	*38487*	*63016*	C_{ope}/ $CO2_{ope}$	*28023*	*19615*
	TAC/ TCE	**76248**	**69460**	**TAC/ TCE**	**77368**	**29362**

Table 7.21: Results of the design of the configuration B for a residential building corresponding to the 50 dwellings case-Scenario 3.

Technology	**Scenario 3**		
	Install Cap	**CIA[€/yr]**	CO_2**fix [kg**CO_2eq**/yr]**
$Pct_{1,2,3}$ [kW]	$43.6_{1,2,3}$	-	-
PV	641 m^2	16092	5160
Inv	120 kW	8283	2292
HP	297 kWt	20751	2375
GB	125 kWt	1754	63
BB	48 kWt	2025	24
TSR	27 kWht	1292	164
	CIA / $CO2_{fix}$	*50196*	*10078*
	Annual operational costs		
Fuel	**Consumption [kWh/yr]**	**Energy cost [€/yr]**	CO_2**ope [kg**CO_2eq**/yr]**
Electricity (Purchased)	104686	25311	6210
Electricity (Sold)	81330	-14692	
Natural Gas	6560	608	1341
Biomass	186390	9021	11743
	C_{ope}/ $CO2_{ope}$	*20249*	*19294*
	TAC/ TCE	**70446**	**29372**

investment cost of 78% leads to reduce the total annual cost in about 22% and total CO_2eq emissions in about 70%. For the scenario 3, by doubling the investment cost, the total annual cost can be reduced in about 26% and total CO_2eq emissions in about 80%. In the case of 24 dwellings, for the scenario 1, an additional investment cost of 48% leads to reduce the total annual cost in about 13% and total CO_2eq emissions in about 54%. For the scenarios 2 and 3, by doubling the investment cost, the total annual cost can be reduced about 5% and 22% respectively, and the total CO_2eq emissions in about 84% in both scenarios. In the case of 50 dwellings, for the scenario 1, an additional investment cost of 41% leads to reduce the total annual cost in about 13% and total CO_2eq emissions in about 29%. For scenarios 2 and 3, an additional investment cost in about 85% leads to reduce the total annual cost in about 12% and 20% respectively, and total CO_2eq emissions of about 70%.

7.3 Closure

The effect of the two recent self-consumption regulations on the optimal configuration of polygeneration systems for the residential sector has been studied from the economic and environmental point of view. The study has encompassed the individual installations (households) and residential buildings.

Attending to the comparison of the individual vs collective installations results, the collective ones are more economically profitable than individual installations in the application of both regulations. However, from the environmental point of view, polygeneration systems for collective installations based on both regulations lead to increase CO_2eq emissions with respect to individual installations.

In general, by promoting collective installations, the RD 244/2019 encourages the investment in different renewable energy technologies unlike RD 900/2015, which established a specific taxation to self-consumption installations higher than 10 kW, in spite of that they were profitable, which represented a barrier to competitive distributed generation. However, the current Spanish regulation is still not enough to achieve a significant reduction of CO_2eq emissions with respect to the individual installations. Based on the obtained results, through the optimal configuration of individual installations it is possible to achieve higher CO_2eq emissions reduction than those obtained by using collective installations. Therefore, more appropriate regulations with a wider perspective leading to further CO_2eq emissions reduction in collective installations should be evaluated. The obtained results provide conclusions that are also valid for most of European countries, where the natural gas price for household consumers decreases when increasing the level of consumption. A more appropriate pricing of natural gas, in which its cost was not reduced when increasing its consumption, and in which greenhouse-gas emissions were considered, would lead to the design and installation of energy systems for building providing the required energy systems (polygeneration systems) with significant reduction of CO_2eq emissions at reasonable and even profitable costs.

For this reason, the legal restrictions in accordance to the current Spanish self-consumption regulation (Boletin Oficial del Estado, 2019) was taken into account to evaluate the potential of reduction of CO_2eq emissions at an affordable cost, as well as its alignment with the European objectives on greenhouse gases emissions reduction (European Commission, 2018). Different scenarios were studied in residential buildings (12, 24 and 50 dwellings) located in Zaragoza (Spain), with and without selling electricity to the electrical grid. It was demonstrated in all the analysed cases, the feasibility of using polygeneration systems

for residential buildings to reduce both the economic costs and the environmental impact. Therefore, it is possible to achieve remarkable CO_2eq emissions reduction (above 65% with respect to conventional systems) at an affordable cost.

Several technologies were also evaluated, nonetheless the most selected technologies along the Pareto curves were PV, HP and TSR, highlighting the important role of the reversible HP in the objective to reduce CO_2eq emissions at an affordable cost, particularly when its integration with PV is feasible. In this respect, whatever regulation fostering energy efficiency and reduction of greenhouse gas emissions should not represent a barrier for the installation of HP and renewable energy technologies and should facilitate the integration of HP with renewable energies considering at the same time the economic feasibility. Technologies such as CM and ACH were barely selected, due to their high investment cost as well as to the consumption of fossil fuels of the former. In the case of WT, ST, and BAT, due to their high investment cost were mainly selected in the trade-off solutions close to the environmental optimum. In the case of BB, it was observed the high potential of this technology to reduce CO_2eq emissions, since it was one of the most selected technologies along the Pareto curves, and it displaced the GB technology in the pathway to reduce CO_2eq emissions.

Although under a self-consumption scheme only, without allowing electricity sale to the electrical grid, was achieved a significant reduction of CO_2eq emissions, it was not possible to offset 100% of greenhouse gas emissions. This objective, zero CO_2eq emissions, only could be reached allowing also the sale of electricity produced with renewable energy sources. However, under the current conditions, although high prices of electricity sale foster the investment in renewable energy technologies, the potential reduction of CO_2eq emissions is limited owing to the net billing restriction.

Based on the obtained results, a concluding remark from the lessons learnt from the Spanish self-consumption regulation is that the installation of i) polygeneration energy supply systems based on PV, HP, TSR and BB technologies properly integrated, under ii) self-consumption scheme, with iii) net billing of renewable electricity sale, iv) at an appropriate electricity price (spot market price in the analysed cases), with v) an adequate limitation of the installation of renewable electrical power in vi) collective energy supply systems, is an interesting approach properly oriented to reach carbon neutral energy supply for buildings.

Chapter 8

Closure

"Sometimes it's not to arrive first, but to reach your destination."

A summary of the main conclusions and contributions of the thesis as well as the potential future works is presented in this chapter.

8.1 Synthesis

In this thesis is addressed the complex problem of the integrated design, synthesis and operation optimization (IDSOO) of polygeneration systems for small-scale residential buildings integrating renewable energy technologies and thermal and electric energy storage. Economic and environmental aspects are the leading objectives, considering the important constraints imposed by legal regulations. A Mixed Integer Linear Programming model has been specifically developed to research these aspects and thermoeconomic analysis has been applied to analyse and unveil the synergies and interactions among the components of these highly complex systems. More specifically, along this research work five main issues have been addressed, namely:

I) The suitable way to select appropriate representative days in order to deal with the complex problem of optimization of polygeneration systems, in particular when resources characterized by a stochastic dynamical behaviour are considered (Chapter 3).

II) The study of the feasibility of using residential buildings as a microgrid considering different energy demands such as electricity, heating and cooling to explore a wider perspective as smart energy system (Chapter 5). This approach is particularly interesting, because it can facilitate the integration of renewable energy technologies in the residential sector.

III) The analysis of the integration of thermal and electric components, especially thermal energy storage and batteries in the polygeneration systems for residential buildings (Chapter 6).

IV) The study of the impact of legal restrictions on the design of polygeneration systems for small-scale residential buildings (Chapter 7).

V) Development and analysis of guidelines for the optimal design of affordable polygeneration systems for small-scale residential buildings oriented to the transition towards decarbonized energy supply systems (Chapter 7).

Furthermore, the entire research work involved also i) the determination of the state of the art of the different thematics comprised in this research (Chapter 1); ii) a thoroughly revision of updated technical, economic and environmental data (Chapter 2) of the equipment and energy resources considered along the thesis and iii) a tailored MILP model (Chapter 4) for the optimization of polygeneration systems for small-scale residential buildings, in the different cases of study considered. A more detailed description of the topics covered throughout the thesis is presented below.

Chapter 1 showed the state of the art of different aspects addressed along the thesis. Thus, it has been presented an overview of the use of polygeneration systems for residential buidings as a suitable alternative to reduce both economic costs and environmental impact in the residential sector and the optimization process as a technique to address the design of such energy systems. Besides, the integration of thermal and electric parts within the energy systems is a cutting edge topic that has been presented to achieve a better approach to design polygeneration systems for residential buildings, showing thermoeconomic analysis as a suitable technique to study such integration thoroughly. Also, an overview of the legal framework was presented highlighting its importance on the design of polygeneration systems to fulfil the international agreements to combat the climate change. The chapter ends defining the objectives and structure of the thesis.

Chapter 2 presented the technical, economic and environmental data used for the optimization of polygeneration systems for residential buildings along

the research work. Firstly, the climatic data and the available natural resources in Zaragoza and Gran Canaria were presented followed by the potential hourly renewable energy (photovoltaic, solar thermal and wind turbine) production in each location. Secondly, the hourly energy demands for the residential buildings such as heating, cooling and electricity for appliances were calculated for each location. Thirdly, a comprehensive description of the technical, economic and environmental parameters of the different energy supply technologies for residential buildings was presented. Finally, the description of different economic and environmental aspects of the different fuels and the electric grid was presented.

From the hourly time series obtained such as renewable energy production, energy demands, among others as input data for the optimization of polygenerations systems, a very important issue to address was the data processing, since the solution of Mixed Integer Linear Programming (MILP) problems is a computational demanding task. Thus, the chapter 3 presented a thorough comparison between different methods for the selection of representative days to address the optimization of polygeneration systems such as Averaging, k-Medoids and OPT method. The advantages and disadvantages of these methods were studied and a new method, the kM-OPT method, was developed improving some characteristics of the previous methods studied. A comprehensive analysis based on metrics and the duration curves of the different time series used along the research work was carried out to evaluate the feasibility of the representative days obtained from different methods. The validation of the representative days was carried out optimizing a grid connected and standalone polygeneration system for residential buildings composed of 40 dwellings in Zaragoza and Gran Canaria. The results obtained from the representative days calculated from the different methods were compared to those obtained using 8760 hours data. The use of representative days allowed a remarkable reduction in computational time, of about three orders of magnitude, with respect to the use of 8760 hours data for the optimization of polygeneration systems for residential buildings with a good accuracy in the obtained results. Besides, it was highlighted the importance of taking into account the time series variability to select the suitable method for the selection of representative days.

Once the technical, economic and environmental data are available and the data processing method is well established, the Mixed Integer Linear Programming (MILP) model for the optimization of polygeneration systems of residential buildings must be developed. Therefore, the chapter 4 described the MILP optimization model utilized along the research work for the study of grid connected and standalone polygeneration systems for residential buildings. Firstly,

the integrated design, synthesis and operation optimization (IDSOO) process was described and presented as the basis of the study. Secondly, a thoroughly description of the superstructure that considers all the candidate technologies studied along the thesis was also presented. Thirdly, the optimization model was described including both economic and environmental objective functions subject to different technical and physical restrictions such as energy balance, equipment efficiency and installed capacities, among others. Finally, it was carried out an explanation about multiobjective optimization for polygeneration systems.

Chapter 5 evaluated the feasibility of using residential buildings as an energy community or microgrid from the economic viewpoint. To this end, three cases namely conventional energy supply systems, grid connected polygeneration systems and grid connected self-sufficient polygeneration sytems for residential buildings, were studied. It was demonstrated the benefits of polygeneration systems, highlighting the feasibility of the PV panels, the heat pump and thermal energy storage for cooling. Besides, it was studied the profitability of self-sufficient energy supply systems for residential buildings connected to the electric grid and as standalone energy system. Along the study interesting insights regarding the thermal and electric parts integration were found.

Taking into account the standalone energy system as an appealing alternative to cover the energy demands of a residential building and focused on the insights found through the study of the feasibility of using residential buildings as an energy community or microgrid, the chapter 6 developed a thermoeconomic analysis in order to identify different synergies between components of an energy supply system to achieve a deeper understanding on the design of energy supply systems for residential buildings and the integration of different technologies. Firstly, it was carried a brief description about thermoeconomics, highlighting fundamental aspects such as the definition of the productive structure. Then, different optimal configurations were obtained from the optimization of the different superstructures which were progressively increasing in complexity along the integration process of different candidate technologies. Along this procedure, different aggregation levels were studied, highlighting its importance on the analysis of the formation costs process and to achieve a fair allocation costs to the final energy services. Regarding the thermal and electric integration, from the thermoeconomic analysis it was explained why the use of batteries can be replaced by thermal energy storage and in general, the advantage of the thermal and electric integration to achieve more cost-effective energy supply systems.

Finally, taking into account the importance of the legal framework to foster low carbon technologies in the pathway to reduce the greenhouse emissions,

the chapter 7 evaluated the two recent Spanish self-consumption regulations through the optimization of grid connected polygeneration systems for residential buildings from the economic and environmental point of view. The RD 900/20015 and RD 244/2019 were compared through the economic optimization of polygenerations systems for individual installations (households) and residential buildings. In addition, a multiobjective optimization was carried out under the legal restrictions imposed by the RD 244/2019 to evaluate the potential of reduction of CO_2eq emissions at an affordable cost, as well as its alignment with the European objectives on greenhouse gases emissions reduction. It was demonstrated in all the analysed cases, the feasibility of using polygeneration systems for residential buildings to reduce both the economic costs and the environmental impact.

8.2 Contributions

- ✓ This thesis compiled significant information utilized for the optimization of polygeneration systems for small-medium size residential buildings. This includes i) information about the available natural energy resources in Zaragoza and Gran Canaria, ii) technical, economic and environmental data of different energy supply technologies for small-scale residential buildings, and iii) economic and environmental aspects associated to different fuels and the electric grid.

- ✓ The development of a methodology for the optimization of the synthesis, design and operation of either grid connected or standalone polygeneration systems for small-medium size residential buildings. To this end, a Mixed Integer Linear Programming (MILP) optimization model was developed including both economic and environmental objective functions subject to different physical and technical restrictions such as the energy balance and the efficiency and capacities of the equipment, among others.

- ✓ A comprehensive analysis of methods for the selection of representative days was carried out. A new method called kM-OPT was developed for the selection of representative days in order to address the optimization of polygeneration systems for residential buildings, improving some characteristics of the methods which have been studied previously. It was highlighted the importance of the right selection of the method for the selection of representative days to obtain suitable results from the optimization of polygeneration system, especially when resources with stochastic

behaviour such as wind energy are considered.

- ✓ One of the cutting-edge research topics nowadays is about the deployment of microgrids. Consequently, this thesis evaluated the use of residential buildings as microgrid from the economic viewpoint, finding it profitable with respect to the current conventional energy systems. However, according to the obtained results its deployment depends on allowing sale of electricity at a competitive electricity price, or considering feed-in tariff schemes.
- ✓ A thoroughly analysis of the thermal and electrical integration for the optimization of polygeneration systems for residential buildings was carried out. It was demonstrated the importance of taking into account both thermal and electrical parts in the design process of the energy systems in order to achieve more cost-effective and sustainable solutions. Heat pumps and energy storage are key technologies for the thermal an electrical integration and to achieve higher shares of renewable energy. Concerning energy storage, it was demonstrated that although batteries are considered a key technology for standalone and microgrids systems, the obtained results remark the importance of thermal energy storage to achieve more cost-effective energy systems for residential buildings.
- ✓ The evaluation of the recent Spanish self-consumption regulations was carried out obtaining remarkable differences between the current Spanish energy policy and the international goals about energy and environmental policies in the pathway to combat the climate change. The obtained results highlight that inappropriate regulations and/or energy pricing may lead to results which may differ from the pursued objective of, for instance, promoting decentralized energy production and/or reduction of CO_2eq emissions. Therefore, future efforts should be devoted to improve self-consumption regulation, with a broader perspective than the current policy, oriented to a more significant reduction of CO_2eq emissions at an affordable cost. The results obtained herein could help policy makers to take suitable decisions aligned to the international policies.
- ✓ Through the multiobjective optimization of grid connected polygeneraton systems for residential buildings considering the current legal restrictions, several technologies were evaluated. The most selected technologies along the Pareto curves were PV, HP and TSR, highlighting the important role of the reversible HP in the objective to reduce CO_2eq emissions at an affordable cost, particularly when its integration with PV is feasible. In this

respect, whatever regulation fostering energy efficiency and reduction of greenhouse gas emissions should not represent a barrier for the installation of HP and renewable energy technologies and should facilitate the integration of HP with renewable energies considering at the same time the economic feasibility. In the pathway to achieve remarkable CO_2eq emissions reductions, technologies such as CM and ACH were barely selected, due to their high investment cost as well as to the consumption of fossil fuels of the former. In the case of WT, ST, and Bat, due to their high investment cost were mainly selected in the trade-off solutions close to the environmental optimum. In the case of BB, it was observed the high potential of this technology to reduce CO_2eq emissions, since it was one of the most selected technologies along the Pareto curves, and it displaced the GB technology in the pathway to reduce CO_2eq emissions.

✓ The multiobjective optimization also allowed to evaluate the feasibility of achieving zero CO_2eq emissions energy supply system for residential buildings under legal restrictions. Thus, although under a self-consumption scheme only, without allowing electricity sale to the electrical grid, was achieved a significant reduction of CO_2eq emissions, it was not possible to offset 100% of greenhouse gas emissions. This objective, zero CO_2eq emissions, only could be reached allowing also the sale of electricity produced with renewable energy sources. However, despite the high prices of electricity sale foster the investment in renewable energy technologies, the potential reduction of CO_2eq emissions is limited because of the net billing restriction. Therefore, good signals of electricity sale prices must be considered to overcome this issue. In the analysed cases, the sale of electricity at spot price provided high potential of CO_2eq emissions reduction obtaining also economic benefits. This means that the production of electricity from renewable energies can be competitive, without any subsidy, allowing a very important reduction of CO_2eq emissions in buildings at an affordable cost and aligned with short term EU objectives on climate change, as well as with the objective of reaching affordable carbon neutral energy supply systems for buildings in the long term of 2050.

8.3 Future perspectives

Along the thesis development, many ideas have come up. Some of them are presented below:

† Forecasting and control are interesting topics to be included in the optimization model aiming to achieve a more robust and practical tool.

† The model developed could be modified in a simple way to the analysis and study of the impact of different regulations. In this respect, it would be interesting to compare and study thoroughly the interest and impact of the future regulations for the energy sector oriented to foster carbon neutral energy supply systems.

† A deeper analysis of energy storage which includes the influence of the size and energy losses in the design of the energy system could be advisable.

† A trending topic nowadays is related to the effect of the integration of renewable energies on the electric grid. Thus, to study the advantages of the integration of thermal energy storage to overcome some technical issues on the electric grid due to the integration of renewable energy technologies could be interesting.

† In the pathway to achieve 100% renewable energy systems, new technologies/systems and energy resources should be included in the design of such systems, such as fuel cells, electric vehicles, hydrogen, synthetic fuels, etc.

Capítulo 8

Conclusión

"A veces no hay que llegar primero, pero hay que saber llegar...♫"

Este capítulo presenta un resumen de los principales resultados y conclusiones obtenidos a lo largo de la tesis, así como las contribuciones realizadas y las perspectivas de trabajos futuros.

8.1 Síntesis

En esta tesis se estudia un problema complejo como es la optimización conjunta de la síntesis, el diseño y la operación de sistemas de poligeneración para edificios residenciales de pequeña escala integrando tecnologías de energías renovables y de almacenamiento de energía térmica y eléctrica. Los aspectos económicos y ambientales son los principales objetivos, considerando también las importantes limitaciones impuestas por el marco legal. Para investigar estos aspectos, se ha desarrollado un modelo de programación lineal entera mixta y se ha aplicado el análisis termoeconómico para analizar e identificar las sinergias e interacciones que existen entre los diferentes componentes de estos sistemas que tienen un alto nivel de complejidad. Más concretamente, a lo largo de este trabajo de investigación se han abordado cinco cuestiones principales:

I) La forma adecuada de seleccionar los días representativos con objeto de reducir sensiblemente el alto coste computacional que conlleva la solución de los problemas de síntesis y optimización de los sistemas de poligeneración

de forma que permitan abordar este complejo problema con fiabilidad, especialmente cuando se consideran recursos caracterizados por un comportamiento dinámico aleatorio (Capítulo 3).

II) El estudio de la viabilidad del uso de edificios residenciales como microrredes, en un paso más hacia la concepción de sistemas energéticos inteligentes en los que se tienen en cuenta diferentes demandas energéticas más allá de la electricidad, considerando en este caso también las demandas de calefacción y refrigeración (Capítulo 5). Asimismo, esta aproximación es muy interesante puesto que su viabilidad facilita la integración de energías renovables y, por tanto, la decarbonización y reducción del impacto ambiental de la producción de energía en el sector residencial.

III) El análisis de la integración de equipos térmicos y eléctricos, especialmente el almacenamiento de energía térmica y las baterías en los sistemas de poligeneración para edificios residenciales (Capítulo 6).

IV) El estudio del impacto de las restricciones legales en el diseño de sistemas de poligeneración para edificios residenciales de pequeña escala (Capítulo 7).

V) El desarrollo de orientaciones/recomendaciones para el diseño óptimo de sistemas de poligeneración asequibles para edificios residenciales de pequeña escala que sirvan de referencia en la transición energética hacia sistemas de suministro de energía descarbonizados (Capítulo 7).

El trabajo completo de investigación requirió también i) determinar el estado del arte de las diferentes temáticas abordadas a lo largo de la tesis (Capítulo 1); ii) una revisión actualizada de los datos técnicos, económicos y medioambientales (Capítulo 2) de los diferentes equipos y recursos energéticos empleados en la tesis y iii) el desarrollo de un modelo MILP orientado a la optimización de sistemas de poligeneración para edificios residenciales de pequeña escala. A continuación, se presenta una descripción más detallada de los temas tratados a lo largo de la tesis.

El capítulo 1 presentó el estado del arte de las diferentes temáticas abordadas a lo largo de la tesis. De esta forma, se ha hecho un repaso general de las tecnologías empleadas en los sistemas de poligeneración para edificios residenciales como alternativa para reducir los costes económicos y medioambientales en el sector residencial y las técnicas de optimización para abordar el diseño de dichos sistemas energéticos. Además, la integración de equipos térmicos y eléctricos

dentro de los sistemas energéticos se ha presentado y constituye un tema de vanguardia que permite mejorar el diseño de sistemas de poligeneración para edificios residenciales, empleando el análisis termoeconómico como una técnica adecuada para estudiar a fondo dicha integración. Asimismo, se ha mostrado el panorama del marco legal regulatorio destacando el importante papel que juega en el diseño de sistemas de poligeneración para edificios residenciales y se ha analizado su contribución y alineamiento con los acuerdos internacionales para combatir el cambio climático. El capítulo finaliza definiendo los objetivos y la estructura general de la tesis.

El Capítulo 2 presentó los datos técnicos, económicos y medioambientales utilizados a lo largo de la investigación para la optimización de los sistemas de poligeneración de edificios residenciales. En primer lugar, se presentaron los datos climáticos y los recursos naturales disponibles en Zaragoza y Gran Canaria, así como la producción horaria potencial de energía renovable (fotovoltaica, solar térmica y eólica) en cada localidad. En segundo lugar, se calcularon las demandas de energía horaria en los edificios residenciales como son la calefacción, la refrigeración y la electricidad, en cada localidad. En tercer lugar, se llevó a cabo una descripción completa de los parámetros técnicos, económicos y medioambientales de las diferentes tecnologías empleadas a lo largo de la investigación. Finalmente, se presentaron los diferentes aspectos económicos y ambientales de los distintos combustibles que fueron usados y de la red eléctrica.

A partir de las series de datos horarios obtenidas para describir la producción de energía renovable y las demandas de energía, entre otras, como datos de entrada para la optimización de sistemas de poligeneración, se estudió la forma más adecuada de procesar el conjunto de series de datos de entrada con el fin de facilitar la solución de los problemas de Programación Lineal Entera Mixta (MILP, por sus siglas en inglés), ya que cuanto mayor es la cantidad de variables, mayor es el costo computacional para la solución de este tipo de problemas. Por lo tanto, el capítulo 3 presentó una comparación exhaustiva entre diferentes métodos para la selección de días representativos usados en la optimización de los sistemas de poligeneración, como el método Averaging, k-Medoids y OPT. Se estudiaron las ventajas y desventajas de esos métodos y se desarrolló un nuevo método, el método kM-OPT, que mejora algunas características de los métodos mencionados anteriormente. También, se llevó a cabo un análisis integral basado en métricas y en las curvas de duración de las diferentes series temporales utilizadas a lo largo del trabajo de investigación para evaluar la viabilidad del uso de los días representativos obtenidos a partir de los diferentes métodos. La validación de los días representativos se ha realizado optimizando un sistema de poligeneración para un edificio residencial compuesto

por 40 viviendas en las locaciones de Zaragoza y Gran Canaria. Los resultados obtenidos usando los días representativos calculados a partir de los diferentes métodos estudiados fueron comparados con los resultados obtenidos usando la serie de datos original que comprendía los 365 días (8760 horas). Se concluyó que el uso de días representativos en la optimización de sistemas de poligeneración para edificios residenciales permitía una notable reducción del tiempo computacional, de unos tres órdenes de magnitud, con respecto al uso de la serie original de datos de 8760 horas, con una buena precisión en los resultados de la optimización. Además, se destacó la importancia de tener en cuenta la variabilidad de las series temporales en la elección del método adecuado para la selección de los días representativos.

Una vez establecidos los datos técnicos, económicos y medioambientales requeridos, así como el método de procesamiento de datos, se desarrolló el modelo de Programación Lineal Entero Mixto (MILP) para la optimización de los sistemas de poligeneración de edificios residenciales. Así, en el capítulo 4 se ha descrito el modelo de optimización MILP utilizado a lo largo del trabajo de investigación para el estudio de los sistemas de poligeneración para edificios residenciales conectados a red y aislados. En primer lugar, se describió y presentó como base del estudio la metodología de optimización simultánea de la síntesis, el diseño y la operación (IDSOO, por sus siglas en inglés) de los sistemas de poligeneración. En segundo lugar, se describió de forma detallada la superestructura que considera todas las tecnologías candidatas estudiadas a lo largo de la tesis. En tercer lugar, se desarrolló el modelo de optimización que incluye las funciones objetivo, económica y medioambiental, sujetas a distintas restricciones técnicas y físicas como el balance energético, la eficiencia de equipos y las capacidades instaladas, entre otras. Finalmente, se presentó una técnica de optimización multiobjetivo para obtener diferentes soluciones que tengan en cuenta aspectos tanto económicos como medioambientales.

En el capítulo 5 se ha evaluado la viabilidad del uso de edificios residenciales como microred desde el punto de vista económico. Para llevar a cabo esta evaluación, se estudiaron tres sistemas energéticos diferentes para suplir las demandas energéticas de un edificio residencial: sistemas convencionales de energía, sistemas de poligeneración conectados a red y sistemas de poligeneración autosufientes conectados a red. A lo largo de la evaluación se ha demostrado la viabilidad económica del uso de algunas tecnologías como los paneles fotovoltaicos, la bomba de calor y el sistema de almacenamiento térmico para el frío. Además, se evaluó también la rentabilidad de los sistemas de suministro energético autosuficientes para edificios residenciales conectados a red y aislados, resultando estos últimos una alternativa viable. A lo largo del estudio, se

obtuvieron resultados interesantes respecto a la integración de equipos térmicos y eléctricos en el sistema de suministro de energía para edificios residenciales.

Teniendo en cuenta la viabilidad de la implementación de sistemas energéticos aislados como una alternativa atractiva para cubrir las demandas de energía de un edificio residencial, partiendo de los resultados obtenidos en el capítulo 5, en el capítulo 6 se llevó a cabo un análisis termoeconómico con el fin de identificar sinergias entre los componentes de un sistema de suministro energético para edificios residenciales conducente a lograr una comprensión más profunda del diseño de los sistemas energéticos y la integración de las diferentes tecnologías. En primer lugar, se realizó una breve introducción a la termoeconomía, destacando aspectos fundamentales como la definición de la estructura productiva y sus diferentes componentes, entre otros. Luego, se obtuvieron diferentes configuraciones a partir de la optimización de las diferentes superestructuras que fueron estudiadas, en las que su complejidad se ha ido aumentando progresivamente a lo largo del proceso de integración, al incluir sistemáticamente las diferentes tecnologías candidatas. Asimismo, se estudiaron diferentes niveles de agregación, destacando su importancia en el análisis de formación de costes internos y en la asignación apropiada de los costes a los productos finales. En cuanto a la integración térmica y eléctrica, a partir del análisis termoeconómico se explicó por qué el uso de baterías puede ser reemplazado/desplazado por almacenamiento de energía térmica y en general, la ventaja de la integración térmica y eléctrica para lograr sistemas de suministro de energía más rentables.

Finalmente, teniendo en cuenta la importancia que tienen las políticas y los aspectos regulatorios en el fomento de las llamadas tecnologías verdes con el fin de reducir las emisiones de gases de efecto invernadero, en el capítulo 7 se evaluaron las dos últimas normativas españolas de autoconsumo desde el punto de vista económico y medioambiental. Los reales decretos RD 900/20015 y RD 244/2019 se compararon mediante la optimización económica de los sistemas de poligeneración para instalaciones individuales (viviendas) y edificios residenciales. Además, se llevó a cabo una optimización multiobjetivo teniendo en cuenta las restricciones legales impuestas por el RD 244/2019 con el fin de evaluar el potencial de reducción de emisiones de CO_2eq a un coste asequible, así como su nivel de concordancia con los objetivos europeos de reducción de emisiones de gases de efecto invernadero. En todos los casos analizados se demostró la viabilidad de utilizar sistemas de poligeneración para edificios residenciales en pro de reducir tanto los costes económicos como el impacto ambiental.

8.2 Contribuciones

- ✓ La tesis ha recopilado información actualizada relevante para la optimización de sistemas de poligeneración para edificios residenciales de tamaño pequeño. Esto incluye i) información sobre los recursos energéticos naturales disponibles en Zaragoza y Gran Canaria, ii) datos técnicos, económicos y ambientales de diferentes tecnologías empleadas para el suministro de energía de edificios residenciales de pequeña-mediana escala, y iii) diferentes aspectos económicos y medioambientales asociados a distintos tipos de combustible y a la red eléctrica.

- ✓ Se ha llevado a cabo el desarrollo de una metodología para la optimización de la síntesis, el diseño y la operación de sistemas de poligeneración conectados a red o aislados para edificios residenciales de tamaño pequeño. Para ello, se creó un modelo de optimización de Programación Lineal Entera Mixta (MILP) que incluye funciones objetivo tanto económica como medioambiental sujetas a diferentes restricciones físicas y técnicas, como el balance energético y las eficiencias y capacidades de los equipos, entre otras.

- ✓ Se llevó a cabo un análisis exhaustivo de diferentes métodos para la selección de días representativos. Este análisis permitió desarrollar un nuevo método de selección de días representativos, el kM-OPT, para abordar la optimización de los sistemas de poligeneración para edificios residenciales, mejorando algunas características de los métodos estudiados. Se destacó la importancia de llevar cabo una adecuada elección del método para la selección de días representativos con el fin de obtener buenos resultados en la optimización del sistema de poligeneración, especialmente cuando se consideran recursos y/o series de datos con alta variabilidad como es el caso de la energía eólica.

- ✓ Uno de los temas de investigación de vanguardia en la actualidad es el desarrollo de microrredes. En consecuencia, esta tesis evaluó el uso de edificios residenciales como microrred desde el punto de vista económico, y se evaluó su rentabilidad con respecto a los sistemas energéticos convencionales actuales. Sin embargo, según los resultados obtenidos, su despliegue depende de la venta de electricidad autogenerada con energías renovables a un precio competitivo o de considerar esquemas con incentivos tarifarios.

- ✓ Se realizó un análisis exhaustivo de la integración térmica y eléctrica para la optimización de sistemas de poligeneración para edificios residenciales. Se demostró la importancia de tener en cuenta tanto las partes térmicas como las eléctricas en el proceso de diseño de los sistemas energéticos para lograr soluciones más rentables y sostenibles. Entre las tecnologías estudiadas, las bombas de calor y el almacenamiento de energía son las tecnologías claves para la integración térmica y eléctrica y para lograr mayor participación de las energías renovables en los sistemas energéticos. En cuanto al almacenamiento de energía, se demostró que, si bien las baterías se consideran una tecnología clave para los sistemas aislados y microrredes, los resultados obtenidos destacan la importancia de incluir el almacenamiento de energía térmica para lograr sistemas de suministro de energía más rentables para edificios residenciales.
- ✓ Se han evaluado las recientes regulaciones españolas de autoconsumo evidenciando importantes diferencias entre la actual política energética española y los objetivos internacionales en materia de políticas energéticas y medioambientales en la lucha contra el cambio climático. Los resultados obtenidos destacan que una normativa y/o un precio de la energía inapropiados pueden conducir a resultados que pueden diferir del objetivo perseguido, por ejemplo, promover la producción de energía descentralizada y/o la reducción de emisiones de CO_2eq. Por lo tanto, los esfuerzos futuros deben dedicarse a mejorar la regulación del autoconsumo, con una perspectiva más amplia que la política actual, orientada a una reducción más significativa de las emisiones de CO_2eq a un costo asequible. Los resultados aquí obtenidos proporcionan orientaciones que podrían ayudar a los agentes políticos a tomar decisiones adecuadas alineadas a las políticas internacionales.
- ✓ A través de la optimización multiobjetivo de sistemas de poligeneración conectados a red para edificios residenciales considerando las restricciones legales vigentes, se evaluaron varias tecnologías. Las tecnologías más seleccionadas a lo largo de las curvas de Pareto fueron la fotovoltaica (PV), la bomba de calor (HP) y el almacenamiento térmico para el frío (TSR), destacando el importante papel de la bomba de calor cuando se quieren reducir las emisiones de CO_2eq a un costo asequible, especialmente cuando su integración con los paneles fotovoltaicos es factible. En este sentido, cualquier normativa que fomente la eficiencia energética y la reducción de emisiones de gases de efecto invernadero no debe representar una barrera para la instalación de tecnologías de bomba de calor y energías renovables,

y por el contrario debería facilitar su integración considerando al mismo tiempo la viabilidad económica. Por otro lado, cuando se requiere alcanzar reducciones notables de emisiones de CO_2eq, tecnologías como la cogeneración (CM) y la máquina de absorción (ACH) fueron prácticamente descartadas, debido a su alto costo de inversión, así como al consumo de combustibles fósiles de las primeras. En el caso de las turbinas eólicas (WT), los colectores solares térmicos (ST) y las baterías (BAT), fueron seleccionadas principalmente en las configuraciones óptimas cercanas al óptimo medioambiental, debido a su alto costo de inversión. En el caso de la caldera de biomasa (BB), se observó el alto potencial que tiene esta tecnología para reducir las emisiones de CO_2eq, ya que fue una de las tecnologías más seleccionadas a lo largo de las curvas de Pareto, desplazando la caldera de gas natural (GB) a medida que se requería una mayor reducción de emisiones de CO_2eq.

- ✓ La optimización multiobjetivo también permitió evaluar la viabilidad de lograr un sistema de suministro de energía con cero emisiones de CO_2eq para edificios residenciales bajo las restricciones legales vigentes. Se encontró que, bajo un esquema de autoconsumo, sin permitir la venta de electricidad a la red eléctrica, se logra una reducción significativa de las emisiones de CO_2eq, pero no es posible alcanzar una reducción del 100 % de las emisiones de gases de efecto invernadero. Este objetivo, alcanzar cero emisiones de CO_2eq, solo podría alcanzarse permitiendo la venta de electricidad producida con fuentes de energía renovables. Sin embargo, a pesar de que los altos precios de venta de electricidad fomentan la inversión en tecnologías de energía renovable, la reducción potencial de emisiones de CO_2eq estaría limitada debido a la restricción de facturación neta (net billing). Por lo tanto, se deben considerar señales de precios de venta de electricidad que se ajusten para superar este problema. En los casos analizados, la venta de electricidad a precio de mercado (spot price) proporcionó un alto potencial de reducción de emisiones de CO_2eq obteniendo también un beneficio económico. Esto significa que la producción de electricidad a partir de energías renovables puede ser competitiva, sin ningún tipo de subvención, permitiendo una reducción muy importante de las emisiones de CO_2eq en los edificios a un coste asequible y alineado con los objetivos a corto plazo de la UE sobre cambio climático, así como con el objetivo de alcanzar sistemas asequibles de suministro de energía neutros en carbono para edificios a largo plazo, en el horizonte 2050.

8.3 Perspectivas futuras

A lo largo del desarrollo de la tesis, han surgido muchas ideas. Algunas de estas ideas se presentan a continuación:

† La previsión y el control de la operación pueden afectar en gran medida a la eficiencia energética de los sistemas estudiados. Estos aspectos no se han estudiado y son temas interesantes a incluir en el modelo de optimización con el objetivo de conseguir una herramienta más robusta y ajustada al comportmiento real de la instalación.

† El modelo MILP desarrollado podría ser modificado facilmente con el fin de comparar y estudiar detalladamente la viabilidad y el impacto de futuras regulaciones del sector energético orientadas a fomentar los sistemas energéticos que permitan combatir el cambio climático.

† Podría ser recomendable un análisis más profundo del almacenamiento de energía que incluya la influencia del tamaño y las pérdidas de energía en el diseño del sistema energético.

† Un tema de gran interés en la actualidad es el estudio del efecto de la integración de las energías renovables en la red eléctrica. En este sentido, estudiar las ventajas de la integración del almacenamiento de energía térmica para superar algunos problemas técnicos en la red eléctrica debido a la integración de las energías renovables podría resultar interesante.

† Cuando el objetivo es lograr sistemas energéticos 100 % renovables, se debería incluir nuevas tecnologías/sistemas y recursos energéticos en el diseño de dichos sistemas tales como las pilas de combustible, los vehículos eléctricos, el hidrógeno, los combustibles sintéticos, etc.

Appendix

Appendix A

Model capacity of batteries

A.1 Lead Acid Batteries LA

Lead Acid Batteries are described by Manwell and McGowan (1993) as a voltage source which is modelled as two tanks separated by a conductance. One tank, which width is c, holds the charge that is immediately available to be used for the demand. The other tank, which width is $1 - c$, holds the charge that is chemically bound. The combined width of the two tanks gives a combined tank area of unity. The combined volume of the tank is q_{max}. The conductance K corresponds to the rate constant of a chemical reaction/diffusion process by which the bound charge becomes available. The rate at which bound charge becomes available is proportional to the levels difference of the two tanks (Figure A.1).

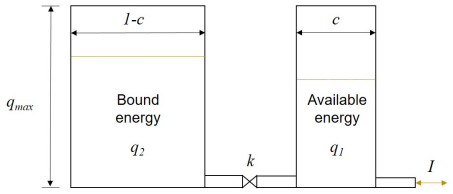

Figure A.1: Scheme of the $KiBaM$ model.

The equations describing the model are the following:

$$q_1 = q_{1,0} \cdot e^{-K \cdot t} + \frac{(q_0 \cdot K \cdot c - I) \cdot (1 - e^{-K \cdot t})}{K} - \frac{I \cdot c \cdot (K \cdot t - 1 + e^{-K \cdot t})}{K} \tag{A.1}$$

$$q_2 = q_{2,0} \cdot e^{-K \cdot t} + q_0 \cdot (1 - c) \cdot (1 - e^{-K \cdot t}) - \frac{I \cdot (1 - c) \cdot (K \cdot t - 1 + e^{-K \cdot t})}{K} \tag{A.2}$$

Where, I is the charge or discharge current when is negative or positive respectively in the time step t, and $q_{1,0}$ and $q_{2,0}$ are the amount of available and bound charge respectively, at the beginning of the calculation, being their sum q_0.

Because the voltage is not considered explicitly in the model, three constants are needed for the model: q_{max}, the maximum capacity of the battery; c, the fraction of capacity that may hold available charge; and K, the rate constant. They can be found from the battery capacity data provided by manufacturers. The procedure to determine these three constants is described as follows:

First of all, the capacities are normalized with respect to a slow discharge rate capacity, corresponding to discharge time $t = t_2$. The data can be expressed in terms of a ratio, $F_{t_1 - t_2}$ of capacities as follows:

$$F_{t_1 - t_2} = \frac{q_{t_1}}{q_{t_2}} \tag{A.3}$$

Where q_{t_i} is the discharged capacity at discharge time t_i. In turn, the discharge capacity is the multiplication of the current and discharge time:

$$F_{t_1 - t_2} = \frac{t_1 \cdot I_{t_1}}{t_2 \cdot I_{t_2}} \tag{A.4}$$

By using $KiBaM$ equations, discharge current can be expressed as a function of the constant c and K as:

$$F_{t_1 - t_2} = \frac{t_1}{t_2} \cdot \frac{(1 - c) \cdot (1 - e^{-K \cdot t_2}) + K \cdot c \cdot t_2}{(1 - c) \cdot (1 - e^{-K \cdot t_1}) + K \cdot c \cdot t_1} \tag{A.5}$$

When the same c is obtained from a given K at two different discharge relations, those are the constants to be used in the model. When multiple values of $F_{t_1 - t_2}$ are known, a least-squares fit could be used to find the best values of the constants. Once calculated c and K constants, q_{max} can be calculated. To

Table A.1: Values of c and K for OPz batteries

Parameter	OPzS	OPzV
K [1/h]	0.11	0.1
c	0.53	0.61

do it, it is convenient to consider a slow discharge rate capacity q_n as a reference, for instance 20 hours rate, this means q_{20}.

$$q_{max} = \frac{q_n \cdot \left((1 - e^{-K \cdot t_n}) \cdot (1 - c) + K \cdot c \cdot t_n\right)}{K \cdot c \cdot t_n} \tag{A.6}$$

Known the three constants, maximum discharge and charge currents $I_{d,max}$ and $I_{c,max}$ respectively, can be calculated in each time step as follows:

$$I_{d,max} = \frac{K \cdot q_{1,0} \cdot e^{-K \cdot t} + q_0 \cdot K \cdot c \cdot (1 - e^{-K \cdot t})}{1 - e^{-K \cdot t} + c \cdot (K \cdot t - 1 + e^{-K \cdot t})} \tag{A.7}$$

$$I_{c,max} = \frac{-K \cdot c \cdot q_{max} + K \cdot q_{1,0} \cdot e^{-K \cdot t} + q_0 \cdot K \cdot c \cdot (1 - e^{-K \cdot t})}{1 - e^{-K \cdot t} + c \cdot (K \cdot t - 1 + e^{-K \cdot t})} \tag{A.8}$$

By applying the procedure described above, taking as a reference OPz (from German Ortsfeste Panzerplatte) batteries of the branch Sunlight (2015), the c and K constants have been obtained for OPzS (Flooded or Vented) and OPzV (VRLA: Valve Regulated Lead Acid) batteries. The results are presented in the Table A.1.

The Table A.2 presents additional technical parameters which have been considered to model the Lead Acid batteries in polygeneration systems. These data have been estimated based on the international renewable energy agency report IRENA (2017).

In this work, OPzS batteries data have been taken as a reference for modelling Lead Acid batteries.

A.2 Lithium Ion Batteries $Li - Ion$

A capacity model is also used for this technology. The Li-Ion battery is modelled as a tank of charge, removing and adding charge as needed (DiOrio et al., 2015).

$$q = q_0 - I \cdot t \tag{A.9}$$

Table A.2: Technical parameters for Lead acid batteries-Opz.

Technical Parameters	**OPzS**	**OPzV**
Round trip efficiency η_{rt} [%]	82	85
Number of cycles failure $N_{c,failure}$	1500	1500
Deep of discharge DOD [%]	50	50
Self-discharge [%/hour]	0.0104	0.0042
Lifetime [Years]	9	9

Table A.3: Technical parameters for Lithium-Ion batteries.

Technical Parameters	**Lithium-Ion**
Round trip efficiency η_{rt} [%]	95
Number of cycles failure $N_{c,failure}$	2000
Deep of discharge DOD [%]	90
Self-discharge [%/hour]	0.0042
Lifetime [Years]	12

Where q is the charge available in the battery in each time step, q_0 is the available charge at the beginning of the calculation an I is the current, assuming that positive current implies discharging from the battery. The maximum charge current allowed is calculated by means the formula used by Homer Energy (2016):

$$I_{c,max_{Li-Ion}} = (1 - e^{-\alpha_c \cdot t}) \cdot (q_{max} - q) \tag{A.10}$$

Where α_c is the maximum charge ratio [A/Ah], which value is assumed 0.4 as the default value used by Homer Energy (2016), and q_{max} is the maximum capacity of the battery bank.

Table A.3 presents additional technical parameters which have been considered to model the Li-Ion batteries in polygeneration systems. Although there are many types of Li-Ion batteries, the Lithium Nickel Manganese Cobalt Oxide - NMC technology has been considered as a reference, since they are a common choice for stationary applications. These data have been estimated based on the international renewable energy agency report IRENA (2017).

Since the polygeneration system model is based on energy, this means, in terms of kWh, the battery capacity S_{bat} is expressed in energy units multiplying the capacity q in Ah by the system voltage Vdc.

$$S_{bat}[kWh] = \frac{q[Ah] \cdot Vdc[V]}{1000} \tag{A.11}$$

The system voltage depends on the size of the energy system. This was shown in detail in the Inverter-Charger technical data (Chapter 2-Figure 2.23).

Appendix B

Primary energy savings PES for cogeneration

Primary energy savings PES are calculated as follows:

$$PES = 1 - \frac{F_{cogen}}{\frac{E_{cogen}}{Ref_E} + \frac{Q_{cogen}}{Ref_Q}} \tag{B.1}$$

Where,

E_{cogen}: CM electricity production [kWh/yr].
F_{cogen}: CM fuel production [kWh/yr].
Q_{cogen}: CM useful heat production [kWh/yr].
Ref_Q: reference efficiency value to produce heat (for domestic hot water) in a conventional system, 0.92 (EU, 2015).
Ref_E: reference efficiency value to produce electricity in a conventional system, 0.53 (EU, 2015).
Moreover, some correction factors must be applied on Ref_E, as follows:

- Correction factors relating to the average climatic situation (F_{cz}): For Zaragoza, average temperature is about 15 °C (IDAE, 2008), therefore, the correction factor is 0.
- Correction factors for avoided grid losses (F_{gl}): This study is for low voltage (below 450 V). The correction factors to apply are 0.888 for electricity exported to the grid and 0.851 for electricity consumed on-site, according

to the Spanish version of the establishing harmonised efficiency reference values (EU, 2015).

$$Ref_E^* = (Ref_E + F_{cz}) \cdot F_{gl} \tag{B.2}$$

Appendix C

Thermoeconomic model for the calculation of the costs of the internal flows and final energy products

This appendix describes the thermoeconomic model used to obtain the costs of the internal flows and final energy products of the productive structure of the optimal standalone energy system with PV panels depicted in the Figure C.1. The thermoeconomic model comprises both costs balance and structural equations. They consists of a set of 25 equations with 25 unknowns corresponding to the internal costs. In addition, different data and parameters such as unit investment costs, energy flows, among others, are also considered to obtain the final results.

- ⊛ **Unknowns:** These are the unit costs of the different energy flows of the productive structure [€/kWh]: c_{E_d}, $c_{E_{HP2}}$, c_{Q_b}, $c_{Q_{bq}}$, $c_{Q_{cq}}$, c_{Q_d}, $c_{Q_{HP1}}$, $c_{Q_{HP2}}$, $c_{R_{ACH1\_r}}$, c_{R_d}, $c_{R_{HP1}}$, $c_{R_{HP1\_r}}$, $c_{R_{HP1\_TSR2}}$, $c_{R_{HP2}}$, $c_{R_{HP2\_r}}$, $c_{R_{HP2\_TSR2}}$, $c_{R_{in2}}$, $c_{R_{out}}$, $c_{R_{out1}}$, $c_{R_{out2}}$, $c_{W_{c-E_d}}$, $c_{W_{PVe}}$, $c_{W_{PV-E_d}}$, $c_{W_{HPR2}}$, $c_{W_{HPQ2}}$.
- ♯ **Data and parameters:** These encompass different technical and economic data of the equipment, fuel prices and energy flows of the productive

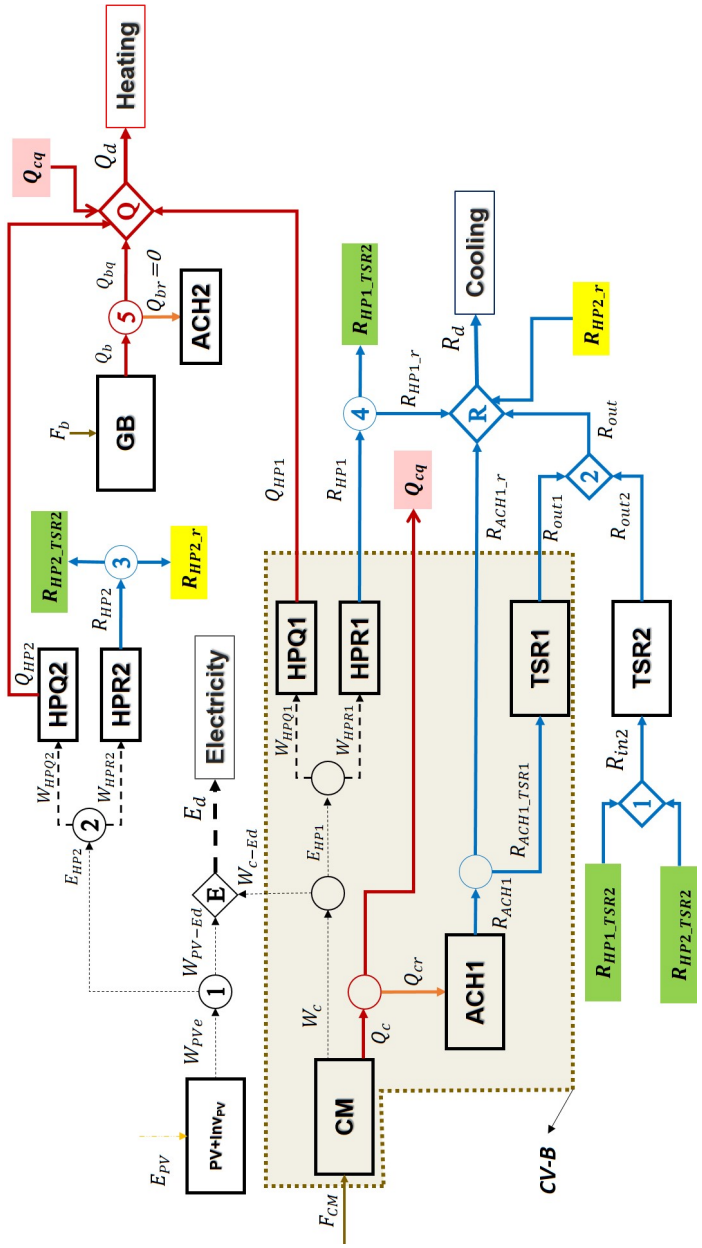

Figure C.1: Productive structure of the optimal standalone energy system with PV panels.

structure:

- ♢ Annual investment costs [€/yr]: $Invest_{ACH}$, $Invest_{CM}$, $Invest_{GB}$, $Invest_{HP}$, $Invest_{PV+Inv}$, $Invest_{TSR}$.
- ↬ Annual energy flows [kWh/yr]: F_{CM}, Q_b, Q_{bq}, Q_{cq}, Q_{HP}, Q_{HP1}, Q_{HP2}, R_{ACH1}, R_{ACH1_r}, R_{HP}, R_{HP1}, R_{HP1_r},R_{HP1_TSR2}, R_{HP2}, R_{HP2_r},R_{HP2_TSR2}, R_{in2}, R_{out}, R_{out1}, R_{out2}, W_{c-E_d}, W_{PVe}, W_{PV-E_d}.
- ⁕ Annual unit investment cost of the different components of the productive structure per unit of product [€/kWh]: z_{ACH1}, z_{CM}, z_{GB}, z_{HPQ}, z_{HPQ1}, z_{HPQ2}, z_{HPR}, z_{HPR1}, z_{HPR2}, z_{PV+Inv}, z_{TSR1}, z_{TSR2}.
- ⧫ Fuel prices [€/kWh]: c_{F_b}, $c_{F_{CM}}$.
- ⊙ Reference unit costs energy services [€/kWh]: $c_{Q_{ref}}$, $c_{R_{ref}}$, $c_{W_{ref}}$.

The set of equations can be divided in two types of equations: Costs balance equations and structural equations. The former includes operational and investment costs of the different components of the productive structure. The later describes the productive model of junctions and branches.

C.1 Costs balance equations

These equations associate the costs of the resources consumed by the component, both operational and investment costs, to the costs of the product, in accordance to the Eq. 6.4.

PV panels:

$$c_{W_{PVe}} = z_{PV+Inv} \tag{C.1}$$

$$z_{PV+Inv} = \frac{Invest_{PV+Inv}}{W_{PVe}} \tag{C.2}$$

Gas boiler:

$$c_{Q_b} = c_{F_b} \cdot k_{F_b} + z_{GB} \tag{C.3}$$

$$z_{GB} = \frac{Invest_{GB}}{Q_b} \tag{C.4}$$

Virtual heat pumps set of equations: The heat pump is divided in two virtual heat pumps $HP1$ and $HP2$ according to the origin of the electricity consumed. Thus, $HP1$ is driven with the electricity generated in the cogeneration module, and $HP2$ is driven with the renewable electricity produced in the PV panels. In turn, each virtual heat pump is divided according to its production of cooling and heating in $HPR1$, $HPQ1$, $HPR2$ and $HPQ2$ respectively. In this case, the virtual heat pump $HP1$ is included in the control volume $CV-B$. As a result, only the cost balance equations of the $HP2$ are presented below:

$$c_{R_{HP2}} = \frac{c_{W_{HPR2}}}{EER} + z_{HPR2} \tag{C.5}$$

$$c_{Q_{HP2}} = \frac{c_{W_{HPQ2}}}{COP} + z_{HPQ2} \tag{C.6}$$

As mentioned in the chapter 6, the investment cost of the heat pump $Invest_{HP}$ is distributed in the virtual heat pumps HPR and HPQ proportionally to their annual productions. Thus, solving the equations 6.19 and 6.20:

$$z_{HPR} = \frac{Invest_{HP} \cdot R_{HP}}{(Q_{HP})^2 + (R_{HP})^2} \tag{C.7}$$

$$z_{HPQ} = \frac{Invest_{HP} \cdot Q_{HP}}{(Q_{HP})^2 + (R_{HP})^2} \tag{C.8}$$

Likewise, the investment cost of the heat pump is distributed in each virtual heat pump namely $HP1$ and $HP2$, and in turn, proportional to their respective annual productions $HPR1$, $HPQ1$, $HPR2$ and $HPQ2$:

$$z_{HPR1} = \frac{(z_{HPR} \cdot R_{HP}) \cdot R_{HP1}}{(R_{HP1})^2 + (R_{HP2})^2} \tag{C.9}$$

$$z_{HPQ1} = \frac{(z_{HPQ} \cdot Q_{HP}) \cdot Q_{HP1}}{(Q_{HP1})^2 + (Q_{HP2})^2} \tag{C.10}$$

$$z_{HPR2} = \frac{(z_{HPR} \cdot R_{HP}) \cdot R_{HP2}}{(R_{HP1})^2 + (R_{HP2})^2} \tag{C.11}$$

$$z_{HPQ2} = \frac{(z_{HPQ} \cdot Q_{HP}) \cdot Q_{HP2}}{(Q_{HP1})^2 + (Q_{HP2})^2} \tag{C.12}$$

Control volume $CV-B$ set of equations: The control volume $CV-B$ includes the cogeneration module CM, the absorption chiller $ACH1$, the virtual thermal energy storage for cooling $TSR1$ and the virtual heat pump $HP1$. Thus, in accordance to the Eq. 6.23 the cost balance equation is:

$$\begin{aligned} &c_{W_{c-E_d}} \cdot W_{c-E_d} + c_{Q_{cq}} \cdot Q_{cq} + c_{R_{ACH1\_r}} \cdot R_{ACH1\_r} + \\ &+ c_{Q_{HP1}} \cdot Q_{HP1} + c_{R_{HP1}} \cdot R_{HP1} + c_{R_{out1}} \cdot R_{out1} = \\ &c_{F_{CM}} \cdot F_{CM} + z_{CM} \cdot W_c + z_{ACH1} \cdot R_{ACH1} + z_{HPQ1} \cdot Q_{HP1} + \\ &+ z_{HPR1} \cdot R_{HP1} + z_{TSR1} \cdot R_{out1} \end{aligned} \tag{C.13}$$

The unit investment costs for the cogeneration module CM and the absorption chiller $ACH1$ are presented below:

$$z_{CM} = \frac{Invest_{CM}}{W_c} \tag{C.14}$$

$$z_{ACH1} = \frac{Invest_{ACH}}{R_{ACH1}} \tag{C.15}$$

Note that there is not $ACH2$ as there is not heat production in the boiler to drive the absorption chiller $Q_{br} = 0$.

In order to determine the unit cost of the products, it applies the same discount ϱ (Eq. 6.24) to all cogenerated products crossing the border of the control volume $CV-B$, in this case W_{c-E_d}, Q_{cq}, Q_{HP1}, R_{HP1}, R_{ACH1_r} and R_{out1} with respect to the reference unit costs of each energy services $c_{W_{ref}}$, $c_{Q_{ref}}$, $c_{R_{ref}}$ obtained from the reference energy system. Thus, it is obtained the set of equations below:

$$\frac{c_{W_{c-E_d}}}{c_{W_{ref}}} = \frac{c_{Q_{cq}}}{c_{Q_{ref}}} \tag{C.16}$$

$$\frac{c_{Q_{cq}}}{c_{Q_{ref}}} = \frac{c_{Q_{HP1}}}{c_{Q_{ref}}} \tag{C.17}$$

$$\frac{c_{Q_{HP1}}}{c_{Q_{ref}}} = \frac{c_{R_{HP1}}}{c_{R_{ref}}} \tag{C.18}$$

$$\frac{c_{R_{HP1}}}{c_{R_{ref}}} = \frac{c_{R_{ACH1\_r}}}{c_{R_{ref}}} \tag{C.19}$$

$$\frac{c_{R_{ACH1\_r}}}{c_{R_{ref}}} = \frac{c_{R_{out1}}}{c_{R_{ref}}} \tag{C.20}$$

Virtual thermal energy storage set of equations: The unit cost of the product of the virtual thermal energy storage for cooling $TSR1$ is subject to the costs balance of the control volume $CV - B$ presented above. On the other hand, the unit cost of the product of the virtual thermal energy storage for cooling $TSR2$ is calculated through the expression below:

$$c_{R_{out2}} \cdot R_{out2} = c_{R_{in2}} \cdot R_{in2} + z_{TSR2} \cdot R_{out2} \tag{C.21}$$

Concerning the investment cost of the thermal energy storage for cooling, similar to the procedure carried out in the case of the heat pump, the investment of the TSR is distributed in its virtual thermal energy storage for cooling $TSR1$ and $TSR2$ proportional to their respective annual productions R_{out1} and R_{out2}:

$$z_{TSR1} = \frac{Invest_{TSR} \cdot R_{out1}}{(R_{out1})^2 + (R_{out2})^2} \tag{C.22}$$

$$z_{TSR2} = \frac{Invest_{TSR} \cdot R_{out2}}{(R_{out1})^2 + (R_{out2})^2} \tag{C.23}$$

C.2 Structural equations

Structural equations are those equations describing the productive model of junctions (rhombs) and branches (circles), which relate the productive interaction among the components of the energy system. They show how the resources consumed by the energy system are distributed through the different components, i.e. they show how the components are connected from a productive point of view. Thus, the equations presented below are set in accordance to the equations 6.5 and 6.6.

Electrical part set of equations

From junction E:

$$c_{E_d} \cdot E_d = c_{W_{PV-E_d}} \cdot W_{PV-E_d} + c_{W_{c\_E_d}} \cdot W_{c\_E_d} \tag{C.24}$$

From the branching 1:

$$c_{W_{PVe}} = c_{W_{PV-E_d}} \tag{C.25}$$

$$c_{W_{PVe}} = c_{E_{HP2}} \tag{C.26}$$

From the branching 2:

$$c_{E_{HP2}} = c_{W_{HPQ2}} \tag{C.27}$$
$$c_{E_{HP2}} = c_{W_{HPR2}} \tag{C.28}$$

Cooling part set of equations

From junction R:

$$c_{R_{HP1\_r}} \cdot R_{HP1\_r} + c_{R_{HP2\_r}} \cdot R_{HP2\_r} + c_{R_{ACH1\_r}} \cdot R_{ACH1\_r} + c_{R_{out}} \cdot R_{out} = c_{R_d} \cdot R_d \tag{C.29}$$

From junction 1:

$$c_{R_{in2}} \cdot R_{in2} = c_{R_{HP1\_TSR2}} \cdot R_{HP1\_TSR2} + c_{R_{HP2\_TSR2}} \cdot R_{HP2\_TSR2} \tag{C.30}$$

From junction 2:

$$c_{R_{out}} \cdot R_{out} = c_{R_{out1}} \cdot R_{out1} + c_{R_{out2}} \cdot R_{out2} \tag{C.31}$$

From branching 3:

$$c_{R_{HP2}} = c_{R_{HP2\_r}} \tag{C.32}$$
$$c_{R_{HP2}} = c_{R_{HP2\_TSR2}} \tag{C.33}$$

From branching 4:

$$c_{R_{HP1}} = c_{R_{HP1\_r}} \tag{C.34}$$
$$c_{R_{HP1}} = c_{R_{HP1\_TSR2}} \tag{C.35}$$

Heating part set of equations

From junction Q:

$$c_{Q_{cq}} \cdot Q_{cq} + c_{Q_{bq}} \cdot Q_{bq} + c_{Q_{HP1}} \cdot Q_{HP1} + c_{Q_{HP2}} \cdot Q_{HP2} = c_{Q_d} \cdot Q_d \tag{C.36}$$

From branching 5:

$$c_{Q_b} = c_{Q_{bq}} \tag{C.37}$$

Appendix D

Surface area restriction for PV panels and ST collectors

The surface area restriction is included in the optimization model based on the procedure described by IDAE (2011c) to consider the shading effects on both PV panels and ST collectors. The Figure D.1 illustrates the collectors array configuration based on the minimum distance δ between rows. The minimum distance δ is defined as follows:

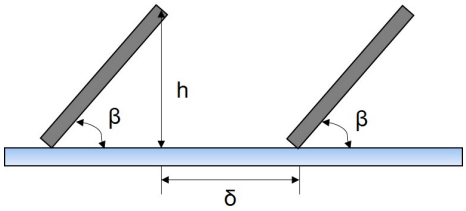

Figure D.1: Shading effect in array collectors.

$$\delta = \chi \cdot h \tag{D.1}$$

$$\chi = \frac{1}{tan(61° - \varphi)} \tag{D.2}$$

$$h = L_{col} \cdot sin\beta \tag{D.3}$$

Where, L_{col} is the length of the collector (hypotenuse), β is the slope of the surface collector and φ is the latitude of the location, 41.7 ° for Zaragoza-Spain.

Therefore, the total area required for the installation of each type of technology (PV panels or solar thermal collectors) A_t can be calculated as:

$$A_{t_{col}} = A_{col} \cdot cos\beta + \delta \cdot b_{col} \cdot n_{col} \tag{D.4}$$

$$n_{col} = \frac{A_{col}}{A_{nom_{col}}} \tag{D.5}$$

Where, A_{col} is the surface area of the collector, b_{col} is the wide of the collector, n_{col} is the number of collectors, and $A_{nom_{col}}$ is the nominal area of each type of collector. The subindex $_{col}$ is to indicate the type of collector, i.e PV panel or solar thermal collector. Thus, the total area restriction is modelled as:

$$A_t \geq A_{t_{PV}} + A_{t_{ST}} \tag{D.6}$$

Bibliography

Abel, E. (1994). Low-energy buildings. *Energy and Buildings*, 21(3):169–174.

AENOR (2005). Instalaciones solares térmicas para producción de agua caliente sanitaria-UNE 94.002.

Aeolos (2006). Aeolos Wind Turbine 30kW Specification. http://www.verdeplus.gr/files/Aeolos H-30kw Brochure.pdf. Accessed on 2019-05-28.

Al-falahi, M. D. A., Jayasinghe, S. D. G., and Enshaei, H. (2017). A review on recent size optimization methodologies for standalone solar and wind hybrid renewable energy system. *Energy Conversion and Management*, 143:252–274.

Al Moussawi, H., Fardoun, F., and Louahlia, H. (2017). Selection based on differences between cogeneration and trigeneration in various prime mover technologies. *Renewable and Sustainable Energy Reviews*, 74:491–511.

Al Moussawi, H., Fardoun, F., and Louahlia-Gualous, H. (2016). Review of trigeneration technologies: Design evaluation, optimization, decision-making, and selection approach. *Energy Conversion and Management*, 120:157–196.

Aldersey-Williams, J. and Rubert, T. (2019). Levelised cost of energy – A theoretical justification and critical assessment. *Energy Policy*, 124:169–179.

Andiappan, V. (2017). State-Of-The-Art Review of Mathematical Optimisation Approaches for Synthesis of Energy Systems. *Process Integration and Optimization for Sustainability*, 1(3):165–188.

Ardani, K., O'Shaughnessy, E., Fu, R., McClurg, C., Huneycutt, J., and Margolis, R. (2016). Installed Cost Benchmarks and Deployment Barriers for

Residential Solar Photovoltaics with Energy Storage: Q1 2016. Technical report, NREL.

ASHRAE (2009). *Fundamentals Handbook*. American Society of Heating, Refrigerating and Air-Conditioning Engineers., Atlanta.

Atersa (2017). Specifications of photovoltaic module A-255P. http://www.atersa.com/Common/pdf/atersa/manuales-usuario/modulos-fotovoltaicos/Ficha_Tecnica_A-255P-A-265P_Ultra.pdf. Accessed on 2018-01-06.

Atersa (2019). Precios de paneles fotovoltaicos. https://atersa.com/es/. Accessed on 2020-11-13.

Aura Energía (2019). Electricity price for Gran Canaria. https://www.aura-energia.com/tarifas-luz-empresa-canarias/. Accessed on 2019-05-29.

Axiom Energy Group (2020). Micro Combined Heat & Power. https://www.axiom-energy.com/microchp. Accessed on 2020-11-13.

Ayerbe (2018). Catálogo de grupos electrógenos 2018. http://www.ayerbe.net/AYERBE-CATALOGO-2018.pdf. Accessed on 2018-10-03.

Baxi (2020). Catálogo de precios. https://www.baxi.es/productos/catalogo-tarifa. Accessed on 2020-03-21.

Beccali, M., Cellura, M., Longo, S., and Mugnier, D. (2016). A Simplified LCA Tool for Solar Heating and Cooling Systems. *Energy Procedia*, 91:317–324.

Bejan, A., Tsatsaronis, G., and Moran, M. J. (1996). *Thermal Design and Optimization*. Wiley, New York.

Boletin Oficial del Estado (2015). RD 900/2015. https://www.boe.es/boe/dias/2015/10/10/pdfs/BOE-A-2015-10927.pdf. Accessed on 2018-10-15.

Boletin Oficial del Estado (2019). RD 244/2019. https://www.boe.es/boe/dias/2019/04/06/pdfs/BOE-A-2019-5089.pdf. Accessed on 2019-05-06.

Bonou, A., Laurent, A., and Olsen, S. I. (2016). Life cycle assessment of onshore and offshore wind energy-from theory to application. *Applied Energy*, 180:327–337.

Bornay (2017). 3 kW nominal capacity wind turbine specifications. https://www.bornay.com/es/productos/aerogeneradores/wind-plus. Accessed on 2018-01-06.

Buoro, D., Pinamonti, P., and Reini, M. (2014). Optimization of a Distributed Cogeneration System with solar district heating. *Applied Energy*, 124:298–308.

Cagnano, A., De Tuglie, E., and Mancarella, P. (2020). Microgrids: Overview and guidelines for practical implementations and operation. *Applied Energy*, 258:114039.

Caro, D. (2019). Carbon Footprint. pages 252–257. Elsevier, Oxford.

Carvalho, M. (2011). *Thermoeconomic and environmental analyses for the synthesis of polygeneration systems in the residential-commercial sector*. PhD thesis, Universidad de Zaragoza.

Carvalho, M., Lozano, M. A., and Serra, L. M. (2012). Multicriteria synthesis of trigeneration systems considering economic and environmental aspects. *Applied Energy*, 91(1):245–254.

Chauhan, A. and Saini, R. P. (2014). A review on Integrated Renewable Energy System based power generation for stand-alone applications: Configurations, storage options, sizing methodologies and control. *Renewable and Sustainable Energy Reviews*, 38:99–120.

Chauhan, R. K., Chauhan, K., Subrahmanyam, B. R., Singh, A. G., and Garg, M. M. (2020). Distributed and centralized autonomous DC microgrid for residential buildings: A case study. *Journal of Building Engineering*, 27:100978.

Chen, S. G. (2013). Bayesian approach for optimal PV system sizing under climate change. *Omega*, 41(2):176–185.

Cho, J., Jeong, S., and Kim, Y. (2015). Commercial and research battery technologies for electrical energy storage applications. *Progress in Energy and Combustion Science*, 48:84–101.

CogenGreen (2014). 7.5 to 402 kW natural gas-fired ecoGEN CHP units. https://www.cogengreen.com/en/75-402-kw-natural-gas-fired-ecogen-chp-units-natural-gas-fired-condensing-micro-and-mini-chp-units. Accessed on 2019-01-31.

Daikin (2019). Tarifa Daikin 2019. https://gduran.com/tarifas/fontaneria/aire-acondicionado-catalogo-precios-fontaneria-DAIKIN.pdf. Accessed on 2019-09-10.

Darrow, K., Tidball, R., Wang, J., and Hampson, A. (2017). Catalog of CHP technologies. Technical report, U.S Environmental Protection Agency.

Dincer, I., Rosen, M. A., and Ahmadi, P. (2017). *Optimization of Energy Systems*. Wiley.

DiOrio, N., Dobos, A., Janzou, S., Nelson, A., and Lundstrom, B. (2015). Technoeconomic Modeling of Battery Energy Storage in SAM. Technical report, NREL.

Domínguez-Muñoz, F., Cejudo-López, J. M., Carrillo-Andrés, A., and Gallardo-Salazar, M. (2011). Selection of typical demand days for CHP optimization. *Energy and Buildings*, 43(11):3036–3043.

Duffie, J. A. and Beckman, W. A. (2013). *Solar Engineering of Thermal Processes*. John Wiley & Sons, 4th edition.

Dufo-López, R. and Bernal-Agustín, J. L. (2015). A comparative assessment of net metering and net billing policies. Study cases for Spain. *Energy*, 84:684–694.

Dufo-López, R., Lujano-Rojas, J. M., and Bernal-Agustín, J. L. (2014). Comparison of different lead–acid battery lifetime prediction models for use in simulation of stand-alone photovoltaic systems. *Applied Energy*, 115:242–253.

El-Sayed, Y. M. (2003). *The Thermoeconomics of Energy Conversions*. Elsevier, Oxford.

El-Sayed, Y. M. and Evans, R. B. (1970). Thermoeconomics and the Design of Heat Systems. *Journal of Engineering for Power*, 92(1):27–35.

El-Sayed, Y. M. and Gaggioli, R. A. (1989). A Critical Review of Second Law Costing Methods—I: Background and Algebraic Procedures. *Journal of Energy Resources Technology*, 111(1):1–7.

Enair (2019). Small Wind Turbines. https://www.enair.es/en/. Accessed on 2020-11-13.

Endesa (2014). Guía vademécum para instalaciones de enlace en baja tensión. Technical report.

Endesa (2018). Precios de gas y electricidad para contratos firmados hasta abril 2019. https://www.solucionesintegralesendesa.com/media/wysiwyg/endesa/Condiciones/tarifas_electricidad_y_gas_SI.pdf. Accessed on 2019-01-29.

Endesa (2019). Anexo de precios de electricidad para empresas. Válido para contrataciones realizadas hasta octubre 2019. https://www.endesaclientes.com/static/iberia/empresas/condiciones/anexo-precio-electricidad-es.pdf. Accessed on 2019-05-29.

Enertres (2017). Catálogo de bombas de calor tarifa 11E. https://enertres.com/aerotermia/. Accessed on 2019-05-02.

EU (2004). DIRECTIVE 2004/8/EC-on the promotion of cogeneration based on a useful heat demand in the internal energy market and amending Directive 92/42/EEC. https://eur-lex.europa.eu/LexUriServ/LexUriServ.do?uri=OJ:L:2004:052:0050:0060:EN:PDF. Accessed on 2020-11-13.

EU (2015). Establishing harmonised efficiency reference values for separate production of electricity and heat in application of Directive 2004/8/EC.

European Commission (2018). 2030 climate & energy framework. https://ec.europa.eu/clima/policies/strategies/2030_en. Accessed on 2019-11-25.

European Commission JRC (2019). PVGIS-Photovoltaic Geographical Information System. http://re.jrc.ec.europa.eu/pvg_tools/en/tools.html#PVP. Accessed on 2020-03-11.

Eurostat (2020). Gas prices for household consumers- bi-annual data (from 2007 onwards). http://appsso.eurostat.ec.europa.eu/nui/show.do?dataset=nrg_pc_202&lang=en. Accessed on 2020-03-07.

Fazlollahi, S. and Maréchal, F. (2013). Multi-objective, multi-period optimization of biomass conversion technologies using evolutionary algorithms and mixed integer linear programming (MILP). *Applied Thermal Engineering*, 50(2):1504–1513.

Fleck, B. and Huot, M. (2009). Comparative life-cycle assessment of a small wind turbine for residential off-grid use. *Renewable Energy*, 34(12):2688–2696.

footprint, C. (2016). 2016 Carbon conversion factors. https://www.carbonfootprint.com/2016_carbon_conversion_factors.html. Accessed on 2019-02-14.

Frangopoulos, C. A. (1987). Thermo-economic functional analysis and optimization. *Energy*, 12(7):563–571.

Frangopoulos, C. A. (1991). Intelligent functional approach; A method for analysis and optimal synthesis-design-operation of complex systems.

Frangopoulos, C. A., Spakovsky, M. V., and Sciubba, E. (2002). A Brief Review of Methods for the Design and Synthesis Optimization of Energy Systems. *International Journal of Thermodynamics*, 5:151–160.

Frederiksen, S. and Werner, S. (2013). *District heating and cooling*. Studentlitteratur.

Frischknecht, R., Itten, R., Sinha, P., de Wild-Scholten, M., and Zhang, J. (2015). Life Cycle Inventories and Life Cycle Assessments of Photovoltaic Systems. Technical report, International Energy Agency.

Fronius (2016). Data sheet Fronius PRIMO. https://www.fronius.com/en/solar-energy/installers-partners/technical-data/all-products/inverters/fronius-primo/fronius-primo-3-0-1. Accessed on 2020-11-13.

Fthenakis, V. and Raugei, M. (2017). 7 – Environmental life-cycle assessment of photovoltaic systems. *The Performance of Photovoltaic (PV) Systems*, pages 209–232.

Fu, R., Feldman, D., Margolis, R., Woodhouse, M., and Ardani, K. (2017). U.S. Solar Photovoltaic System Cost Benchmark: Q1 2017. Technical report, NREL.

Gaggioli, R. A. (1961). *Thermodynamics and the Non-Equilibrium Systems*. PhD thesis, Winsconsin, Madison.

GAMS Development Corporation (2019). General Algebraic Modeling System (GAMS). https://www.gams.com/. Accessed on 2020-11-13.

Ghaem Sigarchian, S., Malmquist, A., and Martin, V. (2018). The choice of operating strategy for a complex polygeneration system: A case study for a residential building in Italy. *Energy Conversion and Management*, 163:278–291.

Giuntoli, J., Agostini, A., Edwards, R., and Marelli, L. (2017). Solid and gaseous bioenergy pathways: input values and GHG emissions. Calculated according to the methodology set in COM(2016) 767.

Gong, J. and You, F. (2015). Sustainable design and synthesis of energy systems. *Current Opinion in Chemical Engineering*, 10:77–86.

Grossmann, I. E. (2002). Review of Nonlinear Mixed-Integer and Disjunctive Programming Techniques. *Optimization and Engineering*, 3(3):227–252.

Guadalfajara, M. (2016). *Economic and environmental analysis of central solar heating plants with seasonal storage for the residential sector. Ph. D. Thesis.* PhD thesis, Universidad de Zaragoza.

Guelpa, E. and Verda, V. (2020). Exergoeconomic analysis for the design improvement of supercritical CO2 cycle in concentrated solar plant. *Energy*, 206:118024.

Haimes, Y. Y., Lasdon, L. S., and Wismer, D. A. (1971). On a bicriterion formation of the problems of integrated system identification and system optimization. *IEEE Transactions on Systems, Man, and Cybernetics*, 3:296–297.

Hiremath, M., Derendorf, K., and Vogt, T. (2015). Comparative Life Cycle Assessment of Battery Storage Systems for Stationary Applications. *Environmental science & technology*.

Homer Energy (2016). HOMER® Pro Version 3.7 User Manual. https://www.homerenergy.com/pdf/HOMERHelpManual.pdf. Accessed on 2017-10-20.

Honda (2003). Household Gas Engine Cogeneration Unit. https://global.honda/innovation/technology/power/cogeneration-picturebook.html. Accessed on 2019-08-22.

IBM (2019). CPLEX Optimizer. https://www.ibm.com/analytics/cplex-optimizer. Accessed on 2020-11-13.

IDAE (2008). Technical guide to measure and determine useful heat, electricity and primary energy savings on high efficiency. Technical report.

IDAE (2009). Escala de calificación energética para edificios de nueva construcción. Technical report.

IDAE (2011a). Consumos del Sector Residencial en España - Resumen de Información Básica. Technical report, IDAE.

IDAE (2011b). Plan de Energías Renovables (PER) 2011-2020. Technical report, IDAE.

IDAE (2011c). Pliego de Condiciones Técnicas de Instalaciones Conectadas a Red.

IDAE (2011d). PROYECTO SECH-SPAHOUSEC. Análisis del consumo energético del sector residencial en España. Technical report, IDAE.

IDAE (2016). Informe de precios energéticos regulados. Technical report.

IDAE (2017). Código Técnico de la Edificación-Ahorro de energía.

IDAE (2018). Estudios, informes y estadísticas. http://www.idae.es/estudios-informes-y-estadisticas. Accessed on 2019-01-30.

IDAE (2019a). Informe de Precios de la Biomasa para Usos Térmicos.

IDAE (2019b). Plan Nacional Integrado de Energía y Clima (PNIEC) 2021-2030. https://www.idae.es/informacion-y-publicaciones/plan-nacional-integrado-de-energia-y-clima-pniec-2021-2030. Accessed on 2019-09-09.

IEA (2020). Global Energy Review 2020: The impacts of the Covid-19 crisis on global energy demand and CO2 emissions. Technical report, IEA.

International Energy Agency (2017). Global Status Report 2017. https://www.worldgbc.org/sites/default/files/UNEP 188_GABC_en %28web%29.pdf.

International Energy Agency (2018). World Energy Outlook 2018. https://www.iea.org/weo2018/. Accessed on 2019-09-25.

International Organization for Standardization (2006). ISO 14040: Environmental management-Life cycle assessment-Principles and framework.

International Renewable Energy Agency (2019). Innovation landscape brief: Net billing schemes. Technical report, Abu Dhabi.

IRENA (2017). Electricity storage and renewables: Costs and markets to 2030. https://www.irena.org/publications/2017/Oct/Electricity-storage-and-renewables-costs-and-markets. Accessed on 2020-11-13.

IRENA (2020a). Battery Storage Paves Way for a Renewable-powered Future. Accessed on 2020-08-18.

IRENA (2020b). Global Renewables Outlook: Energy transformation 2050. https://www.irena.org/publications. Accessed on 2020-11-13.

ISSF (2015). Stainless Steel and CO2 : Facts and Scientific Observations. http://www.worldstainless.org/Files/issf/non-image-files/PDF/ISSF_Stainless_Steel_and_CO2.pdf. Accessed on 2018-05-18.

Jana, K., Ray, A., Majoumerd, M. M., Assadi, M., and De, S. (2017). Polygeneration as a future sustainable energy solution – A comprehensive review. *Applied Energy*, 202:88–111.

Kaderbhai, M. (2017). Understanding ISO 8528-1 Generator Set Ratings. Technical report, Cummins, Inc.

Kasaeian, A., Bellos, E., Shamaeizadeh, A., and Tzivanidis, C. (2020). Solar-driven polygeneration systems: Recent progress and outlook. *Applied Energy*, 264:114764.

Kemp, I. C. (2007). *Pinch Analysis and Process Integration*. Elsevier.

Khalilpour, R. and Vassallo, A. (2015). Leaving the grid: An ambition or a real choice? *Energy Policy*, 82:207–221.

Kiran, D. (2017). Quality Function Deployment. *Total Quality Management*, pages 425–437.

Kotzur, L., Markewitz, P., Robinius, M., and Stolten, D. (2018). Impact of different time series aggregation methods on optimal energy system design. *Renewable Energy*, 117:474–487.

Lapesa (2020). Depósitos y equipamientos para agua caliente sanitaria, producción y acumulación. http://www.lapesa.com/. Accessed on 2020-11-13.

Lazzaretto, A., Toffolo, A., Reini, M., Taccani, R., Zaleta-Aguilar, A., Rangel-Hernandez, V., and Verda, V. (2006). Four approaches compared on the TADEUS (thermoeconomic approach to the diagnosis of energy utility systems) test case. *Energy*, 31(10):1586–1613.

LINDO Systems Inc (2013). Lingo-Optimization Modeling Software for Linear, Nonlinear, and Integer Programming. https://www.lindo.com/. Accessed on 2020-11-13.

Liu, M., Shi, Y., and Fang, F. (2014). Combined cooling, heating and power systems: A survey. *Renewable and Sustainable Energy Reviews*, 35:1–22.

Liu, P., Georgiadis, M. C., and Pistikopoulos, E. N. (2011). Advances in Energy Systems Engineering. *Industrial & Engineering Chemistry Research*, 50(9):4915–4926.

López-Ochoa, L. M., Las-Heras-Casas, J., López-González, L. M., and Olasolo-Alonso, P. (2018). Environmental and energy impact of the EPBD in residential buildings in hot and temperate Mediterranean zones: The case of Spain. *Energy*, 161:618–634.

Lozano, M. and Valero, A. (1993). Theory of the exergetic cost. *Energy*, 18(9):939–960.

Lozano, M., Valero, A., and Serra, L. (1996). Local optimization of energy systems. *ASME Book G01022*, 36:241–250.

Lozano, M. A., Ramos, J. C., Carvalho, M., and Serra, L. M. (2009). Structure optimization of energy supply systems in tertiary sector buildings. *Energy and Buildings*, 41(10):1063–1075.

Lozano, M. A., Ramos, J. C., and Serra, L. M. (2010). Cost optimization of the design of CHCP (combined heat, cooling and power) systems under legal constraints. *Energy*, 35(2):794–805.

Lund, H., Andersen, A. N., Østergaard, P. A., Mathiesen, B. V., and Connolly, D. (2012). From electricity smart grids to smart energy systems – A market operation based approach and understanding. *Energy*, 42(1):96–102.

Lund, H., Østergaard, P. A., Connolly, D., and Mathiesen, B. V. (2017). Smart energy and smart energy systems. *Energy*, 137:556–565.

Lund, H., Werner, S., Wiltshire, R., Svendsen, S., Thorsen, J. E., Hvelplund, F., and Mathiesen, B. V. (2014). 4th Generation District Heating (4GDH): Integrating smart thermal grids into future sustainable energy systems. *Energy*, 68:1–11.

Mancarella, P. (2009). Matrix modelling of small-scale trigeneration systems and application to operational optimization. *Energy*, 34(3):261–273.

Mancarella, P. (2014). MES (multi-energy systems): An overview of concepts and evaluation models. *Energy*, 65:1–17.

Manwell, J. F., McGowan, J., and Rogers, A. (2009). *Wind Energy Explained*. WILEY, 2nd edition.

Manwell, J. F. and McGowan, J. G. (1993). Lead acid battery storage model for hybrid energy systems. *Solar Energy*, 50(5):399–405.

Marín Giménez, J. (2004). *Evaluation of alternatives for the energy supply of a residential building in Zaragoza*. PhD thesis, Universidad de Zaragoza.

Masson, G., Briano, J. I., and Baez, M. J. (2016). Review and analysis of PV Self-Consumption policies. Technical report, IEA.

Masson-Delmotte, V., Zhai, P., Pörtner, H.-O., Roberts, D., Skea, J., Shukla, P. R., Pirani, A., Moufouma-Okia, W., Péan, C., Pidcock, R., Connors, S., Matthews, J. B. R., Chen, Y., Zhou, X., Gomis, M. I., Lonnoy, E., Maycock, T., Tignor, M., and Waterfield, T. (2018). IPCC, 2018: Global Warming of 1.5°C.An IPCC Special Report on the impacts of global warming of 1.5°C above pre-industrial levels and related global greenhouse gas emission pathways, in the context of strengthening the global response to the threat of clim. Technical report, IPCC.

Mathiesen, B., Lund, H., Connolly, D., Wenzel, H., Østergaard, P., Möller, B., Nielsen, S., Ridjan, I., Karnøe, P., Sperling, K., and Hvelplund, F. (2015). Smart Energy Systems for coherent 100% renewable energy and transport solutions. *Applied Energy*, 145:139–154.

McManus, M. (2012). Environmental consequences of the use of batteries in low carbon systems: The impact of battery production. *Applied Energy*, 93:288–295.

Mehigan, L., Deane, J., Gallachóir, B., and Bertsch, V. (2018). A review of the role of distributed generation (DG) in future electricity systems. *Energy*, 163:822–836.

Meteotest (2017). Meteonorm Software. http://www.meteonorm.com/. Accessed on 2017-11-03.

Ministerio de Industria turismo y comercio (2006). Tabla de potencias activas normalizadas. https://www.boe.es/boe/dias/2006/09/27/pdfs/A33821-33821.pdf. Accessed on 2020-11-13.

Miteco (2020). FACTORES DE EMISIÓN: Registro de huella de carbono, compensación y proyectos de absorción de dióxido de carbono. Technical report.

Modi, A., Bühler, F., Andreasen, J. G., and Haglind, F. (2017). A review of solar energy based heat and power generation systems. *Renewable and Sustainable Energy Reviews*, 67:1047–1064.

Morales Pedraza, J. (2019). Chapter 4 - Current Status and Perspective in the Use of Coal for Electricity Generation in the North America Region. pages 211–257. Elsevier.

Muselli, M., Poggi, P., Notton, G., and Louche, A. (2000). Classification of typical meteorological days from global irradiation records and comparison between two Mediterranean coastal sites in Corsica Island. *Energy Conversion and Management*, 41(10):1043–1063.

Muselli, M., Poggi, P., Notton, G., and Louche, A. (2001). First order Markov chain model for generating synthetic "typical days" series of global irradiation in order to design photovoltaic stand alone systems. *Energy Conversion and Management*, 42(6):675–687.

Nejat, P., Jomehzadeh, F., Taheri, M. M., Gohari, M., and Muhd, M. Z. (2015). A global review of energy consumption, CO2 emissions and policy in the residential sector (with an overview of the top ten CO2 emitting countries). *Renewable and Sustainable Energy Reviews*, 43:843–862.

NREL (2016). Distributed Generation Energy Technology Operations and Maintenance Costs. https://www.nrel.gov/analysis/tech-cost-om-dg.html. Accessed on 2020-03-16.

Oleinikova, I. and Hillberg, E. (2020). Micro vs MEGA: trends influencing the development of the power system. Technical report, International Energy Agency (IEA).

Orrell, A. and Poehlman, E. (2017). Benchmarking U.S. Small Wind Costs With the Distributed Wind Taxonomy. Technical report, Pacific Northwest National Laboratory.

Ortiga, J., Bruno, J., and Coronas, A. (2011). Selection of typical days for the characterisation of energy demand in cogeneration and trigeneration optimisation models for buildings. *Energy Conversion and Management*, 52(4):1934–1942.

Ortiga, J., Bruno, J. C., Coronas, A., and Grossman, I. E. (2007). Review of optimization models for the design of polygeneration systems in district heating and cooling networks. *Computer Aided Chemical Engineering*, 24:1121–1126.

Parra, D., Swierczynski, M., Stroe, D. I., Norman, S., Abdon, A., Worlitschek, J., O'Doherty, T., Rodrigues, L., Gillott, M., Zhang, X., Bauer, C., and Patel, M. K. (2017). An interdisciplinary review of energy storage for communities: Challenges and perspectives. *Renewable and Sustainable Energy Reviews*, 79:730–749.

Peters, J. F., Baumann, M., Zimmermann, B., Braun, J., and Weil, M. (2017). The environmental impact of Li-Ion batteries and the role of key parameters – A review. *Renewable and Sustainable Energy Reviews*, 67:491–506.

Pina, E. A. (2019). *Thermoeconomic and environmental synthesis and optimization of polygeneration systems supported with renewable energies and thermal energy storage applied to the residential-commercial sector*. PhD thesis, Universidad de Zaragoza.

Pina, E. A., Lozano, M. A., and Serra, L. M. (2020). A multiperiod multiobjective framework for the synthesis of trigeneration systems in tertiary sector buildings. *International Journal of Energy Research*, pages 1140–1166.

Pinto, E. and Serra, L. (2018). Optimization of the design and operation of a polygeneration system for a residential building integrating renewable energy, electric energy storage and heat pumps. In *ECOS 2018 - Proceedings of the 31st International Conference on Efficiency, Cost, Optimization, Simulation and Environmental Impact of Energy Systems*.

Pinto, E. S., Serra, L. M., and Lázaro, A. (2019). Economic and environmental assessment of renewable energy and energy storage integration in standalone polygeneration systems for residential buildings. In *International Conference on Solar Heating and Cooling for Buildings and Industry. Santiago de Chile, Chile, November 04-07.*

Pinto, E. S., Serra, L. M., and Lázaro, A. (2020). Evaluation of methods to select representative days for the optimization of polygeneration systems. *Renewable Energy*, 151:488–502.

Poncelet, K., H. H oschle, Delarue, E., Virag, A., and W.D'haeseleer (2017). Selecting representative days for capturing the implications of integrating intermittent renewables in generation expansion planning problems. *IEEE TRANSACTIONS ON POWER SYSTEMS*, 32.

Rainbow Power Company (2019). Retail Price List-Inverters. https://www.rpc.com.au/pricelists/pricelist-retail.pdf. Accessed on 2020-03-26.

Ramos, J. (2012). *Optimization of the design and operation of cogeneration systems for the residential and commercial sector. Ph. D. Thesis.* PhD thesis, Universidad de Zaragoza.

REE (2019a). Demanda y producción en tiempo real. http://www.ree.es/es/actividades/demanda-y-produccion-en-tiempo-real. Accessed on 2019-05-28.

REE (2019b). El Sistema electrico español 2018. https://www.ree.es/es/datos/publicaciones/informe-anual-sistema/informe-del-sistema-electrico-espanol-2018.

REE (2019c). Sistema de información del operador del sistema. https://www.esios.ree.es/es?locale=es. Accessed on 2019-05-28.

Renzulli, P. A., Notarnicola, B., Tassielli, G., Arcese, G., and Capua, R. D. (2016). Life Cycle Assessment of Steel Produced in an Italian Integrated Steel Mill. *Sustainability.*

Rockenbaugh, C., Dean, J., Lovullo, D., Lars Lisell, G. B., Hanckock, E., and Norton, P. (2016). High Performance Flat Plate Solar Thermal Collector Evaluation. Technical report, NREL.

Rong, A. and Lahdelma, R. (2016). Role of polygeneration in sustainable energy system development challenges and opportunities from optimization viewpoints. *Renewable and Sustainable Energy Reviews*, 53:363–372.

Rong, A. and Su, Y. (2017). Polygeneration systems in buildings: A survey on optimization approaches. *Energy and Buildings*, 151:439–454.

Salvador Escoda S.A (2017a). Colectores solares planos GK 5000. https://www.salvadorescoda.com/productos/energias-renovables-y-calderas/. Accessed on 2018-01-06.

Salvador Escoda S.A (2017b). Libro blanco de energías renovables. https://www.salvadorescoda.com/. Accessed on 2020-11-13.

Schütz, T., Schraven, M. H., Fuchs, M., Remmen, P., and Müller, D. (2018). Comparison of clustering algorithms for the selection of typical demand days for energy system synthesis. *Renewable Energy*, 129:570–582.

Serra, L. M. (1994). *Optimización exergoeconómica de sistemas térmicos*. PhD thesis, Universidad de Zaragoza.

Serra, L. M., Lozano, M.-A., Ramos, J., Ensinas, A. V., and Nebra, S. A. (2009). Polygeneration and efficient use of natural resources. *Energy*, 34(5):575–586.

Shin, M. and Do, S. L. (2016). Prediction of cooling energy use in buildings using an enthalpy-based cooling degree days method in a hot and humid climate. *Energy and Buildings*, 110:57–70.

SMA (2013). Specifications SUNNY ISLAND 6.0H / 8.0H. http://files.sma.de/dl/2485/SI_6H8H-AEN131411W.pdf. Accessed on 2020-03-20.

SMA (2014). Data sheet Sunny Tripower 5000TL – 12000TL. https://loopsolar.com/datasheet/sma-solar/sma-sunny-tripower-three-phase5-12kw-string-inverter-india.pdf. Accessed on 2020-11-13.

Sunlight (2015). Batteries for Renewable Energy. https://www.systems-sunlight.com/product/product_category/applications/renewable-energy/.

Tapia-Ahumada, K., Pérez-Arriaga, I., and Moniz, E. (2013). A methodology for understanding the impacts of large-scale penetration of micro-combined heat and power. *Energy Policy*, 61:496–512.

Tawfik, T. M., Badr, M. A., El-Kady, E. Y., and Abdellatif, O. E. (2018). Optimization and energy management of hybrid standalone energy system: a case study. *Renewable Energy Focus*, 25:48–56.

Ton, D. T. and Smith, M. A. (2012). The U.S. Department of Energy's Microgrid Initiative. *The Electricity Journal*, 25(8):84–94.

Tremeac, B. and Meunier, F. (2009). Life cycle analysis of 4.5 MW and 250 W wind turbines. *Renewable and Sustainable Energy Reviews*, 13(8):2104–2110.

Tribus, M. and Evans, R. B. (1962). A Contribution to the Theory of Thermoeconomics. Technical report, UCLA.

Tsatsaronis, G. (1998). Recent Development in Energy Economics. In *ECOS'98*, pages 37–38, Nancy, France.

U.S. Department of Energy (2017). Absorption Chillers for CHP Systems. Technical report.

Valero, A., Serra, L., and Uche, J. (2005). Fundamentals of Exergy Cost Accounting and Thermoeconomics. Part I: Theory. *Journal of Energy Resources Technology*, 128(1):1–8.

Valor, E., Meneu, V., and Caselles, V. (2001). Daily Air Temperature and Electricity Load in Spain. *American Meteorological Society*.

Victron (2017). Inversores Multiplus. https://www.victronenergy.com/inverters-chargers/multiplus-12v-24v-48v-800va-3kva. Accessed on 2019-08-28.

Victron Energy (2019). Price list-Inverters. https://www.victronenergy.com/information/pricelist. Accessed on 2020-03-26.

Viti, A. (1996). *DTIE 1.01 Preparación de agua caliente para usos sanitarios*. ATECYR.

von Spakovsky, M. R. and Evans, R. B. (1993). Engineering Functional Analysis—Part I. *Journal of Energy Resources Technology*, 115(2):86–92.

Wakui, T., Kawayoshi, H., and Yokoyama, R. (2016). Optimal structural design of residential power and heat supply devices in consideration of operational and capital recovery constraints. *Applied Energy*, 163:118–133.

Wakui, T. and Yokoyama, R. (2014). Optimal structural design of residential cogeneration systems in consideration of their operating restrictions. *Energy*, 64:719–733.

Wünsch, M., Eikmeier, B., Jochem, E., and Gailfuss, M. (2014). Potential analysis and cost-benefit analysis for cogeneration applications (transposition of the EU Energy Efficiency Directive) and review of the Cogeneration Act in 2014. Technical report, Prognos;Fraunhofer IFAM;IREES.

Yalaoui, A., Chehade, H., Yalaoui, F., and Amodeo, L. (2013). *Optimization*, chapter 2, pages 61–91. John Wiley & Sons, Ltd.

Yanmar (2017). Combined Heat & Power. http://www.yanmar-es.com/products/mchp/. Accessed on 2018-01-06.

Yokoyama, R., Shinano, Y., Taniguchi, S., Ohkura, M., and Wakui, T. (2015). Optimization of energy supply systems by MILP branch and bound method in consideration of hierarchical relationship between design and operation. *Energy Conversion and Management*, 92:92–104.

Zinaman, O., Aznar, A., Linvill, C., Darghouth, N., Dubbeling, T., and Bianco, E. (2017). Grid-Connected Distributed Generation: Compensation Mechanism Basics. Technical report, NREL.